Escola de Camins
Escola Tècnica Superior d'Enginyeria de Camins, Canals i Ports
UPC BARCELONATECH

Seismic design of a multi-story steel building with moment resisting frames using prequalified earthquake haunched joints

TREBALL FINAL DE MÀSTER

Trabajo realizado por:

DAVID SEMPERE GÓMEZ

Dirigido por:

ENRIQUE MIRAMBELL ARRIZABALAGA

Máster en:

Ingeniería de Caminos, Canales y Puertos

Barcelona, 21 de junio de 2021

Departamento de Ingeniería Civil y Ambiental

ACKNOWLEDGEMENT

Me gustaría agradecer a todos los profesores que me han impartido clase durante la especialidad en ingeniería estructural del máster, ya que gracias a ellos he podido adquirir una gran cantidad de conocimientos técnicos en el ámbito de la obra civil y la edificación, los cuales estoy deseando poder aplicar en el mundo profesional.

También me gustaría agradecer a mi tutor, el profesor Enrique Mirambell, por haberme dado la oportunidad de profundizar en el ámbito de las estructuras metálicas y mixtas con la realización de este trabajo final de máster.

Por último, me gustaría dar las gracias a mi madre por todo el apoyo ofrecido en los momentos más difíciles, desde el inicio del grado en 2014, hasta la actual finalización del máster. Ya que, sin este apoyo, a día de hoy no sería ingeniero de caminos, canales y puertos.

ABSTRACT

The current master thesis presents the design of a high ductility steel multi-storey building located in L'Aquila, which is one of the Italian regions with the highest seismic hazard. The structure is a moment resisting frame system (MRFs), which presents a large capacity to exhibit large deformations in inelastic field without significant reduction in strength.

In addition to support gravity and wind loads, the structure has been designed using the capacity design method in order to resist frequent and rare seismic actions. Besides using steel profiles, composite steel-concrete cross-sections have been used owing to the several advantages that present in terms of strength and stiffness.

Several seismic analyses have been applied during the designing process in order to determine the dynamical behaviour and the internal forces produced by the seismic actions, specifically the lineal modal response spectrum and the nonlinear static analysis (pushover).

Furthermore, the displacement-based design method N2, have been introduced to determine the inelastic demand of the dissipative elements under the specific seismic actions of the L'Aquila.

For the case of the beam-to-column joints, prequalified earthquake haunched joints have been considered. These types of connections designed as full-strength, are an excellent solution for the MRF system, since they remain in the elastic range during the application of the seismic actions, allowing the dissipation of energy exclusively by the dissipative elements.

These joints have been designed following the guidelines provided from the investigations carried out by several European universities, in which several prequalified joints to be placed in seismic zones have been studied.

On the other hand, the beam-to-beam joints that connect the secondary beams with the girders, have also been treated in the document. A design procedure that avoids the brittle failure mechanism and allows enough rotation capacity has been presented.

Finally, an evaluation of the performance of the designed building has been carried out, proposing possible improvements and alternatives that may be interesting to be considered for buildings located in important seismic zones.

RESUMEN

El trabajo final de master presenta el dimensionamiento de un edificio metálico compuesto por varios pisos. Al encontrarse en la ciudad de L'Aquila, la cual es una de las regiones con mayor riesgo sísmico de Italia, la estructura está dimensionada para presentar una alta ductilidad. Para ello, se ha utilizado un sistema aporticado (MRF) al presentar gran capacidad para producir deformaciones en el régimen plástico sin reducciones significativa de resistencia.

El diseño por capacidad ha sido utilizado para el dimensionamiento de la estructura, la cual además soportar cargas gravitacionales y de viento, resiste acciones sísmicas frecuentes y poco probables. Se destaca, que además de utilizar perfiles metálicos, se han utilizado secciones mixtas de acero-hormigón debido a las diversas ventajas que presentan en cuanto a resistencia y rigidez.

Varios tipos de análisis dinámicos se han aplicado durante el proceso de cálculo estructural con el fin de determinar el comportamiento bajo cargas dinámicas y los esfuerzos internos producidos por las acciones sísmicas. Específicamente, se han utilizado el análisis dinámico modal espectral y el análisis estático no lineal (pushover).

Además, se ha introducido el método de diseño basado en desplazamiento N2, para así determinar la demanda plástica de los elementos disipativos bajo las acciones sísmicas específicas de L'Aquila.

En el caso de las uniones de viga-columna, se han utilizado uniones acarteladas precalificadas para sismo. Este tipo de unión, dimensionada como de resistencia total, son una excelente solución para el sistema MRF, ya que permanecen en el rango elástico durante la aplicación de las acciones sísmicas, permitiendo que la disipación de energía se produzca exclusivamente en los elementos disipativos.

Para cálculo de dichas uniones, han sido utilizadas las pautas propuestas por un proyecto de investigación llevado a cabo por diversas universidades europeas, dónde se estudian diferentes tipologías de uniones precalificadas para sismo.

Por otro lado, en el documento también son tratadas las uniones viga-viga, las cuales conectan las vigas secundarias con las vigas principales. Se presenta un procedimiento de dimensionamiento que evita la rotura frágil de la unión y proporcionar suficiente capacidad de rotación frente a posibles momentos flectores que puedan aparecer.

Finalmente, se ha realizado una evaluación del desempeño del edificio, proponiendo posibles mejoras y alternativas que pueden que pueden ser interesantes para edificios ubicados en elevadas zonas sísmicas.

INDEX

CHAPTER 1: INTRODUCTION

1.1 MOTIVATION OF THE WORK

Earthquakes may produce buildings to collapse if they are not prepared to resist seismic actions, causing human life and enormous economic losses. For example, in one of the areas of highest seismic hazard in Italy, which is the city of L'Aquila, an earthquake caused 309 deaths and 1600 injuries owing to the collapse of several reinforced concrete and masonry buildings in 2009. Posteriorly, the same natural disaster occurred in the same region, in the city of Amatrice, in 2016, causing 296 deaths and 388 injuries (Fig. 1.1).

Fig.1.1 Earthquakes of Amatrice and L'Aquila cities; Di Trapani and Cavalieri (2018)

The majority of the buildings in Italy were constructed during the seventies and eighties, when technical codes were not sufficiently developed to guide the designer to perform structures resistant to gravity and seismic loads. Therefore, this limited knowledge has conditioned the damage or collapse of several structures.

Since there is an important heritage of reinforced concrete and masonry structures in the Italian territory, several retrofitting interventions to reduce the global and local vulnerabilities of the current structures are necessary to be performed (Di Trapani and Cavalieri, (2018)).

The utilization of steel material for the construction of new buildings located in high seismic areas may be an important alternative to consider owing to the several advantages. Presents high ductility and overstrengh resistance, which are relevant characteristics when the plastic range is reached, commonly used for seismic design. Furthermore, steel buildings present lower mass than reinforced concrete structures, meaning the inertial forces produced by the seismic actions to be applied to the structure would be reduced. Finally, an important reduction of time in the construction process can be produced since several storeys may be built at the same time.

Nevertheless, the problem related to the steel buildings located in seismic areas is the design of the connections, which constitute a critical part that may induce the collapse of the structure if the joint is not designed properly.

Nowadays, procedures for design bolted joints in seismic areas are missing in Europe. Hence, the utilization either of full-strength or partial-strength bolted connections should be supported by experimental evidence to ensure the connections are compatible with the different ductility classes and the structural typology. In such cases, the plastic rotation capacity should be prequalified by relevant test and numerically based procedures, in which the designer cannot practically perform it due to its resources and lack of time.

In contrast to Europe, countries with high seismic hazard such as the US and Japan propose a design methodology based on codified and easy-to-use design tools and procedures derived from the experience and research.

However, as a response, the research project EqualJoints (Landolfo et al. (2018)), carried out by several European universities has been prequalified several full-strength and dissipative joints to be utilized in seismic areas. In fact, these recommendations are expected to appear in the new version of Eurocode 8.

1.2 GENERAL AND SPECIFIC OBJECTIVES OF THE WORK

The aim of this master thesis is to design a multi-storey office building located in L'Aquila (Italy), using a steel moment resistant frame system (MRFs). The structure should be capable to resist gravity loads and the seismic actions associated to the place. For the design, linear and nonlinear seismic analyses shall be applied to determine the performance of the building and verify the hierarchy of resistance.

Moreover, the design of the beam-to-column prequalified haunched joints to be place in the building shall carry out using the guidelines provided by the EqualJoints project (Landolfo et al. (2018). Finally, a study of how to design beam-to-beam simple joints shall be also included.

The specific objectives treated along the document are:

- Carry out a study of the area where the building is considered to be located, defining all the gravity and wind loads which will applied to the structure according its use in order to perform the static analysis.
- Perform the design of all structural elements that composes the structure using the specific codes related to the design of steel and composite buildings.
- Verify that the building presents an optimal dynamic behaviour avoiding global collapse mechanisms as well implement the modal linear response spectrum analysis.
- Introduce the nonlinear modelling with lumped plasticity to perform the static nonlinear analysis to apply the displacement-based design method, specifically the N2 method, to determine the performance of the building in the inelastic field.
- Carry out a research on how to design moment resisting connections using the analytical approach, which is the component method, to design the prequalified haunched connections.
- Understanding of how simple connections work and study the specific codes in order to design the beam-to-beam joints.

- Make an assessment of the designed structure determining if it is a competitive solution and proposing several improvements and alternatives.

1.3 METHODOLOGY

The document is divided in two differentiated parts, due to the fact that the design of the structure and the joints are independent to each other because of using continuous and simple joints, which have been modelled as rigid and pinned connections in the numerical model. Thus, a traditional approach has been applied, which consist in designing the joints according to the previously determined structural elements.

This approach is less time consuming and easier to be applied for the designer, as opposed to using semi-rigid joints, in which case an iteration process in the design process should be required since the stiffness of the connections have an important influence in the internal forces of the structure.

In a first phase, the geometry of the structure was determined according to the needs of an office building. The modelling of the structure was performed in the software SAP2000, using initial cross-sections calculated by hand. All the gravity loads applied to the building used to perform the static analysis were obtained from the Eurocode 1 (EN 1991-1).

The ultimate limit state (ULS) and the serviceability limit state (SLS) that the building had to face under static and seismic conditions, were determined using the Eurocode 0 (EN 1990-1). Subsequently, Eurocode 3 (EN 1993-1), and Eurocode 4 (EN 1994-1) were considered to design the cross-sections of the steel and composite structural elements. Moreover, the Italian code (NTC18) were also taken into account to determine several specific loads such as the wind loads and the seismic actions.

In a second phase, the modal analysis was performed to study the dynamical behaviour of the building and made possible improvements. The linear modal response spectrum was also performed using SAP2000 in order to determine the internal forces produced by the seismic actions, following the considerations of Eurocode 8 (EN 1998-1).

Therefore, an iterative process of both design phases was carried out, since the change of any structural element modifies the dynamical behaviour of the building varying the internal forces produced by the seismic actions.

In a final step, the nonlinear modelling of the building was introduced considering as reference the American code (FEMA 356) and Eurocode 8 (EN 1998-1-3), in order to perform the nonlinear static analysis (Pushover) and the N2 method was applied.

In a second part of the document, the design of the prequalified joints was performed using the component method, which is an analytical approach, taking as reference the guidelines of the EqualJoints project and Eurocode 3 (EN 1993-1-8). Moreover, the Idea StatiCa software was also used during the first steps of the calculations of the prequalified haunched joints. Finally, the simple joints have also been designed using an analytical approach.

1.4 STRUCTURE OF THE RESEARCH WORK

The master's thesis is organized in the following chapters.

Chapter 1. **Introduction** of the document, where the background and the methodology followed in the master thesis is exposed.

Chapter 2. State of the art where the different assumptions for the design of steel structures in seismic areas have been explained, specifically for the MRF typology. Subsequently, basic dynamical concepts have been exposed to introduce the linear modal response spectrum and the nonlinear static analysis, including the N2 method. Finally, the background of the prequalified haunch joints and the specific assumptions that must be considered in order to perform its design are analysed.

Chapter 3. Design of the building. In the chapter is exposed all the steps followed to design the building under gravity and seismic actions applying all the concepts shown in the chapter 2. In the final part of the section, the structural performance is revised using the pushover analysis to verify the final design.

Chapter 4. Design of the joints. The chapter covers the design and the behaviour of prequalified beam-to-column joints to be placed in the building. Moreover, the beam-to-column simple joints design is performed applying different national codes.

Chapter 5. Conclusions and alternatives. In the last chapter, a final assessment of the designed steel building and the steel joints used has been presented, suggesting possible improvements and alternatives.

CHAPTER 2: STATE OF THE ART

2.1 PERFORMANCE CRITERIA FOR THE SEISMIC DESIGN OF STEEL STRUCTURES

2.1.1 Limit states for the seismic design

When it comes to buildings located in zones with important seismic hazard, beyond considering the ultimate limit state (ULS) and the serviceability limit state (SLS) in static conditions against vertical and wind loads, the dynamical behaviour as well as the solicitations produced by the seismic actions must be considered. In fact, according to the clause 2.1 of EN 1998-1 (CEN, 2004), structures located at seismic regions should be met the two following requirements:

- Non-collapse requirement: local or global collapse of the structure under rare seismic actions has to be prevented in order to protect the human lives while preserves the structural integrity with a residual load capacity. This performance is achieved applying the capacity design rules. The non-collapse requirement corresponds to the ultimate limit state (ULS).

- Damage limitation requirement: for frequent seismic events, it aims to prevent the damage of structural elements, retaining its initial stiffness and strength while the damage of non-structural elements is limited. The requirement has the purpose of reducing the cost of reparations without limiting the use of the structure. The performance is achieved limiting the lateral interstorey drift. The damage limitation requirement corresponds to the damage limitations state (DLS).

According to the clause 3.21 of the Italian code (NTC 2018), for a design life of the building of 50 years, the ULS and DLS limits states are characterised by statistical methods defined by return periods (T_r) as shows the Table 2.1.

Table 2.1 Return period for the DLS and ULS

Damage Limitation State (DLS)	Ultimate Limit state (ULS)
Return Period (Tr) = 50 years	Return Period (Tr) = 475 years
Probability of exceedance in 50 years = 63%	Probability of exceedance in 50 years = 10%

Furthermore, two different approaches for the design of earthquake-resistant buildings are specified in clause 6.1.2 of EN 1998-1 (CEN, 2004c).

- Concept a): Low-dissipative structural behaviour
- Concept b): Dissipative structural behaviour

In the first approach, the action effects may be analysed without taking into account the non-linear behaviour of the building, remaining in the elastic range since the building may not fulfil the conditions to apply the plastic design due to poor post-elastic deformation capacity. The structures designed with this concept belong to the category DCL (Ductility Class Low).

Thus, the design of the steel building and the joints following this first approach can be performed using the Eurocode 3, without taking into account more considerations. These assumptions should only be used for buildings located in low seismic areas, as for example with peak ground accelerations (PGA) lower than $0.1g$. Indeed, for PGA lower than $0.05g$ the seismic action may be neglected (Landolfo et al. (2017)).

On the other hand, concept b) classifies the structures into medium structural ductility class (DCM) or high ductility classes (DCH) related to the capacity of dissipating energy trough the inelastic behaviour. Depending on the structural typology, specific requirements are established for the local and global aspects in order to guarantee a ductile response. The Table 2.2 summarizes a range of behaviour factors (q) for each approach that may be used for the elastic seismic analysis.

Table 2.2 Behaviour factors q for approach a) and b); (CEN, 2004c)

Design concept	Structural ductility class	Range of the reference values of the behaviour factor q
Concept a) Low dissipative structural behaviour	DCL (Low)	≤ 1,5 - 2
Concept b) Dissipative structural behaviour	DCM (Medium)	≤ 4 also limited by the values of Table 6.2
	DCH (High)	only limited by the values of Table 6.2

2.1.2 Specific rules for steel moment resistant frames (MRF)

The steel moment resisting frame system (MRFs) is the most dissipative one due to its flexibility, allowing to use large behaviour factors (q). In consequence, the forces produced by seismic actions are considerably reduced due to the inelastic behaviour, which is ideal for buildings which are located in important seismic areas.

In contrast, the flexibility of MRFs produces important interstorey drift ratios, meaning it is an inter-storey drift sensitive typology. This could lead to an oversizing of the structural elements in order to increase the lateral stiffness as well as being necessary to considerer second order effects during the design phase.

The horizontal forces are resisted by the dissipative zones acting in a flexural manner, which should be placed either in the beams or in the joints (if partial-strength joints are used). On the other hand, columns are considered as non-dissipative elements which must remain in the elastic domain to avoid instability problems.

However, the apparition of the plastic hinges in the columns are allowed in specific points such as the base of the columns in the ground floor and in the roof for multi-storey buildings.

These assumptions are satisfied if the strong column – weak beam principle is applied to the design (Eq. 2.1).

$$\sum M_{rc} \geq 1.3 \sum M_{rb} \tag{2.1}$$

where

$\sum M_{rc}$ is the sum of the design values of the moments of resistance of the columns framing the joint. The minimum value of column moments of resistance within the range of column axial forces produced by the seismic design situation should be used.

$\sum M_{rb}$ is the sum of the design values of the moments of resistance of the beams framing the joint.

Furthermore, clause 4.4.2.3(4) of EN 1998-1, (CEN, 2004c) establishes that the formation of soft storeys, brittle failure modes and premature activation of the plastic hinges for low seismic actions must be prevented to avoid a collapse of the structure.

These requirements may be satisfied providing a regular building in plan and elevation, as well as applying the capacity design approach, where besides including the strong column-weak beams principle, establishes specific rules for the dissipative and non-dissipative structural elements.

For the dissipative elements such as beams, enough rotation capacity should be guarantee. Thus, for the approach b), steel cross-sections Class 2 for DLH and Class 1 for DCH must be provided. Moreover, the compression and shear forces are limited to avoid affecting the rotation capacity of the structural element as establishes the clause 6.6.2.

$$\frac{M_{Ed}}{M_{pl,Rd}} \leq 1 \tag{2.2}$$

$$\frac{N_{Ed}}{N_{pl,Rd}} \leq 0.15 \tag{2.3}$$

$$\frac{V_{Ed}}{V_{pl,Rd}} \leq 0.5 \tag{2.4}$$

where

M_{Ed}, N_{Ed} and V_{Ed} are the design forces due to gravity loads in the seismic combination plus the seismic forces

$M_{pl,Rd}, N_{pl,Rd}$ and $V_{pl,Rd}$ are the resign resistances of the dissipative member

In the case of the columns, the criteria for verifying non-dissipative elements consist in applying overstrengh factors to the designing forces as shows the following equations.

$$M_{Ed} = M_{Ed,G} + 1.1\gamma_{ov}\Omega M_{Ed} \quad (2.5)$$

$$N_{Ed} = N_{Ed,G} + 1.1\gamma_{ov}\Omega N_{Ed} \quad (2.6)$$

$$V_{Ed} = V_{Ed,G} + 1.1\gamma_{ov}\Omega V_{Ed} \quad (2.7)$$

where

$M_{Ed,G}, N_{Ed,G}$ and $V_{Ed,G}$ are the forces applied the columns due to gravity loads in the seismic combination

M_{Ed}, N_{Ed} and V_{Ed} are the forces applied to the column due to seismic actions

γ_{ov} is the material overstrengh factor

Ω is the minimum value of $M_{Pl,rd}/M_{Ed}$ of all the dissipative beams, which is evaluated in each principal direction

The Ω factor is decisive to the design under seismic actions, since the use of oversized dissipative structural elements produces a considerably increase in the designing forces of the columns, being necessary to increase their cross-sections to satisfy the capacity design method.

2.1.3 Damage limitation criteria

The damage limitation requirements under frequent earthquakes should be verified to guarantee the structural cooperativeness under frequent earthquakes as well as to reduce the cost of repairing non-structural elements.

The requirement consists in limiting the interstorey-drift ratio (α) under the DLS, which depends on the non-structural elements placed in the building. The interstorey-drift ratio values are defined in the clause 4.4.3 of EN 1998-1 (CEN, 2004c);

- 0.5% if there are brittle non-structural elements attached to the structure.
- 0.75% if the non-structural elements attached to the structure are ductile.
- 1% if there are no non-structural elements attached to the structure.

Thus, the interstorey-drift ratio of each storey of the building should be determined from the seismic analysis under the seismic actions in the DLS using the following expression.

$$d_r \nu \leq \alpha h \quad (2.8)$$

where

d_r is the inter-storey drift, evaluated as the difference between the drift of the storey analysed and upper one

h is the storey height

ν is a displacement reduction factor depending on the importance class

α is the displacement inter-storey ratio defined previously

2.2 LINEAR AND NONLINEAR SEISMIC ANALYSIS

2.2.1 Seismic action

The seismic action due to an earthquake produces a motion in the base of the structure. In consequence, a response in terms of restoring forces related to the stiffness, damping forces produced by the internal friction and the damage of the dissipative zones, and inertial forces due to the mass of the structure appear (Fig. 2.1).

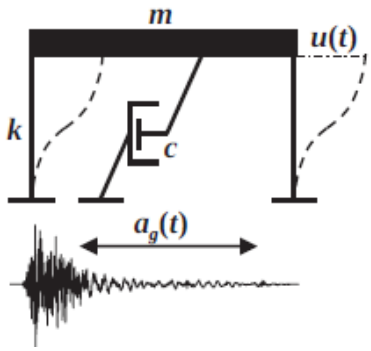

Fig. 2.1. Dynamic action applied to a SDOF; Landolfo et al. (2017)

The structural response under dynamic loading depends on the dynamic properties of the system, such as the fundamental period of vibration and the effective mass participation. For a single-degree-of-freedom system (SDOF) the structural response is computed in Eq. 2.9.

$$m\ddot{u} + c\dot{u} + ku = -m\ddot{u}_g \tag{2.9}$$

where

m is the mass of the system

c is the damping factor

k is the stiffness matrix

$\ddot{u}$ is the acceleration vector

$\dot{u}$ is the velocity vector

u is the displacement vector

Considering a system without damping and under free vibration ($\ddot{u}_g = 0$), which corresponds to a simple harmonic case, the Eq. 2.10 can be obtained.

$$m\ddot{u} + ku = 0 \tag{2.10}$$

The solution of the differential equation using the analytical approach is given in the Eq. 2.11.

$$u = A\cos\omega t + B\sin\omega t \tag{2.11}$$

where

A and B are factors which depends on the boundary conditions

ω is the circular frequency expressed in rad/sec expressed as;

$$\omega = \sqrt{\frac{k}{m}} \tag{2.12}$$

The natural period of vibration expressed in second can be obtained from the circular frequency of the structure (Eq. 2.13).

$$T = \frac{2\pi}{\omega} = 2\pi\sqrt{\frac{m}{k}} \tag{2.13}$$

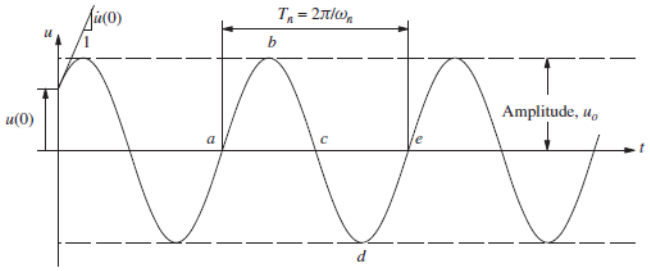

Fig. 2.2 Free vibration of a system without damping; Chopra, (2012)

On the other hand, more complex structures such as buildings composed by several storeys must modelled as multi-degree-systems-of-freedom (MDOF), since their motion cannot be described by a single displacement. There are present N fundamentals modes as shows Fig. 2.3.

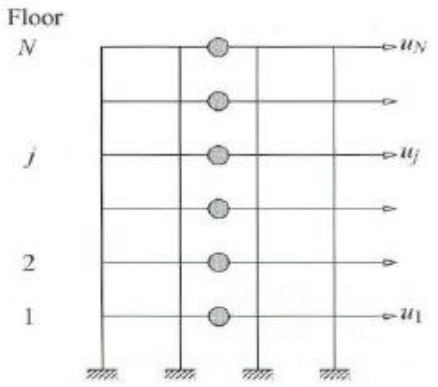

Fig. 2.3 Example of MDOF; Chopra (2005)

The equation that governs the dynamic behaviour is the same as Eq. 2.9.

$$[M]\ddot{u} + [C]\dot{u} + [K]u = -[M]\ddot{u}_g \tag{2.14}$$

where

$[M]$ is the mass matrix of the system

$[C]$ is the damping matrix of the structure

$[K]$ is the stiffness matrix of the structure

$\ddot{u}$ is the acceleration vector

$\dot{u}$ is the velocity vector

u is the displacement vector

In order to determine the general dynamical behaviour of a MDOF system, the Eq. 2.14 should be solved for each natural mode of vibration independently and posteriorly combine all the responses.

Each mode presents its natural mode of vibration (ϕ_n), natural frequency (ω_n), and its own damping ratio (ξ_n). Thus, each modal analysis can be computed as a SDOF using the equations shown previously (Chopra, 2005). In order to treat each mode as independent, is necessary to transform into modal coordinates the Eq. 2.13, replacing $u(t) = \phi\eta$.

$$[\phi]^T[M][\phi]\ddot{\eta(t)} + [\phi]^T[K][\phi]\eta(t) = 0 \tag{2.15}$$

Now, the harmonic solution of Eq. 2.11 may be applied to the Eq. 2.14 for the N_i modes of vibration. From the previous expression is possible to obtain two important dynamic properties, which are the participation factor (Γ_1) and the effective modal mass ($m_{eff,N}$) for each mode.

$$\Gamma_1 = \frac{[\phi]^T[M]\{1\}}{[\phi]^T[M][\phi]} = \frac{\bar{L}_i}{\hat{m}_{ii}} \tag{2.16}$$

$$m_{eff,i} = \frac{\bar{L^2}_i}{\hat{m}_{ii}} \tag{2.17}$$

where

$\hat{m}$ is the generalized mass matrix

The effective modal mass ($m_{eff,i}$) represents the amount of mass participating in one specific mode characterizing the contribution of each mode to the global dynamic response of the system. Then, the sum of the $\sum m_{eff,i}$ is equal to the total mass (M_{tot}).

2.2.2 Linear modal response spectrum analysis

The linear modal response spectrum analysis is the reference method to be applied to the structures under seismic actions according to the clause 4.3.3.3 of EN 1998-1,(CEN, 2004c).

In order to perform the linear modal response spectrum analysis, is necessary to decoupling the equation of motion as it was established in the Eq. 2.15. Subsequently, to determine the eigenvalues (natural frequencies) and the eigenvectors (vibrations modes) the following expressions should be applied.

$$[k] - \omega_n^2[m]\{\phi\}_n = 0 \tag{2.18}$$

Then, the structural response from the pseudo-acceleration spectrum, which depends on the period of vibration (T_i), can be determined for each for mode N_i, as shows the Fig. 2.4.

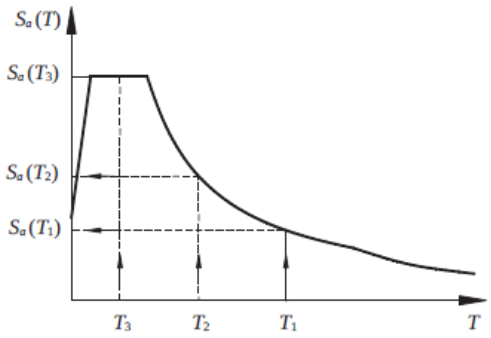

Fig. 2.4 Structural response for each mode N; Landolfo et al. (2017))

Finally, in order to combine of all the modes of vibration, it is usually used the complete quadratic approach (CQC) due to their flexibility in combining modal responses, especially when is not possible to guarantee the modes are independent of each other.

$$E_E = \sqrt{\sum_{i=1}^{n}\sum_{j=1}^{n}\rho_{ij}E_{E,i}E_{E,j}} \tag{2.19}$$

where

ρ_{ij} is the correlation factor, between 0 and 1

$E_{E,i}$ and $E_{E,j}$ are the modal responses peak values

E_E is the seismic action under consideration (force, displacement)

The correlation factor is obtained from;

$$\rho_{ij} = \frac{8\xi^2(1+\beta_{ij})\beta_{ij}^{\frac{3}{2}}}{(1-\beta_{ij}^2)+4\xi\beta_{ij}(1+\beta_{ij}^2)} \tag{2.20}$$

where

ξ is the damping ratio of the structure

β_{ij} is the modal frequencies ratio ω_i/ω_j

2.2.3 Nonlinear static analysis (Pushover). N2 Method

The pushover analysis is a static nonlinear analysis under conditions of constant gravity loads in the seismic combination while incremental horizontal loads are applied to the structure. The analysis allows accounting the nonlinear behaviour of the structural elements.

In order to carry out the nonlinear analysis, commonly the displacement control strategy is used, which consist in monitoring a control node located at the top of the building until reaches a specific displacement established prior to performing the analysis. In the meantime, lateral forces gradually increase.

Fig. 2.5 shows as example all the steps followed during the pushover analysis, whose objective is to determine the capacity curve, composed by the base shear force (V_b) and the displacement of the control node (Δ) of the structure.

In the step "0", only the gravitational loads are applied to the structure. Subsequently, the lateral forces are increased until reaching the yielding strength of the system defined by the formation of the first the plastic hinge. After that point, the stiffness of the structure decreases with the formation of each new one plastic hinge, until it reaches the plastic mechanism, in which the structure is no longer able to resist horizontal loads, reducing drastically its resistance.

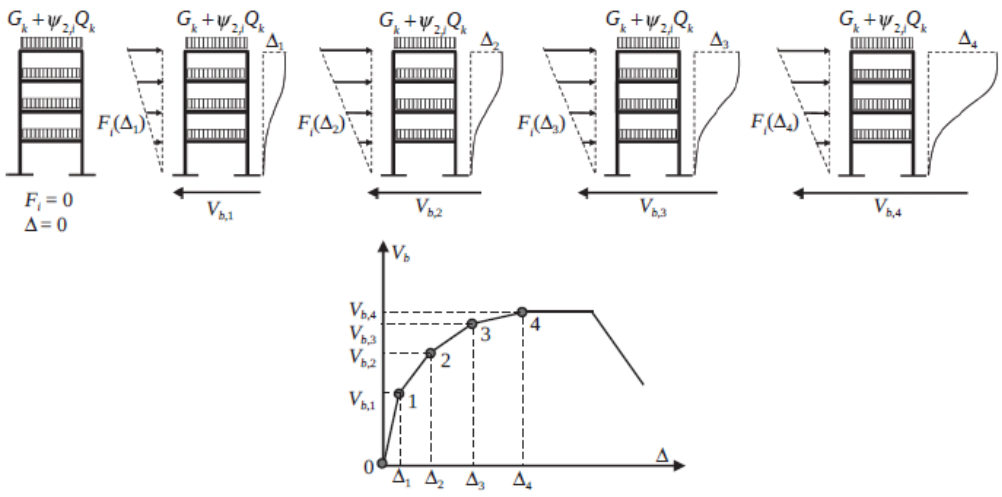

Fig. 2.5 Steps of the nonlinear static analysis principle; Landolfo et al. (2017)

For the case of the non-adaptive pushover, whose simplicity and low computational cost allows its easy implementation, the lateral forces shape is defined by the elastic stiffness of the structure. Hence, it remains constant during all the analysis process changing only in amplitude, without taking into account the variation of the stiffness produced in each storey after the formation of each new plastic hinge.

Due to this simplification, clause 4.3.3.4.2.2 of EN 1998-1 (CEN, 2004c), establishes that two vertical distributions of lateral loads, which are the boundaries of the actual behaviour should be applied (Fig.2.6);

- a "uniform" distribution, which is proportional to mass of each storey regardless of height.
- a "modal" pattern, where forces are related to the first mode of vibration weighted with the mass at each storey.

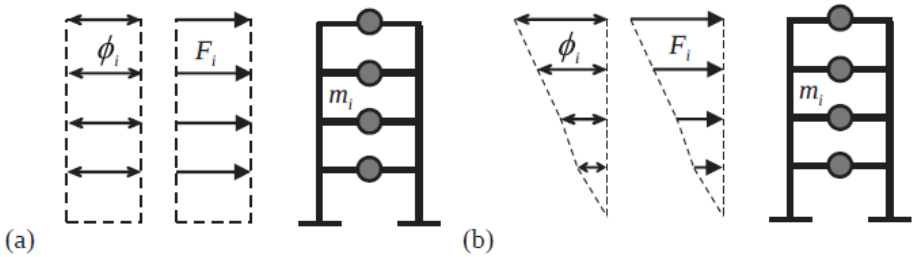

Fig. 2.6 Uniform and modal distribution for lateral forces; Landolfo et al. (2017)

The aim of applying the nonlinear static analysis according to clause 4.3.3.4.2 is:

- to verify the overstrengh ratio α_u/α_i
- to estimate the expected plastic mechanisms and the distribution damage
- as alternative to the design based on linear-elastic analysis which uses the behaviour factor q

Despite the fact that the overstrengh ratio and the plastic mechanism can be obtained through the capacity curve of the multi-degree-freedom-system (MDOF), pushover itself cannot be use directly for the design of the structure since it is not related to any seismic action.

The displacement-based design method, specifically the N2 method, proposed by Fajfar (2000) and posteriorly presented in the Annex B of EN 1998-1 (CEN, 2004c), presents a solution for this limitation.

The method establishes a target displacement derived from the elastic spectrum in the control node in terms of an equivalent single-degree-of-system (SDOF). Once the target displacement has been imposed in the analysis, the performance of the structure is obtained by comparing the displacement demand and the corresponding plastic capacity provided by the structure. The following steps should be followed.

First, the structure may be transformed into a SDOF system with the transformation factor (Γ), which is the same factor exposed previously in the seismic action, named as the participation factor.

$$\Gamma = \frac{\Phi^{t} M 1}{\Phi^{t} M \Phi} = \frac{\sum m_i \Phi_i}{\sum m_i \Phi_i^2} = \frac{m^*}{\sum m_i \Phi^2} \tag{2.21}$$

where

Φ is the displacement shape normalized (value in the top is set equal to 1), obtained from the fundamental mode of vibration

M is the diagonal matrix of mass

m^* is the mass of a equivalent SDOF system

Thus, the force (V_b^*) and displacement (d^*) of the SDOF are computed applying the transformation factor (Γ) in the capacity curve performed previously for the MDOF system.

$$V_b^* = \frac{V_b}{\Gamma} \tag{2.22}$$

$$d^* = \frac{d_n}{\Gamma} \tag{2.23}$$

Secondly, in order to evaluate the initial stiffness (k^*) and period (T^*) of the SDOF system, a bilinearization of the capacity curve should be applied (Fig. 2.7).

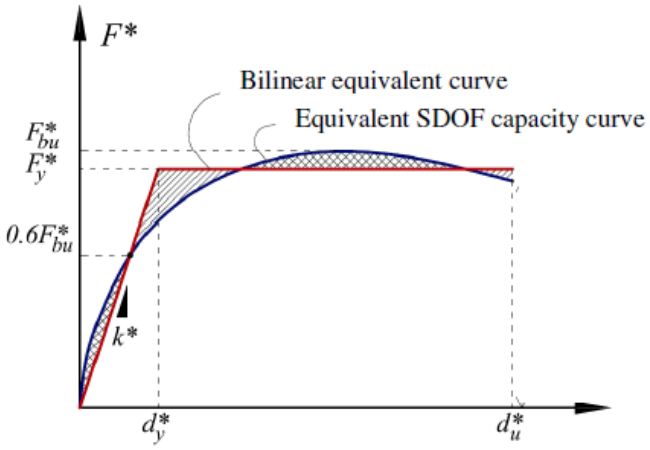

Fig. 2.7 Bilinearization of the SDOF capacity curve; Di Trapani and Cavalieri (2018)

The first part of the curve is a straight line drawn from the origin that intersects the point of the SDOF capacity curve characterized by $0.6F_{bu}^*$. To compute the resistance (F_y^*) of the system, the equivalence of areas for both curves should be applied.

$$k^* = \frac{F_y^*}{d_y^*} \tag{2.24}$$

$$T^* = 2\pi\sqrt{\frac{m^*}{k^*}} \tag{2.25}$$

Finally, the determination of the target displacement (d_t^*) for the SDOF system may be obtained from the displacement related to the period of vibration (T^*) considering unlimited elastic behaviour (d_{et}^*).

$$d_{et}^* = S_e(T^*)\left[\frac{T^*}{2\pi}\right]^2 \tag{2.26}$$

where

$S_e(T^*)$ is the elastic acceleration response spectrum at period T^*

The target displacement depends if the structure presents a short period range ($T^*<T_c$) or a medium and long period range ($T^* > T_c$).

For a short period, the following equations apply for an elastic response (Eq. 2.27) or nonlinear response (Eq. 2.28).

$$d_t^* = d_{et}^* \qquad \text{if} \quad \frac{F_y^*}{m^*} \geq S_e(T^*) \tag{2.27}$$

$$d_t^* = \frac{d_{et}^*}{q_u}(1 + (q_u - 1)\frac{T_C}{T^*} \geq d_{et}^* \qquad \text{if} \quad \frac{F_y^*}{m^*} \leq S_e(T^*) \tag{2.28}$$

$$q_u = \frac{S_e(T^*)m^*}{F_y^*} \tag{2.29}$$

For medium and long period range, only the following expression applies.

$$d_t^* = d_{et}^* \tag{2.30}$$

Following the previous steps, the target displacement (d_t^*) is obtained for the SDOF system. In order to be implemented in the MDOF, the transformation factor (Γ) should be applied again.

$$d_t = \Gamma d_t^* \tag{2.31}$$

The target displacement is utilized for perform the nonlinear static analysis to determine the local plastic deformations demands (θ_{demand}) in the structural elements and connections (Fig. 2.8).

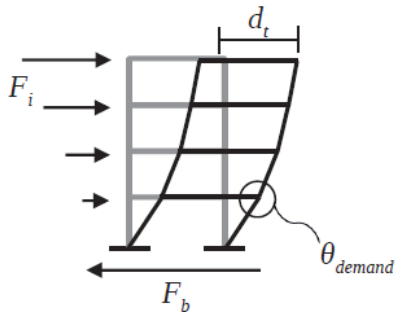

Fig. 2.8 Deformation demands imposing the target displacement; Landolfo et al. (2017)

The performance of the structure is assumed if the plastic rotation capacity ($\theta_{capacity}$) is sufficient to satisfy the demand.

$$\theta_{demand} \leq \theta_{capacity} \tag{2.32}$$

Despite the fact that nonlinear static analysis provides information about the strength and ductility of the structure as well as exposes possible weaknesses of the structure as opposite to the linear methods, presents several limitations.

A restrictive assumption is imposed, a time-independent displacement shape, meaning the structural must be regular to transform the MDOF system to a SDOF system, according to Fajfar (2000). Furthermore, assuming a non-adaptive analysis where the distribution of forces do not change depending on the resultant stiffness produced by the formation of plastic hinges is an approximation.

2.2.4 Nonlinear modelling of the building

Before the application of the pushover analysis, a non-linear modelling of the structural elements should be applied. Since EN 1998-1, (CEN, 2005c) does not specify exhaustive information about this topic for steel buildings, assumptions of FEMA 356 (ASCE, (2000)) has been considered.

In particular, the finite element model applied is the lumped plasticity, whose nonlinear behaviour is concentrated at both ends of the length of the structural element.

The force-deformation relationship depends on the brittle and ductile behaviour. For brittle elements, a force-controlled behaviour is characterized by an elastic range followed by a loss of strength, after reaching the peak.

For steel ductile elements, it is considered the strain hardening and strength-degradation with the residual strength capacity (Fig. 2.9).

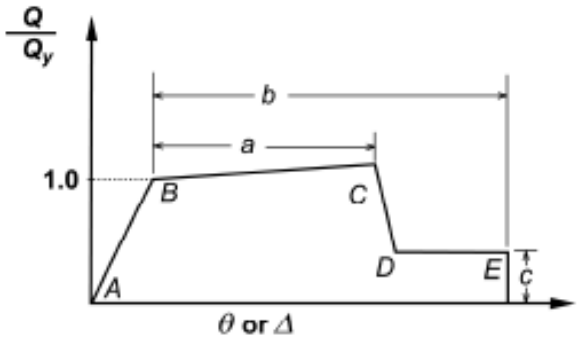

Fig. 2.9 Generalized Force-Deformation for steel elements; FEMA 356 (ASCE, 2000)

The point A corresponds to the unload condition and point B with the yield strength. Once the yield strength has been reached, the region BC of the plastic domain is considered, whose slope depends on the material, usually been a 10% of the elastic stiffness. Point C corresponds to the point of peak-strength prior to failure. Then, branch CD represents the loss of strength due to the failure and branch DE, is the residual strength for the case of ductile elements.

Subsequently, an acceptance criterion is defined for the acceptable damage associated to the three seismic limit states located in the plastic field (Branch BC) established by the Table 5-5 of FEMA 356 (ASCE, 2000), shows the Fig. 2.10.

- The Immediate Occupancy (IO) state, corresponding to the Damage Limitation (DL),
- Life safety (LS) state, which stands for significant damage (SD)
- Collapse prevention (CP) state, related to the near to collapse (NC).

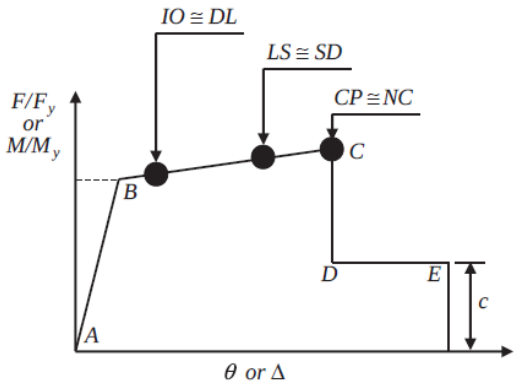

Fig. 2.10 Relevant acceptance criteria in the plastic field; Landolfo et al. (2017)

That criterion depends on the rotation capacity (θ_y) of the structural elements. Table 2.3 shows the acceptance criteria for sections Class 1 according to the Table 5-5.

Table 2.3 Acceptable damage

Type	a	b	c	DL	SD	NC
Beam	$9\theta_y$	$11\theta_y$	$0.6M_p$	$1\theta_y$	$6\theta_y$	$8\theta_y$
Column	$9\theta_y$	$11\theta_y$	$0.6M_p$	$1\theta_y$	$6\theta_y$	$8\theta_y$

2.3 PREQUALIFIED JOINTS

2.3.1 Component approach

The design of joints may carry out using either elastic or plastic analysis. In the first approach, the Von Mises stress should not exceed the yielding strength of the connection. Nevertheless, to take advantage of significant ductility capacity of steel, the plastic approach is commonly use, which allows local stress redistributions.

Several considerations establish clause 2.5(1) of EN 1993-1-8, (CEN, 2005c) to use this second approach, advising of possible limitations such as the lack of ductility of the steel material or specific components (bolts, welds, reinforced concrete in tension). After considering the limitations, the clause stablishes the use of the static theorem of the limit analysis which is commonly applied to cross section under bending forces with the rectangular-stress pattern for Class 1 and 2.

The static theorem requires the determination of an admissible internal distribution of forces, such as a set of stresses in equilibrium with the external forces acting in the joint from global analysis. Subsequently, this redistribution should be statically admissible without violating the plastic resistance and ductility criteria at any point of the connection.

Thus, there may be a large number of statically and plastically admissible distributions, even though only the actual distribution satisfies all the requirements; equilibrium, plasticity and compatibility with the displacements. However, as long as sufficient deformation capacity is available at places where plasticity develops, the static theorem ensures the resistance of the joint associated to any statically and plastically distribution is lower than the actual one, being on the safe side.

From these assumptions, an analytical approach which is the component method, appears in order to characterize joints in terms of resistance, stiffness and ductility. Hence, the approach allows predicting the joint response from the knowledge of the geometrical and mechanical properties of the connection components (Jaspart and Weynand, 2016).

In fact, the component method is exposed in the Eurocodes as general procedure to analyse a variety of joints subjected to different load situations. For each component, its resistance and stiffness under compression, tension and shear forces should be evaluated as well as the consideration of possible interaction between components which may lead to a decrease in individual resistance.

The following steps should be followed to apply the component method.

1. identification of the active components of the joint to be analysed.
2. evaluation of the resistance and stiffness of each component individually.
3. assembly all the components together to obtain the global response.

Table 6.1 of EN 1993-8, (CEN, 2005c) defines all the possible components and how to evaluate its design resistance, stiffness and rotation capacity.

In order to assembly all the components of the joint, it is necessary to define how the external forces that act on the connection are distributed into internal forces acting in each component, satisfying the equilibrium as establishes the static theorem.

Even though the scope of application of the component method is quite large and versatile regarding the joint configurations and connections types, there are some configurations that are not covered. As example, the lack of knowledge for applying the component method is present in the tubular configurations and less traditional designs, as well as beam-to-column joints connected in the weak-axis for I or H members. In these particular cases, a FEM approach should be used.

2.3.2 Design procedure for the prequalified joints

This section stablishes the design procedure developed within the EqualJoints project (Landolfo et al. (2018)), for the different prequalified connections.

According to the design procedure exposed, joints are composed by three macro-components; the web panel, the connection and the beam (Fig. 2.11). Each component is designed individually according to three different design goals, where the resistance of the joint is related to the flexural strength of the beam.

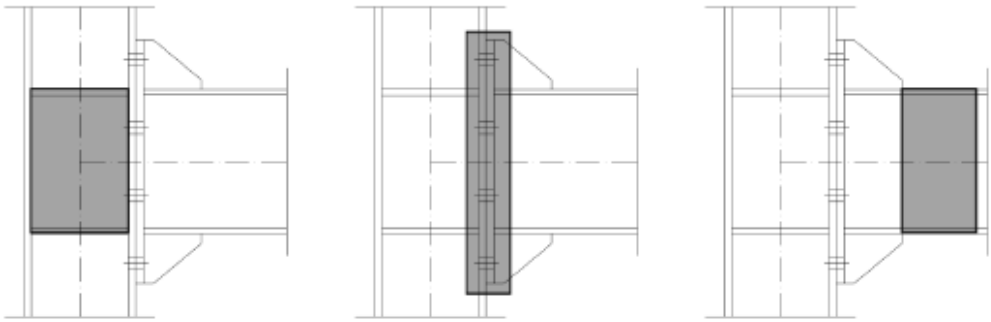

Fig. 2.11 Web panel a), b) connection and c) beam

- Full strength joints are designed to present more resistance than the connected elements to guarantee the plastic deformations occurs in the beams.
- Equal strength is characterized with the yielding of the beam and connection at the same time.
- Partial strength connections; where the plastic connections occur in the connection and the web panel.

The capacity design requirement is satisfy guaranteeing the following equation.

$$M_{wp,Rd} \geq M_{con,Rd} \geq M_{con,Ed} = \alpha(M_{B,Rd} + V_{B,Ed}S_h) \tag{2.33}$$

where

$M_{wp,Rd}$ is the flexural resistance of the corresponding to the strength of the column web panel

$M_{con,Rd}$ is the flexural strength of the connection

$M_{con,Ed}$ is the design bending moment at the column face

α is a factor which depends on the performance level

S_h is the distance between the column face and the tip of the stiffener (rib or haunch)

For the case of the full-strength joints, α is equal to $\gamma_{sh}\gamma_{ov}$; where γ_{ov} is the overstrengh factor and γ_{sh} is the strain hardening factor related to the ratio between the yielding and plastic strength of the connected beam.

For equal strength connections, α should be equal to 1, while for partial-strength connections should be equal to 0.6-0.8 to avoid several damages in the beam.

$V_{B,Ed}$ is the shear force corresponding to the occurring of the plastic hinge in the connected beam;

$$V_{B,Ed} = V_{B,Ed,M} + V_{B,Ed,G} \tag{2.34}$$

where

$V_{B,Ed,G}$ is the contribution of the gravity loads in the seismic combination

$V_{B,Ed,M}$ is the shear force due to the formation of plastic hinges at beam-ends

$$V_{B,Ed,M} = \frac{2M_{con,Ed}}{L_h} \tag{2.35}$$

where

L_h is the approximate distance between plastic hinges

Concerning the overstrengh factors, several authors considerer that factor 1.1 may be not conservative leading to an unsafe design. The solution purposed is to use the hardening overstrengh factor (γ_{sh}) provided by the AISC 358-16**,** instead of the value 1.1.

$$\gamma_{sh} = \frac{f_y + f_u}{2f_y} \leq 1.2 \tag{2.36}$$

where

f_y is the yield strength of the steel element

f_u is the ultimate strength of the steel element

Moreover, a classification is also made for the web panel component;

- Strong web panel. The plastic demand is concentrated in the connection or in the beam.
- Balance web panel. The plastic demand is balance between the connection and the column web panel
- Weak web panel. All the plastic demand is concentrated in the column web panel (partial strength joint) or in the web panel and in the beam

The design assumption for columns web panel zone is expressed in the following equation.

$$V_{wp,Ed} = \frac{M_{con,Ed}}{Z_{wp}} - V_c \tag{2.37}$$

where

$V_{wp,Ed}$ is the design shear force for the column web panel

Z_{wp} is the internal lever arm, being equal to $Z_{wp} = (d_p + \xi b - 0.5t_{f,b})$ for haunched joints

V_c is the sear force in the column

The shear strength of the web panel ($V_{wp,Rd}$) given by the following expression.

$$V_{wp,Rd} = V_{wc,Rd} + V_{wp,add,Rd} = \frac{0.9 f_{y,wc} A_{vc}}{\sqrt{3}\gamma_{m0}} + \frac{4M_{pl,fc,Rd}}{d_s} \tag{2.38}$$

where

$V_{wc,Rd}$ is the plastic shear strength of the unstiffened column web and $V_{wp,add,Rd}$ are the contribution of the stiffeners

A maximum contribution of the 30% of the plastic rotation capacity by the web panel is accepted. However, several studies shown that allowing plastic deformations in the web panel reduces the plastic rotation demand in the connected beam and the plastic shear distortion may lead to brittle failures due to excessive strain demands to the welds. Therefore, the reparability capacity of the column panel after an earthquake may be compromised (Landolfo et al. (2017)).

Thus, it is recommended to verify the shear strength of the web panel without taking into account the contribution of the column stiffeners to avoid plastic deformations. If higher strength is required, additional plates welded to column web should be placed.

2.3.3 Specific assumption for prequalified haunched joints

The specific assumptions of the haunched joints provided by the EqualJoints project (Landolfo et al. (2018)) have been considered in order to design the prequalified haunched joints.

Haunched extended end-plate beam-to-columns joints are intended to provide a full-strength rigid connection, using a strong or balance column web panel. They are composed by an extended end-plate, hight strength bolts and a haunch plate located at the lower beam flange at an angle between 30º and 45º. Transverse stiffeners in the web column and web beam are mandatory to provide enough rigidity. Moreover, continuity plates may be placed in the column panel to increase its strength.

Single-side and double-side configurations which can be used in the major-axis of the column, only in perpendicular and non-slope connections are shown in Fig. 2.12.

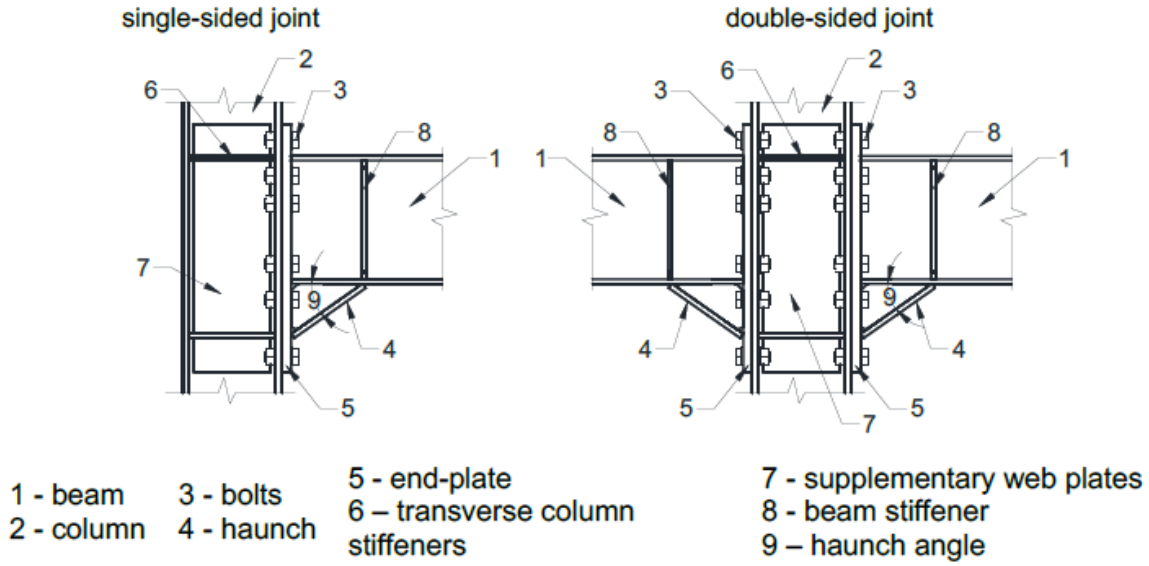

Fig. 2.12 Prequalified haunched joints; Landolfo et al. (2018)

The haunched extended end-plate beam-to column connection is prequalified to be used in:

- Moment Resisting Frames systems (MRFs)
- Dual Concentrically Braced Frames systems (CBFs)
- Dual Eccentrically Braced Frames systems (EBFs)

Despite the fact that the design procedure of the joints is based in the component method implemented in the Eurocode 3, to determine the flexural and shear resistance as well as the stiffness, important design considerations have been established by the guidelines of the EqualJoints project.

Different numerical simulations carried out concluded that the centre of compression of the connection is shifted up by 50% of the haunched depth ($A_c = 0.5h_h$) under negative moments. This is an important assumption when compared to the Eurocode, that stablishes the centre of compression is located at the bottom part of the haunch overestimating the bending capacity.

Furthermore, bolt-rows located near to the centre of compression develop negligible tension forces due to the flexibility of the end-plate and the limit ductility of the bolt-rows at the tension

flange. For this reason, only the rows above the mid depth of the beam-cross section (without haunch) are active under negative moments (Fig. 2.13 a)).

On the other hand, it is assumed the centre of compression is located at the middle part of the upper flange of the beam, activating the bolt-rows located beyond the mid-depth of the beam cross-section (including the haunch) for positive bending moments (Fig. 2.13 b)).

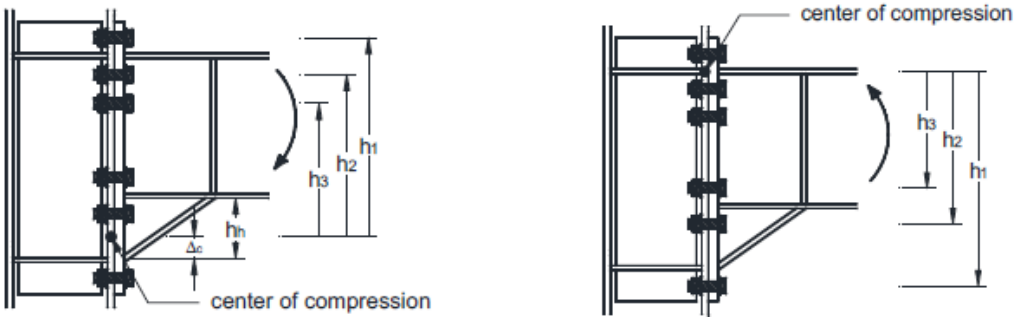

Fig. 2.13 Assumption for negative a) and positive bending moments b) applied to the haunched connections; Landolfo et al. (2018)

In order to highlight the assumptions provided by EqualJoints project, the comparison between the analytical procedure of the standard component method (EC3), the modified one (EC3-M) as well as the laboratory test under negative and positive moments are shown in Fig. 2.14.

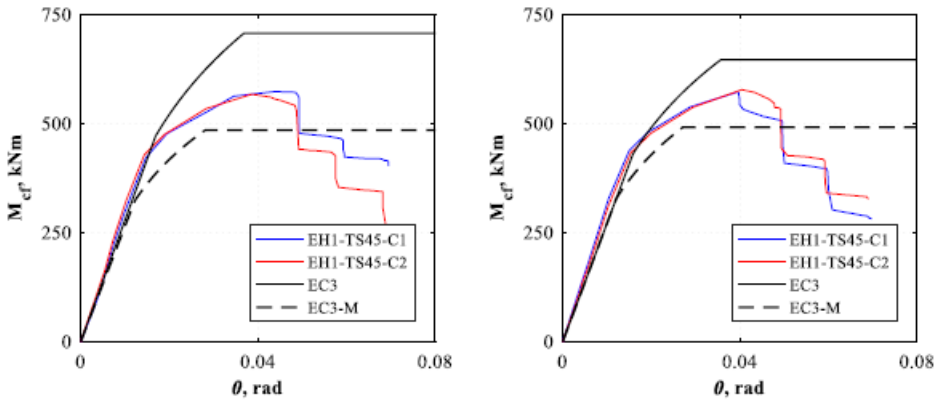

Fig. 2.14 M-Ø diagrams comparing both analytical approaches and laboratory test; EqualJoints project (Landolfo *et al.* (2018)).

As it was mentioned, the unmodified component method (EC3) overestimates the resistance of the joint owing to not considering the beam strength at the end of the haunch, while the modified approach (EC3-M) is a good estimation located in the safety side.

Moreover, the initial stiffness proposed by EN 1993-1-8 presents a good agreement in both models with the experimental results. However, for the nonlinear filed, located between $2/3M_{jrd}$ and M_{jrd}, the analytical model does not present a good estimation for full-strength joints.

The performance parameters of the joints, such as the hysteric behaviour under cyclic loading, stiffness and strength degradation were also studied in the case of the prequalified haunched joints.

They were tested under cyclic loads obtaining the envelope by connecting the points of peak moments for each cycle of loading, while beyond the maximum moment points of largest moment at a given deformation were used, determining the ultimate deformation θ_u when drop of moment of 0.8 times the maximum one occurs (Fig. 2.15).

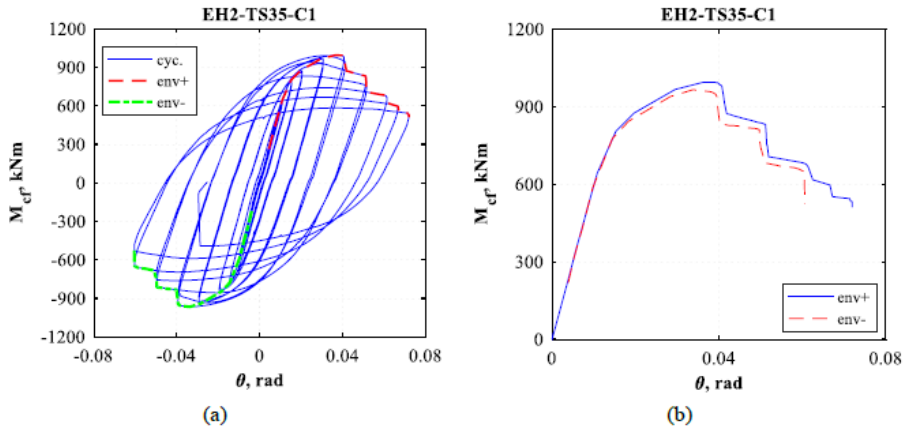

Fig. 2.15 Cyclic loading diagram a) and envelope of largest moments b); EqualJoints (Landolfo et al. (2018)).

The conclusions reached for the haunched joints with respect its behaviour under cyclical loads are they present a stable hysteric response with plastic deformations concentrated in the beam next to the haunch, in addition, the failure mode was characterized by gradual strength deration due to the local buckling of the beam.

After the study of several types of different of haunched joints, it was established the ultimate inter-storey drift (θ_u) is generally larger than 0.04 rad, producing a maximum drop of 20% in the flexural strength. Hence, it is concluded that the prequalified haunched joints designed using the assumptions of the EqualJoints project can be placed in seismic zones. However, for larger beam sizes such us IPE 600 and haunches forming an angle of 45º, the ultimate inter-storey drift decreased to a range between 0.03 and 0.04 rad.

CHAPTER 3: DESIGN OF THE BUILDING

3.1 DESCRIPTION OF THE STRUCTURE

The designed structure is a steel-frame multi-storey office building placed in L'Aquila (Italy), where there is a significant seismic hazard.

For the seismic design of buildings, structural simplicity, uniformity, bi-directional resistance and stiffness, torsional resistance, diaphragmatic behaviour at each storey level and an adequate foundation in the first stages of the phase design should be aimed, according to clauses 4.2.1 and 4.2.2 of EN 1998-1 CEN(2004).

In fact, structures are divided in primary and secondary elements. The first contributes to the resistance and stiffness of the building against the horizontal actions. Therefore, they must satisfy all the requirements of the capacity design, while secondary elements are designed to resist only gravitational loads.

Since there are no bracings or infills, the structure is classified as a moment resisting frame system (MRFs), where the horizontal actions due to seismic load are mainly resisted by bending. In fact, this typology is the most dissipative and flexible for steel buildings, being useful in zones where the seismic loads are quite significant.

Hence, primary elements are designed with continuous joints in order to withstand the horizontal loads in a flexural manner. The secondary elements correspond to the secondary beams which are designed to support the composite slab. Pinned joints have been used to connect the secondary beams with the girders.

Furthermore, it has to be highlighted that most of the mass of the building is concentrated in the floors, where significant inertial forces appear during the earthquake. To distribute the inertial forces to the vertical members, which provides an overall structural stability, the floors develop an important role due to its rigid diaphragm behaviour. This behaviour is an indispensable requirement for seismic design of buildings (Landolfo et al. (2017)).

Despite the fact that the MRF system is one of the best choices for important seismic areas, its flexibility prevents to be used for tall buildings because of the lateral displacements produced, since they may not satisfy the serviceability limit states. This issue shall be discussed during the current chapter.

In an initial stage, a pre-design with simplified models was carried out. However, structural stability issues appeared, consequently, the structural elements obtained by hand calculations were not useful and a significant increase in the size of cross-sections of the structural elements was necessary.

Nowadays, with the computational tools is much more efficient to generate in a first stage of the design more sophisticated models representing in a better way the reality, increasing the speed of the design and reducing the uncertainness (Silva et al. (2013)).

3.2 GEOMETRY

The building is form by six storeys with rectangular plan shape. The area of each floor is equal to 744 square meters, of which 31 meters are long and 24 meters wide. The storey height is 3.5 meters as opposed to the ground floor, which is 4 meters. Thus, the total height of the building is 21.5 meters. Moreover, the roof has been designed in the same geometric shape as the other storeys, being accessible by occupancy.

The beams and columns of the structure are composed by hot-rolled I and H profiles. As it shall be shown in section 3.5.1, the composite slab is connected to the secondary beams by ductile-headed shear studs welded to the upper beam flange.

Normally, countries subject to low seismic actions commonly use either solid or waffle slabs in two ways minimizing the number of beams to be placed in the buildings. However, for the seismic design should be use one-way floor slabs and dissipative beams placed in principal directions in order to resist the horizontal forces.

At the ground floor, fixed connections are mandatory to be placed at the bottom of the columns to guarantee sufficient stability under horizontal forces since there is no bracing system in the building.

The Figure 3.1 shows a general view in 3D of the structure, while the figure 3.2 a) and b) shows respectively the views in the X and Y directions.

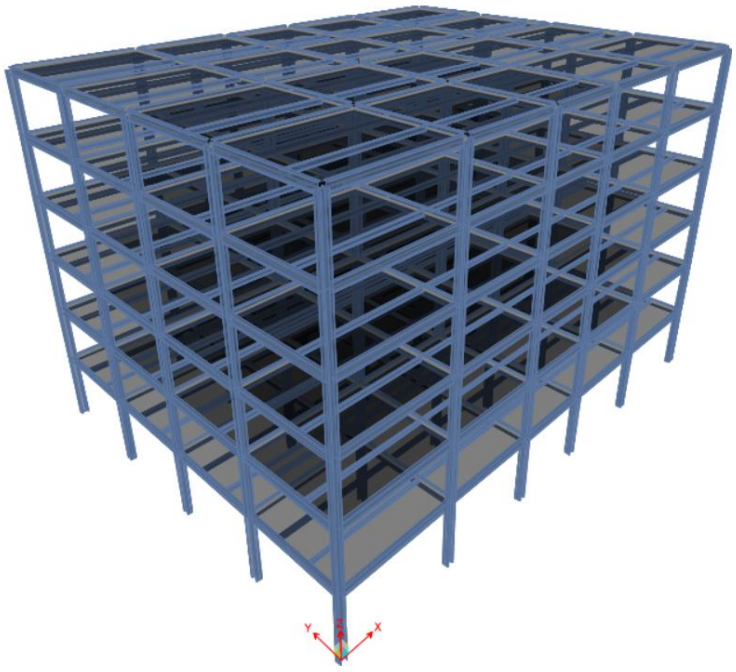

Fig.3.1 3D view of the building

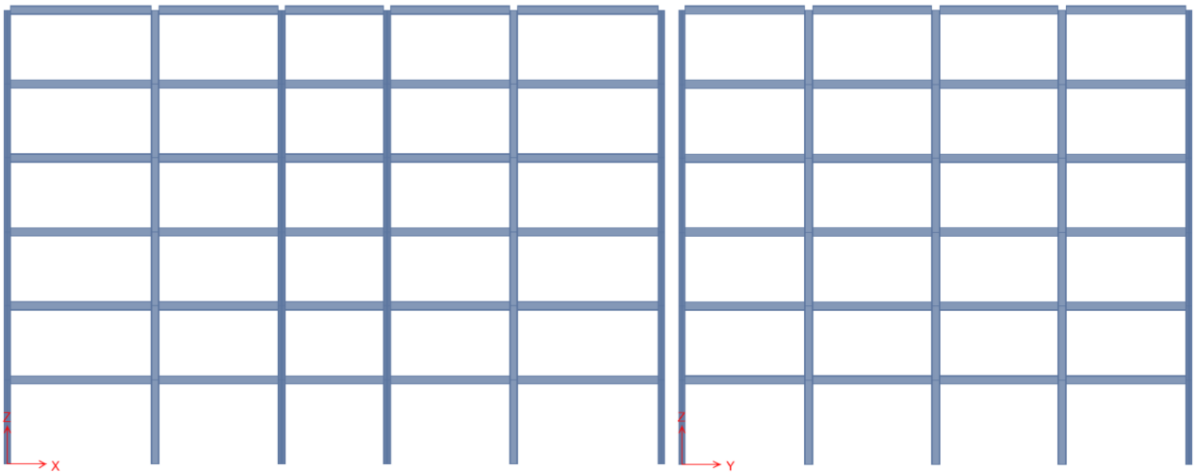

Fig. 3.2. Plan in X and Y directions a), b)

In the geometry plan of the building, along the length there are five bays of 7, 6 and 5 meters while in the width, there are four equal bays of 6 meters length (Fig. 3.3). Moreover, the composite slab is supported by a system of principal beams (filled in black) connected with the supports with continuous joints and secondary beams (filled in grey), presenting a separation of 2 meters.

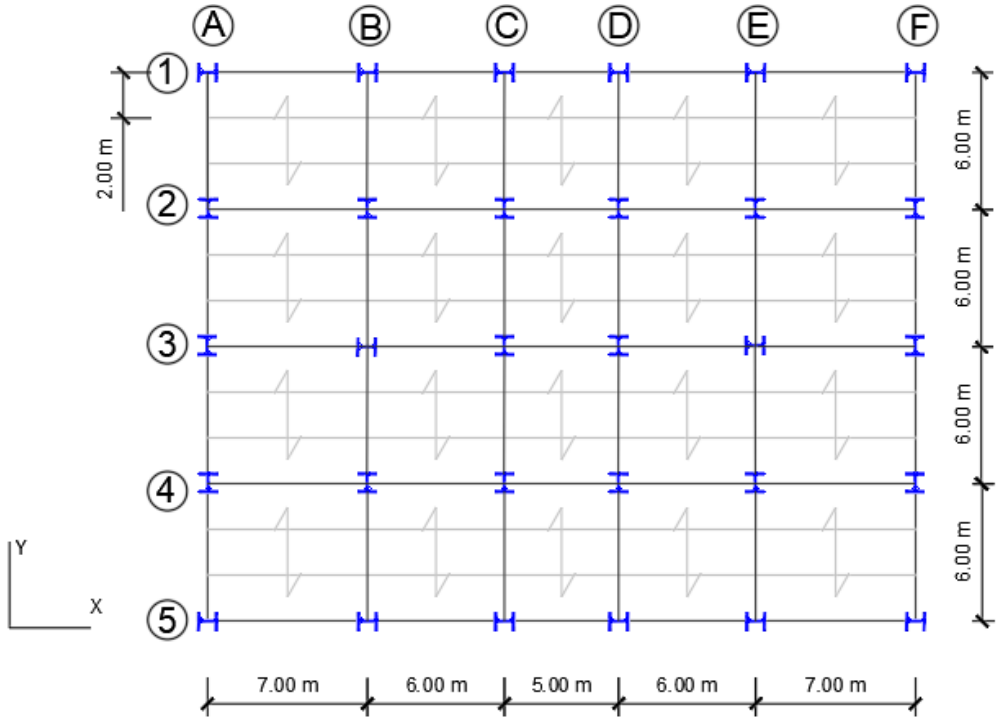

Fig. 3.3 Plan shape view of the building

The use of continuous joints for all the frames of the structure have been necessary in order to provide the building with sufficient lateral stiffness to avoid excessive lateral displacements and instabilities due to its height.

Moreover, the aim of the orientation of the columns is to equilibrate the lateral stiffness in both principal directions. For this reason, 14 columns have been placed in the X direction and 16 in the Y direction.

All the structural elements, which are the same for the 6-storeys in order to provide a constant strength along the elevation, are summarized in the Table 3.1.

Table 3.1 Definition of the structural elements

Structural Elements	Type	Seismic Behaviour	Cross-Section	Steel Grade
A1-A5, C1-C5, D1-D5, F1-F5, A1-F1, A2-F2, A3-F3, A4-F4, A5-F5	Primary Element	Dissipative	IPE400	S235
B1-B5, E1-E5	Primary Element	Dissipative	IPE450	S235
Secondary beams of 6 and 5 meters span	Secondary Element	-	IPE220	S275
Secondary beams 7 meters span	Secondary Element	-	IPE240	S275
Columns	Primary Element	Non-Dissipative	HEM360	S275

Two different steel grades for the structural elements have been used in order to develop the dual-steel concept for buildings in seismic areas, approach which leads to more reliable and cost efficient structures (Landolfo et al. (2017)).

Therefore, mild carbon steel has been chosen for dissipative elements to secure the formation of plastic hinges, while steel with higher yielding resistance has been used for non-dissipative elements.

3.3 STATIC ANALYSIS

3.3.1 Vertical Loads

Permanent structural and non-structural loads

For the permanent structural and non-structural loads, in absence of more specific studies about them, it has been considered the same assumptions of the guidelines for the EqualJoints project (Landolfo et al. (2018)).

The loads considered are:

- Composite Slab: HI-BOND A 75/760P with a total thickness of 130mm. The self-weight is equal to 2.03kN/m^2.
- Internal Partition walls: which according to EN 1991 CEN (2002), it can be assumed equal to 0.5kN/m^2.
- Sound proof isolation: with a thickness of 10mm and a weight per unit of 0.3kN/m^3.
- Floor screed: made with light concrete with a thickness of 70 mm and weight per unit volume equal to 10kN/m^3.

- Floor: Made of ceramic with a weight per unit volume equal to 10kN/m^3 and a thickness of 20mm.
- Thermal insulation: made of fiberglass of 100mm of thickness with a weight per unit volume equal to 0.1kN/m^3.
- Ceiling: made by plasterboards with a superficial load equal to 0.177kN/m^2.

The Table 3.2 shows a summary of the all loads permanent loads.

Table 3.2. Total Permanent Loads

Elements	$\Upsilon_{(kN/m3)}$	thickness(mm)	Q(kN/m^2)
Composite Slab	-	130	2.03
Internal Partition Loads	-	-	0.5
Sound Proof insulation	0.3	10	0.003
Flour Screed	10	50	0.5
Floor	10	20	0.2
Thermal Insulation	0.1	100	0.01
Ceiling	-	-	0.177
Total_G_k	-	-	3.42

Furthermore, in the exterior frames, the self-weight produced by the façade has been taking into account. The load to be considered depends on the material and thickness of the curtain walls. Without more information, it has been assumed 0.8kN/m^2 applied in one meter of width, corresponding to a linear load equal to 0.8kN/m.

Live Loads

According to the table 6.2 of EN 1991-1, CEN (2005), the live load to be considered in the structure depends on the specific use. Since the structure have been designed as an office building, category B is assumed, varying the live load between 2kN/m^2 and 3kN/m^2 (Fig. 3.4). In this case; 3kN/m^2 have been applied.

Categories of loaded areas	q_k [kN/m^2]	Q_k [kN]
Category A		
- Floors	1,5 to2,0	2,0 to 3,0
- Stairs	2,0 to4,0	2,0 to 4,0
- Balconies	2,5 to 4,0	2,0 to 3,0
Category B	2,0 to 3,0	1,5 to 4,5
Category C		
- C1	2,0 to 3,0	3,0 to 4,0
- C2	3,0 to 4,0	2,5 to 7,0 (4,0)
- C3	3,0 to 5,0	4,0 to 7,0
- C4	4,5 to 5,0	3,5 to 7,0
- C5	5,0 to 7,5	3,5 to 4,5
category D		
- D1	4,0 to 5,0	3,5 to 7,0 (4,0)
- D2	4,0 to 5,0	3,5 to 7,0

Fig. 3.4 Live loads according the use of the building; (CEN, 2002)

The roof has been designed to be accessible with occupancy. Hence, its category is equal to I according to the table 6.9 of EN 1991 CEN (2005), which means the same live load of the storeys has been applied on the roof.

Categories of loaded area	Specific Use
H	Roofs not accessible except for normal maintenance and repair.
I	Roofs accessible with occupancy according to categories A to G
K	Roofs accessible for special services, such as helicopter landing areas

Fig. 3.5 Categories for the roof; (CEN, 2002)

Taking into account the non-structural loads plus the live loads, the total value is 4.39kN/m^2, which is lower than the maximum load supported by the composite slab to satisfy the serviceability limit states.

Finally, load arrangements have been applied for the live loads, being placed at the most unfavourable part of the influence area of the actions effects considered, according to clause 6.2 of EN 1991-1, (CEN, 2002).

Snow Loads

The snow loads applied to the building have been obtained considering clause 3.4.1 of the national Italian normative, NTC (2018)**.**

$$q_s = q_{sk} u_i C_e C_t \tag{3.1}$$

where

q_{sk} is the load reference for snow

u_i is the shape factor of the roof

C_e is the exposition factor

C_t is the thermic factor.

L'Aquila is located at zone II, meaning the load reference for snow (q_{sk}) is equal to 1.00kN/m^2 for buildings placed in altitudes minor than 200 meters.

The shape factor of the roof (u_i) can be obtained from the table 3.4.II (Fig. 3.6), depending on the angle of the roof with the horizontal plane. In the building, the roof is flat, being u_i equal to 0.8.

Tab. 3.4.II – *Valori del coefficiente di forma*

Coefficiente di forma	$0° \le \alpha \le 30°$	$30° < \alpha < 60°$	$\alpha \ge 60°$
μ1	0,8	$0{,}8 \cdot \frac{(60-\alpha)}{30}$	0,0

Fig.3.6 Shape factor; NTC (2018)

Finally, the exposition factor (C_e) is equal to 1,0, because it has considered a normal topography. The same value is applied to the thermic factor (C_t), because no research for the isolating materials located at the roof has been carried out. Thus, the snow load (q_s) is equal to **0**.8kN/m^2 .

3.3.2 Wind Loads

The calculation of the wind loads has been performed with clause 3.3 of NTC (2018). In a first step, the basic mean wind velocity at 10 meters height has been calculated with Eq. 3.2.

$$V_b = V_{b,0} * c_a \tag{3.2}$$

where

$V_{b,0}$ is the basic mean wind velocity at sea level

C_a is the altitude coefficient

$$C_a = 1 \quad for \quad a_s \leq a_0 \tag{3.3}$$
$$C_a = 1 + K_s \left(\frac{a_s}{a_0} - 1\right) \quad for \quad a_s \leq a_0$$

being a_s the building altitude with the sea level reference. a_0 and K_s are parameters which are given in the Table 3.3.I.c which depends n the region on that is being analysed, in this case the Abruzzo region (Fig. 3.7).

Tab. 3.3.I -*Valori dei parametri* $v_{b,0}$, a_0, k_s

Zona	Descrizione	$v_{b,0}$ [m/s]	a_0 [m]	k_s
1	Valle d'Aosta, Piemonte, Lombardia, Trentino Alto Adige, Veneto, Friuli Venezia Giulia (con l'eccezione della provincia di Trieste)	25	1000	0,40
2	Emilia Romagna	25	750	0,45
3	Toscana, Marche, Umbria, Lazio, Abruzzo, Molise, Puglia, Campania, Basilicata, Calabria (esclusa la provincia di Reggio Calabria)	27	500	0,37
4	Sicilia e provincia di Reggio Calabria	28	500	0,36
5	Sardegna (zona a oriente della retta congiungente Capo Teulada con l'Isola di Maddalena)	28	750	0,40
6	Sardegna (zona a occidente della retta congiungente Capo Teulada con l'Isola di Maddalena)	28	500	0,36
7	Liguria	28	1000	0,54
8	Provincia di Trieste	30	1500	0,50
9	Isole (con l'eccezione di Sicilia e Sardegna) e mare aperto	31	500	0,32

Fig.3.7 Specific parameters for equation 3.2; NTC (2018)

Therefore, $V_{b,0}$ and a_0 are equal to 27m/s and 500m respectively. Since it has been assumed the building is situated at sea level, the coefficient c_a is equal to 1,0. The wind pressure to be applied is given by Eq. 3.3.

$$p = q_r c_e c_p c_d \tag{3.4}$$

where

q_r is the kinetic pressure

c_e is the external pressure coefficient

c_p is the exposition coefficient

c_d is the dynamic coefficient which it can be considered equal to one for regular buildings less than 80 meters of height

The kinetic pressure (q_r) is obtained considering the reference wind load (v_r) which is equal to the basic mean velocity (V_b) for a return period of 50 years. Then, it has to be accounted the air density (ρ) equal to 1.25 kg/m^3.

$$q_r = \frac{1}{2}\rho v_r^2 \tag{3.5}$$

In order to obtain the exposition coefficient (c_p) are applied the following expressions.

$$C_e(Z) = K_r^2 c_t \ln\frac{z}{z_0}[7 + c_t \ln\frac{z}{z_0}] \quad for\ Z > Z_0 \tag{3.6}$$

$$C_e(Z) = c_e(Z_{min}) \quad for\ Z > Z_0$$

where K_r, z_0 and Z_{min} are factors given in the table 3.3.II. The topographic factor (c_t) it may be assumed equal to one in this case.

The exposition category is III obtained considering the building is located at urban area, Category B of table 3.3.III**,** not being close to the sea. The figure x shows the variation of the exposition coefficient (c_p) with the height.

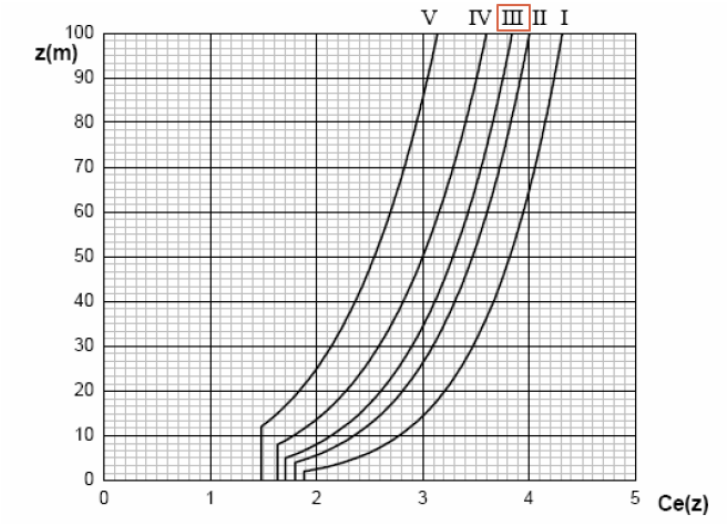

Fig. 3.8 Variation of the exposition coefficient regarding the height; NTC 2018

For the case of 21.5 m of height, c_p is equal to 2.66.

The last step consist in the calculation of the external coefficient pressure (c_e) with the method exposed in 3.3.8 of the Circolare NTC (2018)**,** which is the same explained in the clause 7.2 of EN1994-1-1, CEN (2004).

Two main directions for the wind loads applied to the building are considered, $\theta = 0º$ and $\theta = 90º$ corresponding to the X and Y direction respectively (Fig.3.9).

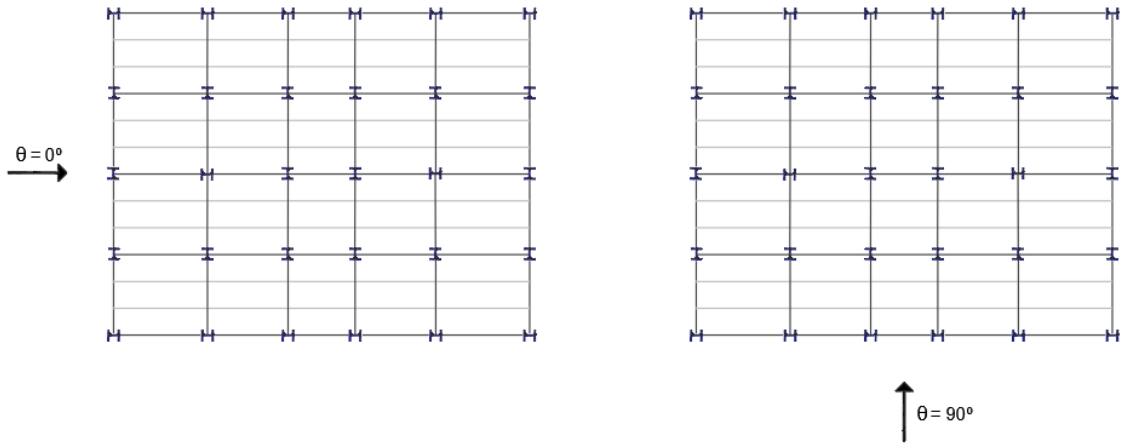

Fig. 3.9 Directions for the wind loads

The external pressure coefficients vary depending on the orientation of the wind. There are five different zones; A, B, C, D, E. Zones D and E corresponds to the windward and leeward zones (Fig. 3.10), while the zones A, C, D are the lateral ones (Fig 3.11).

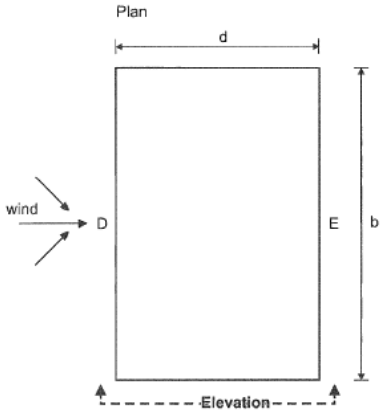

Fig. 3.10 Windward and leeward zones; (CEN, 2004a)

In both principal directions the condition $h \leq b$ is satisfied, therefore, only one shape of profile of velocity pressure is used.

The lateral zones are conditioned by the factor $e = \min(2h; b)$.

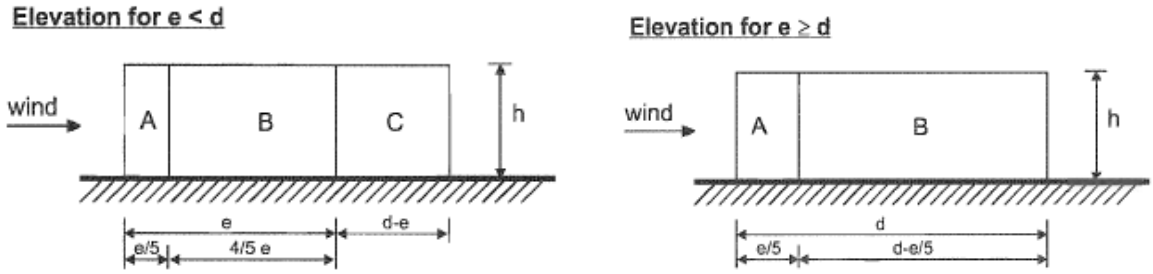

Fig. 3.11 Lateral wind zones; (CEN, 2004a)

Values for the external pressure coefficients for each wind zone provided by EN 1991-1-4 are considered (Fig. 3.12)

Zone	A		B		C		D		E	
h/d	$c_{pe,10}$	$c_{pe,1}$	$c_{pe,10}$	$c_{pe,1}$	$c_{pe,10}$	$c_{pe,1}$	$c_{pe,10}$	$c_{pe,1}$	$c_{pe,10}$	$c_{pe,1}$
5	-1,2	-1,4	-0,8	-1,1	-0,5		+0,8	+1,0	-0,7	
1	-1,2	-1,4	-0,8	-1,1	-0,5		+0,8	+1,0	-0,5	
≤ 0,25	-1,2	-1,4	-0,8	-1,1	-0,5		+0,7	+1,0	-0,3	

Fig. 3.12 External pressure coefficients for each wind zone; (CEN, 2004a)

In the tables 3.4 and 3.5 are summarize the length of the wind loads as well as the external coefficient factors to be considered for each wind direction. The negative sign corresponds to a suction zone while the positive one means a pression zone. Subsequently, they are shown graphically in the Fig. 3.12.

Table 3.4 External coefficient pressure factors for the X Direction (0º)

Dimensions		Zone	m	Cpe
b(m)	24	A	4.8	-1.2
h(m)	21.5	B	19.2	-0.8
d(m)	31	C	7	-0.5
e(m)	24	D	24	0.74
h/d	0.69	E	24	-0.38

Table 3.5 External coefficient pressure factors for the Y Direction (0º)

Dimensions		Zone	m	Cpe
b(m)	31	A	6.2	-1.2
h(m)	21.5	B	17.8	-0.8
d(m)	24	C	0	-0.5
e(m)	31	D	31	0.80
h/d	0.90	E	31	-0.50

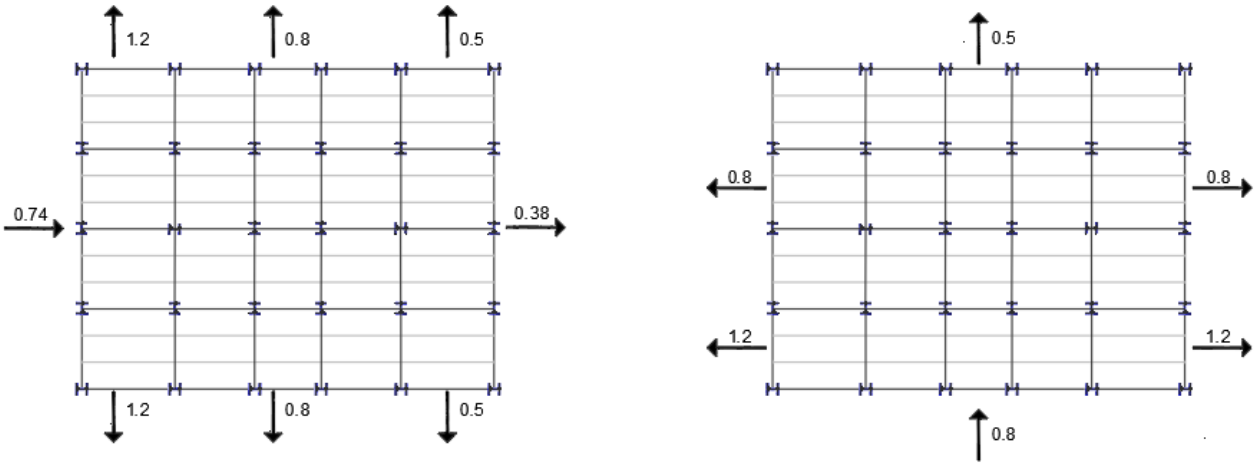

Fig.3.13 External Coefficients pressure in +X and +Y directions respectively.

Once the external coefficients have been calculated, it is possible to obtain the wind pressure values which are considered in the model of the building, applying the Eq. 3.4 as shows the Table 3.6 and Fig. 3.14 and 3.15 for the X and Y directions of the wind loads respectively.

Table 3.6 Wind pressure expressed in kN/m²

Zone	0º	90º
	q(kN/m²)	q(kN/m²)
A	-1.5	-1.5
B	-1	-1
C	-0.6	-0.6
D	0.9	1
E	-0.5	.0.6

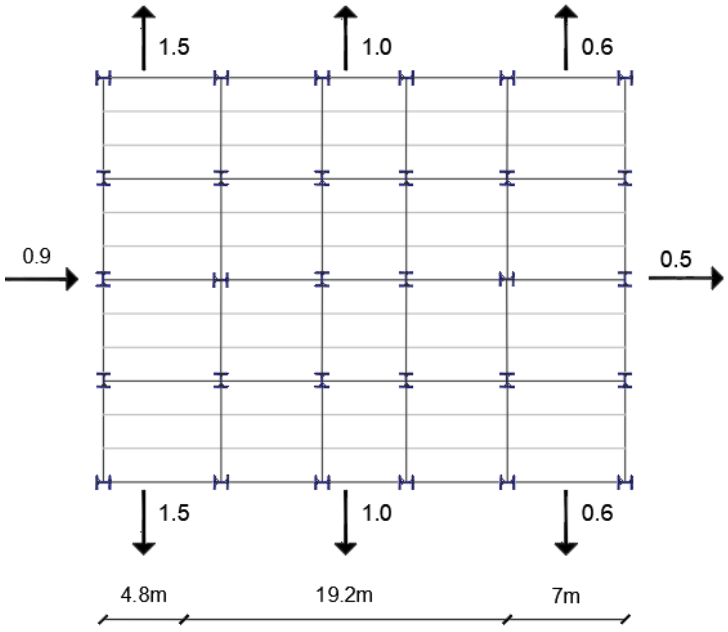

Fix. 3.14 Wind pressure (kN/m²) in X direction ($\theta = 0º$)

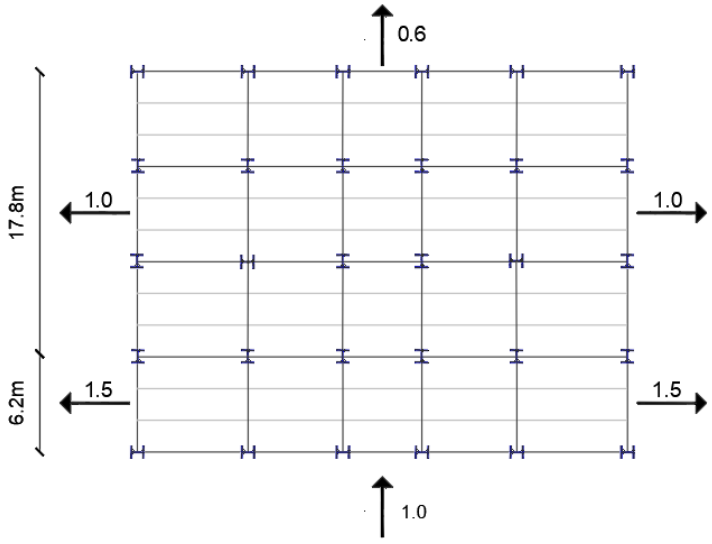

Fix. 3.15 Wind pressure (kN/m²) in Y direction ($\theta = 90º$)

Finally, the roof should also be analysed under the wind loads, especially in the suction zones. The simplify method presented in the clause C.3.3.8.1.2 (Ministerio delle Infraestructure e dei Transporti, 2018b) have been used to determine the external pressure coefficients and its area of application (Fig. 3.16) and Table 3.7.

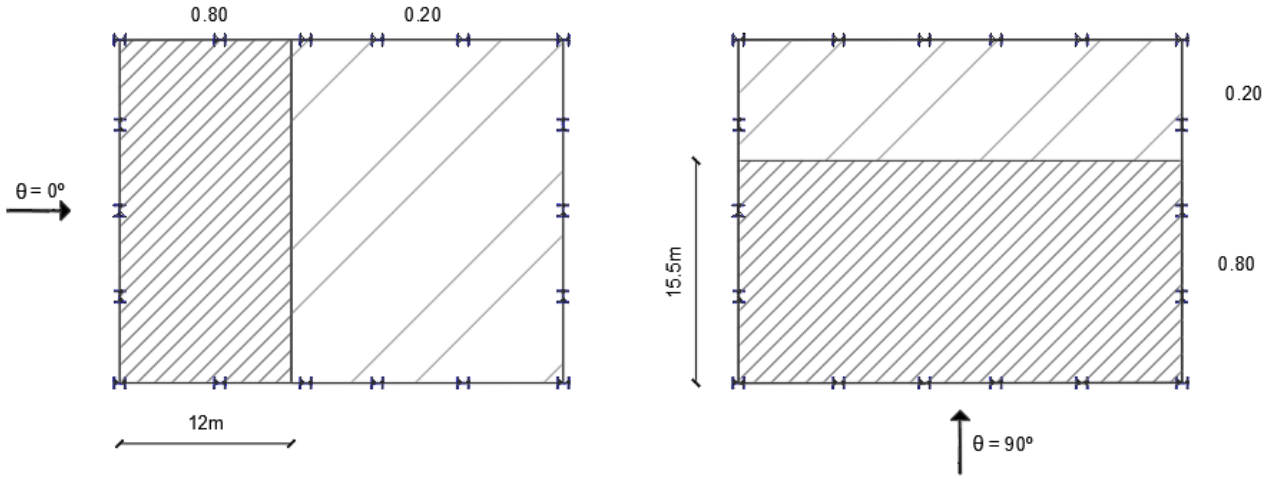

Fix. 3.16 Fig. External pressure coefficients in the roof in +X and +Y directions.

Table 3.7 Wind loads for the roof

Zone	Cpe	q(kN/m^2)
Pression	0.2	0.24
Suction	-0.8	-0.97

3.3.4 Non-seismic load combinations

The current section shows the load combinations for the ultimate limit states (ULS) and serviceability limit states (SLS) used to design the structural elements against vertical and wind loads for the building without considering the seismic actions.

In order to verify the state of equilibrium and strength of the structure (ULS), it is applied the Equation 6.10 of EN 1990, CEN (2005), which considers the persistent and transient design situations.

$$\sum_{j\geq 1} \gamma_G \, G_{k,j} + \gamma_{Qk,1} Q_{k,1} + \sum_{i\geq 1} \gamma_{Qj} \, \psi_{0,j} Q_{i,j} \tag{3.7}$$

where

γ_G is equal to 1.35 for unfavourable actions and 1.0 for favourable ones

$G_{k,j}$ are the permanent actions

$Q_{k,1}$ is the leading variable action

$\gamma_{Qk,1}$ is equal to 1.5 for unfavourable actions and zero for favourable ones

$Q_{i,1}$ is accompanying variable action

$\psi_{0,j}$ are the combination factors given in the Fig. 3.17

Table A1.1 - Recommended values of ψ factors for buildings

Action	ψ_0	ψ_1	ψ_2
Imposed loads in buildings, category (see EN 1991-1-1)			
Category A : domestic, residential areas	0,7	0,5	0,3
Category B : office areas	0,7	0,5	0,3
Category C : congregation areas	0,7	0,7	0,6
Category D : shopping areas	0,7	0,7	0,6
Category E : storage areas	1,0	0,9	0,8
Category F : traffic area, vehicle weight ≤ 30kN	0,7	0,7	0,6
Category G : traffic area, 30kN < vehicle weight ≤ 160kN	0,7	0,5	0,3
Category H : roofs	0	0	0
Snow loads on buildings (see EN 1991-1-3)*			
Finland, Iceland, Norway, Sweden	0,70	0,50	0,20
Remainder of CEN Member States, for sites located at altitude H > 1000 m a.s.l.	0,70	0,50	0,20
Remainder of CEN Member States, for sites located at altitude H ≤ 1000 m a.s.l.	0,50	0,20	0
Wind loads on buildings (see EN 1991-1-4)	0,6	0,2	0
Temperature (non-fire) in buildings (see EN 1991-1-5)	0,6	0,5	0
NOTE The ψ values may be set by the National annex. * For countries not mentioned below, see relevant local conditions.			

Fig. 3.17 Combination factor the load combinations; (CEN, 2005a)

On the other hand, for the design of the building in the serviceability limit states for the characteristic combination Table A2.6 of EN 1990-1, (CEN, 2005a) have been applied.

$$\sum_{j\geq 1} \gamma_G \, G_{k,j} + Q_{k,1} + \sum_{j\geq 1} \gamma_{Qj} \, \psi_{0,j} Q_{k,j} \tag{3.8}$$

In order to define the limits for the vertical deflections and horizontal displacements, the clause 4.2.4.2 of NTC (2018) have neem taking into account since the Eurocode encourages to use the national values. The total vertical deflections (δ_{max}) are limited to $L/250$ and the deflections due to variable loads are limited to $L/300$ (Fig 3.18). Moreover, the maximum interstorey-drift allowed is h/300 while the maximum horizontal displacement at the top of the building is $H/500$ (Fig. 3.19).

Tab. 4.2.XII - *Limiti di deformabilità per gli elementi di impalcato delle costruzioni ordinarie*

Elementi strutturali	Limiti superiori per gli spostamenti verticali	
	$\frac{\delta_{max}}{L}$	$\frac{\delta_2}{L}$
Coperture in generale	$\frac{1}{200}$	$\frac{1}{250}$
Coperture praticabili	$\frac{1}{250}$	$\frac{1}{300}$
Solai in generale	$\frac{1}{250}$	$\frac{1}{300}$
Solai o coperture che reggono intonaco o altro materiale di finitura fragile o tramezzi non flessibili	$\frac{1}{250}$	$\frac{1}{350}$
Solai che supportano colonne	$\frac{1}{400}$	$\frac{1}{500}$
Nei casi in cui lo spostamento può compromettere l'aspetto dell'edificio	$\frac{1}{250}$	
In caso di specifiche esigenze tecniche e/o funzionali tali limiti devono essere opportunamente ridotti.		

Fig. 3.18 Maximum deflections allowed in the characteristic combination for the SLS; (Ministerio delle Infraestructure e dei Transporti, 2018a)

Tab. 4.2.XIII - *Limiti di deformabilità per costruzioni ordinarie soggette ad azioni orizzontali*

Tipologia dell'edificio	Limiti superiori per gli spostamenti orizzontali	
	$\frac{\delta}{h}$	$\frac{\Delta}{H}$
Edifici industriali monopiano senza carro-ponte	$\frac{1}{150}$	/
Altri edifici monopiano	$\frac{1}{300}$	/
Edifici multipiano	$\frac{1}{300}$	$\frac{1}{500}$

In caso di specifiche esigenze tecniche e/o funzionali tali limiti devono essere opportunamente ridotti.

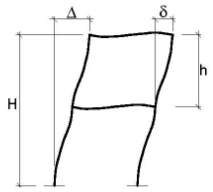

Fig. 3.19 Maximum horizontal displacements allowed in the characteristic combination for the SLS; (Ministerio delle Infraestructure e dei Transporti, 2018a)

In the following, Tables 3.8 and 3.9 shows all the load combinations considered for the ULS and SLS respectively taking into account the gravity loads as well as the wind loads applied the positive and negative orientations.

.

Table 3.8. Load combinations for the ULS

	Combinations	Dead Load	L1 Permanent Load	L2 Live Loads	L3 Roof Load	L4 Snow	L5 Wind_+X	L6 Wind_+Y	L7 Wind_-X	L8 Wind_-Y	Comments
ULS STR	ULS1	1	1				1.5				Favorable Dead Load+Wind
	ULS2	1	1					1.5			Favorable Dead Load+Wind
	ULS3	1	1						1.5		Favorable Dead Load+Wind
	ULS4	1	1							1.5	Favorable Dead Load+Wind
	ULS5	1.35	1.35	1.5							Induced Load
	ULS6	1.35	1.35		1.5						Roof
	ULS7	1.35	1.35			1.5					Snow
	ULS8	1.35	1.35				1.5				Wind
	ULS9	1.35	1.35					1.5			Wind
	ULS10	1.35	1.35						1.5		Wind
	ULS11	1.35	1.35							1.5	Wind
	ULS12	1.35	1.35	1.5	1.05						Induced Load+roof
	ULS13	1.35	1.35	1.5			0.9				Induced Load+Wind
	ULS14	1.35	1.35	1.5				0.9			Induced Load+Wind
	ULS15	1.35	1.35	1.5					0.9		Induced Load+Wind
	ULS16	1.35	1.35	1.5						0.9	Induced Load+Wind
	ULS17	1.35	1.35	1.5	1.05		0.9				Induced Load+roof+wind
	ULS18	1.35	1.35	1.5	1.05			0.9			Induced Load+roof+wind
	ULS19	1.35	1.35	1.5	1.05				0.9		Induced Load+roof+wind
	ULS20	1.35	1.35	1.5	1.05					0.9	Induced Load+roof+wind
	ULS21	1.35	1.35	1.5		0.75	0.9				Induced Load+Snow+wind
	ULS22	1.35	1.35	1.5		0.75		0.9			Induced Load+Snow+wind
	ULS23	1.35	1.35	1.5		0.75			0.9		Induced Load+Snow+wind
	ULS24	1.35	1.35	1.5		0.75				0.9	Induced Load+Snow+wind
	ULS25	1.35	1.35	1.05	1.5						Roof+Induced Load
	ULS26	1.35	1.35		1.5		0.9				Roof +Wind
	ULS27	1.35	1.35		1.5			0.9			Roof +Wind
	ULS28	1.35	1.35		1.5				0.9		Roof +Wind
	ULS29	1.35	1.35		1.5					0.9	Roof +Wind
	ULS30	1.35	1.35	1.05	1.5		0.9				Roof+Induced Load+Wind
	ULS31	1.35	1.35	1.05	1.5			0.9			Roof+Induced Load+Wind
	ULS32	1.35	1.35	1.05	1.5				0.9		Roof+Induced Load+Wind
	ULS33	1.35	1.35	1.05	1.5					0.9	Roof+Induced Load+Wind
	ULS34	1.35	1.35	1.05			1.5				Wind+Induced Load
	ULS35	1.35	1.35	1.05				1.5			Wind+Induced Load
	ULS36	1.35	1.35	1.05					1.5		Wind+Induced Load
	ULS37	1.35	1.35	1.05						1.5	Wind+Induced Load
	ULS38	1.35	1.35		1.05		1.5				Wind+Roof
	ULS39	1.35	1.35		1.05			1.5			Wind+Roof
	ULS40	1.35	1.35		1.05				1.5		Wind+Roof
	ULS41	1.35	1.35		1.05					1.5	Wind+Roof
	ULS42	1.35	1.35			0.75	1.5				Wind+Snow
	ULS43	1.35	1.35			0.75		1.5			Wind+Snow
	ULS44	1.35	1.35			0.75			1.5		Wind+Snow
	ULS45	1.35	1.35			0.75				1.5	Wind+Snow
	ULS46	1.35	1.35	1.05	1.05		1.5				Wind+induced Load+Roof
	ULS47	1.35	1.35	1.05	1.05			1.5			Wind+induced Load+Roof
	ULS48	1.35	1.35	1.05	1.05				1.5		Wind+induced Load+Roof
	ULS49	1.35	1.35	1.05	1.05					1.5	Wind+induced Load+Roof
	ULS50	1.35	1.35	1.05		0.75	1.5				Wind+Snow+Induced Load
	ULS51	1.35	1.35	1.05		0.75		1.5			Wind+Snow+Induced Load
	ULS52	1.35	1.35	1.05		0.75			1.5		Wind+Snow+Induced Load
	ULS53	1.35	1.35	1.05		0.75				1.5	Wind+Snow+Induced Load
	ULS54	1.35	1.35	1.05		1.5					Snow+Induced Load
	ULS55	1.35	1.35			1.5	0.9				Snow+Wind
	ULS56	1.35	1.35			1.5		0.9			Snow+Wind
	ULS57	1.35	1.35			1.5			0.9		Snow+Wind
	ULS58	1.35	1.35			1.5				0.9	Snow+Wind
	ULS59	1.35	1.35	1.05		1.5	0.9				Snow+Induced Load+Wind
	ULS60	1.35	1.35	1.05		1.5		0.9			Snow+Induced Load+Wind
	ULS61	1.35	1.35	1.05		1.5			0.9		Snow+Induced Load+Wind
	ULS62	1.35	1.35	1.05		1.5				0.9	Snow+Induced Load+Wind

Table 3.9. Load combinations for the SLS

	Combinations	Dead Load	L1 Permanent Load	L2 Live Loads	L3 Roof Load	L4 Snow	L5 Wind_+X	L6 Wind_+Y	L7 Wind_-X	L8 Wind_-Y	Comments
SLS Characteristic	SLS1	1	1				1				Favorable Dead Load+Wind
	SLS2	1	1					1			Favorable Dead Load+Wind
	SLS3	1	1						1		Favorable Dead Load+Wind
	SLS4	1	1							1	Favorable Dead Load+Wind
	SLS5	1	1	1							Induced Load
	SLS6	1	1		1						Roof
	SLS7	1	1			1					Snow
	SLS8	1	1				1				Wind
	SLS9	1	1					1			Wind
	SLS10	1	1						1		Wind
	SLS11	1	1							1	Wind
	SLS12	1	1	1	0.7						Induced Load+roof
	SLS13	1	1	1			0.6				Induced Load+Wind
	SLS14	1	1	1				0.6			Induced Load+Wind
	SLS15	1	1	1					0.6		Induced Load+Wind
	SLS16	1	1	1						0.6	Induced Load+Wind
	SLS17	1	1	1	0.7		0.6				Induced Load+roof+wind
	SLS18	1	1	1	0.7			0.6			Induced Load+roof+wind
	SLS19	1	1	1	0.7				0.6		Induced Load+roof+wind
	SLS20	1	1	1	0.7					0.6	Induced Load+roof+wind
	SLS21	1	1	1		0.5	0.6				Induced Load+Snow+wind
	SLS22	1	1	1		0.5		0.6			Induced Load+Snow+wind
	SLS23	1	1	1		0.5			0.6		Induced Load+Snow+wind
	SLS24	1	1	1		0.5				0.6	Induced Load+Snow+wind
	SLS25	1	1	0.7	1						Roof+Induced Load
	SLS26	1	1		1		0.6				Roof +Wind
	SLS27	1	1		1			0.6			Roof +Wind
	SLS28	1	1		1				0.6		Roof +Wind
	SLS29	1	1		1					0.6	Roof +Wind
	SLS30	1	1	0.7	1		0.6				Roof+Induced Load+Wind
	SLS31	1	1	0.7	1			0.6			Roof+Induced Load+Wind
	SLS32	1	1	0.7	1				0.6		Roof+Induced Load+Wind
	SLS33	1	1	0.7	1					0.6	Roof+Induced Load+Wind
	SLS34	1	1	0.7			1				Wind+Induced Load
	SLS35	1	1	0.7				1			Wind+Induced Load
	SLS36	1	1	0.7					1		Wind+Induced Load
	SLS37	1	1	0.7						1	Wind+Induced Load
	SLS38	1	1		0.7		1				Wind+Roof
	SLS39	1	1		0.7			1			Wind+Roof
	SLS40	1	1		0.7				1		Wind+Roof
	SLS41	1	1		0.7					1	Wind+Roof
	SLS42	1	1			0.5	1				Wind+Snow
	SLS43	1	1			0.5		1			Wind+Snow
	SLS44	1	1			0.5			1		Wind+Snow
	SLS45	1	1			0.5				1	Wind+Snow
	SLS46	1	1	0.7	0.7		1				Wind+induced Load+Roof
	SLS47	1	1	0.7	0.7			1			Wind+induced Load+Roof
	SLS48	1	1	0.7	0.7				1		Wind+induced Load+Roof
	SLS49	1	1	0.7	0.7					1	Wind+induced Load+Roof
	SLS50	1	1	0.7		0.5	1				Wind+Snow+Induced Load
	SLS51	1	1	0.7		0.5		1			Wind+Snow+Induced Load
	SLS52	1	1	0.7		0.5			1		Wind+Snow+Induced Load
	SLS53	1	1	0.7		0.5				1	Wind+Snow+Induced Load
	SLS54	1	1	0.7		1					Snow+Induced Load
	SLS55	1	1			1	0.6				Snow+Wind
	SLS56	1	1			1		0.6			Snow+Wind
	SLS57	1	1			1			0.6		Snow+Wind
	SLS58	1	1			1				0.6	Snow+Wind
	SLS59	1	1	0.7		1	0.6				Snow+Induced Load+Wind
	SLS60	1	1	0.7		1		0.6			Snow+Induced Load+Wind
	SLS61	1	1	0.7		1			0.6		Snow+Induced Load+Wind
	SLS62	1	1	0.7		1				0.6	Snow+Induced Load+Wind

3.3.5 Buckling analysis

Once the combinations have been established, clause 5.2 of EN 1993-1, CEN (2005) suggest the consideration of the second order effects, which increase the internal forces of the structural elements due to the deformation of the structure, if the following expressions are not satisfied.

$$\alpha_{cr} = \frac{F_{cr}}{F_{Ed}} \geq 10 \text{ for elastisc analysis} \qquad (3.9)$$

$$\alpha_{cr} = \frac{F_{cr}}{F_{Ed}} \geq 15 \text{ for plastic analysis}$$

where

α_{cr} is the factor by which the design loading would have to be increase to cause elastic instability in a global mode

F_{Ed} is the design loading structure

F_{cr} is the elastic critical buckling load for global instability mode based on initial elastic stiffnesses

For structures located in seismic regions, second-order effects under gravitational and wind loads in the predesign phase should be avoid since during the seismic action this behaviour shall be magnified, which may produce the non-verification of the damage limitation states or the instability of the building, Silva et al. (2013). For this reason, the building has been predesigned guaranteeing only first order effects appear under non-seismic actions.

In order to obtain α_{cr}, a buckling analysis of the whole structure has been performed with the software SAP2000 considering the most unfavourable loads of the table 3.8. Each load combination presents six modes of buckling, of which the first modes are translational in the principal directions. Table 3.10 shows the different buckling factors for the load cases taken into account.

Table 3.10 Buckling factors α_{cr} for the most unfavourable ULS combinations

Combination	Mode 1	Mode 2	Mode 3	Mode 4	Mode 5	Mode 6
ULS12	19.5	22.3	28.0	31.0	35.0	43.1
ULS17	19.7	22.5	28.4	31.4	35.4	43.2
ULS18	19.7	22.6	28.4	31.4	35.4	43.2
ULS30	21.5	24.6	30.9	33.8	38.1	47.2
ULS31	21.4	24.6	30.9	33.8	38.2	47.1
ULS46	22.3	25.5	32.3	35.5	39.9	48.8
ULS47	22.2	25.6	32.3	35.4	40.0	48.8

As it can be noticed, the minimum values of α_{cr} are above of the limits to consider in the Eq. 3.9. Thus, second order effects and imperfections have not been introduced in the structural model. As an example, figure 3.20 displays as example the two first sway modes of buckling in the X and Y direction, for the combination ULS12, which is the most unfavourable one.

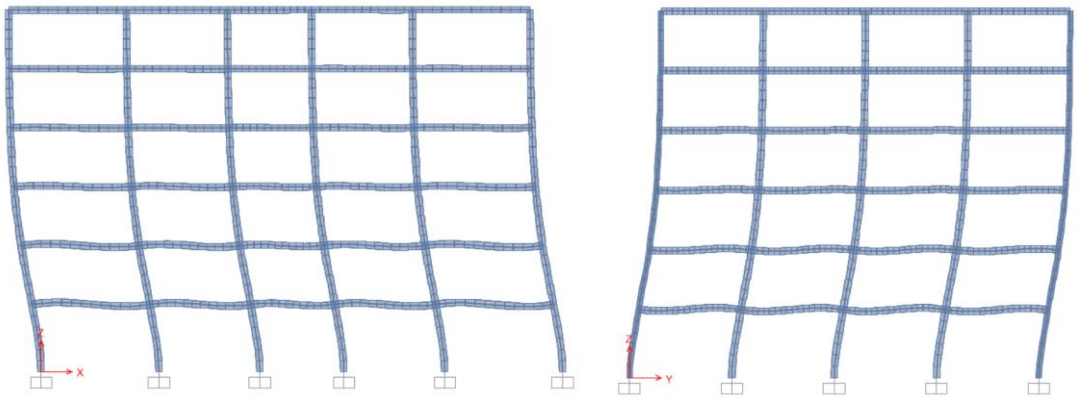

Figure 3.20 Sway modes of buckling in the X and Y directions for the load combinations ULS12

3.4 DESIGN OF THE STRUCTURAL ELEMENTS

3.4.1 Internal forces from the static analysis

The current section discusses the design of the structural elements that composes the building, such as the composite slab, the principal and secondary beams as well as the columns. A static analysis has been performed for the 62 load cases shown in the Tables 3.8 and 3.9 with the support of the software SAP2000.

Despite the fact that the envelopes have been calculated, the verifications for the ULS and SLS states have been performed for the 62 load combinations without considering the envelope in the design, in order to avoid and oversizing of the structural elements due to the consideration of the application of the peak forces acting simultaneously.

As mode of example, the internal forces applied to the principal beams and columns, which are connected with continuous joints, determined by the envelope in the ULS that are located at the exterior frames in the X and Y direction, are shown in the Figures. 3.21, 3.22 and 3.23.

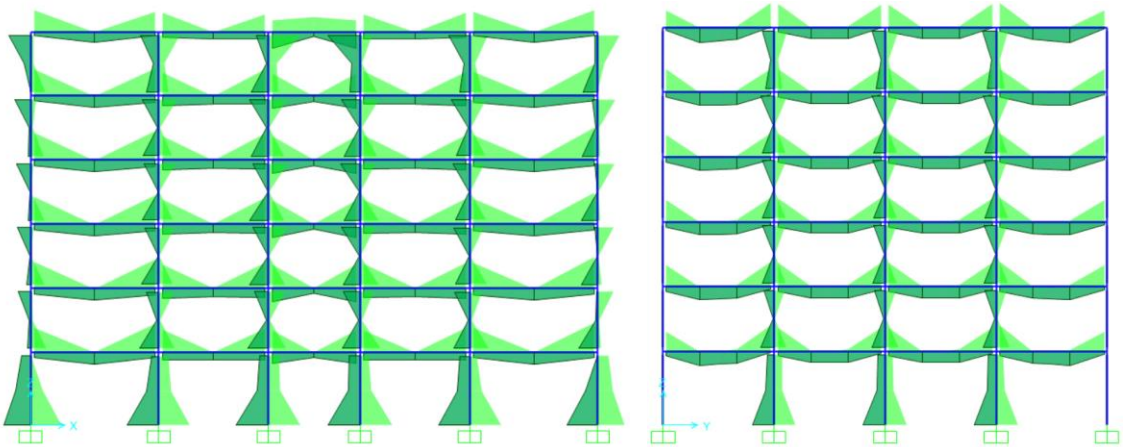

Fig.3.21 Envelope of bending moments in the outside X and Y frames

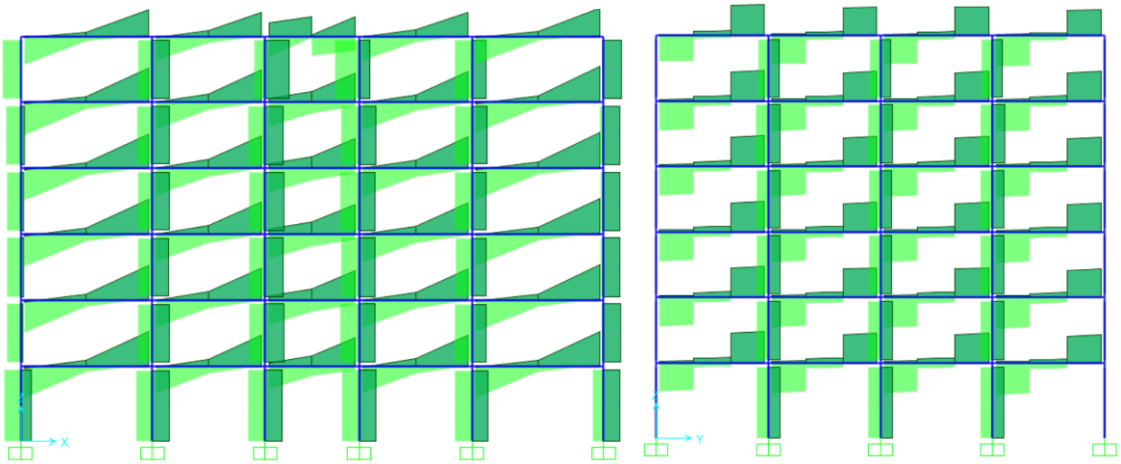

Fig.3.22 Envelope of shear forces in the outside XZ and YZ frames

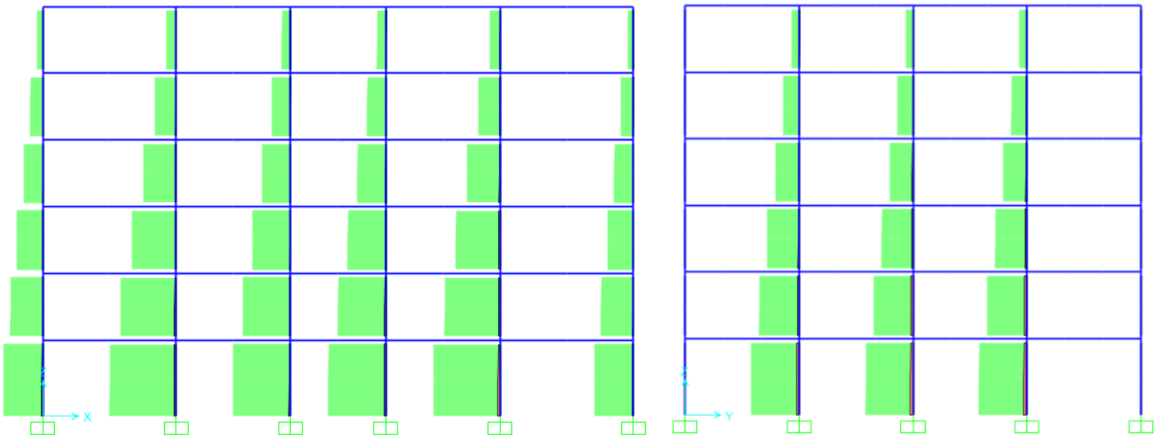

Fig.3.23 Envelope of axial forces in the outside XZ and YZ frames

Moreover, the bending moments and shear forces applied to the secondary beams that are connected to the principal ones with simple connections, are shown in the Fig. 3.24.

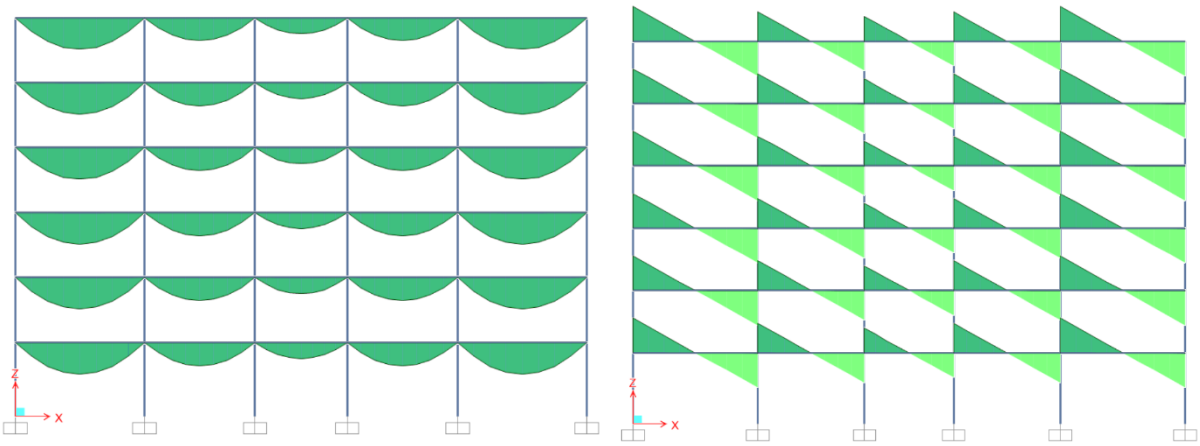

Fig. 3.24 Bending moments and shear forces applied to the secondary beams

3.4.2 Composite slab design

As it was mentioned in the section 3.1, one-way composite slab formed by a profiled steel deck and a slab concrete is use in the building due to the multiple advantages it presents over traditional slabs.

- Provides a fast solution when time is an important factor
- Produces a reduction of the depth and the self-weight of the floor slab
- Props are normally non necessary during the construction

In fact, modern steel buildings widely use composite slabs because they improve significantly the performance of the floor under gravity and seismic actions. In addition, it is necessary less man hours than traditional all steel structural decks (Landolfo et al. (2017)).

The composite steel concrete slab used is the HI-BOND A 75/760P (MeTecno), consisting of a corrugated collaborating steel sheet with a thickness of 1.2mm with a steel grade S260GD. The concrete slab is C20/25 with a characteristic resistance of 20 Mpa. The total thickness of the slab is 130 mm, being 75 mm for the steel sheet and 55 mm for the concrete slab. Both materials work simultaneously improving the resistance against positive and negative bending moments owing to the special prints located at the steel sheet.

The trapezoidal steel deck used in the HI-BOND A 75/760P (Fig. 3.25) which presents a self-weight of 0.15kN/m^2 for a thickness of 1.2mm.

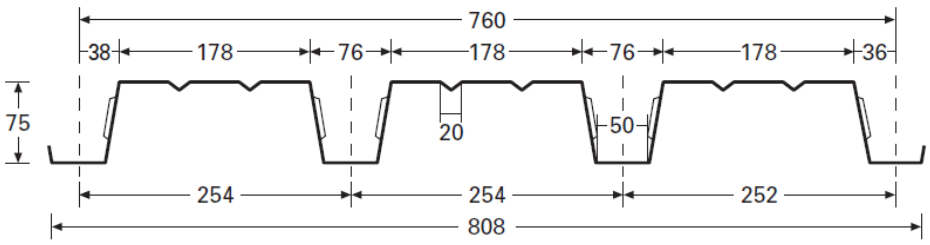

Fig. 3.25 Trapezoidal steel deck used in the HI-BOND A 75/760P

The thickness and height of the steel sheet has been chosen considering the loads applied to the slab and the spacing between the secondary beams. In addition, no shoring shall be used during the construction phase in order to reduce cost and time.

On the other hand, the concrete slab must provide sufficient stiffness to behave as a rigid diaphragm. That behaviour is guarantee if the concrete slab depth is at least 50 mm thick. The self-weight of the concrete slab, considering a density of 25kN/m^3, is equal to 1.88kN/m^2.

Due to the complexity of obtaining the resistance of collaborating composite slabs, the manufacturer's recommendations have been used. For a continuous slab with three or more bays, using a HI-BOND A 75/760P with a total thickness of 130mm, the maximum applicable load is equal to 4.42kN/m^2 in order to satisfice the serviceability limit states.

In case of the building, the composite slab is verified under ULS and SLS, since considering the live loads and permanent loads, 4.40kN/m^2 have been applied.

3.4.3 Design of the secondary beams

The secondary beams have been designed as a composite structure due to the mixed action between the composite slab and the steel profile, whose connection has been guaranteed by placing ductile-headed shear studs.

The use of composite structures presents several advantages since the resistance and the area moment of inertia of the cross-sections increases considerably as opposed to the consideration of the steel profile only. In fact, the structure self-weight was reduced by 3000kN changing the initial profiles IPE 300 determined in the pre-design phase, to IPE 240 and IPE 220 owing to using composite structures.

Even though the mixed action presents several advantages, it has not been considered for the principal beams, which are the dissipative elements under seismic actions. Because improving its resistance may lead to an increase of the columns profiles in order to satisfy the strong column-weak beam principle. Indeed, the criteria for choosing the primary beams were its stiffness and not for their resistance. Therefore, only the minimum headed shear studs are provided to the principal beams for constructional reasons.

Secondary beams have been designed as simply supported beams, which its maximum bending moment and deflection is located at the mid span according to the theory of elasticity.

The resistant moment (M_{rd}) of the composite structures depends on whether there is a total or partial connection. The total connection allows to the section reaching the ultimate internal forces allowed by the cross-sections, while for partial connections, the flexural resistance is related to the number of head shear studs used.

In the case of secondary beams connected to a perpendicular composite slab, the number of shear studs to be placed is limited by the geometry of the steel deck, where in most cases is not possible to guarantee a total connexion (Fig. 3.26).

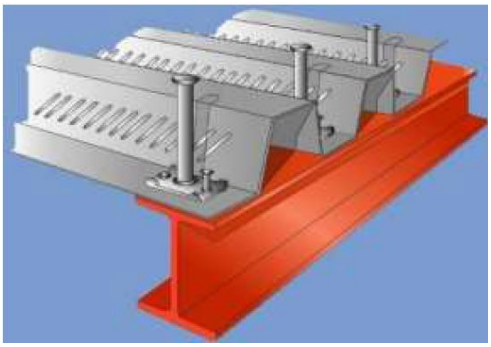

Fig. 3.26 Example of a beam connected to the perpendicular direction of the composite slab; (Tullini, 2019)

In the current building, all the secondary beams are oriented in the X direction, while the composite slab has been placed in the orthogonal direction. Hence, as shown the geometry of the steel deck of the HI-BOND 75 (Fig 3.20), the maximum number of head shear stubs that can be placed in the span of 7 meters are 26 (considering the distance from the supports to the mid span, which is the critical section). For the spans of 6 and 5 meters, the maximum number that can be placed are 22 and 18 respectively.

The number of head shear studs which guarantee a total connexion (N_f) are calculated from the following expression.

$$N_f = \frac{V_{l,Ed}}{P_{rd}} \tag{3.10}$$

where

$V_{l,Ed}$ is the longitudinal shear force

P_{rd} is the resistance of the head shear stud.

Since the steel beam shall be subjected to bending, and the upper flange to compression, the profile is categorized as class 1 according to the clause 5.2 of EN1993-1 (CEN, 2005b). Therefore, the plastic theory can be used to determine the longitudinal shear force ($V_{l,Ed}$).

In the Fig. 3.27 is shown the critic section where the Eq. 3.10 should be applied.

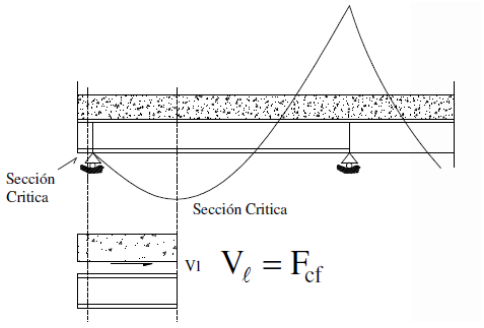

Fig. 3.27 Critical section to determine the number of head shear studs; (Mirambell, 2020)

The longitudinal shear force ($V_{l,Ed}$) may be obtained as the minimal axial force acting on the steel profile and the slab (F_{cd}).

$$F_{cd} = \left[\frac{0.85 f_{ck} A_c}{\gamma_c} + \frac{A_{se}}{\gamma_s}; \frac{A_a f_y}{\gamma_{M0}}\right] \quad (3.11)$$

where

f_{ck} is the characteristic strength of the concrete

A_c is the area of the concrete slab

γ_c is the material safety factor equal to 1.5

A_{se} is the area of the reinforcing steel in the concrete slab

γ_s is the material safety factor equal to 1.15

A_a is the area of the steel profile

f_y is the yield strength of the steel beam

γ_{M0} is the reduction factor equal to 1

In order to obtain A_c , it has to be considered the total depth of the concrete slab and the effective width obtained by the span length, which is equal to 2 meters in both sides, divided by 4.

The internal forces experimented by the secondary beams are positive bending moments meaning with their maximum at the mid span. Thus, only the slab is subjected to compression forces being neglected the contribution of the steel deck. Subsequently, the resistance of the ductile head shear stud (P_{rd}) corresponds to the minimum resistance between the shear stud (Eq. 3.12) and the slab considering the ribs are perpendicular to the secondary beams (Eq. 3.13) according to EN 1994-1, (CEN, 2004b).

$$P_{rd1} = 0.8 f_u \left(\frac{\pi d^2}{4}\right) \frac{1}{\gamma_v} \quad (3.12)$$

where

f_u is the ultimate strength of the studs

d is the diameter of the stud

γ_v is the shear safety factor equal to 1.25

The geometry and the mechanical characteristics of the shear studs that are used in the building are showed in the table 3.11.

Table 3.11 Characteristics of shear studs used in the building

ϕ(mm)	h(mm)	f_y(Mpa)	f_u(Mpa)	P_{rd}(kN)
16	100	350	450	57.9

$$P_{rd2} = \frac{1}{\gamma_v} 0.29 \alpha d^2 (f_{ck} E_{cm})^{0.5} \left[0.6 \frac{b_0}{h_a} \left(\frac{h}{h_a} - 1 \right) \right] k_t \tag{3.13}$$

where

α is a factor considered equal to 1

f_{ck} is the characteristic compression strength of the concrete

E_{cm} is the secant modulus of concrete

k_t is the reduction factor due to the composite slab ribs are oriented perpendicular to the secondary beams

$$K_t = \left(\frac{0.7}{\sqrt{N_r}} \right) \left(\frac{b_0}{h_a} \right) \left(\frac{h}{h_a} - 1 \right) \tag{3.14}$$

being N_r the number of head shear studs located in one rib.

The geometric characteristics are shown in the Fig. 3.28.

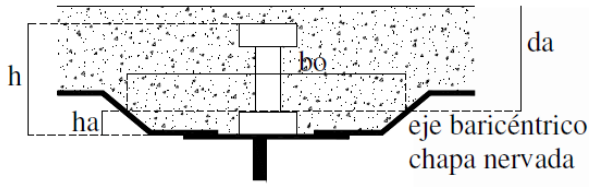

Fig. 3.28. Geometric characteristics to be considered in Eq.3.14; (Mirambell, 2020)

Finally, to guarantee a ductile behaviour of the head shear studs, the followings expressions should be satisfied.

$$\eta \geq 1 - \left(\frac{355}{fy} \right) (0.75 - 0.03 L_e) \quad \eta \geq 0.4 \tag{3.15}$$

where

L_e is the distance between null bending moment

fy is the yield strength of the beam

$$\eta = \frac{N}{N_f} \tag{3.16}$$

being N the number of head shear studs placed on the beam and N_f the number of head shear stubs to guarantee a total connexion.

In the Table 3.12 is summarize the longitudinal shear force ($V_{l,Ed}$) and the resistance of the head shear stud (P_{rd}), which has been conditioned by the resistance of the concrete slab, for all the spans. Moreover, it is shown the head shear studs placed in each secondary beam as well as the verification of the ductile behaviour according to the Eq. 3.15.

Table 3.12 Head shear studs placed in each secondary beam

Span(m)	Profile	$V_{l,Ed}$ (kN)	$P_{rd}(kN)$	N_f	Shear head studs	N	η
7	IPE240	1075	30	36	2ϕ16/ 254mm	26	0.72
6	IPE220	919	30	31	2ϕ16 / 254mm	22	0.71
5	IPE220	919	30	31	2ϕ16/ 254mm	18	0.58

ULS Verifications

Owing to the geometric limitations a total connexion cannot be guarantee, therefore a partial one is performed. In order to obtain the resistance of the secondary beams, an interpolation between the resistance of the steel profile ($M_{\alpha pl,rd}$) and the resistance of the composite structure considering a total connexion (M_{rd}) should be carry out.

The bending resistance of the steel profiles using a steel S275, according to the EN 1993-1, (CEN, 2005b):

$$M_{\alpha pl,rd\,IPE240} = 101\ kNm$$

$$M_{\alpha pl,rd\,IPE220} = 78\ kNm$$

The bending moment resistance of the composite cross-section it has been calculated considering both sections are in the plastic range. Therefore, the plastic neutral axis can be obtained applying the equilibrium equation.

$$x = \frac{0.85 f_{cd} b_{eff}}{A_a f_y} \tag{3.17}$$

For the profile IPE 240 and IPE 220, the neutral axis is located in the composite slab being subjecting the steel profile only under tension. Neglecting the contribution of the concrete, the ultimate bending moment of the cross-section is obtained by the following equation.

$$M_{rd} = 0.85 f_{cd} b_{eff} x (h_{total} - \frac{x}{2} - Z_a) \tag{3.18}$$

Fig. 3.29 shows the interpolation made between the resistance of the steel profiles and the resistance of the composite cross-section if a full connection was used. The actual resistance, which is filled in red, can be obtained considering the grade of connection (η) for each profile.

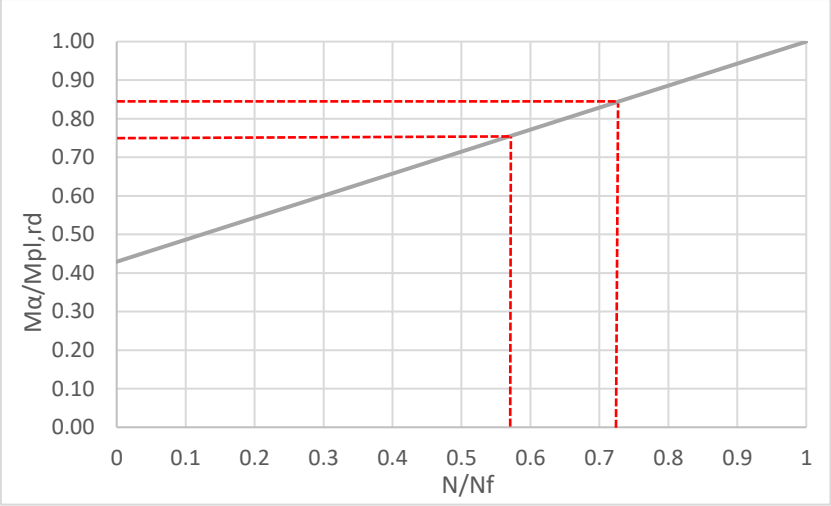

Fig. 3.29 Actual resistance of the cross-section with partial connexions

In addition, the shear forces have been taking into account for possible reductions in the bending resistance of the cross-sections. In the Table 3.12 is summarized the forces applied to each secondary beam due to the gravity loads, which are the same in all the storeys, and their respective ratios for the bending and shear resistance.

Table 3.12 Shear and bending resistance of the secondary beams

Span(m)	Profile	M_{ed}(kNm)	V_{ed}(kN)	M_{α}(kNm)	M_{Rd}(kNm)	$V_{pl,rd}$(kN)	Bending Ratio	Shear Ratio
7	IPE240	170	97	235	197	304	0.70	0.32
6	IPE220	125	58	196	162	252	0.51	0.23
5	IPE220	87	53	196	146	252	0.40	0.21

SLS verifications

In the composite structures, the construction process takes an important relevance, defining in most cases the steel profile that is need to be used. In the case of the building, during the concreting of the composite floor slab, no shoring shall be used to reduce costs and increase the construction speed and allowing to place several floors at the same time.

For this reason, the deflections should be evaluated in two different steps; the first one considers the deflection of the steel beam due to its self-weight and the execution loads and the weight of the fresh concrete (δ_1). The most unfavourable deflection is produced during this first step. Then, a second deflection appears due to the application of the live loads (δ_2), but in this case, the second moment of area of the composite cross-section is taking into account.

According to the elastic theory, the deflection in a simply supported beam under a uniform load can be calculated with the following expression.

$$\delta = \frac{5ql^4}{384EI} \tag{3.19}$$

where

E is the young modulus

I is the second moment of area

l is the span length

q is the uniform applied load

The uniform load applied to the secondary beams has been calculated considering the composite slab supported by 3-bays composed by two principal beams in the edges and two secondary beams in the centre, corresponding to a building frame in the Y direction (Fig. 3.30).

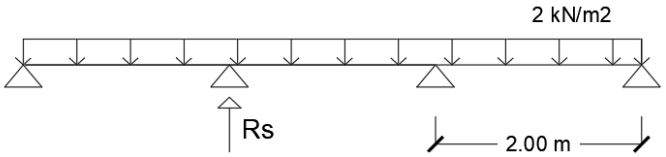

Fig.3.30 Structural scheme of the slab supported by 3 bays

Applying the equilibrium and compatibility equations, the reaction to be applied in the secondary beams is equal to:

$$q = R_s = 1.1 L_{slab} G_{kslab} + SW_{beam} \tag{3.20}$$

where

L_{slab} is the length between beams

G_{kslab} is the permanent weigh of the slab

SW_{beam} is the self-weight of the steel profile of the secondary beam

Then, the same procedure is applied to obtain the reaction produced by the live loads.

A summary of the deflection produced by the first and second phase, and the deflections allowed according for the SLS in the characteristic combination, according to the Italian code (NTC 2018) is shown in the Table 3.13.

Table 3.13 Deflections produced and allowed in the secondary beams

Span(m)	Profile	$\delta_1$mm)	δ_2 (mm)	δ_{Total}(mm)	$L/250$ (mm)	$L/300$ (mm)	Ratio 1	Ratio 2
7	IPE240	18	3	21	28	23	0.75	0.13
6	IPE220	14	3	17	24	20	0.71	0.15
5	IPE221	7	2	9	20	17	0.46	0.13

In conclusion, the composite structures of the secondary beams verify the ULS and SLS for the gravity loads, where the choice of the steel profile has been conditioned by the SLS since no shoring have been considered.

3.4.4 Design of the principal beams

This section discusses the design of the principal beams under the gravity and wind loads. Since the principal beams are connected to the support elements with continuous joints, its structural scheme is represented by a continuous beam. Thus, the maximum bending moments are placed at both ends of the element, where the lower flange is under compression. Moreover, this typology presents considerably lower deflections than the simple-supported beams.

The internal forces applied to the principal beams are bending moments and shear forces, not appearing axial forces due to the rigid diaphragm behave of the floors.

The most loaded elements are those oriented in the Y direction because they support the secondary beams on both sides, especially the beams filled in red (Fig. 3.31). In contrast, beams placed in the X direction, which are parallel to the secondary beams, only receive a fraction of vertical load from the composite slab and the wind actions.

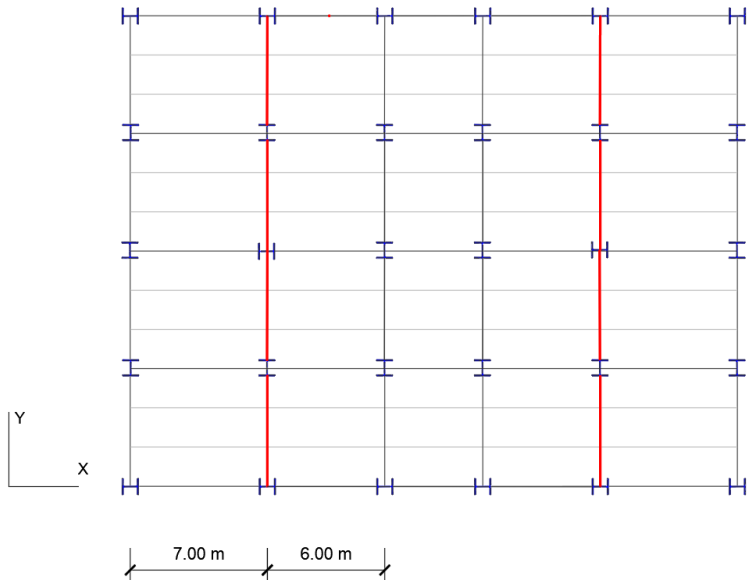

Fig. 3.31 Most solicited principal beams in the building

Moreover, pinned connections between secondary and principal beams have been used in order to avoid the appearance of torsional moments. Furthermore, these joints are simpler and economically favourable in comparison to rigid links.

An important factor that has been conditioned the design of the principal beams is the lateral torsional buckling. In the parts where the bending moments are positive, the upper flange is subjected to compression, which is laterally restrained by the composite slab.

However, at the ends of beams, where negative bending moments appear producing compressions in the lower flange, the structural element is not prevented from lateral deflections by the secondary beams owing to the use of simple connections. Hence, the lateral unrestrained length considered for the principal beams is equal to the length span.

In order to obtaining the bending resistance of the cross-section ($M_{pl,Rd}$) of the principal beams, which are Class 1, clause 6.2.5 of EN 1993-1, CEN (2005b) has been applied.

$$\frac{M_{Ed}}{M_{pl,Rd}} < 1 \tag{3.21}$$

$$M_{pl,Rd} = \frac{W_{pl,y} f_y}{\gamma_{M_o}} \tag{3.22}$$

where

f_y is the yield strength of the steel, in this case 235Mpa

$W_{pl,y}$ is the plastic section modulus

γ_{M_o} is the partial factor for resistance of cross-section

A reduction in the flexural resistance of the cross-section should be applied if the design shear force (V_{ed}) is higher than the 50% of the plastic shear resistance force ($V_{pl,Rd}$), according to clause 6.2.6.

$$\frac{V_{ed}}{V_{pl,Rd}} < 0.5 \tag{3.23}$$

$$V_{pl,rd} = \frac{A_v(f_y/\sqrt{3})}{\gamma_{m_o}} \tag{3.24}$$

where

A_v is the shear area of the cross section

In addition, a laterally unrestrained member subject to major axis bending moment should be verified against the lateral-torsional buckling according to the clause 6.3.2.1.

$$\frac{M_{Ed}}{M_{b,Rd}} < 1 \tag{3.25}$$

The design buckling resistance ($M_{b,Rd}$) can be obtained applying the following expressions.

$$M_{b,Rd} = \frac{\chi_{LT} W_{pl,y} f_y}{\gamma_{M_1}} \tag{3.26}$$

where

γ_{M_1} is the partial redactor factor for instabilities equal to 1

χ_{Lt} is the reduction factor of for lateral torsional buckling

$$\chi_{Lt} = \frac{1}{\phi_{Lt} + \sqrt{\phi_{Lt}^2 - \lambda_{LT}^2}} \tag{3.27}$$

$$\phi_{Lt} = 0.5[1 + \alpha_{Lt}(\lambda_{Lt} - 0.2) + \lambda_{LT}^2] \tag{3.28}$$

$$\lambda_{Lt} = \sqrt{\frac{W_{pl,y} f_y}{M_{cr}}} \tag{3.29}$$

$$M_{cr} = C_1 \frac{\pi^2 I_z}{L_c^2} \sqrt{\frac{I_w}{I_z} + \frac{L_c^2 G I_t}{\pi^2 E I_z}} \tag{3.30}$$

where

α_{Lt} is the imperfection factor depending on the cross-section shape

λ_{Lt} is the slenderness

M_{cr} is the elastic critical moment for lateral-torsional buckling

C_1 Depends on the shape of the bending moments

I_z is the second moment of area determined in the weak axis

I_w is the polar moment of inertia

I_t is the torsional inertia

L_c is the unrestrained length

A summary of the most loaded principal beams of the building under the ULS and SLS are shown in the Tables 3.14 and 3.15, exposing the strength of the cross-sections and the ratios according the Eq. 3.23 and 3.25.

For the case of SLS, the maximum deflection is established as $L/250$ for the total deflection, and $L/300$ produced the live loads, according to the Italian code (NTC18). The results are shown in absolute values.

Further information about the verification of all the primary beams of the building are exposed in the Annex 1.

Table 3.14 Summary of ULS verification for the most loaded principal beams

Element	Direction	Profile	Load Combination	M_{Ed}(kNm)	V_{Ed} (kN)	$M_{b,Rd}$(kNm)	$V_{pl,Rd}$(kNm)	Eq. 3.25	Eq. 3.23
PB641	Y	IPE400	ULS5	-213	-177	230	580	0.93	0.31
PB107	Y	IPE400	ULS13	-211	-140	246	580	0.86	0.24
PB606	Y	IPE450	ULS5	-251	-161	299	690	0.84	0.23

Table 3.15 Summary of SLS verification for the most load beams principal beams

Element	Load Combination	γ_{Total}	γ_Q
PB641	SLS5	L/826	L/8733
PB107	SLS5	L/1627	L/4316
PB606	SLS5	L/810	L/1077

In conclusion, profiles IPE 400 and IPE 450 have been verified under the ULS and SLS for the gravity and wind loads design.

3.4.5 Design of the columns

On the other hand, columns are continuous from the ground floor to the roof using the same cross-sections. Due to the gravity and wind loads, they are subjected to bending moments and shear forces in the major and minor axis, as well as to compression axial forces. Thus, verifications against compression and biaxial-bending moment, flexural and lateral torsional buckling must be performed.

In addition, the orientation of each column has been considered since its resistance varies depending on the position of the strong and weak axis.

Interior and central columns are subjected mainly to compression forces, where the bending moments are almost neglected, being the design governed by the flexural buckling. On the contrary, columns located close to the exterior frames, are subjected to compression forces and bending moments, behaving as beam-columns elements.

The design resistance of the column cross-section under uniform compression ($N_{c,Rd}$) is exposed in the clause 6.2.4.

$$\frac{N_{Ed}}{N_{pl,Rd}} < 1 \tag{3.31}$$

$$N_{pl,Rd} = \frac{Af_y}{\gamma_{M_o}} \tag{3.32}$$

where

A is the area of the cross-section

f_y the yield strength of the steel, in this case 275Mpa

The bending resistance of the cross-section in the major and minor axis should be evaluated using the Eq. 3.21, and subsequently verify the biaxal-bending that considers the axial loads applied to the column according to the clause 6.2.9.

$$\left[\frac{M_{y,Ed}}{M_{N,y,rd}}\right]^{\alpha} + \left[\frac{M_{z,Ed}}{M_{N,z,rd}}\right]^{\beta} \tag{3.33}$$

where

$M_{y,Ed}$ and $M_{z,Ed}$ are the design bending moments in the strong and weak axis respectively

$M_{N,y,rd}$ and $M_{N,z,rd}$ are the plastic moment resistance in the strong and weak axis reduced by the axial forces

α and β are equal to 2 and 5 n

Where $n = \frac{N_{ed}}{N_{pl,rd}}$

Once the resistance of the cross-section has been evaluated, the possible instabilities as the flexural and lateral-torsional buckling should be taking into account.

The flexural buckling may appear due to the compression forces. The buckling resistance of a compression member ($N_{b,Rd}$) according to clause 6.3.1 can be obtained with the following equations.

$$\frac{N_{Ed}}{N_{b,Rd}} < 1 \tag{3.34}$$

$$N_{b,Rd} = \frac{\chi A f_y}{\gamma_{M_1}} \tag{3.35}$$

where

γ_{M_1} is the partial redactor factor for instabilities equal to 1

χ is the reduction factor for flexural buckling

$$\chi_{Lt} = \frac{1}{\phi_{Lt} + \sqrt{\phi_{Lt}^2 - \lambda^2}} \tag{3.36}$$

$$\phi_{Lt} = 0.5[1 + \alpha(\lambda^2 - 0.2) + \lambda^2] \tag{3.37}$$

$$\lambda = \sqrt{\frac{Af_y}{N_{cr}}} \tag{3.38}$$

$$N_{cr} = \frac{\pi^2 EI}{\beta L} \tag{3.39}$$

where

α is the imperfection factor

λ is the slenderness obtained

N_{cr} is the elastic critical force for the relevant buckling mode based on the gross cross-sectional properties

E is the young modulus

I is the second moment of area, evaluated in the strong and weak axis

L is the length of the structural element

β is the buckling factor

The buckling factor (β) depends on whether the structure is sway or non-sway. According to the section 3.5, where a buckling analysis were performed determining the building can be classify as non-sway structure, the buckling factor (β) is between the values 0.5 and 1.

The factor should be calculated considering the boundary conditions and the stiffness of the beams connected at the top and bottom part of each column of the structure. In order to simplify the calculations, it has been considered a buckling factor for all the columns equal to 1, which is the most unfavourable value for a non-sway structure.

The lateral-torsional buckling for the columns in the major-axis should be evaluated with the same assumptions exposed for the principal beams.

Finally, the interaction between the axial forces and bending moments should be verified with the following expressions according to the clause 6.3.3.

$$\frac{N_{Ed}}{\frac{\chi_y N_{Rk}}{\gamma_{M1}}} + k_{yy}\frac{M_{y,Ed}}{\chi_{LT}\frac{M_{y,Rk}}{\gamma_{M1}}} + k_{yz}\frac{M_{z,Ed}}{\frac{M_{z,Rk}}{\gamma_{M1}}} \leq 1 \tag{3.40}$$

$$\frac{N_{Ed}}{\frac{\chi_z N_{Rk}}{\gamma_{M1}}} + k_{zy}\frac{M_{y,Ed}}{\chi_{LT}\frac{M_{y,Rk}}{\gamma_{M1}}} + k_{zz}\frac{M_{z,Ed}}{\frac{M_{z,Rk}}{\gamma_{M1}}} \leq 1 \tag{3.41}$$

where

$N_{Ed}, M_{y,Ed}$ and $M_{z,Ed}$ are the design forces

χ_y and χ_z are the reduction factors due to flexural buckling f

$k_{yy}, k_{yz}, k_{zy}, k_{zz}$ are the interaction factors

To determine the interaction factors, the Method 2 proposed by the Annex B of the EN 1993-1, (CEN, 2005b) has been considered.

A summary of the verification of the columns in ULS is shown in the Table 3.16, where the local axes of the columns are refereed in the Fig. 3.32. The total ratio considers the axial forces acting simultaneously with the bending moments, taking into account the previous expressions for the flexural buckling and the biaxial-bending.

Further information about the verification of the columns is shown in the Annex 1.

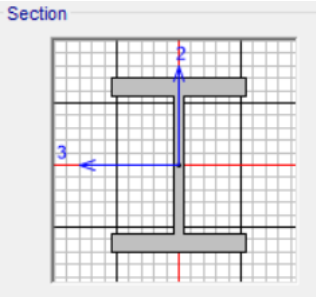

Fig.3.32 Local axes for the columns; SAP2000

Table 3.16 Summary of ULS verification for the most loaded columns

Item	Profile	Load combination	N_{Ed}(kN)	M_{Ed3}(kNm)	M_{Ed2}(kNm)	V_{Ed2}(kN)	V_{Ed3}(kN)	Total Ratio
DB1	HE360M	ULS5	-3441	11	1	9	1	0.51
DE1	HE360M	ULS5	-3441	11	-1	-14	7	0.51
AB6	HE360M	ULS5	-262	-15	161	10	-93	0.30
CB1	HE360M	ULS13	-3182	60	-10	15	8	0.50

Despite considering the interaction with compression and bending forces acting in the columns, the highest requests are under axial compression loads in the case of the gravity and wind loads design since the bending moments are quite low under static conditions.

3.4.6 Building under wind loads

The last step consists in analyse the horizontal displacements when the wind loads are acting in the façade of the building without the application of the live loads, which it is the worst condition.

The inter-storeys displacements produced in the X and Y directions for the load combinations SLS34 and SLS35, which are the most unfavourable are shown in the Fig. 3.33.

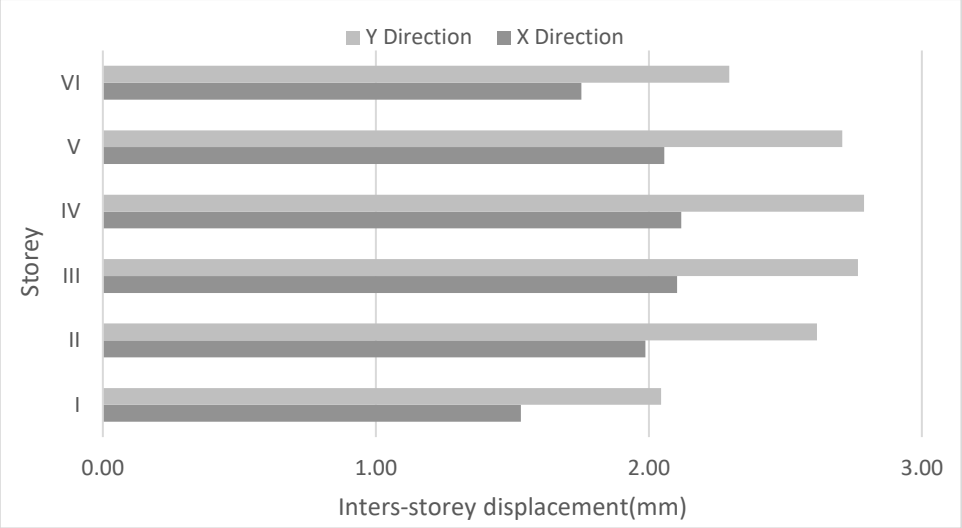

Fig. 3.33 Inter-storey displacements in the X and Y direction

According to the Italian code (NTC 2018), the maximum inter-storey value allowed is $h/300$, meaning is equal to 13 mm for the first floor and 11 for the other storeys. Thus, this condition is verified. Moreover, the top displacement produced is equal to 13 mm which is lower to the $H/500$.

In conclusion, all the structural elements verify the ULS and SLS for the static analysis. Despite the building seems to be oversized under the gravity loads, during the application of the seismic action the solicitations increase considerably, and the final design of the building is the result of an interaction process between the static and seismic analysis.

3.5 SEISMIC DESIGN

3.5.1 Behaviour factor of the building

The building has been conceived with a high ductility class (DCH), exhibiting the ability to dissipate energy through the inelastic behaviour. Therefore, a sufficient rotational capacity must be ensured in the plastic hinges, consequently, all the dissipative elements are be class 1.

Depending on the structural system and the ductility class, different structural behaviours (q) are defined in the clause 6.1.3 of EN 1998-1(CEN, 2004c) as shown the Fig. 3.34. Those factors are used in the linear seismic analysis through the designing spectrum.

STRUCTURAL TYPE	Ductility Class	
	DCM	DCH
a) Moment resisting frames	4	$5\alpha_u/\alpha_1$
b) Frame with concentric bracings Diagonal bracings V-bracings	 4 2	 4 2,5
c) Frame with eccentric bracings	4	$5\alpha_u/\alpha_1$
d) Inverted pendulum	2	$2\alpha_u/\alpha_1$
e) Structures with concrete cores or concrete walls	See section 5	
f) Moment resisting frame with concentric bracing	4	$4\alpha_u/\alpha_1$
g) Moment resisting frames with infills Unconnected concrete or masonry infills, in contact with the frame	2	2
Connected reinforced concrete infills	See section 7	
Infills isolated from moment frame (see moment frames)	4	$5\alpha_u/\alpha_1$

Fig. 3.34 Behaviour factor q for each structural typology

where

α_i is the value witch the horizontal seismic design action is multiplied to reach the plastic resistance in any member of the structure

α_u is the value which the horizontal seismic design action is multiplied to produce the structural instability owing to the plastic hinges appeared in the structural elements

To determine redistribution parameter (α_u/α_i), the nonlinear static analysis should be performed. However, as a first approximation to apply the linear seismic analysis, it can be assumed equal to 1.3 for a regular multi-storey building.

Thus, for the current building, the behaviour factor becomes 6.5 for the ULS analysis. This is the highest value that can be obtained, meaning the structure presents large flexibility and ductility. In the case of the DLS verifications, a structural factor equals to 1.5 has been considered.

3.5.2 Criteria for structural regularity

Regularity in plan

To considerer a building regular in plan, the building should have symmetrical lateral stiffness and mass distribution with respect to the principal directions. Otherwise, eccentricity appears inducing torsional effects according to clause 4.2.3.2 of EN 1998-1, CEN (2004).

During the seismic action, inertial forces are applied in the mass of each story, which can be assumed to be concentrated at one point named as centre of mass (MC). Subsequently, the shear resistant forces, whose stiffness is proportional the structural members, appear in the opposite direction at the centre of stiffness (CS). If there is an eccentricity between both centres, the shear forcers applied to the columns increase due to the torsional effects (Fig. 3.35) according to Petrini et al. (2004).

Instead, if the eccentricity is equal to zero, the building only is subjected to translational solicitations. However, the technical codes establish a minimum eccentricity of 5% since during the construction process, some eccentricity always appears in the structure.

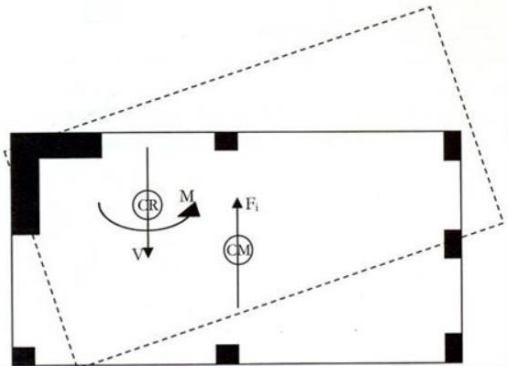

Fig 3.35 Torsional effects due to the eccentricity; Petrini et al. (2004)

In multi-story buildings, the centre of stiffness depends on the shape and the distribution of the lateral forces, being necessary to apply the lateral force method. Nevertheless, there is a simplified procedure that consist in obtaining the centre of stiffness for each floor as the centre of inertia. This simplification is allowed to be used when the lateral load resisting systems are continuous from the foundation to the top of the building, although for dual systems such as moment resistant frames with concrete walls, this simplified procedure is no longer valid.

The centre of inertia can be computed with the following equations.

$$X_{cs} = \frac{\sum x_i K_{yi}}{\sum K_{yi}} \tag{3.42}$$

$$Y_{cs} = \frac{\sum y_i K_{xi}}{\sum K_{xi}} \tag{3.43}$$

where

X_{cs} and Y_{cs} are the centre of inertia in the X and Y axis respectively

x_i and y_i are the distances from each vertical element to the centre of origin stablished

K is the stiffness of the structural element, considering the vertical elements. For the columns can be assumed as $K = 12EI/L^3$.

In the case of the centre of mass, a similar procedure should be performed for each storey considering the seismic mass, which is deeply discussed in section 3.6.3.

$$X_{cm} = \frac{\sum y_i mi}{\sum mi} \tag{3.44}$$

$$Y_{cm} = \frac{\sum xmi}{\sum mi} \tag{3.45}$$

In addition, if the following inequalities are not satisfied, the building should be considered as torsional deformable, meaning the dynamical behaviour would not be optimal, having to decreasing the structural behaviour factor (q).

$$e_x \leq 0.30 r_x \qquad e_y \leq 0.30 r_y \tag{3.46}$$
$$r_x \geq l_s \qquad r_y \geq l_s$$

where

e_x and e_y are the eccentricity in the X and Y directions

r_x and r_y are the torsional radius defined as the square root of the ratio of the torsional stiffness to the lateral stiffness

l_s is the radius of gyration of the floor masses calculated as the ratio between the polar moment of inertia of masses in plan with the respect to the centre of mass of the floor and floor mass.

The torsional radius can be calculated for a simplify way as.

$$r_x = \sqrt{\frac{\sum(x^2 K_y + y^2 K_x)}{\sum K_y}} \tag{3.47}$$

$$r_y = \sqrt{\frac{\sum(x^2 K_y + y^2 K_x)}{\sum K_x}} \tag{3.48}$$

Being x and y the distance from each column to the centre of stiffness and K_x and $K_y$the stiffness of each element as specified in the expression.

For a rectangular area, ls may approximate as:

$$l_s = \sqrt{\frac{{l_x}^2 + {l_y}^2}{12}} \tag{3.49}$$

The centre of inertia and mass for each storey, as well as the torsional radius of the building are shown in the Table 3.17.

Table 3.17 Eccentricity for each storey

	Centre of Inertia(m)		Centre of Mass(m)		Eccentricity(m)		Ls(m)	r_x(m)	r_y(m)
Storey	X	Y	X	Y	e_x	e_y			
I	15.5	12	15.5	12	0	0	11.32	14.51	15.29
II	15.5	12	15.5	12	0	0	11.32	14.51	15.29
III	15.5	12	15.5	12	0	0	11.32	14.51	15.29
IV	15.5	12	15.5	12	0	0	11.32	14.51	15.29
V	15.5	12	15.5	12	0	0	11.32	14.51	15.29
VI	15.5	12	15.5	12	0	0	11.32	14.51	15.29

It can be noticed the eccentricity for each floor is equal to zero as well as the building is not torsional deformable, since the Eq. 3.46 is satisfied, performing an excellent dynamic behaviour.

Other consideration for regularity in plan is the slenderness of the building, $\lambda = L_{max}/L_{min}$, should not be higher than 4. In this case, L_{max} is equal to 31 meters and L_{min} 24 min, therefore the slenderness is equal to 1.29.

In conclusion, it can be stated the building is regular in plant. In fact, it is expected the structure experiences two fundamental translational modes of vibration and a third rotational mode, which shall be uncoupled.

Regularity in elevation

There are several criteria to be met in order to ensure the regularity in elevation:

- Lateral forces resisting system must be continuous along the height without interruptions
- Lateral stiffness and mass of the structure must be constant or gradually decrease with height
- In frame buildings, the ratio between the effective resistance of each storey and the necessary design resistance should not vary disproportionally between adjacent stories.

Since all these conditions are satisfied, the building is regular in elevation. In consequence, no soft stories are expected to appear.

3.5.3 Seismic action

The purpose of this subchapter is to discuss the elastic and design spectrums corresponding to the L'Aquila (Abruzzo), which have been applied in the linear analysis and the N2 method.

Clause 3.23 of the Italian code, NTC (2018) establishes that the following expressions should be applied to define the elastic spectrums.

$$S_a(T) = a_g S \eta F_0 \left[\frac{T}{T_B} + \frac{1}{\eta F_0}\left(1 - \frac{T}{T_B}\right)\right] \qquad 0 \le T \le T_B \tag{3.50}$$

$$S_a(T) = a_g S \eta F_0 \qquad T_B \le T \le T_C \tag{3.51}$$

$$S_a(T) = a_g S \eta F_0 \left[\frac{T_C}{T}\right] \qquad T_c \le T \le T_D \tag{3.52}$$

$$S_a(T) = a_g S \eta F_0 \left[\frac{T_C T_D}{T^2}\right] \qquad T_D \le T \tag{3.53}$$

where

T the period of vibration of a linear single-degree-of-freedom system

a_g is the design ground acceleration

T_B is the lower limit of the period of the constant spectral acceleration branch

T_C is the upper limit of the period of the constant spectral acceleration branch

T_D is the value of deining the beginning of the constant displacement response range of the spectrum

S corresponds to the soil factor

η is the damping correction factor equal to 1 for 5% viscous damping

F_0 is the factor that magnifies the maximum spectral amplification with a minimum value of 2.2

The designing spectrums can be obtained applying the behaviour factor (q) equal to 6.5 for the ULS, and 1.5 for the DLS in the previous equations.

The displacement spectrum $S_{De}(T)$, should be calculated transforming the elastic spectrum $S_e(T)$ with the following expression according to the clause 3.2.3.2.3.

$$S_{De}(T) = S_e(T)\frac{T}{2\pi} \tag{3.54}$$

The parameters that characterize the elastic spectrum are related to the ground type; A, B, C, D or E (Fig. 3.36). The classification is made by the average shear wave velocity ($v_{s,30}$) assigned to each ground type. As the shear-wave velocity decreases, the acceleration response spectra become higher, increasing the forces applied to the structures.

Categoria	Caratteristiche della superficie topografica
A	*Ammassi rocciosi affioranti o terreni molto rigidi* caratterizzati da valori di velocità delle onde di taglio superiori a 800 m/s, eventualmente comprendenti in superficie terreni di caratteristiche meccaniche più scadenti con spessore massimo pari a 3 m.
B	*Rocce tenere e depositi di terreni a grana grossa molto addensati o terreni a grana fina molto consistenti*, caratterizzati da un miglioramento delle proprietà meccaniche con la profondità e da valori di velocità equivalente compresi tra 360 m/s e 800 m/s.
C	*Depositi di terreni a grana grossa mediamente addensati o terreni a grana fina mediamente consistenti* con profondità del substrato superiori a 30 m, caratterizzati da un miglioramento delle proprietà meccaniche con la profondità e da valori di velocità equivalente compresi tra 180 m/s e 360 m/s.
D	*Depositi di terreni a grana grossa scarsamente addensati o di terreni a grana fina scarsamente consistenti*, con profondità del substrato superiori a 30 m, caratterizzati da un miglioramento delle proprietà meccaniche con la profondità e da valori di velocità equivalente compresi tra 100 e 180 m/s.
E	*Terreni con caratteristiche e valori di velocità equivalente riconducibili a quelle definite per le categorie C o D*, con profondità del substrato non superiore a 30 m.

Fig. 3.36 Ground types category depending on the shear wave velocity; (Ministerio delle Infraestructure e dei Transporti, 2018a)

In order to obtain the ground type that presents L'Aquila, a geotechnical report of the area has been used; Studio viscogliosi tomassi (2010). The report specifies the Down-Hole in-situ test was carry out in the ground to obtain the average shear-wave velocity. Fig. 3.37 displays the results for each layer of soil considered in the analysis until reaching a depth equal to 30 meters.

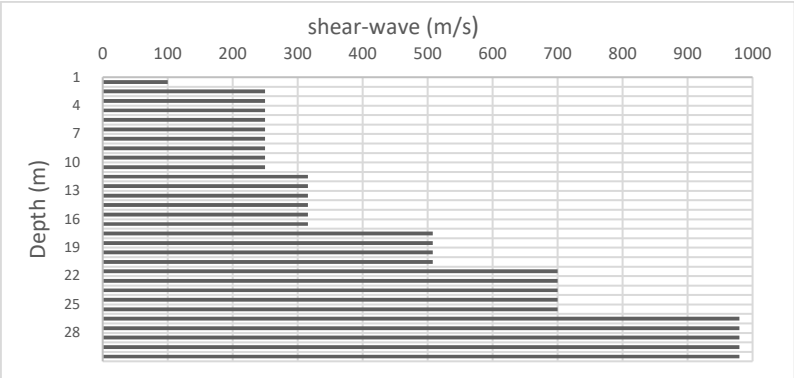

Fig. 3.37 Results of the Down-Hole in-situ test

The average shear-wave velocity ($v_{s,30}$) can be obtained applying the following expression.

$$v_{s,30} = \frac{30}{\sum \frac{h_i}{v_i}} \tag{3.55}$$

where

h_i is the thickness of each soil layer in meters

v_i is the shear-wave velocity for each soil layer

The value obtained for $v_{s,30}$ is equal to 353 m/s, corresponding to a ground type C, which is formed by deep deposits of dense gravel or stiff clay. In absence of more information, these data have been taken as valid to calculate the elastic spectrums.

Table 3.18 shows all the parameters needed to perform the elastic spectrums in the ULS and DLS state for a ground type C, according to the Italian code (NTC 2018). Moreover, Fig. 3.38 and Fig. 3.39 show the different spectrums for the ULS and DLS design respectively.

Table 3.18 Parameters for ground type C

Parameters	Ultimate Limit State (ULS)	Damage Limitation State (DLS)
Tr(years)	475	50
a_gg	0.261g	0.104g
S	1.330	1.500
F0	2.364	2.332
$T_B(s)$	0.172	0.150
$T_C(s)$	0.517	0.449
$T_D(s)$	2.644	2.016
q	6.5	1.5

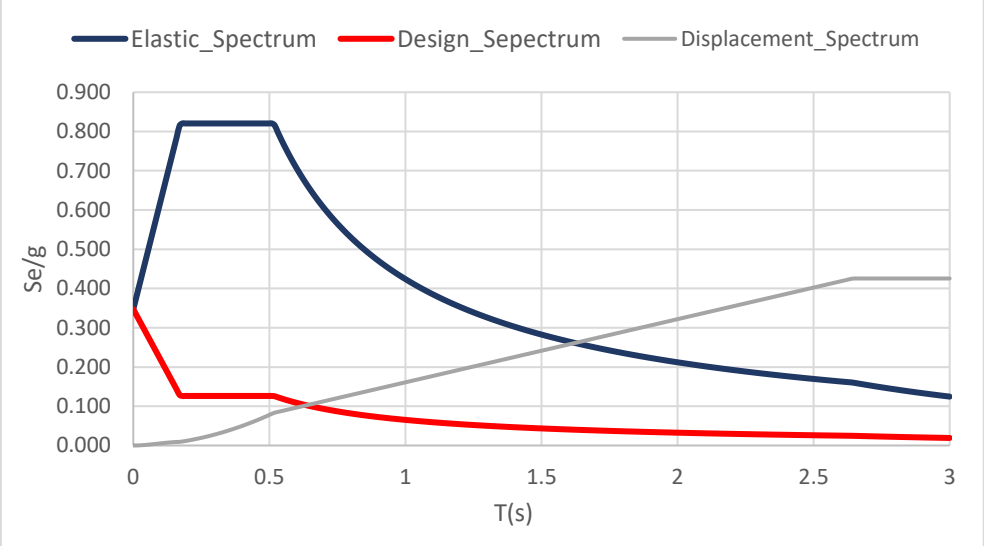

Fig. 3.38 Spectrums for the ULS

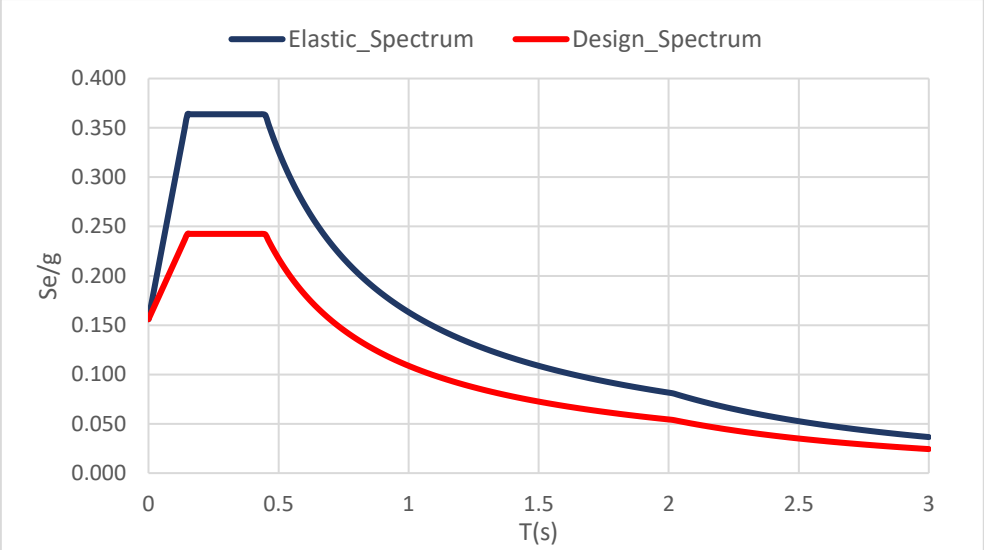

Fig. 3.39 Spectrums for the DLS

3.5.4 Modal analysis

The dynamical behaviour of the building, which is highly influenced by the regularity in plan and elevation, has been analysed applying the modal analysis using the Eq. 2.18.

Before carrying out the analysis and obtain the eigenvalues and eigenvectors, is necessary to define the seismic masses in the building according to clause 3.2.4 of EN 1998-1, CEN (2004).

$$\sum G_{k,j} + \sum \psi_{E,i} Q_{k,i} \tag{3.56}$$

Under seismic actions, only permanent loads ($G_{k,j}$) and the live loads ($Q_{k,i}$) are considered owing to the low probability of occurrence the seismic action while there are other loads such snow or wind. Moreover, the reduction factor $\psi_{E,i}$ considerers live loads are not applied simultaneously in all the structure during the earthquake.

$$\psi_{E,i} = \psi_{2,i}\varphi \tag{3.57}$$

Being φ a factor from the EC8 or the national annexes. In this case, according to the clause 2.5.3 of the NTC 2018.

$$\psi_{E,i} = \psi_{2,i} \tag{3.58}$$

being $\psi_{2,i}$ the factor quasi-permanent value of the variable actions

In the Table 3.19 is shown the seismic mass to considerer of each storey, where total mass of the building is 2308 kN s^2 /m.

Table 3.19 Weight and mass associated for each storey

Storey	G_k(KN)	Q_k(kN)	Weight(kN)	Seismic Mass (kN s^2/m)
I	3110	670	3780	390
II	3137	670	3806	388
III	3137	670	3806	388
IV	3137	670	3806	388
V	3137	670	3806	388
VI	2921	670	3590	366

Considering the first 6 modes vibration, a mass activation of the 94% has been reached in the X and Y direction (Table 3.20). Thus, the remaining modes of vibration may be neglected according to clause 4.3.3.3 of EN 1998-1, (CEN, 2004c).

Table 3.20 Period and mass activation for the relevant modes of vibration

Mode	T(s)	Mass X	Mass Y	RX	Ry	RZ
1	1.159	84%	0%	0%	5%	0%
2	1.083	0%	84%	7%	0%	0%
3	0.964	0%	0%	0%	0%	84%
4	0.360	10%	0%	0%	19%	0%
5	0.338	0%	10%	27%	0%	0%
6	0.298	0%	0%	0%	0%	10%

The fundamental periods of vibration are the three first. Two of them are translational in the X and Y direction, and the third is rotational as shows the Figures 3.40, 3.41 and 3.42.

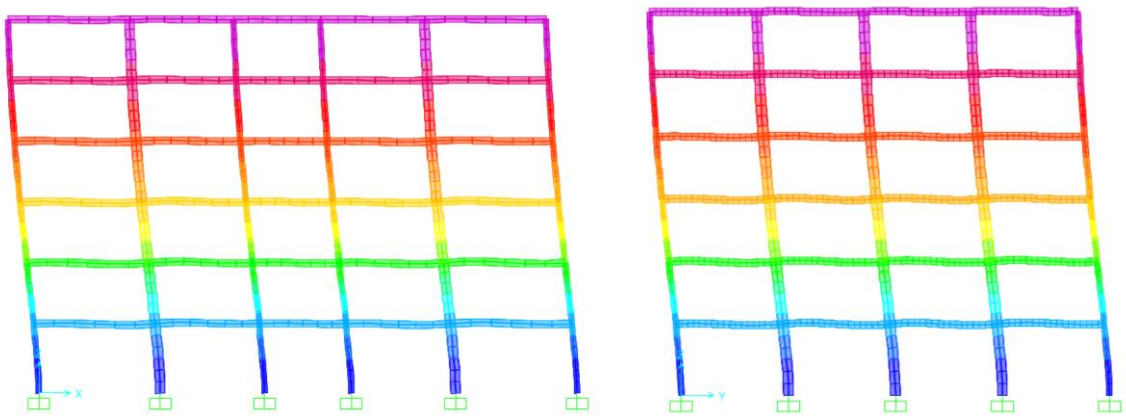

Fig. 3.40 Mode 1. T=1.125s and Mode 2. T=1.036s

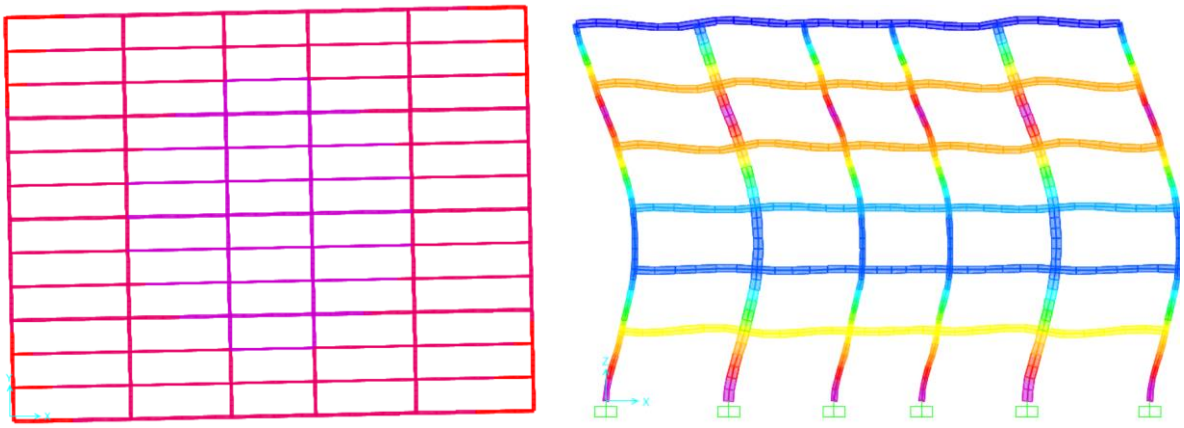

Fig.3.41 Mode 3. T=0.906s and Mode 4 T=0.344s

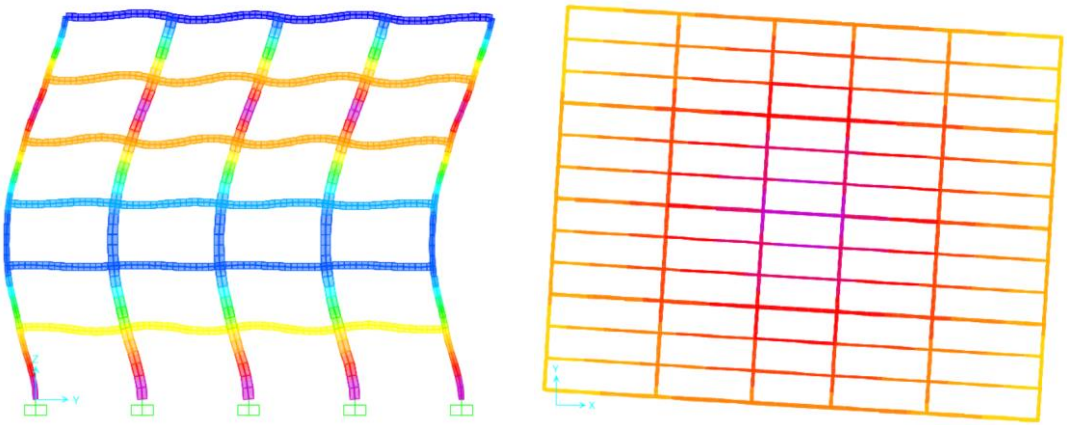

Fig. 3.42 Mode 5. T=0.309s and Mode 6 T=0.275s

3.5.5 Seismic combinations

To perform the seismic combinations which are applied in the linear modal response spectrum analysis, the expression established in clause 3.2.4 has been considered.

$$\sum G_{k,j} + P + A_{ed} + \sum \psi_2 Q_{k,i} \tag{3.59}$$

where

$G_{k,j}$ corresponds to the permanent loads

A_{ed} is the design value of the seismic action

$Q_{k,i}$ is the variable load

P is the pretensioning action

ψ_2 is the coefficient for the quasi-permanent value.

The seismic action (A_{ed}) depends on the limit state that is being analysed, being the ULS or DLS. Moreover, A_{ed} should be evaluated with the importance factor (γ_I) of the building given in clause 4.2.5.

$$A_{ed} = \gamma_I A_{ek} \tag{3.60}$$

Ordinary buildings correspond to the class II, meaning the importance factor is equal to 1. Therefore, the characteristic value of the seismic action A_{ek} is equal to the design value of the seismic action (A_{ed}).

Furthermore, the horizontal components in both principal directions should be considered acting simultaneously. However, considering peak forces at the same time in both directions would lead to and structure oversizing, due to low probability of occurrence. For this reason, the combination of the seismic forces is carried out with the following expression.

$$E_{edx}" + "0.3E_{edy} \tag{3.61}$$
$$0.3E_{edx}" + "E_{edy}$$

where

E_{edx} represents the actions effects due to the seismic action in the X direction

E_{edx} represents the actions effects due to the seismic action in the Y direction.

" + " implies “to be combined with”

On the other hand, despite the building presents no eccentricity between the centre of stiffness and the centre of mass, clause 4.3.2 of EN 1998-1, CEN (2004)**,** specifies the uncertainness in the location of masses and the spatial variation of the seismic motion has to be included in the seismic combinations with the consideration of an accidental eccentricity for each storey, equal to 5%.

$$e_{ai} = \pm 0.05 L_i \tag{3.62}$$

being L_i is the floor-dimension perpendicular to the direction of the seismic force.

In the case of the building, the eccentricity in the e_x and e_y is equal to 1.55 meters and 1.2 meters respectively. It should be applied in the most unfavourable location, for this reason are expressed with the positive and negative sign.

Thus, taking into account Eq. 3.61 and the accidental eccentricity applied in the worst conditions, 32 seismic combinations have been obtained (Table 3.21). These load combinations are the same for the ULS and DLS, residing the difference between both states in the seismic action (A_{ed}).

Table 3.21 Seismic combinations for the ULS and DLS

	Combinations	Dead Load	L1 Permanent Load	L2 Live Loads	L8 Roof	Ex	Ey	Eccentricity_X	Eccentricity_Y	Comments
ULS	ULS1	1	1	0.3	0.3	1	0.3	+5%	+5%	1EX+0.3EY
	ULS2	1	1	0.3	0.3	1	0.3	-5%	+5%	1EX+0.3EY
	ULS3	1	1	0.3	0.3	1	0.3	+5%	-5%	1EX+0.3EY
	ULS4	1	1	0.3	0.3	1	0.3	-5%	-5%	1EX+0.3EY
	ULS5	1	1	0.3	0.3	-1	0.3	+5%	+5%	"-1EX+0.3EY"
	ULS6	1	1	0.3	0.3	-1	0.3	-5%	+5%	"-1EX+0.3EY"
	ULS7	1	1	0.3	0.3	-1	0.3	+5%	-5%	"-1EX+0.3EY"
	ULS8	1	1	0.3	0.3	-1	0.3	-5%	-5%	"-1EX+0.3EY"
	ULS9	1	1	0.3	0.3	1	-0.3	+5%	+5%	"1EX-0.3EY"
	ULS10	1	1	0.3	0.3	1	-0.3	-5%	+5%	"1EX-0.3EY"
	ULS11	1	1	0.3	0.3	1	-0.3	+5%	-5%	"1EX-0.3EY"
	ULS12	1	1	0.3	0.3	1	-0.3	-5%	-5%	"1EX-0.3EY"
	ULS13	1	1	0.3	0.3	-1	-0.3	+5%	+5%	"-1EX-0.3EY"
	ULS14	1	1	0.3	0.3	-1	-0.3	-5%	+5%	"-1EX-0.3EY"
	ULS15	1	1	0.3	0.3	-1	-0.3	+5%	-5%	"-1EX-0.3EY"
	ULS16	1	1	0.3	0.3	-1	-0.3	-5%	-5%	"-1EX-0.3EY"
	ULS17	1	1	0.3	0.3	0.3	1	+5%	+5%	"+0.3EX+1EY"
	ULS18	1	1	0.3	0.3	0.3	1	-5%	+5%	"+0.3EX+1EY"
	ULS19	1	1	0.3	0.3	0.3	1	+5%	-5%	"+0.3EX+1EY"
	ULS20	1	1	0.3	0.3	0.3	1	-5%	-5%	"+0.3EX+1EY"
	ULS21	1	1	0.3	0.3	-0.3	1	+5%	+5%	"-0.3EX+1EY"
	ULS22	1	1	0.3	0.3	-0.3	1	-5%	+5%	"-0.3EX+1EY"
	ULS23	1	1	0.3	0.3	-0.3	1	+5%	-5%	"-0.3EX+1EY"
	ULS24	1	1	0.3	0.3	-0.3	1	-5%	-5%	"-0.3EX+1EY"
	ULS25	1	1	0.3	0.3	0.3	-1	+5%	+5%	"+0.3EX-1EY"
	ULS26	1	1	0.3	0.3	0.3	-1	-5%	+5%	"+0.3EX-1EY"
	ULS27	1	1	0.3	0.3	0.3	-1	+5%	-5%	"+0.3EX-1EY"
	ULS28	1	1	0.3	0.3	0.3	-1	-5%	-5%	"+0.3EX-1EY"
	ULS29	1	1	0.3	0.3	-0.3	-1	+5%	+5%	"-0.3EX+1EY"
	ULS30	1	1	0.3	0.3	-0.3	-1	-5%	+5%	"-0.3EX+1EY"
	ULS31	1	1	0.3	0.3	-0.3	-1	+5%	-5%	"-0.3EX+1EY"
	ULS32	1	1	0.3	0.3	-0.3	-1	-5%	-5%	"-0.3EX+1EY"

3.5.6 Linear modal response spectrum analysis

In order to carry out the verifications of the capacity design, the linear modal response spectrum analysis, which was introduced in the chapter 2, has been applied for the 32 seismic combinations shown in Table 3.21. Normally, since the gravity loads in seismic combination remain constant, they are evaluated separately from the seismic actions. In fact, the capacity design verifications separates both actions.

On the other hand, the seismic actions should be evaluated for all the seismic combinations and posteriorly make an envelope. The seismic actions have been calculated considering the 6 first modes of vibration of the building, which were obtained from the modal analysis shown in section 3.6.4.

The combination of these modes has been performed using a complete quadratic combination (CQC) which applies the Eq. 2.19. Subsequently, an envelope of the 32 load combinations have been considered to determine the internal forces according to the seismic actions.

As mode of example, in Figures 3.43, 3.44 and 3.45 are shown the internal forces due to the gravity loads in the seismic combination of the exterior frames in the X and Y direction. Then, Figures 3.46, 3.47 and 3.48 show the envelope of the internal forces produced by the combination of the 32 seismic combinations.

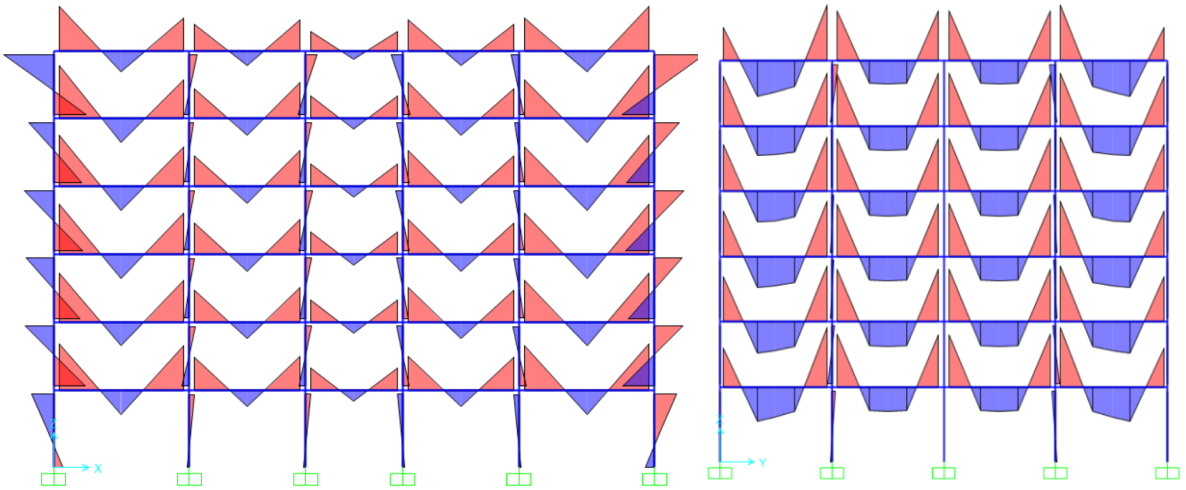

Fig. 3.43 Bending moments in the X and Y directions due to gravity loads in the seismic combination

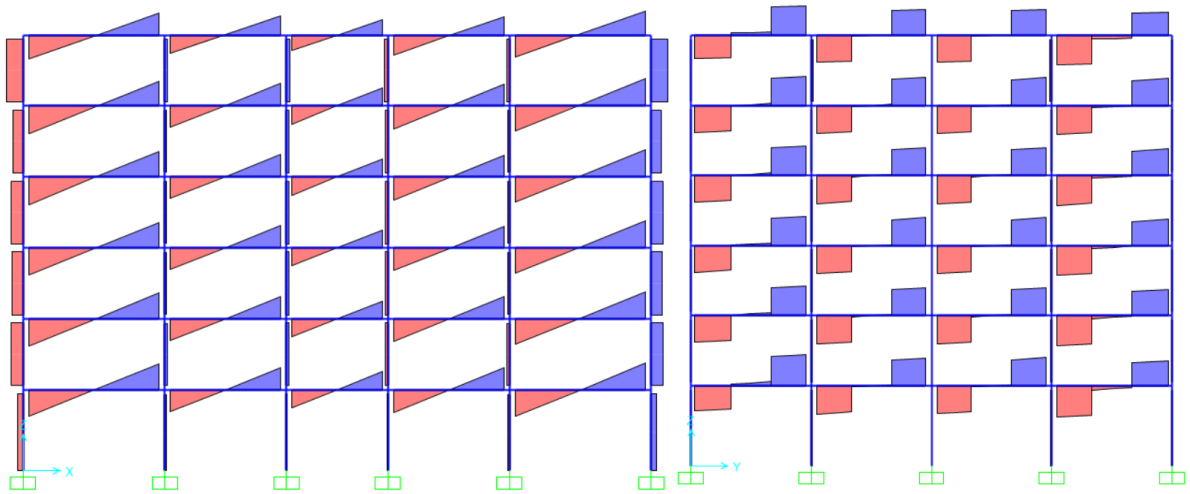

Fig. 3.44 Shear forces in the X and Y directions due to gravity loads in the seismic combination

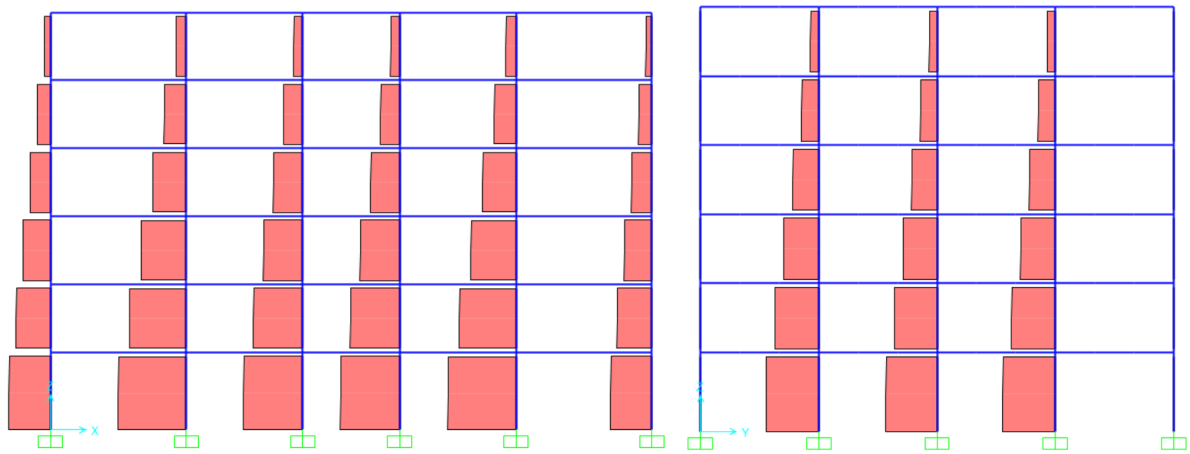

Fig. 3.45 Axial compression forces in the X and Y directions due to gravity loads in the seismic combination

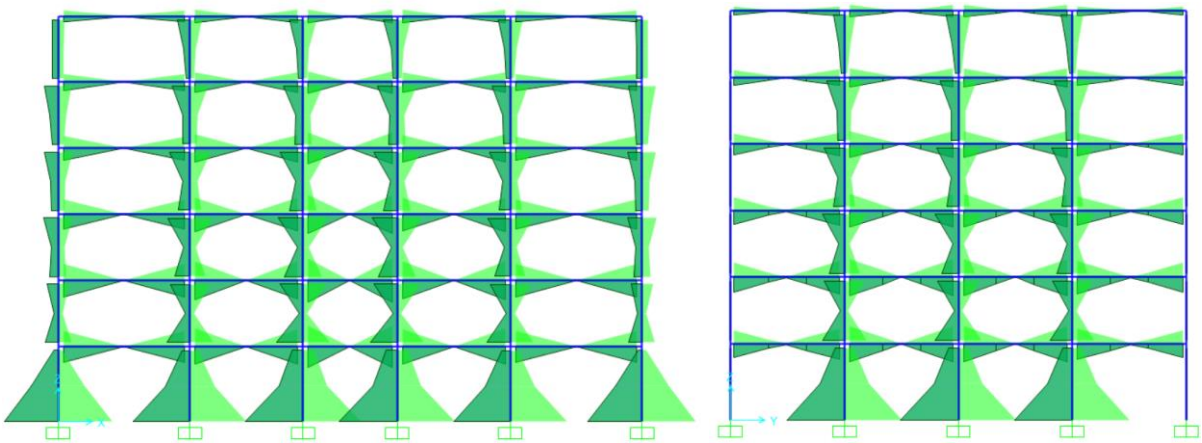

Fig. 3.46 Envelope of bending moments in the X and Y directions due to seismic actions

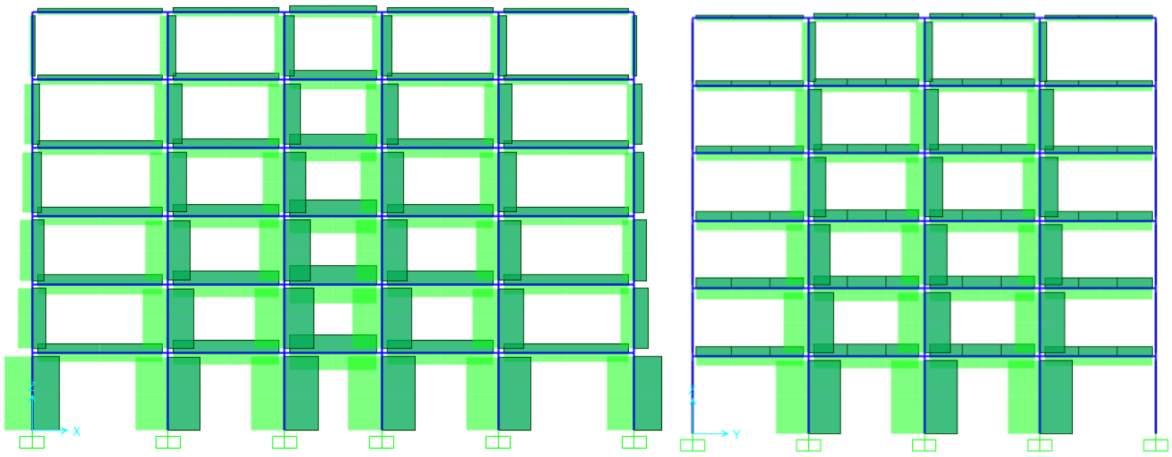

Fig. 3.47 Envelope of shear forces in the X and Y directions due to seismic actions

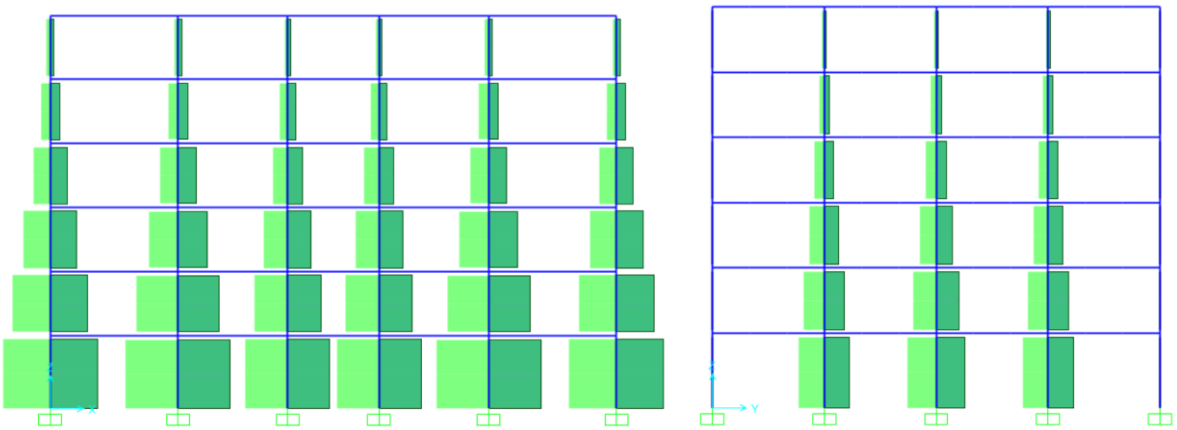

Fig. 3.48 Envelope of axial compression forces in the X and Y directions due to seismic actions

In the Table 3.22 it shown the base shear forces obtained from the linear modal response spectrum in the X and Y directions after performing the envelope of the 32 seismic combinations.

Table 3.22 Base shear forces in each direction due to the linear modal response spectrum

F_x(kN)	F_y(kN)
1072	1168

Contrary to the lateral force method, due to the combination of all modes of vibration in a quadratic way, the sign of the forces disappears, all of them being positive. Therefore, internal forces diagrams do not make physical sense. For this reason, the seismic action (A_{Ed}) should be considered acting in the positive and negative direction.

Furthermore, the modal response spectrum analysis is quite conservative as it only provides the maximum values applied to the structural elements. For instance, the columns are subjected to the maximum bending moments in the strong and weak axis, as well as the maximum axial load simultaneously, because the time variation is not taking into account such as it if does the nonlinear dynamic analysis, (Landolfo et al. (2017)).

Despite these limitations, the linear modal spectrum analysis is the most widely used for seismic design and is the one recommend by EN 1998-1, (CEN, 2004).

On the other hand, once the linear modal response spectrum has been performed in the ULS, second order effects ($P-\Delta$) under the seismic design must be taken into account to guarantee the stability of the structure and prevent any collapse if the following equation is not satisfied as establishes clause 4.4.2.2.

$$\theta = \frac{P_{tot} d_r}{V_{tot} h} \leq 0.1 \tag{3.63}$$

where

θ is the interstorey drift sensitive coefficient

P_{tot} is the total gravity load at and above the storey considered

d_r is the design interstorey drift evaluated as the difference between the current displacement of the storey and the bottom storey

V_{tot} is the total seismic storey shear

h is the interstorey height

If the interstorey drift sensitive coefficient value (θ) is between 0.1 and 0.2, second-order effects can be considered applying the factor α to the seismic internal forces, which is obtained as $1/(1-\theta)$.

For factors greater than 0.2, second order analysis should be performed, while values above 0.3 are not acceptable. In the latter case, the design of the building has to be improved.

The interstorey displacements has been obtained as specifies clause 4.3.4.

$$d_s = q_d d_e \tag{3.64}$$

where

q_d is the displacement behaviour factor equal to q, in this case 6.5

d_e is the displacement of the structural system determined by a linear analysis basic on the design spectrum

d_s is the current displacement of the same point due to the seismic action

Tables 3.23 and 3.24 summarizes the inter-storey drifts and the drift sensitive factors for each storey in the X and Y directions respectively.

3.23 Inter-storey drift and drift sensitive factor for X direction

Storey	P_{total}(kN)	V_{total}(kN)	h(mm)	Displacement(mm)	Interstorey drift(mm)	Θ	α
I	22818	1123	4000	34	34	0.17	1.21
II	18970	1036	3500	74	41	0.21	1.27
III	15158	915	3500	112	37	0.18	1.21
IV	11347	770	3500	142	31	0.13	1.15
V	7535	586	3500	165	22	0.08	-
VI	3723	356	3500	178	14	0.04	-

3.24 Inter-storey drift and drift sensitive factor for Y direction

Storey	P_{total}(kN)	V_{total}(kN)	h(mm)	Displacement(mm)	Interstorey drift(mm)	Θ	α
I	22818	1197	4000	29	34	0.16	1.20
II	18970	1108	3500	64	41	0.20	1.25
III	15158	979	3500	95	37	0.16	1.20
IV	11347	819	3500	121	30	0.12	1.14
V	7535	618	3500	140	22	0.08	-
VI	3723	358	3500	151	13	0.04	-

It is highlighted there is a considerable interstorey drift in the first floors. In consequence, second order effects should be considered in the seismic design with the amplification factor α.

This is a clear consequence of the flexibility of the building due to the structural typology. Furthermore, this expression has conditioned the election of cross-section of the primary beams. Despite the fact that lower profiles would have verified the ULS and SLS for the static and seismic design, it was necessary to reduce the inter-storey drift produced by the seismic actions in the ULS.

3.6 CAPACITY DESIGN VERIFICATIONS

3.6.1 Strong column – weak beam principle

According to clause 4.4.2.3(4) of EN 1998-1, (CEN, 2004c) partial global plastic failures mechanism, for instance the creation of a limited number of plastic hinges, or the formation of soft story mechanism must be avoided.

Therefore, in a first instance, the principle of strong column-weak exposed in the chapter 2 should be verified.

Table 3.25 shows the bending moment resistance of the primary elements.

Table 3.25 Characteristics of the cross sections of the principal beams and columns

Profile	Axis	$f_y(Mpa)$	W_{pl}(cm3)	$M_{pl,Rd}$(kNm)
HEM360	Major	275	4990	1372
HEM360	Minor	275	1942	534
IPE450	Major	235	1702	400
IPE400	Minor	235	1307	307

The Eq. 2.1 has been applied for the beam-column joints of the building to determine if the principle of strong column-weak beam is satisfied. In the following, several examples are shown.

- Exterior joints in the X direction with major axis:

$$\sum M_{rc} = M_{c,major1} + M_{c,major2} = 2744\ kNm$$

$$\sum M_{rb} = M_{rb1,IPE400} = 307\ kNm$$

$$\frac{\sum M_{rc}}{\sum M_{rb}} = 8.93 > 1.3$$

- Interior Joint in the X direction with major axis:

$$\sum M_{rc} = M_{c,major1} + M_{c,major2} = 2744\ kNm$$

$$\sum M_{rb} = M_{rb1,IPE400} + M_{rb2,IPE400} = 614kNm$$

$$\frac{\sum M_{rc}}{\sum M_{rb}} = 4.51 > 1.3$$

- Interior joints in the X direction with minor axis:

$$\sum M_{rc} = M_{c,minor1} + M_{c,minor2} = 1068\ kNm$$

$$\sum M_{rb} = M_{rb1,IPE400} + M_{rb2,IPE400} = 614\ kNm$$

$$\frac{\sum M_{rc}}{\sum M_{rb}} = 1.73 > 1.3$$

- Interior joints in the Y direction with major axis:

$$\sum M_{rc} = M_{c,major1} + M_{c,2} = 2744\ kNm$$

$$\sum M_{rb} = M_{rb1,IPE450} + M_{rb2,IPE450} = 800\ kNm$$

$$\frac{\sum M_{rc}}{\sum M_{rb}} = 3.43 > 1.3$$

- Interior joints in the Y direction with minor axis:

$$\sum M_{rc} = M_{c,minor1} + M_{minor,2} = 1068kNm$$

$$\sum M_{rb} = M_{rb1,IPE450} + M_{rb2,IPE450} = 800\ kNm$$

$$\frac{\sum M_{rc}}{\sum M_{rb}} = 1.34 > 1.3$$

In spite of the fact that the principle is widely verified in the joints where the major axis of the columns connects to the beam, in the minor ones the ratios are closer to 1.3, especially in the joints connecting the beams IPE 450.

In fact, in a previous phase of the building design, HE550B columns were considered. However, the internal joints in the Y direction did not verify the principle because of the lack of inertia in the minor axis of the columns. For this reason, it was decided to use heavy profiles as HEM.

Furthermore, some joints at the top of the building in the roof have not been verified this condition. Hence, several plastic hinges at the roof level may appear.

3.6.2 Verification of the dissipative elements

The dissipative elements of the building, must satisfy the Equations 2.2, 2.3 and 2.4 according to the capacity designing method. Moreover, the bottom part of the columns in the ground storey are considered also as dissipative elements, then the same equations have been applied.

The design forces should be determined combining the gravity loads in the seismic combination as well as the internal forces produced by seismic action, where the magnification factor α to the considerer the P-A effects should be included.

$$M_{Ed} = M_{Ed,G} + \alpha M_{Ed} \tag{3.65}$$

$$N_{Ed} = N_{Ed,G} + \alpha N_{Ed} \tag{3.66}$$

$$V_{Ed} = V_{Ed,G} + \alpha V_{Ed,M} \tag{3.67}$$

where

$M_{Ed,G}$, $N_{Ed,G}$ and $V_{Ed,G}$ are the internal forces due to the gravity loads in the seismic combination

M_{Ed}, N_{Ed} are the internal forces due to the seismic actions

The shear force demand ($V_{Ed,M}$) is calculated considering the apparition of two plastic hinges at both ends of the dissipative beam.

$$V_{Ed,m} = \frac{M_{pl,A} + M_{pl,B}}{L_h} \tag{3.68}$$

where

$M_{pl,A}$ and $M_{pl,B}$ are the plastic moments of the beam at both ends

L_h is the distance between both section considering the actual dimensions of the beam-to-columns joints

The most requested beams under seismic actions are located at the second floor (Fig. 3.49). Since the beams in the X direction are subjected to only a fraction of the gravity loads and this direction presents more flexibility, the requested seismic forces are lower producing a factor Ω higher, which affects to the internal forces applied to the columns in the X direction.

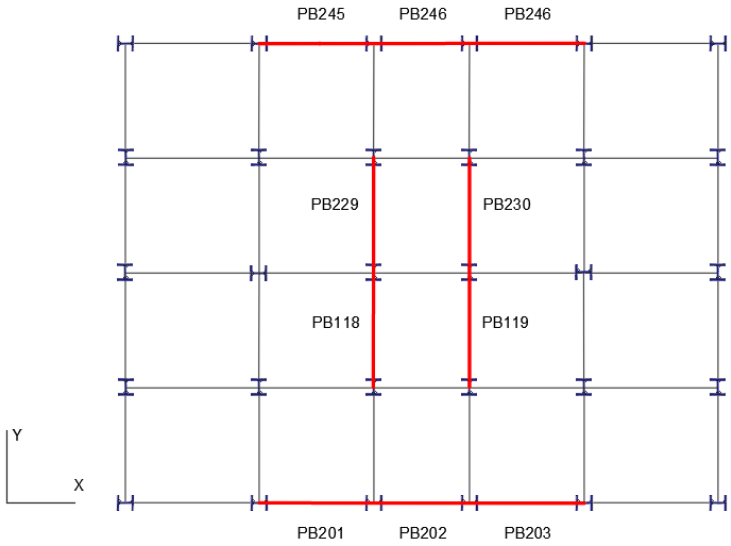

Fig. 3.49 Most requested beams under the seismic actions

Tables 3.26 and 3.27 show the verification of the most requested beams of the building under bending moments (Eq. 2.2) and shear resistance (Eq. 2.4) to verify the capacity design.

Moreover, the Ω factor which accounts the overstrengh, which is the inverse value of the strength ratios, that presents the dissipate elements under the seismic actions has been also included in the tables.

Further information about the verification of all the dissipative elements are shown in the Annex 2.

Table 3.26 ULS ratio and Ω factor for most requested dissipative beams

Direction	Item	Profile	M_{Ed_G}(kNm)	M_{Ed_E}(kNm)	α	M_{Ed_Total}(kNm)	$M_{pl,Rd}$(kNm)	Ω	Eq.2.2
X	PB201	IPE400	-14	83	1.27	119	307	2.58	0.39
X	PB202	IPE400	-10	97	1.27	132	307	2.32	0.43
Y	PB218	IPE450	-59	69	1.21	143	400	2.15	0.46
Y	PB229	IPE450	-59	69	1.21	143	400	2.15	0.47

Table 3.27 Shear ratio for ULS

Direction	Item	Profile	L(m)	L_h(m)	$V_{Ed,G}$(kN)	$V_{Ed,M}$ (kN)	α	V_{Ed_total}(kN)	Eq. 2.4
X	PB201	IPE400	6	5.45	15	113	1.27	128	0.22
X	PB202	IPE400	5	4.45	13	138	1.27	163	0.28
Y	PB218	IPE450	6	5.45	50	113	1.21	86	0.15
Y	PB229	IPE450	6	5.45	51	113	1.21	86	0.15

It can be stated the dissipative elements are capable to resist the seismic actions. Hence, the capacity design has been verified for the dissipative elements.

Due to using a behaviour factor equal to 6.5, a great reduction of the of the values of the internal forces have been produced. In consequence, the dissipative elements present considerably overstrength.

In consequence, the Ω factor to be considered for the columns is equal to 2.32 for the X direction and 2.15 for the Y direction, which are the minimum ones of all the dissipative beams analysed. Therefore, the verifications of the non-dissipative elements became more restrictive to satisfy the capacity design.

3.6.4 Verification of the non-dissipative elements

In order to verify the columns of the building under seismic actions, which are non-dissipative elements, the designing forces may be obtained from the Equations 2.5, 2.6 and 2.7 of the chapter 2. The overstrengh factor of the material equal to 1.25 as well as second order effects with the factor α has been considered.

The most requested columns are located at the second-storey, in the central frame of the building and the outside frame, where important axial forces and bending moments on both axes acts simultaneously (Fig. 3.50).

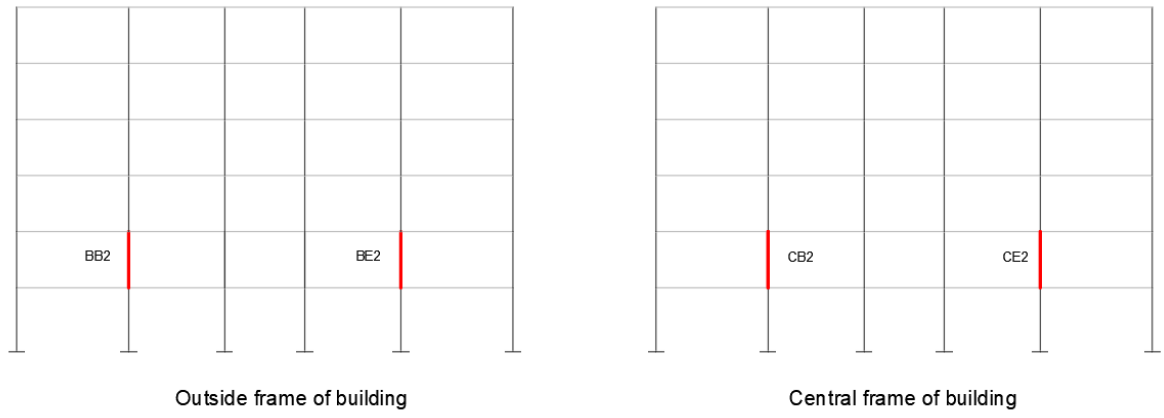

Fig. 3.50 Most requested columns due to the seismic actions

The verification of the columns is shown in the Tables 3.28 and 3.29 considering the orientation of each column, being 0º parallel to the X direction and 90º parallel to the Y direction of the plan view of the building as well as the internal forces produced in the major axis (3) and the minor one (2) shown in absolute values.

Has been considering the resistance of the cross-sections under biaxial-bending (Eq. 3.33) and the interaction of the flexural buckling and lateral torsional buckling by combination factors exposed in the Annex B of EN 1993-1, (CEN, 2005b) which are the Equations 3.40 and 3.41.

The verification under shear forces has been performed to account possible reductions of the flexural capacity of the cross-sections using the Eq. 2.4 applied to the major and minor axis.

Table 3.28 Verification for the most requested non-dissipative elements

Item	Θ	Ω_x	Ω_y	N_{Ed}(kN)	$M_{2,Ed}$(kNm)	$M_{3,Ed}$(kNm)	Eq. 3.33	Eq. 3.40	Eq. 3.41
BB2	0º	2.43	2.09	905	264	272	0.52	0.70	0.92
CB2	90º	2.43	2.09	984	285	297	0.58	0.65	0.88

Table 3.29 Shear ratios for ULS

Item	Θ	Ω_x	Ω_y	$V_{Ed,2}$(kN)	$V_{Ed,3}$ (kN)	Eq. 2.4 (2)	Eq. 2.4 (3)
BB2	0º	2.43	2.09	173	173	0.15	0.10
CB2	90º	2.43	2.09	191	192	0.12	0.12

It is concluded the non-dissipative elements verifies the capacity design. The utilization of heavy profiles HEM has been necessary to present sufficient flexural strength in both axes to verify the internal forces produced by the seismic actions increased considerably by the overstrengh factors mentioned previously.

3.6.5 Damage limitation requirement

The damage limitations under frequent seismic actions, as it was explained in the chapter 2, should be verified taking into account the seismic action in the DLS.

Imposing a limit of the interstorey drift ratio equal to 0.5%, considering there are brittle non-structural elements attached to the structure and a reduction displacement factor ν equal to 0.5 for an importance class II.

In order to perform the verification, the linear modal response spectrum have been applied considering the earthquake in the DLS to obtain the displacement in each storey in the X and Y direction. Subsequently, applying the Eq. 28, which considers the height of the storeys and the interstorey-drift, the following inter-storey drift ratios have been obtained (Fig. 3.51).

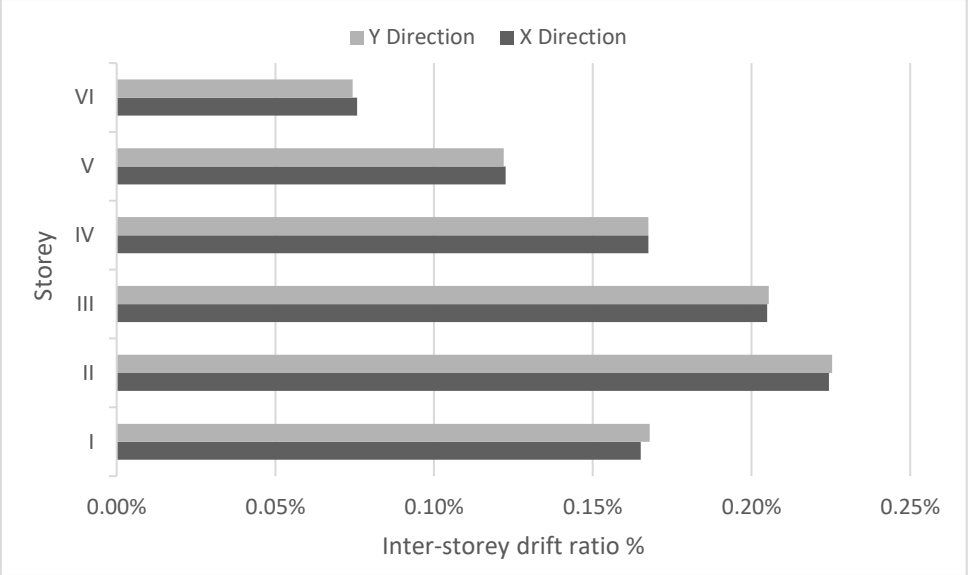

Fig. 3.51 Interstorey-drift ratios produced in each storey

Hence, since all the ratios are below to the impose α factor equal to 0.5%, the building satisfies the damage limitation requisite under the frequent seismic actions.

3.7 NONLINEAR STATIC ANALYSIS

3.7.1 Nonlinear modelling of the building

To finalize the design of the steel building, the nonlinear static analysis (Pushover) and the N2 method exposed in the section 2.2.3 of chapter 2 have been carried out.

In a first step, to model the nonlinear behaviour of the structure, the plastic hinges defined by the FEMA 356 (ASCE, 2000) have been utilized for the primary elements, which are the principal beams and the column, using the software SAP2000 (Fig. 3.52).

In the case of the beams, plastic hinges type M, whose nonlinear behaviour is activated at the end of the beams by flexural solicitations in the major axis, has been considered.

For the columns, the nonlinear behaviour of the structural element is conditioned by the axial forces acting simultaneously with bending moments applied in the major and minor axes. Thus, plastic hinges type N-M that takes into account these interactions have been used in the model. Moreover, the nonlinear modelling of one frame of the building it is shown in Fig. 3.53 as example.

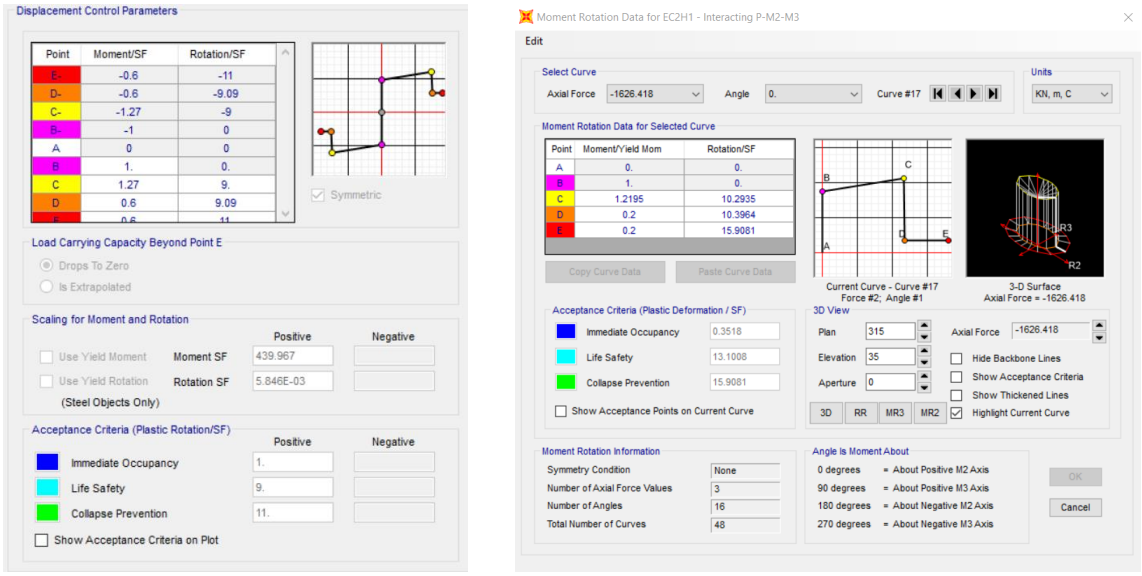

Fig. 3.52 Plastic hinges used for beams a) and columns b); SAP2000

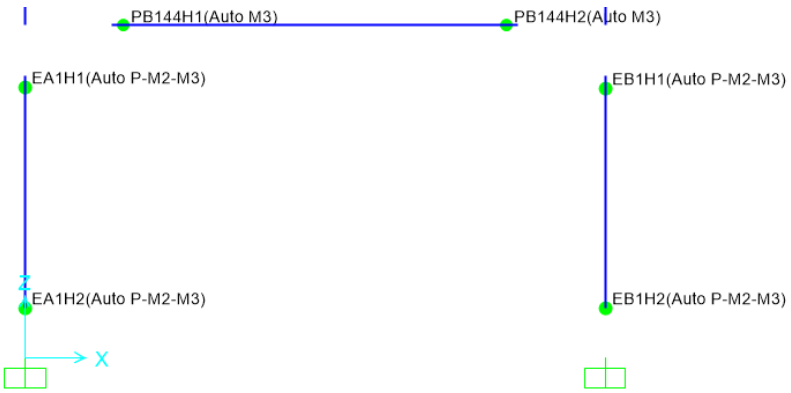

Fig. 3.53 Nonlinear modelling of the frames; SAP2000

3.7.2 Pushover analysis

In order to obtain the modal distribution of lateral forces in the X and Y directions, the eigenvalues (ϕ_i) of the fundamentals period of vibration, which are the Mode 1 for X direction and Mode 2 for the Y direction, have been considered in Eq. 3.69. These vectors have been normalized (ϕ_N) considering a top displacement equal to 1. Moreover, forces also have normalized by the seismic mass (m_i) of the top storey.

On the other hand, for the uniform distribution the Eq. 3.70 has been applied.

Tables 3.30 and 3.31 show the calculation of the distribution forces for the X and Y direction, and the Figures 3.54 and 3.55 show graphically the uniform shape of the lateral loads.

$$F_i = m_i \phi_N \quad (3.69)$$

$$F_i = m_i \quad (3.70)$$

Table 3.30Force shape for the X direction

Storey	m_i(kN s2/m)	1STMode	Modal Pattern			Uniform Pattern		
		ϕ_i(m/s2)	ϕ_N(m/s2)	F_i(kN)	F_N(kN)	ϕ_N(m/s2)	F_i(kN)	F_N(kN)
VI	366	0.029	1.00	366	1.00	1.00	366	1.00
V	388	0.027	0.92	359	0.98	1.00	388	1.06
IV	388	0.023	0.80	310	0.85	1.00	388	1.06
III	388	0.018	0.62	242	0.66	1.00	388	1.06
II	388	0.012	0.41	159	0.44	1.00	388	1.06
I	390	0.005	0.18	72	0.20	1.00	390	1.07

Table 3.31 Force shape for the Y direction

Storey	m_i(kN s2/m	2STMode	Modal pattern			Uniform Pattern		
		ϕi(m/s2)	ϕN(m/s2)	F_i(kN)	F_N(kN)	ϕ_N(m/s2)	F_i(kN)	F_N(kN)
VI	366	0.029	1.00	366	1.00	1.00	366	1.00
V	388	0.026	0.93	359	0.98	1.00	388	1.06
IV	388	0.023	0.80	311	0.85	1.00	388	1.06
III	388	0.018	0.63	243	0.66	1.00	388	1.06
II	388	0.012	0.41	161	0.44	1.00	388	1.06
I	390	0.005	0.19	73	0.20	1.00	390	1.07

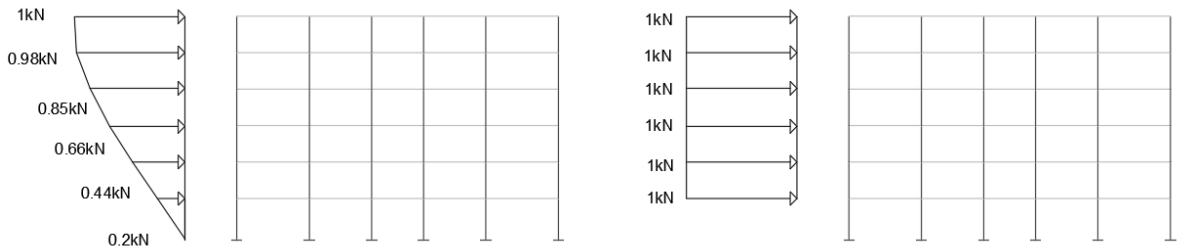

Fig. 3.54 Modal and uniform forces shapes normalized in the X direction

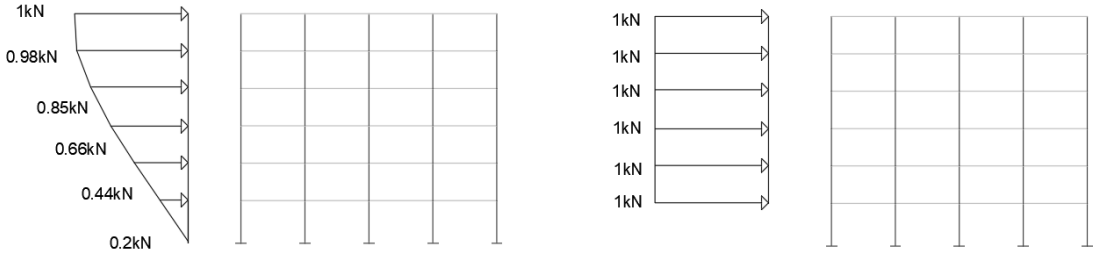

Fig. 3.55 Modal and uniform forces shapes normalized in the Y direction

Normally, the ultimate base shear strength (V_u) of the modal distribution is lower than the uniform one, but present larger displacements. This behaviour can be observed clearly in the Figures 3.56 and 3.57. As it was established in the chapter 2, since the non-adaptive pushover has been performed, the actual behaviour of the building is between both distributions.

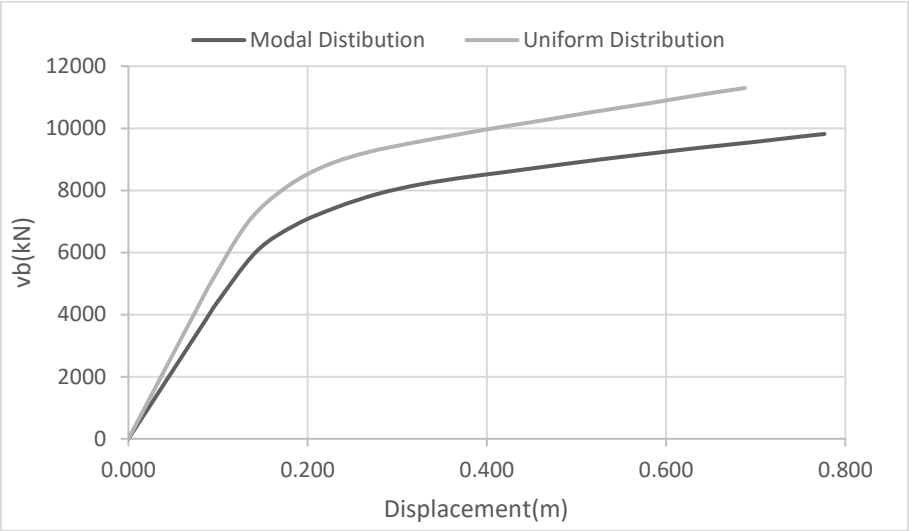

Fig. 3.56 Capacity curve X direction

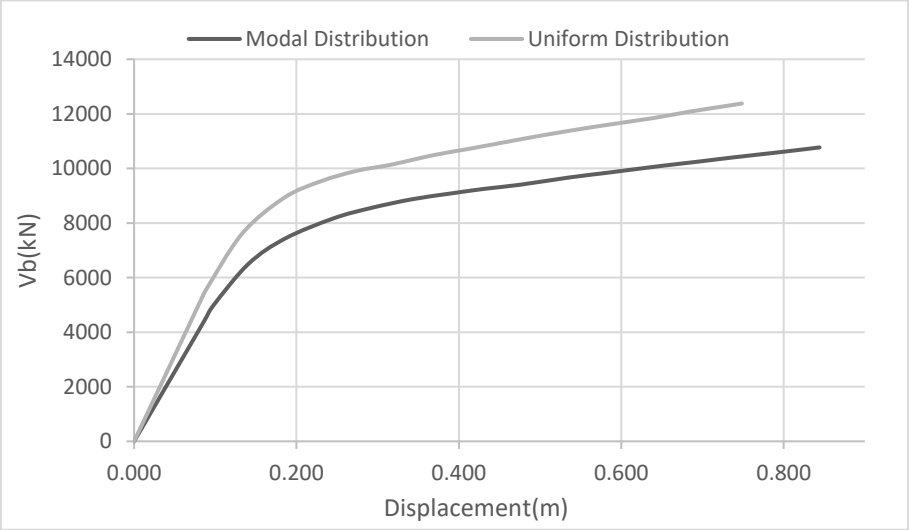

Fig. 3.57 Capacity curve in Y direction

It is highlighted the ductile behaviour that presents the building in both directions, reaching the plastic mechanism without sharply drops of resistance. Since all the primary elements are ductile, and there are no infills or bracings, no brittle shear failure produce the formation of the local mechanism. It is noted that resistance in the Y direction is higher due to the beams IPE 450 placed in this direction.

The yielding forces (V_Y) of the building for each distribution, where the first plastic hinge appears, and ultimate base shear forces (V_u) at the base of the building before reaching the plastic mechanism are summarize in the Table 3.32. Moreover, the overstrengh factor (α_u/α_i) can be determined dividing both forces.

Table 3.32 Overstrengh factor for the 4 pushover analyses

Direction	Force Profile	V_u(kN)	V_y(kN)	α_u/α_i
X	Modal	9724	4368	2.23
X	Uniform	11297	4212	2.68
Y	Modal	10097	4960	2.04
Y	Uniform	12080	5478	2.21

The minimum overstrengh factor obtained by the 4 pushover analyses is equal to 2.04, which is higher than the value 1.3 value used to determine the behaviour factor of the building (q) applied to the linear modal response spectrum analysis. Thus, the assumption of considering a behaviour factor equal to 6.5 can be stated as correct according to the pushover analysis.

On the other hand, the plastic hinges appeared in the building for the X and Y directions before reaching the plastic mechanism are shown in the figures 3.58 and 3.59.

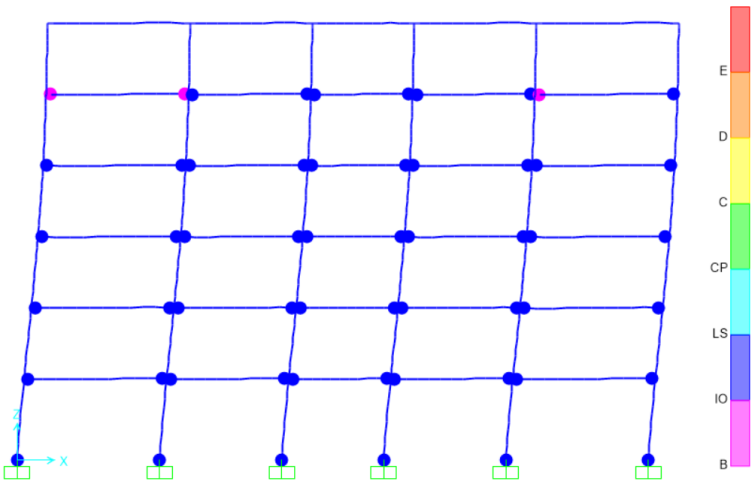

Fig. 3.58 Plastic hinges activated in the X direction before reaching the plastic mechanism

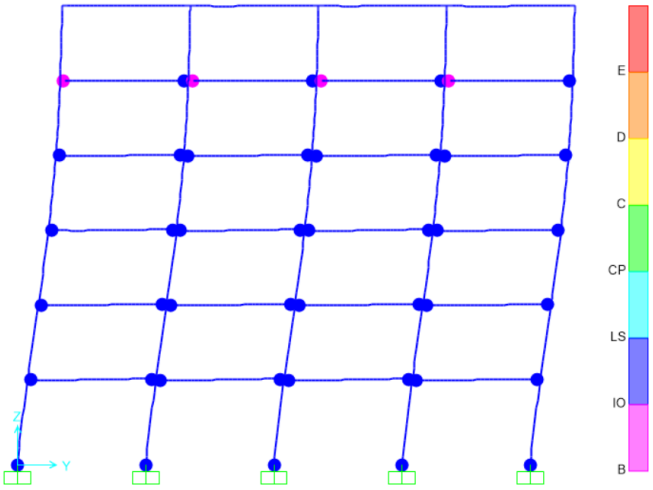

Fig. 3.59 Plastic hinges activated in the 3.33 direction before reaching the plastic mechanism

It can be noticed that for both directions, plastic hinges only appear in the dissipative elements, which are the principal beams, while the columns remain in the elastic domain, verifying the capacity design performed in the building.

Moreover, as it was expected, also appears plastic hinges at the bottom of the columns in the ground floor. Non soft-storeys appears due to the regularity in elevation of the building, performing a ductile behaviour dissipating enough energy.

3.7.3 Application of the N2 method

In order to obtain the structure performance of the building subjected to the seismic actions of the L'Aquila, the N2 method has been carried out. There is no limitation of applying this method in the building since is completely regular in plan and elevation, activating a modal mass of 83% and 84% respectively with the fundamental periods in the X and Y directions.

From Table 3.29 is possible to obtain the mass (m^*) of the SDOF system that is equal to $1508 kN\, s^2/m$. Therefore, applying the Eq. 2.21 for both directions, the transformation factor (Γ) is equal to 1.28.

In order to transform the capacity curves of the MDOF showed in the Figures 3.42 and 3.43 into a SDOF system, Eq. 2.22 and 2.23 have been applied with the transformation factor. Subsequently, the linearization of the capacity curves has been performed applying the procedure presented in the chapter 2 that considers the equivalence of areas.

As example, the transformation of the MDOF capacity curve into a SDOF system with its corresponding bilinear curve for the modal distribution in the X direction is shown in Fig. 3.60.

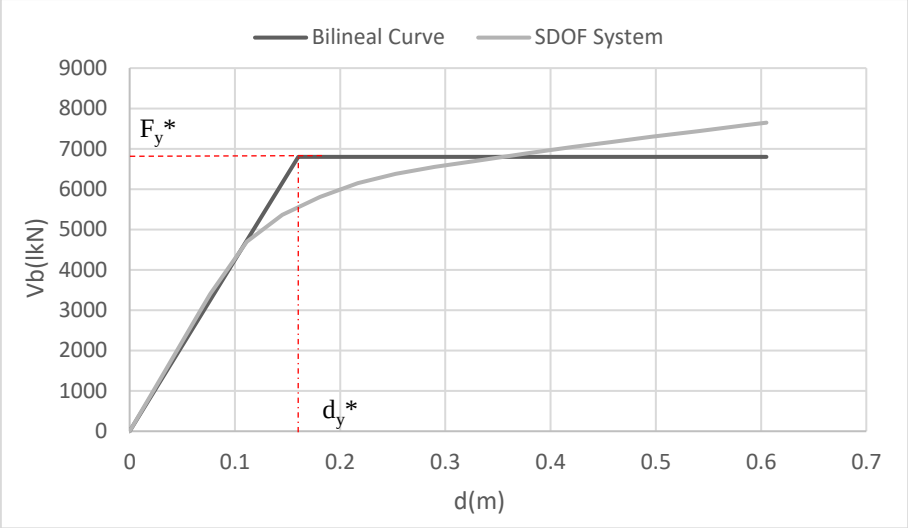

Fig. 3.60 Capacity curve of the SDOF system with its bilinear curve respectively

The same procedure has been carried out four times for each analysis. Once the bilinearization is performed, the yielding force of the system (F_y^*) and its corresponding displacement (d_y^*) can be determined in order to determine the equivalent stiffness (k^*) and the period of vibration (T^*) from Eq. 2.24 and Eq. 2.25.

Subsequently, considering the elastic spectrum of L'Aquila in the ULS, the requested elastic displacement (d_e^*) for the system can be determine using the Eq. 2.30. Owing to the flexibility of the building which produces important periods of vibration, allows determining the target displacement (d_t^*) as the elastic one from the elastic spectra (Table 3.33).

As final step, the transformation factor (Γ) should be multiplied by the target displacement (d_t^*) in order to determine the target displacement for the MDOF system to perform again the nonlinear analysis.

Table 3.33 Calculation of the target displacement for the MDOF

Direction	Force Profile	F_y^*(kN)	d_y^* (m)	T*(s)	d_e^*(m)	d_t^*(m)	d_t(m)
X	Modal	6800	0.18	1.26	0.13	0.13	0.17
X	Uniform	7900	0.17	1.13	0.12	0.12	0.15
Y	Modal	7700	0.22	1.30	0.14	0.14	0.18
Y	Uniform	8800	0.19	1.13	0.12	0.12	0.15

Finally, with the target displacement (d_t), the pushover analyses have been performed with the 4 different distribution forces in other to determine the maximum rotation of the plastic hinges formed in each case ($\theta_{y,demand}$). To determine the capacity rotation of the beams, the following expression has been applied.

$$\theta_y = \frac{M_p L}{6EI} \tag{3.71}$$

where

M_p is the bending resistance of the beam

L is the lenght of the beam

EI is the bending stiffness

This capacity is multiplied by 6 according to the table 5-5 of FEMA 356, (ASCE, 2000) to obtain the $\theta_{y,capacity}$ in the LS for the seismic design.

The Table 3.34 summarizes the maximum rotation of the plastic hinges for the 4 cases.

Table 3.34 Verification of the building design with the N2 approach

Element	Direction	Force Profile	Item	$\theta_{y,demand}$ (rad)	$\theta_{y,capacity}$ (rad)	6Θy=LS	Verification
PB202	X	Modal	IPE 400	0.013	0.007	0.040	YES
PB102	X	Uniform	IPE 400	0.012	0.007	0.040	YES
PB218	Y	Modal	IPE 400	0.015	0.008	0.047	YES
PB118	Y	Uniform	IPE 400	0.014	0.008	0.047	YES

Since in all the cases the rotation capacity is higher than the demand, it is concluded the building resists the seismic actions of L'Aquila in the ULS.

CHAPTER 4: DESIGN OF THE JOINTS

4.1 PREQUALIFIED JOINTS

4.1.1 Beam-to-column joints

Beam-to-column joints are such an important key factor in the performance of the MRFs buildings that need special attention during the design phase. Since the dissipative elements are the beams, where plastic hinges are placed, joints must be designed as full-strength with sufficient overstrengh to guarantee they remain in the elastic field during an earthquake, according to the capacity design.

The objective of the current section is to discuss the design carried out of the rigid non-dissipative beam-column joints, specifically the prequalified haunched connections, which have been prepared to be integrated into a high ductility building (DCH).

The designed connections are underlined in the Fig. 4.1, whose double-sided configuration connects the girders IPE 450 and IPE 400 with the major-axis of the supporting elements HEM360. These particular joints have been studied since they are the most requested in the seismic design of the building. Therefore, the same connections can be placed in all the remaining frames of the structure.

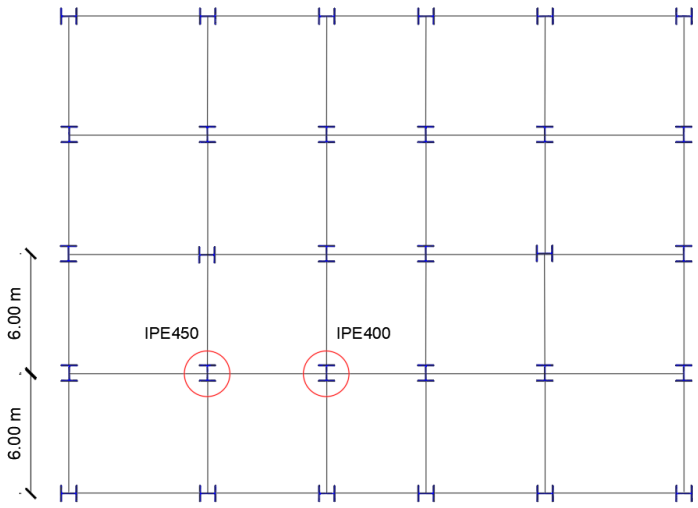

Figure 4.1 Non-dissipative joints designed

Instead of considering the internal forces provided from the different analysis performed in the chapter 3, the flexural strength of the girders (IPE 450 and IPE 400) multiplied by an overstrengh factor has been taking into account for the design of the non-dissipative joints. Hence, there are two different connections, one for each girder, due to the difference in the flexural strength as well as the geometric shape of each beam.

4.1.2 Design requirements for non-dissipative joints

Bending requirements

The first step to design non-dissipative joints is to determine the bending moments at the column face ($M_{con,Ed}$) with the Eq. 2.13. Then, the bending resistance of the connection ($M_{con,Rd}$), which can be evaluated with the component method, should satisfy the following expression.

$$\frac{M_{con,Ed}}{M_{con,Rd}} \leq 1 \tag{4.1}$$

In order to determine $M_{con,Ed}$, α is set equal to $\gamma_{sh}\gamma_{ov}$, since the joints are designed as full-strength. The factor γ_{ov} is taken equal to 1.25 while to determine the overstrengh factor γ_{sh}, Eq. 2.16 has been applied, obtaining a value equal to 1.2.

The distance from the column face to the plastic hinge may be assumed in a simplified way as the length of the haunch (Fig. 4.2).

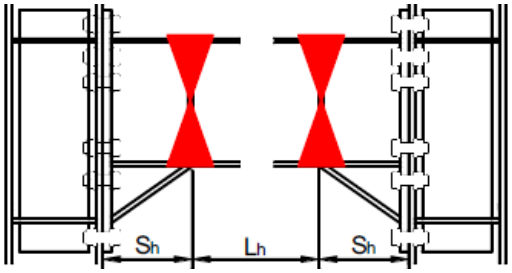

Fig. 4.2 Distance from the column face to the plastic hinge (S_h) and distance between plastic hinges (L_h); EqualJoints (Landolfo et al. 2018)

Shear requirements

The shear requirement must be satisfied to avoid a brittle failure of the connection.

$$\frac{V_{b,Ed}}{V_{con,Rd}} \leq 1 \tag{4. 2}$$

where

$V_{b,Ed}$ is the design shear force, determined by the Eq. 2.34

$V_{con,Rd}$ is the shear resistance obtained applying the component method

On the other hand, the column web panels have been designed as full strength, therefore the following equation applies.

$$\frac{V_{wp,Ed}}{V_{wp,Rd}} \leq 1 \tag{4. 3}$$

where

$V_{wp,Ed}$ is the design shear force in the column web panel (Eq. 2.37)

$V_{wp,Rd}$ is the shear resistance of the web panel, without considering the contribution of the stiffeners (Eq. 2.38).

Stiffness requirements

A minimum amount of stiffness must be guaranteed in the designed joints to satisfy the hypothesis of continuous joints, which was applied in the elastic global analysis. Otherwise, the design performed of the building would no longer valid.

According to clause 5.2.2.5 of EN 1993-1-8, (CEN, 2005c), a connection is classify as rigid if the following expression is fulfilled.

$$S_j \geq \frac{k_b E I_b}{L_b} \tag{4.4}$$

where

k_b is equal to 25 for frames without bracing system

I_b is the second moment of area of the beam

L_b is the span of the beam (centre-to-centre of the columns)

Clause 5.1.2 establishes how to evaluate the stiffness calculated of the joints in the elastic analysis. If the bending moment applied is lower than $2/3M_{j,Rd}$, the initial stiffness$(S_{j,ini})$ should be utilized in the global analysis. In the case of higher moments, a secant stiffness (S_j), which can be obtained in a simplify way, should be taken into account.

$$S_j = \frac{S_{j,ini}}{\mu} \tag{4.5}$$

where

μ is equal to 2 for bolted connections

During the elastic analysis under gravity loads, the bending moments have not been reached the $2/3M_{j,Rd}$ of the joints. Thus, the initial stiffness has been taking into account.

Nonlinear response of the joints

On the other hand, regarding the nonlinear response of the haunched joints, special attention to their ductility is not needed, since the joints are designed to remain in an elastic domain compared to the semi-rigid dissipative connections, which should be performed an exhaustive analysis to guarantee enough ductility if plastic analysis would be performed. However, the bending moment-rotation diagrams (M-Ø) have been displayed in the following section to discuss the non-linear response.

In order to perform the diagrams mentioned previously, the initial stiffness ($S_{j,ini}$) has been applied in the elastic domain, which is assumed for bending moments lower than $2/3M_{j,Rd}$ while for the non-linear response, a secant stiffness (S_j) obtained with μ factor, should be taking into account as shown the Fig. 4.3.

$$\mu = \frac{M_{j,Rd}}{M_{Ed}} \tag{4.6}$$

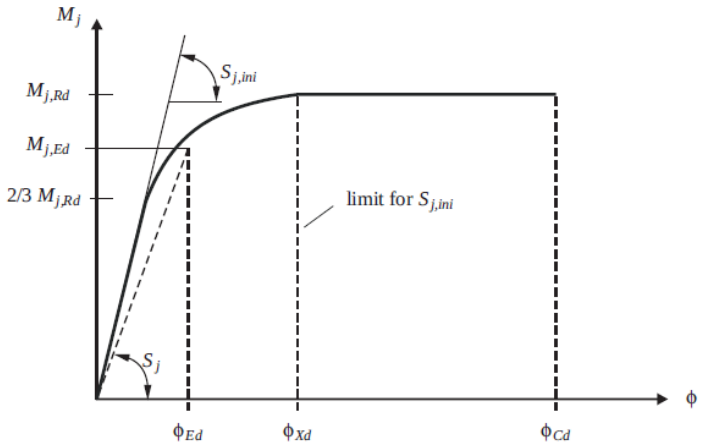

Fig. 4.3 Non-linear behaviour of the connections; Jaspart and Weynand, (2016)

The behaviour shown in the previous figure is only allowed for connections with enough ductility. Otherwise, only the elastic part must be accounted for brittle joints.

Despite the fact that the component method allows calculating the ductility for each component, there is no a proposed method to assembly all the ductility. Instead, EN 1993-1-8 (CEN, 2005c), classifies the joints as ductile or brittle according depending on their rotation capacity.

According to clause 6.4.2, a joint has sufficient ductility if these two following conditions are met:

- Either the column flange in bending or the end plate in bending governs the design bending moment of the connection.
- The thickness (t) of the component that yields should satisfy the expression 4.7.

$$t \leq 0.36d\sqrt{\frac{f_{ub}}{f_y}} \tag{4.7}$$

where

d is the diameter of the bolts

f_{ub} is the ultimate strength of the bolts

f_y is the yielding strength of the component analysed (column flange or the end-plate)

For the designed non-dissipative joints, the yielding of the end-plate governs the bending resistance. However, the thickness of the end-plat does not verify the Eq. 4.7.

Thus, an intermediate ductile behaviour are provided by the connections presenting ductility until reaching the maximum allowed rotation ($\emptyset_{cd}$) as shown in Fig. 4.4 (Jaspart and Weynand (2016)).

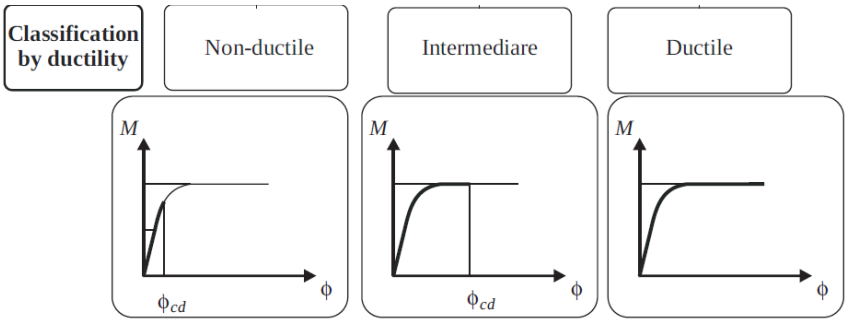

Figure 4.4 Classification by ductility ; Jaspart and Weynand, (2016)

Applying all the formulas mentioned previously, the design forces for the connections placed in beams IPE 450 and IPE 400 are shown in the Table 4.1.

Table 4.1. Design forces applied to the prequalified haunched joints

Connection	Beam	M_{Ed}(kNm)	V_{Ed}(kN)	$V_{wp,Ed}$(kN)	S_j(MN/rad)
Haunched Joint 1	IPE 450	662	296	1021	295278
Haunched Joint 2	IPE 400	510	232	900	202396

4.1.3 Design of the haunched joints

In order to design the prequalified haunched joints an iterative process has been performed to provide enough strength and stiffness to satisfy the designing forces of Table 4.1. For the first iterations, the recommendations by the Equaljoints project (Landolfo et al. (2018)), are taking into account, as well as the utilization of the software Idea StatiCa.

Despite the resistance of the column web and beam flange in tension increases for the double-side configuration, the strength of the connection is the same as the single-side configuration once the resistance of all the components is assembled using the static theorem. Thus, both configurations present same characteristics.

The components of the designed prequalified haunched joints are:

- 6 bolt-rows with 2 bolts per row composed by preloaded bolts M30 GR 10.9 placed along the extended end-plate. The holes have been placed satisfying the minimum spacing required and edge distances provided by the clause 3.5 of EN 1993-1-8 (CEN, 2005c).
- Extended end-plate 30mm thick. The thickness must be between the thickness of the beam and column flanges.
- Haunch placed at the lower part of the beam connected with the extended end-plate. Its height is 180mm and its length is 214 mm, forming an angle of 40º respect to the lower beam flange. Its width is equal to the beam flange, and the thickness of the haunched flange is 1.25 times the thickness of the beam flange, equal to 18mm. For the haunched region, web thickness should be at least the same thickness of the beam web, in this case, 10mm.
- Stiffeners 15 mm thick placed at the column and beam web to ensure a rigid connection. Fillet welds with a throat thickness (a) at least $0.55t$ connect them to the column and beam webs.
- Full penetrations welds reinforced by fillet welds are used in critical sections such as the upper beam flange and the connection of the haunched with the end-plate.

Figures 4.5 and 4.6 show the single and double-side joint configuration for the haunched joints used in the beams IPE 450. The similar layout is assumed for the beams IPE 400 (see Figures 4.7 and 4.8).

In fact, both connections are quite similar, using the same components. The main difference resides in the geometry of the extended-end plate and the bolts spacing, varying in consequence the bending resistance and the stiffness.

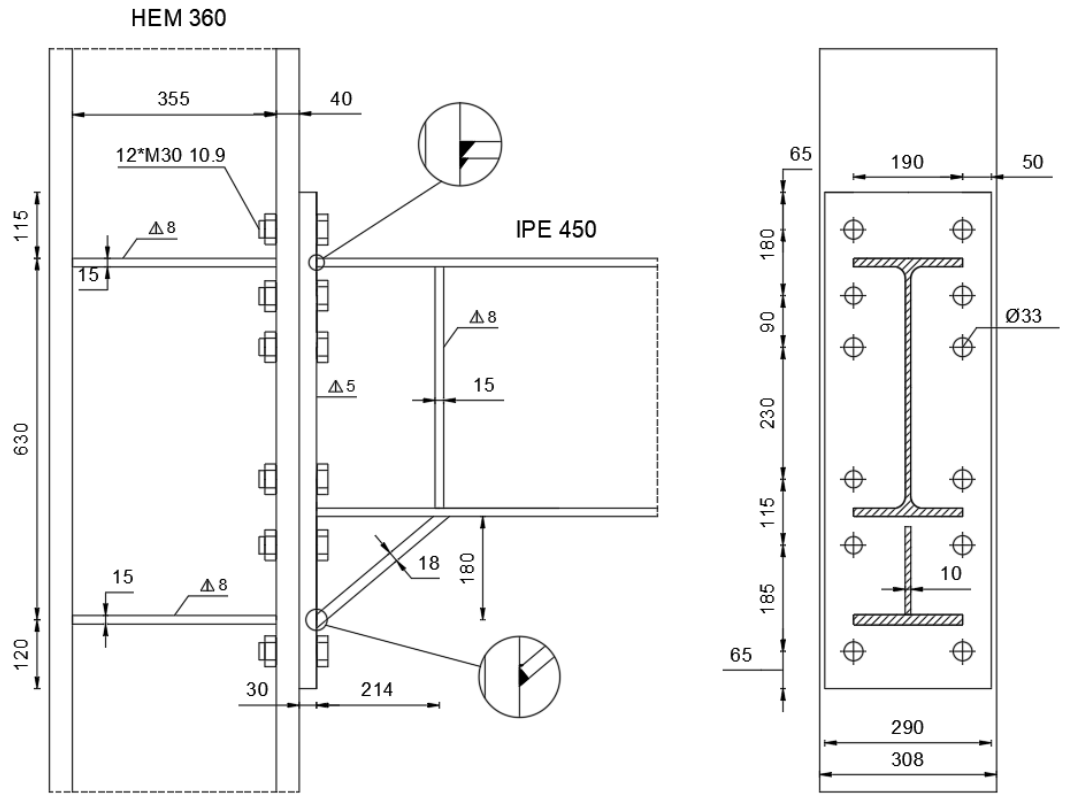

Figure 4.5 Single-side joint configuration of haunched connection of beam IPE 450

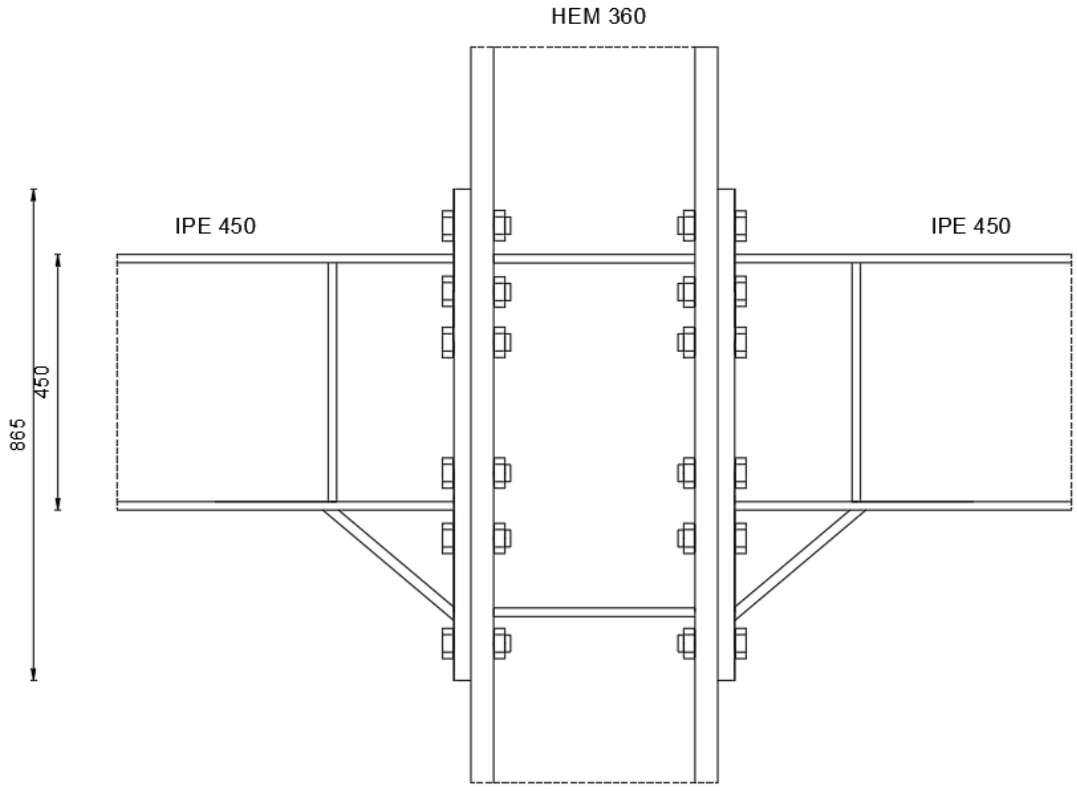

Figure 4.6 Double-side joint configuration of haunched connection of beam IPE 450

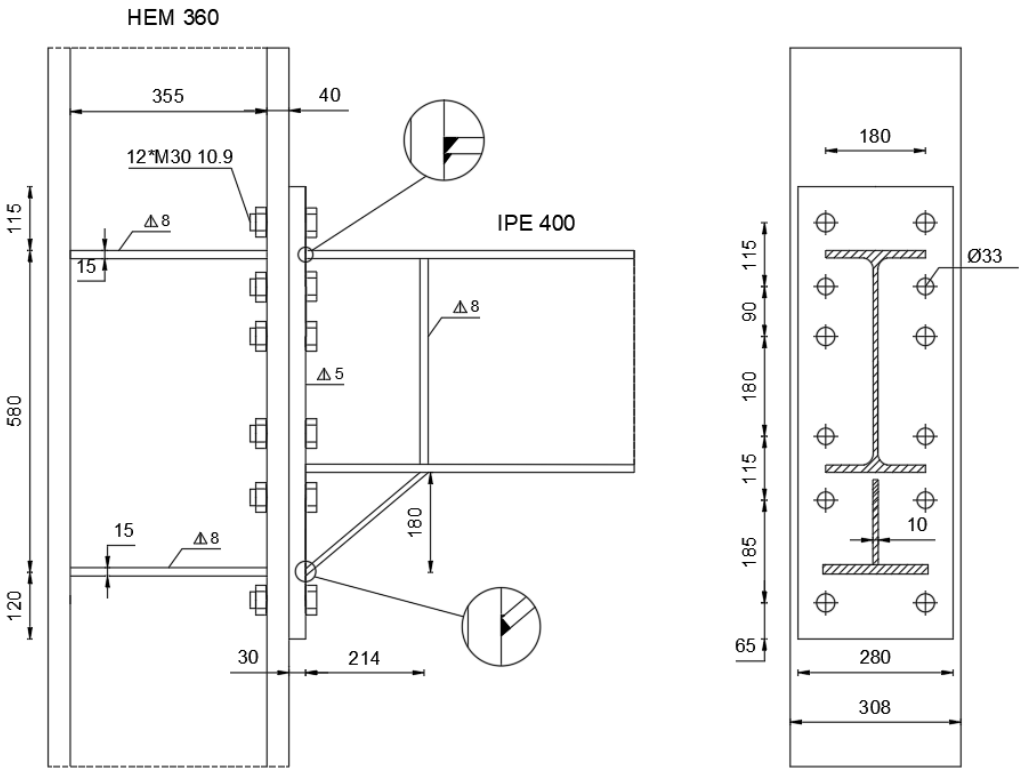

Figure 4.7 Single-side joint configuration of haunched connection of beam IPE 400

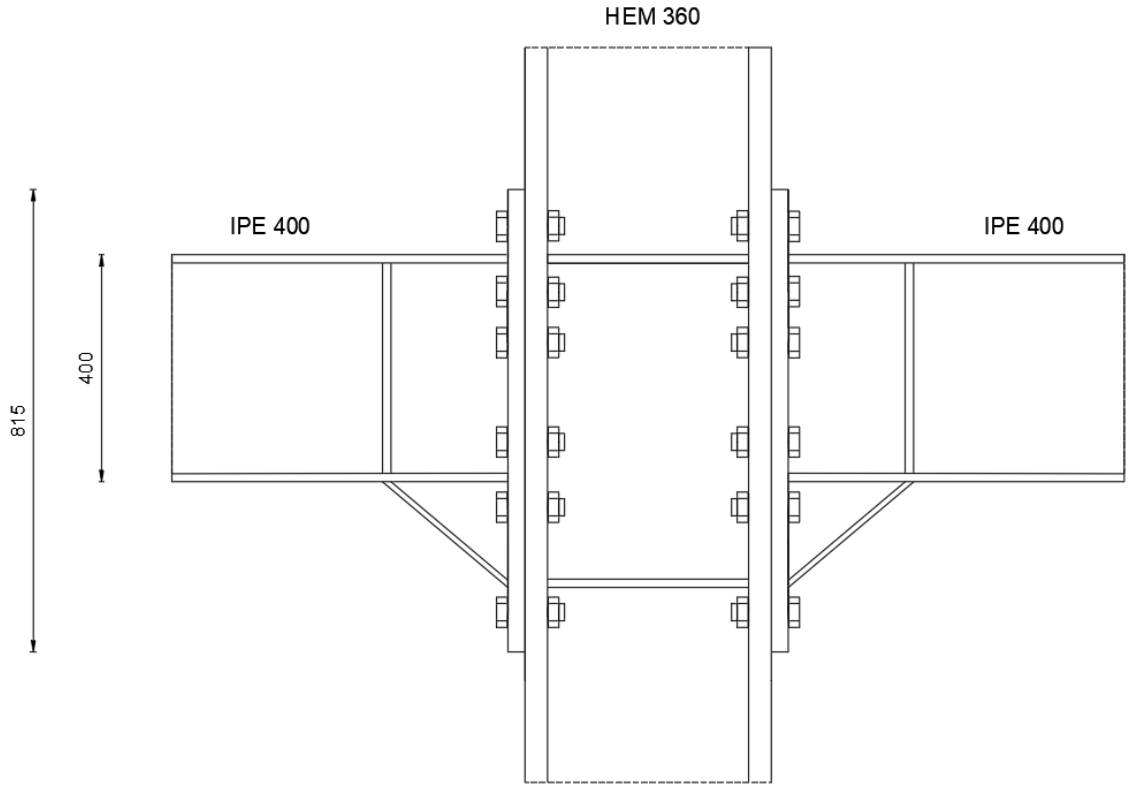

Figure 4.8 Double-side joint configuration of haunched connection of beam IPE 400

Table 4.2 summarizes the bending and shear resistance for each connection, as well as the initial and secant stiffnesses.

Table 4.2 Resistance and stiffness of the haunched joints

Connection	$M_{con,Rd}$(kNm)	V_{con}(kN)	V_{con}(kN)	S_{in}(MN/rad)	S_j(MN/rad)	$\rho_{Bending}$	ρ_{Shear}	ρ_{Colum_Panel}
IPE 450	866	333	1464	628744	479700	0.76	0.88	0.70
IPE 400	722	333	1464	591489	417584	0.70	0.69	0.62

It is concluded the design and stiffness requirements are satisfied for both joints, being able to place at the building connecting the girders with the support elements in the major-axis as non-dissipative connections.

In the following, the M-Ø diagrams which exposes the performance of the connections are shown in the Figures 4.9 and 4.10.

Since they present a limited ductility, the maximum allowable rotation assumed is 0.04 rad/m, obtained from the tests performed by the EqualJoints project. After that rotation, the failure occurs decreasing the drastically the resistance.

As it was exposed in the chapter 2, the laboratory results showed the initial stiffness is suitable to the initial stiffness (S_{in}) obtained by the analytical approach as opposite to the secant one (S_i) for the case of the full-strength joints overestimating the stiffness after reaching the plastic field.

However, since the analytical approach has been applied, they are presented in the following.

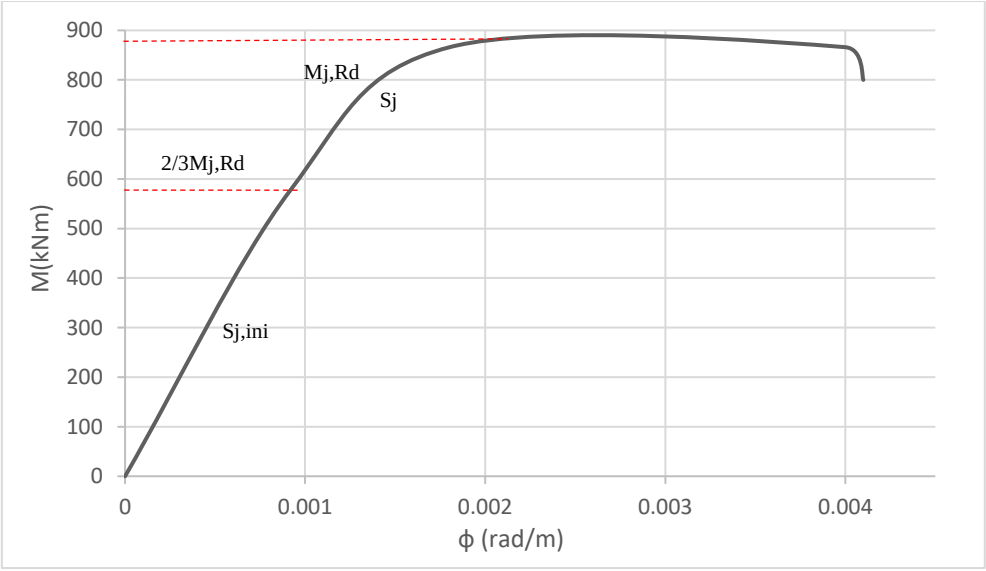

Figure 4.9 Nonlinear behaviour for the haunched joint of beam IPE 450

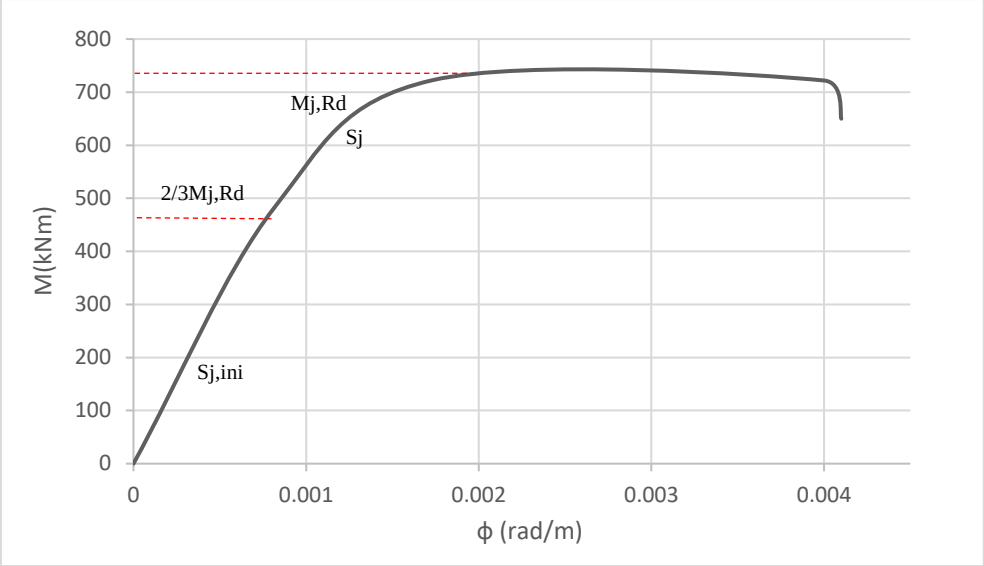

Figure 4.10 Nonlinear behaviour for the haunched joint of beam IPE 400

4.2 APPLICATION OF THE COMPONENT APPROACH

4.2.1 Bending resistance of the prequalified haunched connections

In order to determine the bending resistance of the non-dissipative connections, besides using the component method, the specific considerations proposed by the EqualJoints previously exposed in the chapter 2 have been considered;

- Under negative bending moment, only the bolt rows placed above the mid-depth of the beam cross-section without considering the haunch are assumed active.
- Under positive bending, only the bolts located beyond mid-depth of the beam cross–section including haunch are assume active.
- For negative bending moment, the centre of compression is shifted up by 50% of the haunch depth.
- The following components are not taking into account: column web panel in shear, beam flange and wed (and haunch) in compression.

Hence, the lever arm of each bolt-row to be considered under negative moments is lower than in the case of positive bending moment, owing to the consideration of the shifting of the centre of compression. In consequence, a lower bending resistance is provided in the haunched joints when negative bending moments appear.

For this reason, the most conservative case has been considered to determine the flexural resistance of the connections (Fig. 4.11).

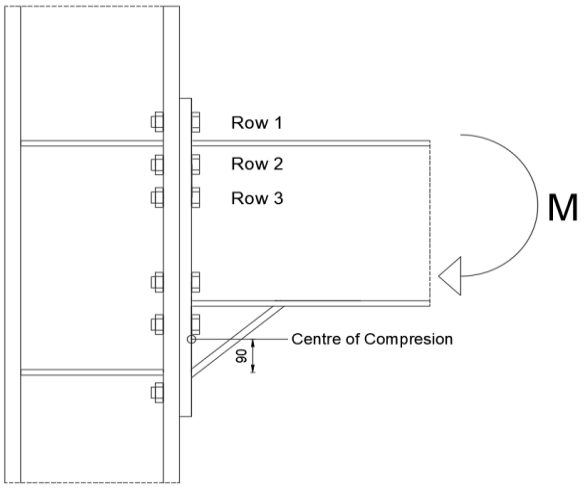

Figure 4.11 Bolt-rows considered in the analysis

The individual resistance for the following components must be calculated to obtain the final bending resistance.

- Column flange in bending
- End-Plate in bending
- Beam flange in tension
- Column web in transverse tension
- Column web in transverse compression

In order to evaluate the resistance of components subjected to tension or bending, an idealization of the tension zone has been performed utilizing the T-stub method, used for the bolted connections as exposed the clause 6.24 of EN 1993-1-8, CEN (2005c). The equivalent T-stubs models are composed by and equivalent length (l_{eff}) as the Fig. 4.12 shows.

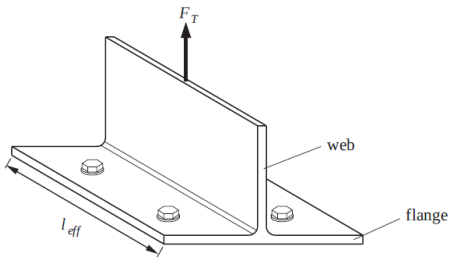

Fig. 4.12 Example of idealization of one T-Stud model; Jaspart and Weynand, (2016)

Three different failures consider the T-stub model:

- Mode 1. Failure due to the yielding of the flange or the end-plate, while the bolts remain in the elastic domain.

$$F_{T,Rd,1} = \frac{4m_{pl,rd}}{m} \tag{4.8}$$

$$m_{pl,rd} = \frac{t^2 f_y l_{eff}}{4\gamma_{m0}} \tag{4.9}$$

where

t is the thickness of the component

l_{eff1} is the effective length

m depends on the geometry of the connection

- Mode 2. Corresponds to a partial yielding of the flange combined with a failure of the bolts in tension.

$$F_{T,Rd,2} = \frac{2m_{pl,rd} + n\sum F_{t,Rd}}{m + n} \tag{4.10}$$

where

n is the geometrical dimension characterising the position of the prying force.

$\sum F_{t,Rd}$ is the summation of the tension resistance of bolts obtained by the following expression.

$$\sum F_{t,Rd} = \frac{0.9 f_u A_s}{\gamma_{M2}} \tag{4.11}$$

where

A_s is the tensile stress area of the bolts

f_u is the ultimate yield strength of the bolts

γ_{M2} is equal to 1.25

- Mode 3. Failure under tension producing low flange deformation.

$$F_{T,Rd,3} = \sum F_{t,Rd} \tag{4.12}$$

Depending on the failure mode, circular or non-circular patterns appear varying the effective length of the T-stub model (Figure 4.13).

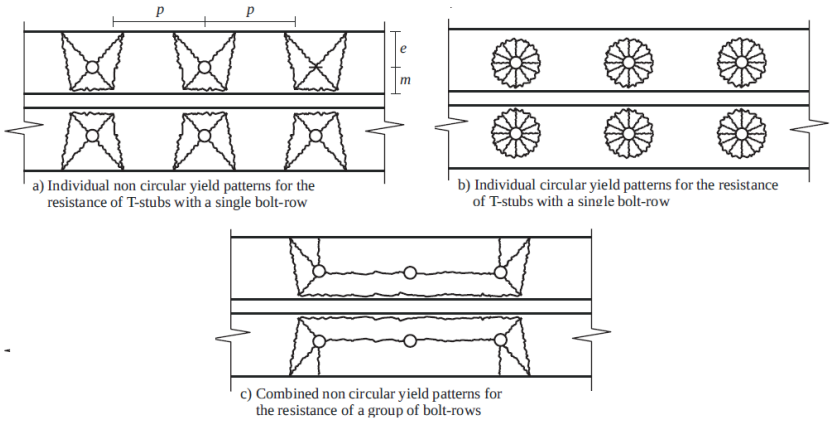

Fig. 4.13 Different failure patterns that appears in the T-Stud model; Jaspart and Weynand, (2016)

Failures 1, 2 and 3 may occur for non-circular patters since prying forces appear, while for circular patterns mode 2 cannot be reached. Hence, the design resistance of the T-stub is the minimum value of expressions 4.14 and 4.15.

$$F_{T,Rd,A} = \min\left(F_{T,Rd,1}; F_{T,Rd,2}; F_{T,Rd,3}\right) \tag{4.13}$$

$$F_{T,Rd,B} = \min\left(F_{T,Rd,1}; F_{T,Rd,3}\right) \tag{4.14}$$

Modes 1 and 2 provides ductility to the connection as opposite to the mode 3, which corresponds to the brittle failure. In the following, a relationship of the failure modes with the factor β, which relates the resistance of the end-plate or column flange with the bolt resistance, is shown (Fig. 4.14).

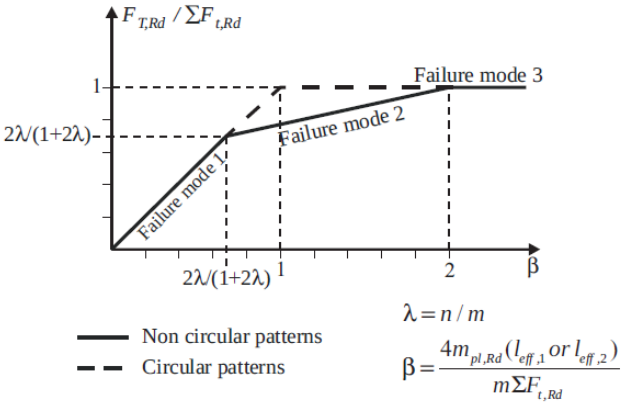

Fig. 4.14 Type of failure of T-Stud model; Jaspart and Weynand (2016)

As the resistance of the end-plate or column web increases respect to the bolt strength, the factor β increases, producing a brittle failure mechanism due to the bolt failure under tension.

In addition, when the T-stub model is applied to a group of bolt-rows, clause 6.2.4.2 establishes that for a group of bolt-rows, it may be necessary to divide the group into individual bolt-rows and use equivalent T-stub models for each one satisfying the following conditions:

- The force at each bolt-row should not exceed the design resistance determined considering only that individual bolt-row
- The total force on each group of bolt-rows, comprising two or more adjacent bolt-rows within the same bolt group, should not exceed the design resistance of the bolt- row group.

Component 1 - Column flange in transverse bending

For the analysis of column flange under transverse bending, two different T-stub models must be utilized since there are stiffeners placed at the column web. The first T-Stud model only considers the bolt-row 1, while the second model includes the bolt-rows 2 and 3.

Depending on the location of the bolt-rows according to the stiffener, Fig. 4.15 shows how they are defined. Fig. 4.16 and 4.17 equivalent length (l_{eff}) to be applied to the expressions each bolt-row.

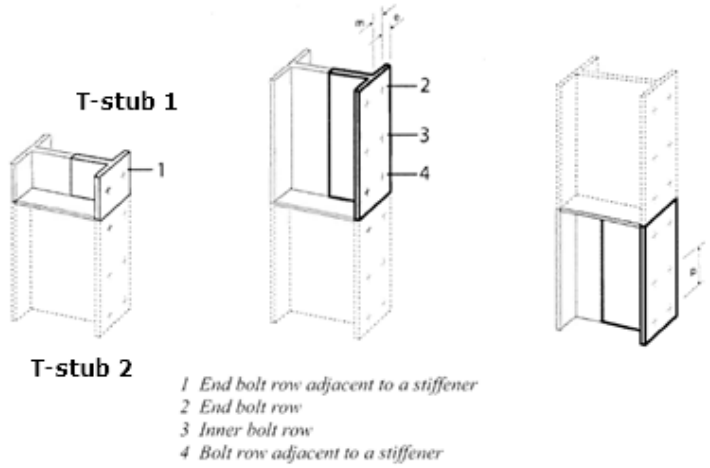

Fig. 4.15 Definition for each bolt-row; CEN, (2005c)

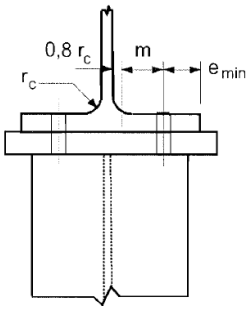

Fig. 4.16 Specific geometric parameters to obtain the equivalent length; CEN, (2005c)

Bolt-row Location	Bolt-row considered individually		Bolt-row considered as part of a group of bolt-rows	
	Circular patterns $\ell_{eff,cp}$	Non-circular patterns $\ell_{eff,nc}$	Circular patterns $\ell_{eff,cp}$	Non-circular patterns $\ell_{eff,nc}$
Bolt-row adjacent to a stiffener	$2\pi m$	αm	$\pi m + p$	$0{,}5p + \alpha m$ $- (2m + 0{,}625e)$
Other inner bolt-row	$2\pi m$	$4m + 1{,}25e$	$2p$	p
Other end bolt-row	The smaller of: $2\pi m$ $\pi m + 2e_1$	The smaller of: $4m + 1{,}25e$ $2m + 0{,}625e + e_1$	The smaller of: $\pi m + p$ $2e_1 + p$	The smaller of: $2m + 0{,}625e + 0{,}5p$ $e_1 + 0{,}5p$
End bolt-row adjacent to a stiffener	The smaller of: $2\pi m$ $\pi m + 2e_1$	$e_1 + \alpha m$ $- (2m + 0{,}625e)$	not relevant	not relevant
For Mode 1:	$\ell_{eff,1} = \ell_{eff,nc}$ but $\ell_{eff,1} \le \ell_{eff,cp}$		$\sum \ell_{eff,1} = \sum \ell_{eff,nc}$ but $\sum \ell_{eff,1} \le \sum \ell_{eff,cp}$	
For Mode 2:	$\ell_{eff,2} = \ell_{eff,nc}$		$\sum \ell_{eff,2} = \sum \ell_{eff,nc}$	

Fig. 4.17 Effective length for each bolt-row; (CEN, 2005c)

Table 4.3 shows the geometric parameters to perform the resistance for the T-stub models while Table 4.4 are shown a summary of the resistances for each model.

Table 4.3. Geometric parameters of the joint

m(mm)	53.4	e1(mm)	65
e(mm)	59	emin(mm)	59
n(mm)	59	λ1	0.48
p(mm)	95	λ2	0.44
m2(mm)	50	α	6.2

Table 4.4 Resistance for each T-stub model

T-stub 1							
ROW 1	Individual	leff,cp-1	336	leff,ncp-1	252	FT,1,Rd(kN)	2080
		leff,cp-2	298	leff,ncp-2	-	FT,2,Rd(kN)	918
		leff,cp	298	leff,ncp	252	FT,3,Rd(kN)	808
		Leff,1(mm)			252	FT,row1(kN)	**808**
		Leff,2(mm)			252		
T-stub 2							
Row 2	Individual	leff,cp	336	leff,ncp	331	FT,1,Rd(kN)	2728
		Leff,1(mm)			331	FT,2,Rd(kN)	1072
		Leff,2(mm)			331	FT,3,Rd(kN)	808
	Group	leff,cp	263	leff,ncp	235	FT,row2_indiviudal(kN)	**808**
		Leff,1(mm)			235		
		Leff,2(mm)			235		
Row 3	Individual	leff,cp	336	leff,ncp	287	FT,1,Rd(N)	2368
		Leff,1(mm)			287	FT,2,Rd(kN)	986
		Leff,2(mm)			287	FT,3,Rd(kN)	808
	Group	leff,cp	263	leff,ncp	191	FT,row3_indiviudal(kN)	**808**
		Leff,1(mm)			191		
		Leff,2(mm)			191		
Group 2-3		Leff,1(mm)			426	FT,1,Rd(kN)	3511
		Leff,2(mm)			426	FT,2,Rd(kN)	1682
						FT,3,Rd(kN)	1616
						FT,row_group(kN)	**1616**

The resistance of the column flange under transverse bending is defined by the tension resistance of the bolts (Mode 3), because the high thickness of column flange (40mm) produces an elevated resistance for Modes 1 and 2. Therefore, no yielding of the column flange shall be occurred.

Component 2 – End Plate in bending

For this second component, the same procedure has been used as for the previous component. The main difference resides in how to define the equivalent length for each bolt-row related to the geometric characteristics of the end-plate (Figures 4.18 and 4.19).

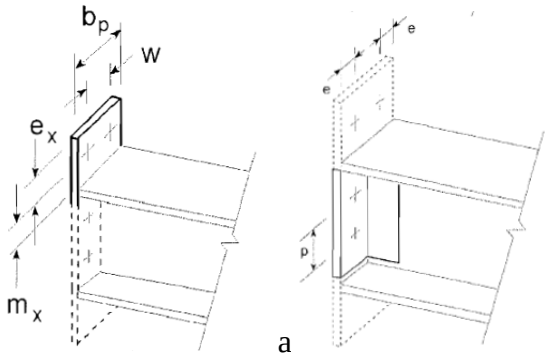

Fig. 4.18 Effective length for each bolt-row considered for the T-stub models; (CEN, 2005c)

Bolt-row location	Bolt-row considered individually		Bolt-row considered as part of a group of bolt-rows	
	Circular patterns $\ell_{eff,cp}$	Non-circular patterns $\ell_{eff,nc}$	Circular patterns $\ell_{eff,cp}$	Non-circular patterns $\ell_{eff,nc}$
Bolt-row outside tension flange of beam	Smallest of: $2\pi m_x$ $\pi m_x + w$ $\pi m_x + 2e$	Smallest of: $4m_x + 1{,}25e_x$ $e+2m_x+0{,}625e_x$ $0{,}5b_p$ $0{,}5w+2m_x+0{,}625e_x$	—	—
First bolt-row below tension flange of beam	$2\pi m$	αm	πm + p	$0{,}5p + \alpha m$ $-(2m + 0{,}625e)$
Other inner bolt-row	$2\pi m$	$4m + 1{,}25\ e$	$2p$	p
Other end bolt-row	$2\pi m$	$4m + 1{,}25\ e$	$\pi m + p$	$2m+0{,}625e+0{,}5p$
Mode 1:	$\ell_{eff,1} = \ell_{eff,nc}$ but $\ell_{eff,1} \le \ell_{eff,cp}$		$\sum\ell_{eff,1} = \sum\ell_{eff,nc}$ but $\sum\ell_{eff,1} \le \sum\ell_{eff,cp}$	
Mode 2:	$\ell_{eff,2} = \ell_{eff,nc}$		$\sum\ell_{eff,2} = \sum\ell_{eff,nc}$	
α should be obtained from Figure 6.11.				

Fig. 4.19 Effective length for each bolt-row in the case of the end-plate; (CEN, 2005c)

All the specific geometric parameters necessary to determine the equivalent length for each T-stub model are shown in the Table 4.5. The resistance presented for each bolt-row is presented in the Table 4.6.

Table 4.5 Geometric parameters of the joint in the case of the end-plate

ex(mm)	65	n	50
mx(mm)	50	λ1	0.62
nx(mm)	62.5	λ2	0.38
e(mm)	50	α	5.4
m(mm)	81	Mpl	61875
m2(mm)	50		

Table 4.6 Resistance for each T-stub model

T-stub 1							
ROW 1	Individual	leff,cp-1	314	leff,ncp-1	281	FT,1,Rd(kN)	718
		leff,cp-2	347	leff,ncp-2	191	FT,2,Rd(kN)	608
		leff,cp-3	257	leff,ncp-3	145	FT,3,Rd(kN)	808
		leff,cp-4	-	leff,ncp-4	236	FT,row1(kN)	**608**
		leff,cp	257	leff,ncp	145		
		Leff,1(mm)			145		
		Leff,2(mm)			145		
T-stub 2							
Row 2	Individual	leff,cp	511	leff,ncp	439	FT,1,Rd(kN)	1337
		Leff,1(mm)			439	FT,2,Rd(kN)	721
		Leff,2(mm)			439	FT,3,Rd(kN)	808
	Group	leff,cp	351	leff,ncp	293	FT,row2_indiviudal(kN)	**721**
		Leff,1(mm)			293		
		Leff,2(mm)			293		
Row 3	Individual	leff,cp	511	leff,ncp	388	FT,1,Rd(kN)	1920
		Leff,1(mm)			388	FT,2,Rd(kN)	673
		Leff,2(mm)			388	FT,3,Rd(kN)	808
	Group	leff,cp	351	leff,ncp	241	FT,row3_indiviudal(kN)	**673**
		Leff,1(mm)			241		
		Leff,2(mm)			241		
Group 2-3		Leff,1(mm)			534	FT,1,Rd(kN)	2645
		Leff,2(mm)			534	FT,2,Rd(kN)	1485
						FT,3,Rd(kN)	1616
						FT,row_group(kN)	**1485**

As opposite of the first component analysed in the Table 4.4, the predominant mode of failure is the second one, due to the thickness of the end-plate (30mm), which is lower than the column flange reducing the resistance in the first two modes of failure. Therefore, there is a combined between the yielding of the end plate and the failure of the bolts in tension providing a more ductile failure.

Component 3 – Column web in transverse tension

The resistance of column web in transverse tension has been calculated as specifies the clause 6.2.6.3.

$$F_{t,wc,Rd} = \frac{\omega b_{eff} t_{wc} f_{y,wc}}{\gamma_{m0}} \tag{4.15}$$

where

b_{eff} is taken equal to the l_{eff} for the equivalent T-stub model used in the column flange

t_{wc} is the thickness of the column web

ω is the reduction factor that considerers the interaction with the shear forces

$f_{y,wc}$ is the yield strength of the column

In this particular case, for single side joint, the transformation parameter β, which transforms the deformability curve of the web panel, is equal to one, meaning ω is:

$$\omega = \omega_1 = \frac{1}{\sqrt{1 + 1.3\left(\frac{b_{eff,c,wc}t_{wc}}{A_{vc}}\right)^2}} \tag{4.16}$$

where

A_{vc} is the shear area of the column

Table 4.7 shows the equivalent effective length considered for each bolt-row as well as its resistance.

4.7 Resistance for each bolt-row

ROW	L_{eff}(mm)	w_1	F_t(kN)
1	252	0.86	1255
2	331	0.79	1647
3	287	0.83	1429
Group 2-3	426	0.71	2119

Component 4 – Beam web in tension

The resistance of the beam web in tension has similarities with the column web in transverse tension. The difference is the absence of the reduction factor ω which considers the interaction with the shear forces. In the point 6.2.6.8 is established the following expression.

$$F_{t,wc,Rd} = \frac{b_{eff}t_{wb}f_{y,wb}}{\gamma_{m0}} \tag{4.17}$$

where

b_{eff} is the effective width in tension of the beam that should be taken into account equal to the effective length of the equivalent T-Stud in bending for the end-plate

t_{wb} is the web thickness of the beam web

$f_{y,wb}$ is the yield strength of the beam

For this component, only the bolt-rows placed along the beam must take into account. Therefore, only the rows 2 and 3 are considered (Table 4.8).

Table 4.8 Resistance for bolt-rows 2 and 3

ROW	$F_{t,wc,Rd}$(kN)
1	-
2	950
3	839
Group 2-3	1155

Component 5 Column web in transverse compression

The last component refers to the column web under transverse compression. According to the point 6.2.6.2, the resistance is given by the following expression.

$$F_{c,wc,Rd} = \frac{\omega k_{wc} b_{eff,c,wc} t_{wc} f_{y,wc}}{\gamma_{m0}} \tag{4.18}$$

where

ω is the reduction factor for the shear forces

k_{wc} is a reduction factor for the axial forces, which in this case can be considered equal to one

t_{wc} is the thickness of the column web

$f_{y,wc}$ is the yield strength for the column web

$b_{eff,c,wc}$ is the effective length given by the following expression for bolted end-connection plate.

$$b_{eff,wc,tp} = t_{fp} + 2\sqrt{2}a_p + 5\left(t_{fc} + s\right) + s_p$$

Which in this case is equal to 402mm.

Applying the same formula given in 4.19 for the ω factor, the resistance of the column web is equal to:

$$F_{c,wc,Rd} = 1692kN$$

The resistance of the column web in compression by the buckling due to the to the low slenderness that present due to their thickness, obtaining a redactor factor ρ equal to one. Producing and slenderness of 0.52. Therefore, the reduction factor for plate buckling is equal to one and no restrictions presents the column web resistance.

Once the resistance for all the components have been obtained, in order to obtain the bearing capacity an assembly of all the resistances has to be perform considering the minimum ones for each bolt-rows as shows the 4.9.

Table 4.9 Minimum resistance obtained for each bolt-row

ROW	F,min(kN)	Component
1	608	End Plate in Bending
2	721	End Plate in bending
3	623	End Plate in bending
Group 2-3	1155	Beam web in tension

Moreover, the fact the summation of the individual resistance of bolt words 2 and 3 (1344kN) is higher than group resistance (1155kN) means the individual resistances cannot be reached. Thus, a reduction of the loads that can be supported the nearest bolt row to the centre of compression (Bolt-row 3) must be applied as follows.

$$F_{3,min,red} = F_{group2-3-}F_{2,min} = 434kN$$

In conclusion, in the figure 4.20 it is shown the final resistance that each bolt-row presents for the single-side connection of beam IPE 450 as well as the respective level arm to the centre of compression for each one.

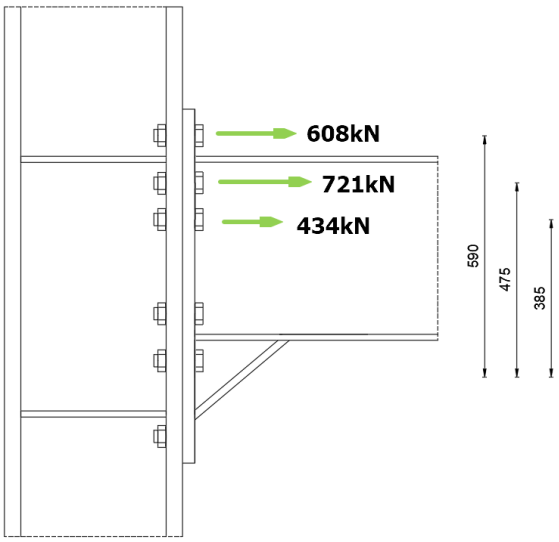

Figure 4.20 Resistance for each bolt-row

Therefore, the bearing resistance can be obtained multiplying each resistance by their respective level arm.

$$M_{j,rd} = 608kN * 590mm + 721kN * 475mm + 434 * 380mm = 866kNm$$

Hence, the bending resistance of the joint is higher than the bending design at the column face.

$$\frac{M_{Con,Rd}}{M_{Con,Ed}} = 1.32$$

Another verification to be made is that the bearing resistance of the end beam considering the haunch must be higher than the design bending moment.

$$\frac{M_{j,Ed}}{M_{bh,Rd}} \leq 1 \tag{4.19}$$

were

$M_{bh,Rd}$ is the plastic bending moment resistance composed of beam top flange, the haunched flange and haunched web neglecting the lower beam flange (Fig. 4.21).

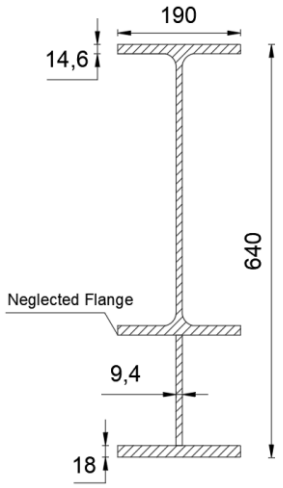

Figure 4.21 Beam plus the haunch

Obtained as following.

$$M_{bh,Rd} = W_{pl,rd} f_{yd} = (867429.8 + 77632028) * 235 + 1063620 * 275 = 679\text{kNm}$$

Therefore, Eq. 4.19 has been satisfied.

$$\frac{662}{679} \leq 1$$

4.2.2 Shear resistance

The shear resistance of the haunched joint has to be checked in order to avoid a brittle failure.

$$\frac{V_{b,Ed}}{V_{con,Rd}} < 1.0 \tag{4.20}$$

where

$V_{con,Rd}$ is the shear resistance of the connection

$V_{b,Ed}$ is the shear design load shown in table 4.1.

The shear resistance of the joints has been determined analysing the components established by the EqualJoints project.

- Beam web in shear
- Bolts in bearing on column flange
- Bolts in bearing on end-plate
- Bolts in shear (only taking into account the bolts not considered for the bending resistance of the connection)

Beam web in shear

The shear resistance of the web beams can be obtained applying the expression 3.24 introduced in the chapter 3.

Bolts in bearing on column flange and end-plate

The calculation of the resistance of bolts in bearing is exposed in clause 6.3.1 of EN 1993-1-8, (CEN, 2005c).

$$F_{b,Rd} = \frac{k_1 \alpha f_u dt}{\gamma_{M2}} \tag{4.21}$$

where

f_u is the ultimate strength for the end plate or column flange, in both cases 460Mpa

d is nominal diameter of the bolt

t is the thickness of the element

γ_{M2} is the safety factor equal to 1.25

k_1 and α are specified in 4.23 and 4.24.

$$\alpha = \min\left(\frac{e_1}{3d_0}; \frac{p_1}{3d_0} - \frac{1}{4}; \frac{f_{ub}}{f_u}; 1.0\right) \tag{4. 22}$$

$$k_1 = \min\left(\frac{2.8e_2}{d_0} - 1.7; \frac{1.4p_2}{d_0} - 1.7; 2.5\right) \tag{4. 23}$$

Bolts in shear

Since preloaded bolts class 10.9 has been used, the slip resistance in the ULS should be obtained according to clause 3.9.1.

$$F_{s,Rd,scr} = \frac{k_s n \mu}{\gamma_{M3}} F_{p,c} \quad (4.\ 24)$$

where

k_s is a factor assumed equal to 1

n is the number of friction planes, in this case 1

μ is the slip factor depending on the friction surface which is assumed equal to 0.3

γ_{M3} is the safety factor equal to 1.25 to guarantee slip resistance in ULS conditions

$F_{p,c}$ is the preloaded force

$$F_{p,c} = 0.7 f_{ub} A_s \quad (4.\ 25)$$

Therefore, considering only 6 bolts for slip resistance, which were not considered for the bending resistance of the connection, no interaction with tensile forces appears.

A summary with all the shear resistances is shown in the Table 4. 10.

Table 4.10 Resistance of each component

Shear resistance	F_{Rd}(kN)
Beam web in shear	690
Bolts in bearing in column flange	444
Bolts in bearing in end-plate	333
Bolts in shear	565

Considering the weakest component, which is the bolts under bearing in the end-plate, the shear requirement of the non-dissipative joint that connects the girder IPE 450 with the supporting element has been verified.

$$\frac{333kN}{281.6kN} = 1.19 > 1$$

4.2.3 Rotational stiffness

The last design step of the prequalified joints is the determine the actual rotational stiffness using also the component method. The flexibility of each component (k_i) should be determined to calculate the initial stiffness ($S_{j,ini}$) according to clause 6.3 of EN 1993-1-8, (CEN, 2005c).

$$S_{j,ini} = \frac{E z^2}{\mu \sum \frac{1}{k_i}} \tag{4.26}$$

where

k_i is the stiffness of each component analysed

z is the level arm

μ is the stiffness ratio described in previously in 4.6

For the haunched joints, the following components must be analysed as specifies Table 10 of clause 6.3.

- Column web in panel shear (k_1)
- Column web in compression (k_2)
- Column web in tension (k_3)
- Column flange in bending (k_4)
- End-plate in bending (k_6)
- Bolts in tension (k_{10})

Deformations of the beam flange and web in compression, beam web in tension and haunches are included in the deformations of the beam in bending, not contributing to the stiffness of the connection.

Column web in panel shear (k_1)

$k_1 = \infty$ For stiffened columns

Column web in compression (k_2)

$k_2 = \infty$ For stiffened columns

Column web in tension (k_3)

$$k_3 = \frac{0.7 b_{eff,t,wc} t_{wc}}{d_c}$$

being $b_{eff,t,ec}$ the effective width of the column web in tension, that should be taken as equal to the smallest of the effective lengths, individually or as a part of a group of bolt row.

Column flange in tension (k_4)

$$k_4 = \frac{0.9 l_{eff} t_{fc}^3}{m^3}$$

being b_{eff} is the smallest length of the effective lengths individually or as part of a bolt group.

End-plate in bending (k_5)

$$k_5 = \frac{0.9 l_{eff} t_p^3}{m^3}$$

Bolts in tension (k_{10})

$$k_{10} = \frac{1.6 A_s}{L_b}$$

where

L_b is the bolt elongation length, that can be taken as equal to the grip length, plus the sum of the height of the bolt and the height of the nut.

In case of two or more bolt-rows in tension, a refined method, must be applied as opposite to the simplify one, utilized when there is only one bolt-row in tension.

As example, a joint with an extended end-plate composed by several bolt-rows in tension with the respective the stiffness of each component ($k_{i,i}$) in Fig. 4.22.

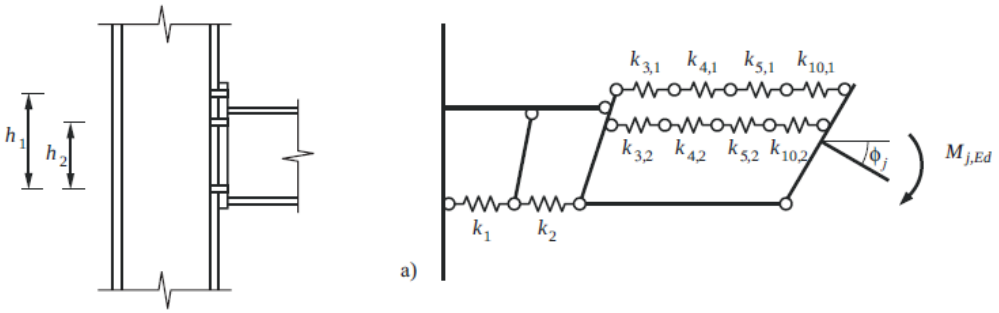

Fig. 4.22 Refined method for two or more bolts in tension ; Jaspart and Weynand, (2016)

The method consists in transforming all the springs shown in the Figure 4.22 into an effective coefficient stiffness $(k_{eff,i})$ for each bolt-row (Fig. 4.23.a), since the bolt-rows deformations are proportional to the distance between the point of application and the centre of compression.

For this reason, an equivalent coefficient (k_{eq}) globalizes all the effective coefficients considering the level arm to the centre of compression (Fig. 23.b). In order to calculate each coefficient, Eq. 4.28, 4.29 and Eq. 4.30 have been applied.

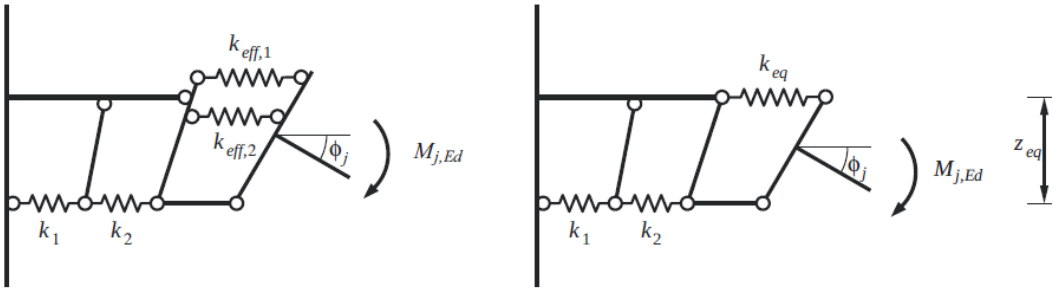

Fig. 4.23 Effective and equivalent stiffness (a and b); Jaspart and Weynand, (2016)

$$k_{eff,i} = \frac{1}{\sum \frac{1}{k_{i,r}}} \tag{4.27}$$

where

$k_{i,r}$ is the stiffness of each component for each bolt-row

$$k_{eq} = \frac{\sum k_{eff,i}\, h_i}{Z_{eq}} \tag{4.28}$$

where

h_i is the distance between bolt-row I to the centre of compression

$k_{eff,i}$ is the effective stiffness coefficient for bolt-row I, taking into account the basic components mentioned previously

The equivalent lever arm Z_{eq} is be determined from:

$$Z_{eq} = \frac{\sum k_{eff,i} h_r^2}{\sum k_{eff,i}\, h_r} \tag{4.29}$$

The results obtained from the joint connecting the beam IPE 450 are shown in Tables 4.11 and 4.12.

Table 4.11 Stiffness of each component of the joint

Stiffness	Component	
k_1	Column web panel in shear	∞
k_2	Column web in compression	∞
$k_{3.1}$	Column web in tension, Row 1	14
$k_{3.2}$	Column web in tension, Row 2	13
$k_{3.3}$	Column web in tension, Row 3	11
$k_{4.1}$	Column flange in bending, Row 1	95
$k_{4.2}$	Column flange in bending, Row 2	89
$k_{4.3}$	Column flange in bending, Row 3	72
$k_{5.1}$	End-Plate in bending, Row 1	28
$k_{5.2}$	End-Plate in bending, Row 2	13
$k_{5.3}$	End-Plate in bending, Row 3	11
k_{10}	Bolts in tension	10

From the stiffness of each component and applying the method discussed previously, the equivalent stiffness for each bolt-row ($k_{eff,i}$) , the equivalent stiffness (k_{eff}) and the level arm (Z_e) has been determine in order to calculate the initial stiffness ($S_{j,ini}$) and the secant one ((S_j) as shown the Table 4.12.

Table 4.12 Initial stiffness of the IPE 450 haunched joint

$k_{eff,1}$	5
$k_{eff,2}$	4
$k_{eff,3}$	3
Z_e(mm)	508
K_e	12
S_{ini}(MN/rad)	628744
S_i (MN/rad)	475345

4.3 SIMPLE JOINTS

4.3.1 Assumptions considered for beam-to-beam connections

The simple connections used for the beam-to-beam joints, which connects the secondary beams with the girders are discussed in the current section.

Simple joints are assumed to transfer no bending moments, being only capable to resist shear and axial forces. They are place out of scope of the non-dissipative joints since they are secondary elements designed to resist only vertical loads.

Despite EN 1993-1-8, (CEN, 2005c) establishes the design of bolts under shear and tension forces, non-specific rules are presented for the design of simple joints. Thus, the recommendations based on different international design codes, compiled by Jaspart and Weynand, (2016), have been followed in order to design the beam-to-beam connections.

Even though simple connections are not supposed to transmit any bending moment to the supporting element, they may actually present some stiffness becoming as semi-rigid instead of a simple one. In consequence, a collapse of the connection can occur since they have been designed only to transmit shear and axial forces, being highly unsafe especially for seismic zones.

In order to avoid modelling the joints as semi-rigid due to its complexity in the global design, the hypothesis of simple joints has been assumed. This assumption is assumed as valid if the following requirements are satisfied.

- Sufficient rotation capacity
- Sufficient ductility

The first criterion aims to allow the rotation of the joint without developing important bending moments. In fact, contact between the lower part of the connecting element and the supporting one should be avoided to not generate compression forces.

On the other hand, the second statement prevents the brittle failure of the connection due to the rupture the bolts of welds in order to promote plastic deformations.

4.3.2 Design of the fin plate connections

For the building, single and double-side configurations single-notched of fin plate connections have been designed to connect the secondary beams with the girders. These types of joints are composed by a fin plate, a fillet weld on both sides of the plate and a single vertical bolt-row (Fig. 4.24).

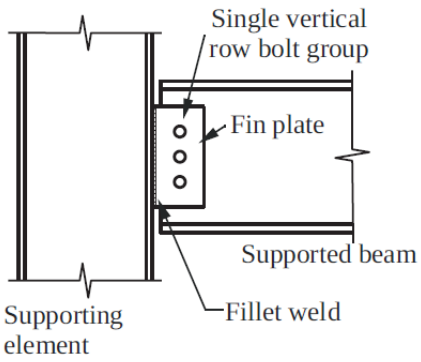

Fig. 4.24 Fin plate connections; Jaspart and Weynand (2016)

Specifically, each single-notched joint designed is composed by the following components.

- Tow bolts M24 GR 6.8
- Fin plates 10mm thick
- Fillet welds with a throat thickness (a) of 6mm

Figure 4.25 shows the single-notched joints that connects the secondary beams IPE 220 and IPE 240 with the girder IPE 450, whose design satisfies the designing shear forces obtained in the elastic analysis under gravity loads as well as the two requirements mentioned previously. Therefore, the proposed designed can be applied in all the beam-to column joints of the building.

Moreover, two different find plates have been utilized owing to the two different geometries that present the secondary beams IPE 220 and IPE 240.

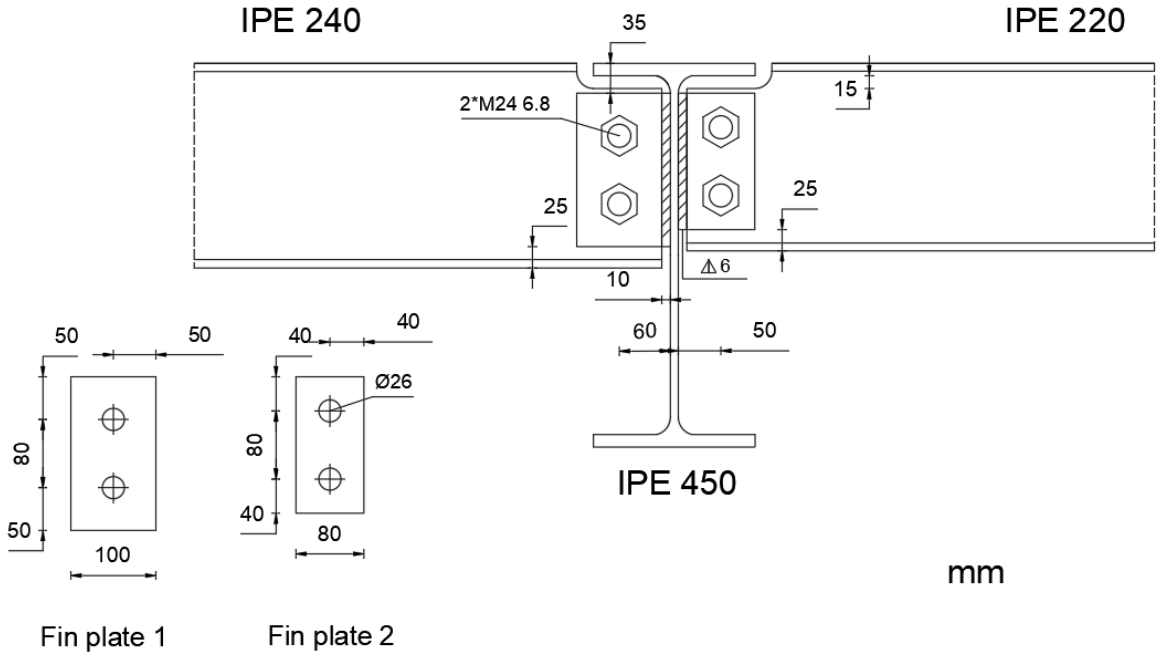

Fig. 4.25 Single-notched fin plate connections designed for connecting the secondary beams IPE 240 and IPE220 with the girders

The shear design forces ($V_{Con,Ed}$) and shear resistance ($V_{Con,Rd}$) for each simple connections are shown in the Table 4.13. Moreover, the required rotation capacity (ϕ_{Ed}) and the admissible one ($\phi_{admisible}$) are also displayed.

Table 4.13 Design requirements and resistance for the simple joints

Beam	$V_{Con,Ed}$(kN)	$V_{Con,Rd}$(kN)	ρ_{Shear}	ϕ_{Ed}(rad)	$\phi_{availaible}$(rad)
IPE 240	97	142	0.68	0.0006	0.9090
IPE220	58	132	0.44	0.0009	0.8251

Therefore, the designed connections meet all the requirements to be place in the building. In the following, the different assumptions considered to guarantee enough rotation capacity and avoiding brittle failures are deeply discussed.

4.3.3 Requirements for sufficient rotation capacity

For rotation requirements, it must be avoided the contact between the lower part of the beam with the supported member. This condition is satisfied if the following expression is applied the connection.

$$h_p \leq d_b \tag{4. 30}$$

where

h_p is the height of the fin plate

d_b is the depth of the supported beam calculated as $h - 2(t_f + r_b)$

Furthermore, the required rotation of the connection should be lower than the admissible one.

$$\emptyset_{Ed} \leq \emptyset_{available} \tag{4. 31}$$

being $\emptyset_{Ed} = \frac{PL^3}{24EI}$ according to the elasticity theory

On the other hand, the available rotation ($\emptyset_{available}$) depends on the geometric shape of the connection.

$$\emptyset_{available} = \sin^{-1}\left(\frac{z}{\sqrt{(z-g_h)^2 + \left(\frac{h_p}{2} + h_e\right)^2}}\right) - \tan^{-1}\left(\frac{z-g_h}{\frac{h_p}{2} + h_e}\right) \tag{4. 32}$$

The geometric parameters to be considered in Eq. 4.33 are shown in the Fig. 4.26.

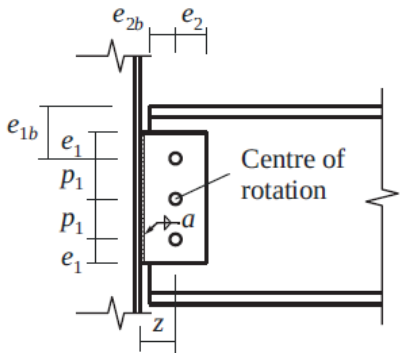

Fig.4.26 Geometric parameters for the fin plate connection; Jaspart and Weynand, (2016)

4.3.4 Requirements for sufficient joint ductility

The minimum throat thickness (a) in the case of double fillet welds is established as $a \geq 0.48t$ to avoid a premature weld failure.

On the other hand, a criterion to permit a plastic redistribution of internal forces is exposed in the following three inequalities.

- The failure produced by the bolts or the buckling of the find plate should be avoided.

$$\min\left(V_{Rd1;}V_{Rd7}\right) > V_{Rd} \tag{4. 33}$$

where

V_{Rd1} is the shear resistance of the bolts

V_{Rd7} is the buckling resistance of the fin plate

V_{Rd} is the shear resistance of the connection

- The component that reaches the yielding must be ductile. In order to satisfy the assumption, one of the following inequalities should be satisfied.

  For the beam web:

$$F_{b,hor,Rd} \leq \min\left(F_{v,Rd}; V_{Rd7}\beta\right) \tag{4. 34}$$

  For the fin plate:

$$F_{b,hor,Rd} \leq \min\left(F_{v,Rd}; V_{Rd7}\beta\right) \tag{4. 35}$$

where

$F_{b,hor,Rd}$ is the bearing resistance of the beam web or the fin plate

$F_{v,Rd}$ is the shear resistance of the bolts

- Finally, the resistance of the shear bolts should be higher the buckling resistance of the fin plate.

$$V_{Rd1} > \min\left(V_{Rd2;}V_{Rd8}\right) \tag{4. 36}$$

The previous requirements can only be checked once the shear resistance of the connection has been obtained. Hence, an iterative process should be carried out to design the simple joints. Once each component has been analysed, the assumed shear strength is the minimum value.

Bolts in shear (V_{Rd1})

$$V_{Rd1} = \frac{nF_{v,Rd}}{\sqrt{1+\left(\frac{6z}{(n+1)p_1}\right)^2}} \tag{4. 37}$$

being n is the number of bolts placed in the fin plate

Fin plate in bearing (V_{Rd2})

$$V_{Rd2} = \frac{1}{\sqrt{\left(\frac{\frac{1}{n}+\alpha}{F_{b,ver,Rd}}\right)^2+\left(\frac{\beta}{F_{b,hor,Rd}}\right)^2}} \tag{4. 38}$$

where

$F_{b,ver,Rd}$ is the vertical bearing capacity of the fin plate

$F_{b,hor,Rd}$ is the horizontal bearing capacity of the fin plate

α is equal to zero for one vertical bolt rows

β is equal to $\beta = \frac{6z}{p_1 n(n+1)}$

In the Table 3.4 of EN 1993-1-8, (CEN, 2005c) the bearing capacity is defined.

$$F_{b,ver,Rd} = \frac{k_1 \alpha_b f_{ubw} d t_w}{\gamma_{M2}} \tag{4. 39}$$

where

k_1 is the min $(2.8\frac{e_2}{d_0} - 1.7; 1.4\frac{p_2}{d_0} - 1.7; 2.5)$

α_b is the min $(\frac{e_1}{3d_0}; \frac{p_1}{3d_0} - \frac{1}{4}\ o;\ \frac{f_{ub}}{f_{up}}\ or\ 1)$

$$F_{b,hor,Rd} = \frac{k_1 \alpha_b f_{ubw} d t_w}{\gamma_{M2}} \quad (4.\ 40)$$

where

k_1 is the min $(2.8\frac{e_1}{d_0} - 1.7; 1.4\frac{p_2}{d_0} - 1.7; 2.5)$

α_b is the min $(\frac{e_2}{3d_0}; \frac{p_2}{3d_0} - \frac{1}{4}; \frac{f_{ub}}{f_{up}}\ or\ 1)$

Fin plate in shear: Gross Section (V_{Rd3})

$$V_{Rd3} = \frac{h_p t_p f_{yp}}{1.27\sqrt{3}\gamma_{M0}} \quad (4.\ 41)$$

Fin plate in shear: Net Section (V_{Rd4})

$$V_{Rd4} = A_{v,net} \frac{f_{up}}{\sqrt{3}\gamma_{M2}} \quad (4.\ 42)$$

Fin plate in shear: Shear Block (V_{Rd5})

$$V_{Rd5} = F_{eff,2,Rd} \quad (4.\ 43)$$

$$F_{eff,2,Rd} = 0.5\frac{f_{up} A_{nt}}{\gamma_{M2}} + \frac{1}{\sqrt{3}} f_{yp} \frac{A_{nv}}{\gamma_{M2}} \quad (4.\ 44)$$

where

A_{nt} is the net area subjected to tension, $A_{nt} = t_p(e_2 - \frac{d_0}{2})$

A_{nv} is the net area subjected to shear, $A_{nv} = t_p(h_p - e_1 - (n - 0.5)d_0)$

Fin plate in bending (V_{Rd6})

$$V_{Rd6} = \infty$$

Bucklin of the fin plate (V_{Rd7})

$$(V_{Rd7}) = \infty$$

Beam web in bearing (V_{Rd8})

For the beam web in bearing Eq. 4.39, 4.40 and Eq. 4.41 applying the geometry of the beam.

Beam web in shear (V_{Rd9}): Gross section

The beam web capacity of the gross section under shear can be obtained applying Eq. 3.24.

Beam web in shear (V_{Rd10}): Net section

Eq. 4.44 applies of fin plate in shear gross section (V_{Rd4}), using the specific forces and shape of the beam web.

Beam web in shear (V_{Rd11}): Shear Block

Eq. 4.45 applies of fin plate in shear gross section (V_{Rd5}), using the specific forces and shape of the beam web.

All the calculations performed for the connection placed in the secondary beam IPE 240 are shown in the Tables 4.14 and 4.15.

Table 4.14 Shear resistance of bolts and

Fv,Rd(kN)		130
Fin Plate	Fb, ver,Rd(kN)	106
	Fb, hor,Rd(kN)	106
Beam Web	Fb, ver,Rd(kN)	122
	Fb, hor,Rd(kN)	122

Table 4.15 Resistance of all the components

Bolts in shear	Vrd1(kN)	193
Fin Plate in bearing	β	0.75
	Vrd2(kN)	147
Find plate in shear(Gross Section)	Vrd3(kN)	225
Find plate in shear(Net Section)	Av,net(mm2)	1280
	Vrd4(kN)	254
Find plate in shear(Shear Block)	Ant(mm2)	370
	Anv(mm2)	910
	Vrd5(kN)	208
Find Plate in bending	Vrd6(kN)	∞
Buckling of the Fin plate	Vrd7(kN)	∞
Beam web in bearinng	Vrd8(kN)	142
Beam web in shear: Gross Section	Vrd9(kN)	304
Beam web in shear: Net Section	Ab,v,net(mm2)	1593
	Vrd10(kN)	316
Beam web in shear: Net Section: Shear Block	Ant(mm2)	229
	Anv(mm2)	831
	Vrd11(kN)	171
Vrd(kN)		142

In conclusion, considering the minimum resistance of all the components, it has been obtained the shear resistance of the joint which is equal to 142kN satisfying the shear requirements in the ULS for the static conditions. Moreover, the inequalities to guarantee a ductile behaviour, which are the Equations 4.33, 4.34, 4.35 and 4.36 have been satisfied.

The same procedure has been carried out in the case of the secondary beams IPE 220.

CHAPTER 5: CONCLUSIONS

5.1 ASSESSMENT OF THE BUILDING

The aim of this final chapter is to discuss the performance of the building once the structural design has been finalized.

The multi-storey steel building is able to resist the gravity loads under static conditions in the ULS and SLS states. Moreover, the buckling phenomena in the sway modes have been prevented by the heavy structural elements used.

In addition, the top displacement in the roof and the inter-storey drifts produced by wind loads, which usually have a significant impact on steel structures, are below from the limits established by the Italian national code, guaranteeing the user comfort.

In the case of the secondary beams, the use of composite structures has allowed to reduce the sizing of steel the cross-sections owing to the increase in strength and bending stiffness. Therefore, a considerable reduction in the mass of the building has been produced.

Furthermore, the building presents the capacity to resist rare and frequent seismic actions of L'Aquila, which are the ULS and DLS states under seismic conditions. The primary elements designed to resist the seismic actions have been satisfied the capacity design method applied to a high ductility class structure (DHC). The activation of the plastic hinges has been produced exclusively in the dissipative zones (principal beams), remaining the non-dissipative ones such as the columns and beam-to-columns joints, in the elastic field.

In fact, global mechanisms such as torsional behaviours or soft-storey mechanisms, which may lead to a structure collapse, have been avoided providing structural regularity in plan and elevation. On the other hand, no local mechanisms, which involves small portions of the building, have been produced, since the shear failure of the structural elements has been avoided.

As a result, the capacity curves obtained from the pushover analysis present a ductile behaviour, resisting important base shear forces before reaching the plastic mechanism, without sharply decreases in strength due to brittle mechanisms, as Fig. 5.1 shows.

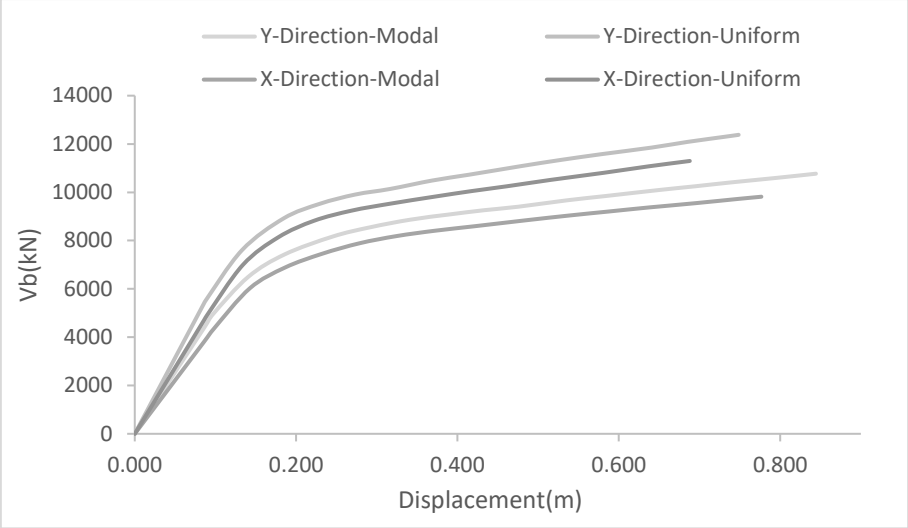

Fig. 5.1 Capacity curves for the 4 pushovers performed

Furthermore, the inelastic demand in form of rotation of the plastic hinges for the ULS, has been determined imposing the target displacements determined from the base-displacement method, N2, into de the pushover analysis.

The maximum rotations, produced mainly in the first storeys are below the Life Safety (LS) criteria, while the less requested beams have been remained in the elastic field or have a demand equal to the Immediate Occupancy (IO), established for frequent seismic actions according to the FEMA 356 (Figures 5.2 and 5.3). Therefore, the building presents an important capacity to dissipate energy in the inelastic field, being able to resist higher target displacements verifying the ULS.

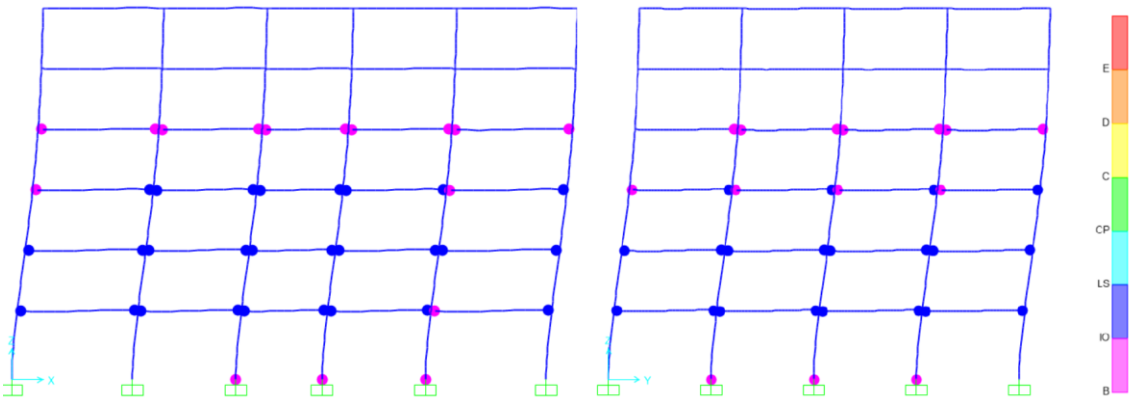

Fig. 5.2 Modal distributions in the X and Y direction considering the target displacement

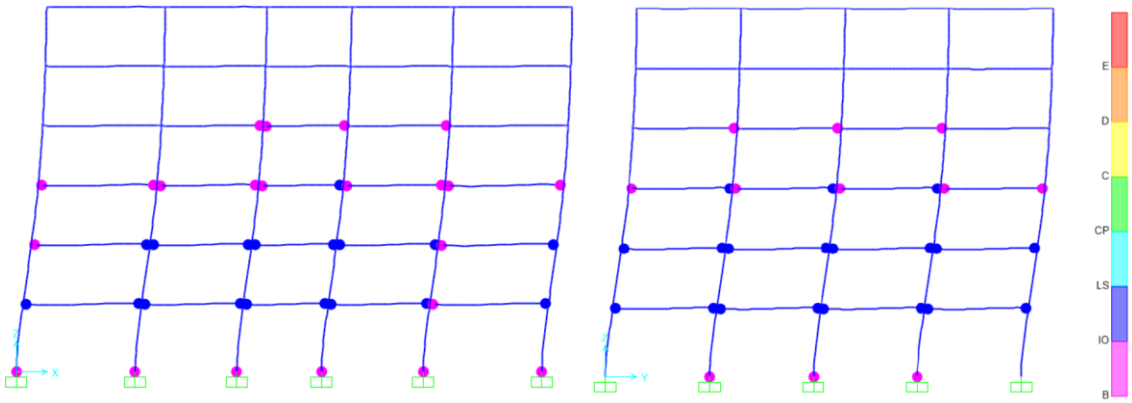

Fig. 5.3 Uniform distributions in the X and Y direction considering the target displacement

To conclude the assessment of the building, an analysis of the primary elements, that must resist the vertical and horizontal forces, has carried out to determine if the building has been designed in an optimal way and to consider possible improvements.

In order to carry out the analysis, the resistance ratio for each structural element have been plotted using a box and whisker diagram, where the designing forces and the strength of the cross-sections are taken into account. The static and seismic conditions in the ULS have been considered.

Principal beams

In the case of the principal beams under static conditions, their design have been conditioned by the lateral-torsional buckling. Therefore, the box and whisker plot shows the ULS ratio accounting the bending designing forces and the buckling resistance of the cross-sections ($M_{Ed}/M_{b,Rd}$), for the principal beams placed along the X and Y directions (Fig. 5.4).

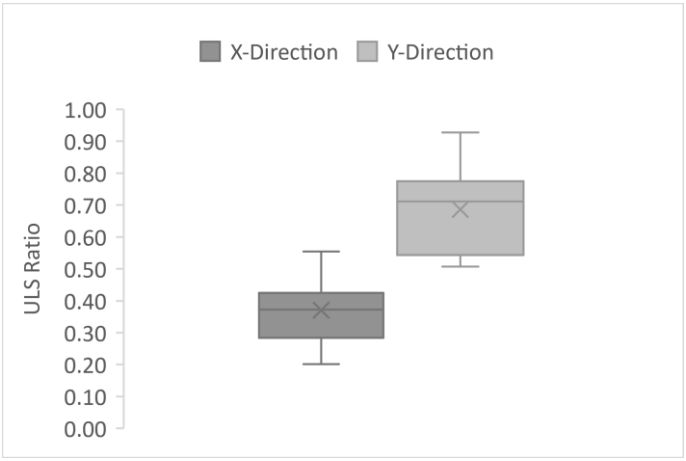

Fig. 5.4 ULS ratios of the principal beams under static conditions

The maximum ratio reached is 0.56, being the median and the average is 0.37 for the beams placed along the X direction.

On the other hand, beams placed in orthogonal direction are quite more requested since they support the secondary beams at both sides. The maximum is 0.93, where the average value is 0.69.

Concerning the seismic actions, the box and whiskers plot accounts ULS the ratio that relates the bending moment design under seismic actions, which have been determined from the linear modal response spectrum, and the flexural strength of the cross-section ($M_{Ed}/M_{pl,Rd}$) considering the capacity design of the dissipative elements, as shows Fig. 5.5.

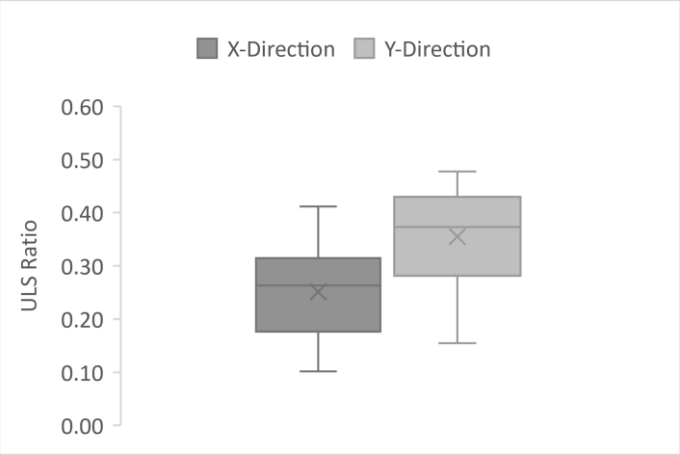

Fig. 5.5 ULSs ratio of the principal beams under seismic conditions

The mean value for the beams under rare seismic actions is equal to 0.25 and 0.35 for the X and Y directions, respectively. However, the most important values are the maximum ones, which are 0.41 and 0.47 respectively, since through them the overstrengh factor Ω to be apply to the columns have been obtained.

In conclusion, profiles IPE 400 and IPE 450 along the Y-direction have taken full advantage of the resistance capacity under static conditions.

On the other hand, under the static and seismic loads, beams placed in the X-direction are oversized. Despite this, steel profiles IPE 400 are necessary to provide sufficient horizontal stiffness. Otherwise, the seismic actions in the ULS would cause excessive inter-storey drift ratios that would invalidate the design.

Despite the fact that the building is located in one of the highest seismic zones in Italy, the internal forces obtained in the rare seismic conditions are lower than the static loads because of the large periods of vibration that present the building owing to its flexibility.

Moreover, it should be noted that the highest structural behaviour factor (q), which is 6.5, has been accounted in the linear modal response spectrum analysis, producing a considerable reduction of the internal forces to be resisted in elastic conditions due to the ductility that presents the MRF system.

Columns

For the case of the columns under the static conditions, the ULS ratio for each structural element accounts the designing compressive axial forces and the buckling resistance of the structural element, since the bending moments hardly influence the cross-section strength due to their low values.

Under seismic conditions, since important axial forces and bending moments are applied simultaneously in both axis, the interaction formulas that accounts the possible flexural and lateral-torsional buckling (Eq. 3.40 and Eq. 3.41), proposed by the Annex B of EN 1993-1, (CEN, 2005b) condition the ULS ratio (Fig. 5.6).

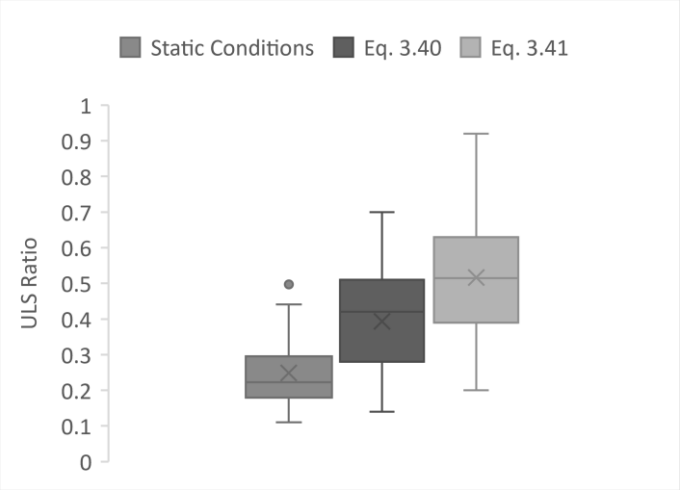

Fig. 5.6 ULS Ratios of the columns under static and seismic conditions

The mean ratio of the columns under static loads are equal to 0.25, being the maximum value equal to 0.53. Most ratios which are between the first and third quartile, present values of 0.2 and 0.3.

On the other hand, under seismic actions, the internal forces increase considerably due to the overstrength presented by the principal beams. The maximum values reached are 0.73 and 0.92 for the Equations 3.40 and 3.41.

In the seismic conditions, the variance of the values increases because the bottom end of the ground floor columns have been designed as dissipative-elements, consequently, no overstrengh factors have been accounted.

Even if the overstrengh of the beams under seismic conditions were reduced, reducing in consequence the internal forces to be considered to verify the capacity design in the columns, heavy profiles would still be necessary. Since several internal joints connect girders IPE 450 with the minor-axis of the columns, which must provide sufficient bending stiffness to guarantee the strong column-weak beam principle.

In addition, the heavy profiles provide considerable lateral stiffness to reduce the lateral displacements produced by horizontal loads and they prevent the buckling phenomena in sway modes under the static conditions.

Moreover, are capable to verify capacity design method applied to a hight ductility class structure (DHC) due its strength. Hence, profiles HEM 360 are an optimal solution for the current MRF building.

In conclusion, the primary elements chosen for the building are the most optimal solution according to geometry and the MRF system, where the design of various structural elements has been conditioned by their rigidity rather than their strength.

These conditions have been produced a structure stronger than strictly needed to resist the earthquake. This usually happens in the case of high-rise buildings whose design is conditioned by the SLS under wind loads. However, for this particular building with a total height of 21.5 m, the chosen design is considered the most optimal for a MRF system in order to verify all the requesting actions.

5.2 EVALUATION OF THE JOINTS

Regarding the beam-to-column, the use prequalified haunched connections has been an excellent choice for the MRF system. Due to strength the joints present, it has been guaranteed the plastic hinges only appear in the dissipative elements instead of the joint or the web panel zone.

The elevated flexural strength required to consider the joint as non-dissipative, has been reached using high resistance preloaded bolts attached to the extended end-plate and the increase in the level arm of the bolt-rows by the presence of the haunch.

It should be noted the design of the prequalified haunched joints based on the EqualJoints project ensures the connection presents sufficient overstrengh, since the current recommendations for the non-dissipative joints proposed by Eurocode 8 are in controversy. Moreover, the joints are supported by the experimental tests carried out to ensure that under cyclic loadings there are no sharply decreases in the strength and stiffness, providing a ductile behaviour at least a rotation of 0.04 rad.

On the other hand, placing stiffeners in the column and beam web a rigid connection is guaranteed, with no relative rotations appearing between the columns and the beams. This is such an important property in the elastic analysis since the MRF system presents high flexibility.

The flexural requirements ($M_{Con,Ed}$) to considerer the connections as non-dissipative, and the actual strength ($M_{Con,Rd}$) of the haunched joints placed at the girders IPE 400 and IPE 450 are shown in the Figures 5.7 and 5.8. Moreover, the required stiffness ($S_{j,Ed}$) to consider the connections as rigid has been also shown.

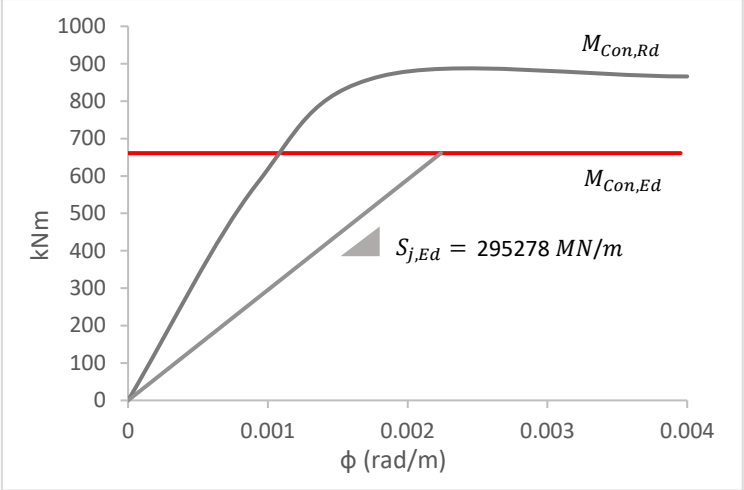

Fig. 5.7 Actual behaviour of the haunched joints placed in the girders IPE 450

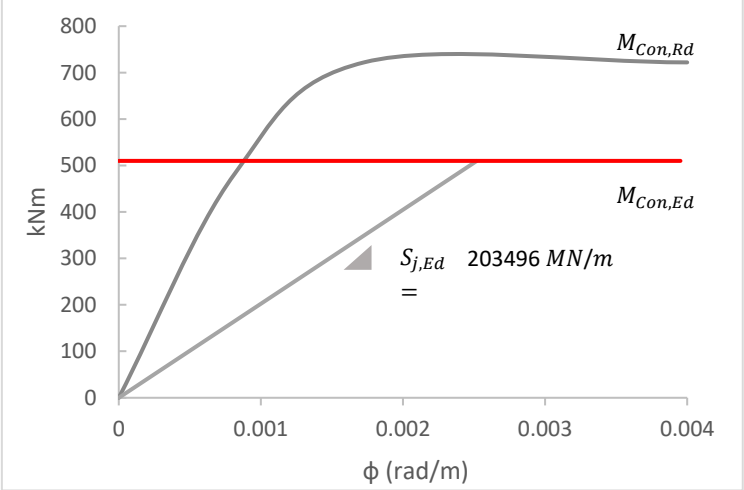

Fig. 5.8 Actual behaviour of the haunched joints placed in the girders IP E400

On the other hand, the assumptions provided by the EqualJoints guidelines allows the use of the component method in a simple way. Therefore, the designer may be able to determine the behaviour of the joint using simple spreadsheets.

However, the use of haunches, high strength preloaded bolts, stiffeners, as well as the full penetration welds in order to provide the required resistance and stiffness increases the cost of the connections. In addition, they should be placed in all the frames of the building since there is no a bracing system, otherwise using beam-co-column simple joints the horizontal actions would not be resisted.

Finally, regarding the fin plate joints that connects the secondary beams with the girders, enough available rotation and a ductile failure has been ensured due to the approach followed for their design.

The advantage of simple joints resides in the simplicity of its components, reducing the cost. Moreover, the use of the simple joints instead of rigid ones to connect the secondary beams with the girders, avoids the occurrence of torsional moments. In contrast, the bending moment and the deflection at the midspan section increases.

5.3 ALTERNATIVES

In the current section, possible alternatives according to the seismic resistant systems and the connections have been presented.

Initially, regarding the flexibility of the building that the MRF system has been presented, an alternative would be the use of frames with concentric bracings (CBF) or eccentric bracings (EBF). Both typologies would increase considerably the lateral stiffness, reducing the inter-storey displacements under the seismic conditions.

The advantage of using bracings would allow to design the frames of the buildings as secondary elements, resisting only against vertical loads. Therefore, ductile-headed shear studs may be placed in all the beams to produce a composite action with the composite slab. In consequence, the depth of the steel profiles may be decreased reducing the weight of the building.

In the case of the CBF system, the dissipative zones are located in the diagonals under tension. Two categories are inside this typology, which are the bracings with cross or single diagonal shape and V inverted, avoiding the K-shape which cannot be used as seismic resistant system.

Using the diagonal shape should more appropriated for hight seismic zones, since presents more ductility. In fact, the Eurocode 8 allows using a maximum factor equal to 4, which is quite similar that one used in the MRF system.

In this case, the diagonal bracings should be designed neglecting the contribution of the diagonals under compression to avoid transmitting compressive forces to the columns. Therefore, the use of slender profiles is recommended to promote the buckling phenomena under compression forces. On the other hand, the frames that supports the bracings should be designed as non-dissipative to guarantee the yielding only occurs in the brace system.

Moreover, during the designing phase, an interactive process should be carried out to determine the cross-sections of the bracings because the overstrengh they can present against the seismic actions is strictly limited. Since the internal forces produced by the seismic actions decreases with the height of the building, each storey should use different bracings to satisfy this assumption.

The use of eccentric braces system (EBF), which presents important ductility to be placed in a hight seismic region, may be an alternative for the CBF system. In this case, the dissipative zones are located at the eccentricity of the layout of the bracings, named as links, which dissipate energy through cyclic bending or cycling shear using long and short links respectively.

However, either using the CBF or EBF seismic system, the fundamentals periods of vibration shall be considerably reduced due to important rise in stiffness, consequently, increasing the seismic actions applied to the building. Thus, the use of bracings or links to dissipate energy may be not sufficient to resist the rare seismic actions of L'Aquila, due to the hight peak ground acceleration (PGA) of the region.

In that case, a dual system composed by moment resisting frames and braced frames (MRF +CBF) may be considered. The horizontal forces would be resisted by both sub-systems proportionally to their stiffness presenting an important inelastic capacity. Therefore, a uniform distribution of the bracings and frames using rigid connections should be guaranteed in order to avoid torsional mechanisms.

In this case, the orientation of the columns would no longer relevant since the bracing system would provide sufficient lateral stiffness. Therefore, connecting principal beams with the minor axis of the columns would be avoid, requiring lower columns cross-sections to verify the strong column-weak beam principle applied to the non-dissipative elements.

Nowadays, the of use dual systems placed in some specific parts of the building, designing the remaining structural elements as secondary ones, is gaining importance among the designers since optimal solutions may be reached reducing the structural cost. However, the complexity of the design increases considerably.

Regarding the joints, since the use of full-strength haunched joints presents an important cost due its components, the use of extended stiffened end-plate, which are simi-rigid joints, would be and alternative if a bracing system is provided to the building.

The extended stiffened end-plate joints have been also prequalified by the EqualJoints project, consequently, they may be placed in seismic zones as full-strength or partial strength. Therefore, depending on the seismic resistant system chosen, the joint may be designed to dissipate energy through the inelastic behaviour, considering the connected beams and columns as non-dissipative.

Due to the simplicity that present the extended stiffened end-plate joints in its components and the limited use of welds, the cost of constructions is considerably reduced comparing to full-strength joints.

Furthermore, the use of them as semi rigid instead of using a simple joints, presents several advantages. There is a reduction in positive bending moments under gravity loads and in the case of very rigid structures placed in seismic locations, the use of the semi-rigid joints produces and increase in flexibility. In consequence, the natural periods of vibrations increase allowing to reduce the internal forces produced by the seismic actions.

ANNEX 1

The Annex 1 presents all the verifications of the primary elements under the static conditions. The designing forces as well as the resistance of the principal beams under the ULS according to the section 3.4.4 are shown. On the other hand, Table A1.2 are displayed the deflections produced under SLS conditions.

Finally, in the Table A.3 the verification of the columns under ULS are displayed according to the section 3.4.5.

Table A1.1 Principal beams under ULS in the static conditions

Frame	Section	Length	Comb	$M_{Ed,i}$(kNm)	$M_{Ed,j}$(kNm)	V_{Ed}(kN)	$M_{pl,Rd}$(kNm)	$M_{b,Rd}$(kNm)	$Eq.3.25$	$Eq.3.23$
PB100	IPE400	7	ULS13	−41	−76	−49	307	227	0.33	0.07
PB101	IPE400	6	ULS13	−22	−65	−39	307	247	0.26	0.06
PB102	IPE400	5	ULS48	−59	−59	−41	307	260	0.23	0.06
PB103	IPE400	6	ULS13	−23	−64	−39	307	247	0.26	0.06
PB104	IPE400	7	ULS13	−39	−79	−48	307	228	0.34	0.07
PB105	IPE400	6	ULS13	−94	−142	−96	307	246	0.58	0.14
PB106	IPE450	6	ULS13	−151	−253	−163	400	323	0.78	0.24
PB107	IPE400	6	ULS13	−139	−211	−140	307	246	0.86	0.20
PB108	IPE400	6	ULS13	−139	−211	−140	307	246	0.86	0.20
PB109	IPE450	6	ULS13	−150	−253	−163	400	323	0.78	0.24
PB110	IPE400	6	ULS13	−94	−142	−96	307	246	0.58	0.14
PB111	IPE400	7	ULS13	−74	−118	−89	307	220	0.54	0.13
PB112	IPE400	6	ULS5	−85	−85	−84	307	234	0.36	0.12
PB113	IPE400	5	ULS13	−44	−69	−62	307	254	0.27	0.09
PB114	IPE400	6	ULS13	−61	−96	−76	307	238	0.41	0.11
PB115	IPE400	7	ULS5	−107	−107	−98	307	216	0.50	0.14
PB116	IPE400	6	ULS5	−126	−126	−107	307	248	0.51	0.15
PB117	IPE450	6	ULS13	−234	−234	−193	400	323	0.72	0.28
PB118	IPE400	6	ULS13	−187	−187	−156	307	248	0.75	0.23
PB119	IPE400	6	ULS5	−186	−186	−156	307	248	0.75	0.23
PB120	IPE450	6	ULS13	−234	−234	−193	400	323	0.72	0.28
PB121	IPE400	6	ULS13	−126	−126	−107	307	248	0.51	0.15
PB122	IPE400	7	ULS13	−65	−125	−84	307	226	0.55	0.12
PB123	IPE400	6	ULS13	−58	−84	−75	307	238	0.35	0.11
PB124	IPE400	5	ULS13	−44	−67	−62	307	254	0.26	0.09
PB125	IPE400	6	ULS13	−56	−93	−72	307	241	0.39	0.10
PB126	IPE400	7	ULS5	−109	−109	−97	307	220	0.49	0.14
PB127	IPE400	6	ULS5	−125	−126	−107	307	248	0.51	0.15
PB128	IPE450	6	ULS13	−220	−234	−179	400	323	0.72	0.26

Frame	Section	Length	Comb	$M_{Ed,i}$(kNm)	$M_{Ed,j}$(kNm)	V_{Ed}(kN)	$M_{pl,Rd}$(kNm)	$M_{b,Rd}$(kNm)	$Eq.3.25$	$Eq.3.23$
PB129	IPE400	6	ULS13	-184	-187	-156	307	248	0.75	0.23
PB130	IPE400	6	ULS5	-184	-186	-156	307	248	0.75	0.23
PB131	IPE450	6	ULS13	-220	-234	-179	400	323	0.72	0.26
PB132	IPE400	6	ULS13	-125	-126	-107	307	248	0.51	0.15
PB133	IPE400	7	ULS13	-74	-118	-89	307	220	0.54	0.13
PB134	IPE400	6	ULS5	-85	-85	-84	307	234	0.36	0.12
PB135	IPE400	5	ULS13	-44	-69	-62	307	254	0.27	0.09
PB136	IPE400	6	ULS13	-61	-96	-76	307	238	0.41	0.11
PB137	IPE400	7	ULS5	-107	-107	-98	307	216	0.50	0.14
PB138	IPE400	6	ULS13	-142	-142	-117	307	246	0.58	0.17
PB139	IPE450	6	ULS13	-253	-253	-207	400	323	0.78	0.30
PB140	IPE400	6	ULS13	-211	-211	-172	307	246	0.86	0.25
PB141	IPE400	6	ULS13	-211	-211	-172	307	246	0.86	0.25
PB142	IPE450	6	ULS13	-253	-253	-207	400	323	0.78	0.30
PB143	IPE400	6	ULS13	-142	-142	-117	307	246	0.58	0.17
PB144	IPE400	7	ULS13	-41	-76	-49	307	227	0.33	0.07
PB145	IPE400	6	ULS13	-22	-65	-39	307	247	0.26	0.06
PB146	IPE400	5	ULS48	-59	-59	-41	307	260	0.23	0.06
PB147	IPE400	6	ULS13	-23	-64	-39	307	247	0.26	0.06
PB148	IPE400	7	ULS13	-39	-79	-48	307	228	0.34	0.07
PB200	IPE400	7	ULS13	-42	-77	-49	307	227	0.34	0.07
PB201	IPE400	6	ULS13	-19	-72	-37	307	248	0.29	0.05
PB202	IPE400	5	ULS48	-68	-68	-45	307	260	0.26	0.06
PB203	IPE400	6	ULS48	-69	-69	-43	307	246	0.28	0.06
PB204	IPE400	7	ULS13	-35	-85	-47	307	230	0.37	0.07
PB205	IPE400	6	ULS13	-109	-135	-100	307	246	0.55	0.15
PB206	IPE450	6	ULS13	-181	-235	-171	400	323	0.73	0.25
PB207	IPE400	6	ULS13	-161	-200	-146	307	246	0.81	0.21
PB208	IPE400	6	ULS13	-160	-200	-146	307	246	0.81	0.21
PB209	IPE450	6	ULS13	-181	-235	-171	400	323	0.73	0.25
PB210	IPE400	6	ULS13	-109	-135	-100	307	246	0.55	0.14
PB211	IPE400	7	ULS13	-83	-115	-90	307	218	0.53	0.13
PB212	IPE400	6	ULS13	-64	-89	-76	307	236	0.38	0.11
PB213	IPE400	5	ULS13	-40	-72	-60	307	255	0.28	0.09
PB214	IPE400	6	ULS13	-61	-94	-75	307	237	0.39	0.11
PB215	IPE400	7	ULS13	-87	-113	-91	307	217	0.52	0.13
PB216	IPE400	6	ULS13	-126	-127	-107	307	248	0.51	0.15
PB217	IPE450	6	ULS13	-228	-228	-191	400	323	0.70	0.28
PB218	IPE400	6	ULS5	-186	-188	-157	307	248	0.76	0.23

Frame	Section	Length	Comb	$M_{Ed,i}$(kNm)	$M_{Ed,j}$(kNm)	V_{Ed}(kN)	$M_{pl,Rd}$(kNm)	$M_{b,Rd}$(kNm)	$Eq.3.25$	$Eq.3.23$
PB219	IPE400	6	ULS13	−186	−188	−157	307	248	0.76	0.23
PB220	IPE450	6	ULS13	−228	−228	−191	400	323	0.70	0.28
PB221	IPE400	6	ULS5	−126	−127	−107	307	248	0.51	0.15
PB222	IPE400	7	ULS13	−75	−122	−86	307	224	0.54	0.12
PB223	IPE400	6	ULS13	−54	−90	−73	307	240	0.38	0.11
PB224	IPE400	5	ULS13	−40	−71	−61	307	255	0.28	0.09
PB225	IPE400	6	ULS13	−56	−95	−73	307	241	0.39	0.11
PB226	IPE400	7	ULS13	−83	−110	−89	307	220	0.50	0.13
PB227	IPE400	6	ULS13	−127	−127	−107	307	248	0.51	0.16
PB228	IPE450	6	ULS13	−222	−228	−179	400	323	0.70	0.26
PB229	IPE400	6	ULS5	−188	−188	−157	307	248	0.76	0.23
PB230	IPE400	6	ULS13	−188	−188	−157	307	248	0.76	0.23
PB231	IPE450	6	ULS13	−222	−228	−179	400	323	0.70	0.26
PB232	IPE400	6	ULS5	−127	−127	−107	307	248	0.51	0.16
PB233	IPE400	7	ULS13	−83	−115	−90	307	218	0.53	0.13
PB234	IPE400	6	ULS13	−64	−89	−76	307	236	0.38	0.11
PB235	IPE400	5	ULS13	−40	−72	−60	307	255	0.28	0.09
PB236	IPE400	6	ULS13	−61	−94	−75	307	237	0.39	0.11
PB237	IPE400	7	ULS13	−87	−113	−91	307	217	0.52	0.13
PB238	IPE400	6	ULS13	−135	−135	−114	307	246	0.55	0.16
PB239	IPE450	6	ULS13	−235	−235	−198	400	323	0.73	0.29
PB240	IPE400	6	ULS13	−200	−200	−167	307	246	0.81	0.24
PB241	IPE400	6	ULS13	−200	−200	−167	307	246	0.81	0.24
PB242	IPE450	6	ULS13	−235	−235	−199	400	323	0.73	0.29
PB243	IPE400	6	ULS13	−135	−135	−114	307	246	0.55	0.16
PB244	IPE400	7	ULS13	−42	−77	−49	307	227	0.34	0.07
PB245	IPE400	6	ULS13	−19	−72	−37	307	248	0.29	0.05
PB246	IPE400	5	ULS48	−68	−68	−45	307	260	0.26	0.06
PB247	IPE400	6	ULS48	−69	−69	−43	307	246	0.28	0.06
PB248	IPE400	7	ULS13	−35	−85	−47	307	230	0.37	0.07
PB300	IPE400	7	ULS13	−43	−77	−49	307	227	0.34	0.07
PB301	IPE400	6	ULS13	−18	−74	−37	307	248	0.30	0.05
PB302	IPE400	5	ULS48	−70	−70	−46	307	260	0.27	0.07
PB303	IPE400	6	ULS48	−72	−72	−44	307	246	0.29	0.06
PB304	IPE400	7	ULS13	−33	−88	−46	307	231	0.38	0.07
PB305	IPE400	6	ULS13	−109	−134	−101	307	246	0.54	0.15
PB306	IPE450	6	ULS13	−184	−230	−173	400	323	0.71	0.25
PB307	IPE400	6	ULS13	−161	−198	−147	307	246	0.80	0.21
PB308	IPE400	6	ULS13	−161	−198	−147	307	246	0.80	0.21

Frame	Section	Length	Comb	$M_{Ed,i}$(kNm)	$M_{Ed,j}$(kNm)	V_{Ed}(kN)	$M_{pl,Rd}$(kNm)	$M_{b,Rd}$(kNm)	$Eq.3.25$	$Eq.3.23$
PB309	IPE450	6	ULS13	−184	−231	−173	400	323	0.71	0.25
PB310	IPE400	6	ULS13	−109	−134	−100	307	246	0.54	0.15
PB311	IPE400	7	ULS13	−84	−113	−91	307	218	0.52	0.13
PB312	IPE400	6	ULS13	−63	−91	−76	307	236	0.39	0.11
PB313	IPE400	5	ULS13	−40	−73	−60	307	256	0.28	0.09
PB314	IPE400	6	ULS13	−62	−93	−76	307	237	0.39	0.11
PB315	IPE400	7	ULS13	−84	−115	−90	307	218	0.53	0.13
PB316	IPE400	6	ULS5	−126	−128	−107	307	248	0.52	0.16
PB317	IPE450	6	ULS13	−228	−228	−191	400	323	0.71	0.28
PB318	IPE400	6	ULS5	−187	−189	−157	307	248	0.76	0.23
PB319	IPE400	6	ULS13	−187	−189	−157	307	248	0.76	0.23
PB320	IPE450	6	ULS13	−228	−228	−191	400	323	0.71	0.28
PB321	IPE400	6	ULS5	−126	−128	−107	307	248	0.52	0.16
PB322	IPE400	7	ULS13	−76	−120	−87	307	223	0.54	0.13
PB323	IPE400	6	ULS13	−53	−92	−73	307	241	0.38	0.11
PB324	IPE400	5	ULS13	−41	−72	−61	307	255	0.28	0.09
PB325	IPE400	6	ULS13	−57	−96	−73	307	241	0.40	0.11
PB326	IPE400	7	ULS13	−81	−112	−89	307	221	0.51	0.13
PB327	IPE400	6	ULS5	−128	−128	−108	307	248	0.52	0.16
PB328	IPE450	6	ULS13	−223	−228	−121	400	323	0.71	0.18
PB329	IPE400	6	ULS5	−189	−189	−158	307	248	0.76	0.23
PB330	IPE400	6	ULS13	−189	−189	−158	307	248	0.76	0.23
PB331	IPE450	6	ULS13	−223	−228	−121	400	323	0.71	0.18
PB332	IPE400	6	ULS5	−128	−128	−108	307	248	0.52	0.16
PB333	IPE400	7	ULS13	−84	−113	−91	307	218	0.52	0.13
PB334	IPE400	6	ULS13	−63	−91	−76	307	236	0.39	0.11
PB335	IPE400	5	ULS13	−40	−73	−60	307	256	0.28	0.09
PB336	IPE400	6	ULS13	−62	−93	−76	307	237	0.39	0.11
PB337	IPE400	7	ULS13	−84	−115	−90	307	218	0.53	0.13
PB338	IPE400	6	ULS13	−134	−134	−114	307	246	0.54	0.16
PB339	IPE450	6	ULS13	−230	−230	−198	400	323	0.71	0.29
PB340	IPE400	6	ULS13	−198	−198	−166	307	246	0.80	0.24
PB341	IPE400	6	ULS13	−198	−198	−167	307	246	0.80	0.24
PB342	IPE450	6	ULS13	−231	−231	−198	400	323	0.71	0.29
PB343	IPE400	6	ULS13	−134	−134	−114	307	246	0.54	0.16
PB344	IPE400	7	ULS13	−43	−77	−49	307	227	0.34	0.07
PB345	IPE400	6	ULS13	−18	−74	−37	307	248	0.30	0.05
PB346	IPE400	5	ULS48	−70	−70	−46	307	260	0.27	0.07
PB347	IPE400	6	ULS48	−72	−72	−44	307	246	0.29	0.06

Frame	Section	Length	Comb	$M_{Ed,i}$(kNm)	$M_{Ed,j}$(kNm)	V_{Ed}(kN)	$M_{pl,Rd}$(kNm)	$M_{b,Rd}$(kNm)	$Eq.3.25$	$Eq.3.23$
PB348	IPE400	7	ULS13	-33	-88	-46	307	231	0.38	0.07
PB400	IPE400	7	ULS13	-44	-76	-50	307	226	0.34	0.07
PB401	IPE400	6	ULS13	-18	-75	-37	307	248	0.30	0.05
PB402	IPE400	5	ULS48	-70	-70	-46	307	260	0.27	0.07
PB403	IPE400	6	ULS48	-72	-72	-44	307	246	0.29	0.06
PB404	IPE400	7	ULS13	-32	-89	-46	307	232	0.38	0.07
PB405	IPE400	6	ULS13	-111	-132	-101	307	246	0.54	0.15
PB406	IPE450	6	ULS13	-189	-226	-175	400	323	0.70	0.25
PB407	IPE400	6	ULS13	-164	-195	-148	307	246	0.79	0.21
PB408	IPE400	6	ULS13	-164	-196	-148	307	246	0.79	0.21
PB409	IPE450	6	ULS13	-189	-227	-174	400	323	0.70	0.25
PB410	IPE400	6	ULS13	-111	-132	-101	307	246	0.54	0.15
PB411	IPE400	7	ULS13	-86	-110	-91	307	217	0.51	0.13
PB412	IPE400	6	ULS13	-62	-93	-76	307	237	0.39	0.11
PB413	IPE400	5	ULS13	-42	-74	-61	307	255	0.29	0.09
PB414	IPE400	6	ULS13	-64	-91	-76	307	236	0.39	0.11
PB415	IPE400	7	ULS13	-82	-117	-90	307	219	0.53	0.13
PB416	IPE400	6	ULS13	-127	-129	-107	307	248	0.52	0.16
PB417	IPE450	6	ULS13	-229	-229	-191	400	323	0.71	0.28
PB418	IPE400	6	ULS5	-188	-190	-157	307	248	0.77	0.23
PB419	IPE400	6	ULS13	-188	-190	-157	307	248	0.77	0.23
PB420	IPE450	6	ULS13	-229	-229	-191	400	323	0.71	0.28
PB421	IPE400	6	ULS5	-127	-129	-107	307	248	0.52	0.16
PB422	IPE400	7	ULS13	-78	-119	-87	307	223	0.53	0.13
PB423	IPE400	6	ULS13	-53	-94	-73	307	241	0.39	0.11
PB424	IPE400	5	ULS13	-42	-73	-61	307	255	0.29	0.09
PB425	IPE400	6	ULS13	-59	-96	-74	307	240	0.40	0.11
PB426	IPE400	7	ULS13	-80	-114	-88	307	221	0.52	0.13
PB427	IPE400	6	ULS13	-129	-129	-108	307	248	0.52	0.16
PB428	IPE450	6	ULS13	-223	-229	-180	400	323	0.71	0.26
PB429	IPE400	6	ULS5	-190	-190	-158	307	248	0.77	0.23
PB430	IPE400	6	ULS13	-190	-190	-158	307	248	0.77	0.23
PB431	IPE450	6	ULS13	-223	-229	-180	400	323	0.71	0.26
PB432	IPE400	6	ULS5	-129	-129	-108	307	248	0.52	0.16
PB433	IPE400	7	ULS13	-86	-110	-91	307	217	0.51	0.13
PB434	IPE400	6	ULS13	-62	-93	-76	307	237	0.39	0.11
PB435	IPE400	5	ULS13	-42	-74	-61	307	255	0.29	0.09
PB436	IPE400	6	ULS13	-64	-91	-76	307	236	0.39	0.11
PB437	IPE400	7	ULS13	-82	-117	-90	307	219	0.53	0.13

Frame	Section	Length	Comb	$M_{Ed,i}$(kNm)	$M_{Ed,j}$(kNm)	V_{Ed}(kN)	$M_{pl,Rd}$(kNm)	$M_{b,Rd}$(kNm)	$Eq.3.25$	$Eq.3.23$
PB438	IPE400	6	ULS13	−132	−132	−113	307	246	0.54	0.16
PB439	IPE450	6	ULS13	−226	−226	−196	400	323	0.70	0.28
PB440	IPE400	6	ULS13	−195	−195	−166	307	246	0.79	0.24
PB441	IPE400	6	ULS13	−196	−196	−166	307	246	0.79	0.24
PB442	IPE450	6	ULS13	−227	−227	−196	400	323	0.70	0.28
PB443	IPE400	6	ULS13	−132	−132	−113	307	246	0.54	0.16
PB444	IPE400	7	ULS13	−44	−76	−50	307	226	0.34	0.07
PB445	IPE400	6	ULS13	−18	−75	−37	307	248	0.30	0.05
PB446	IPE400	5	ULS48	−70	−70	−46	307	260	0.27	0.07
PB447	IPE400	6	ULS48	−72	−72	−44	307	246	0.29	0.06
PB448	IPE400	7	ULS13	−32	−89	−46	307	232	0.38	0.07
PB500	IPE400	7	ULS13	−47	−73	−51	307	225	0.32	0.07
PB501	IPE400	6	ULS13	−18	−74	−37	307	248	0.30	0.05
PB502	IPE400	5	ULS36	−66	−66	−44	307	260	0.25	0.06
PB503	IPE400	6	ULS48	−71	−71	−44	307	246	0.29	0.06
PB504	IPE400	7	ULS13	−32	−88	−46	307	231	0.38	0.07
PB505	IPE400	6	ULS13	−113	−130	−102	307	246	0.53	0.15
PB506	IPE450	6	ULS13	−195	−221	−176	400	323	0.68	0.26
PB507	IPE400	6	ULS13	−168	−191	−149	307	246	0.78	0.22
PB508	IPE400	6	ULS13	−168	−192	−149	307	246	0.78	0.22
PB509	IPE450	6	ULS13	−194	−221	−176	400	323	0.68	0.26
PB510	IPE400	6	ULS13	−113	−130	−102	307	246	0.53	0.15
PB511	IPE400	7	ULS5	−110	−110	−98	307	216	0.51	0.14
PB512	IPE400	6	ULS13	−60	−95	−75	307	238	0.40	0.11
PB513	IPE400	5	ULS13	−40	−71	−37	307	255	0.28	0.05
PB514	IPE400	6	ULS13	−67	−89	−78	307	235	0.38	0.11
PB515	IPE400	7	ULS13	−80	−120	−89	307	220	0.55	0.13
PB516	IPE400	6	ULS5	−125	−129	−107	307	248	0.52	0.15
PB517	IPE450	6	ULS13	−227	−227	−191	400	323	0.70	0.28
PB518	IPE400	6	ULS5	−185	−190	−156	307	248	0.76	0.23
PB519	IPE400	6	ULS5	−185	−190	−156	307	248	0.76	0.23
PB520	IPE450	6	ULS13	−227	−227	−191	400	323	0.70	0.28
PB521	IPE400	6	ULS5	−125	−129	−107	307	248	0.52	0.15
PB522	IPE400	7	ULS13	−83	−115	−89	307	221	0.52	0.13
PB523	IPE400	6	ULS13	−52	−96	−72	307	241	0.40	0.10
PB524	IPE400	5	ULS13	−41	−71	−37	307	255	0.28	0.05
PB525	IPE400	6	ULS13	−63	−92	−75	307	239	0.38	0.11
PB526	IPE400	7	ULS13	−78	−117	−88	307	222	0.53	0.13
PB527	IPE400	6	ULS5	−129	−129	−108	307	248	0.52	0.16

Frame	Section	Length	Comb	$M_{Ed,i}$(kNm)	$M_{Ed,j}$(kNm)	V_{Ed}(kN)	$M_{pl,Rd}$(kNm)	$M_{b,Rd}$(kNm)	$Eq.3.25$	$Eq.3.23$
PB528	IPE450	6	ULS13	−224	−227	−180	400	323	0.70	0.26
PB529	IPE400	6	ULS5	−190	−190	−158	307	248	0.76	0.23
PB530	IPE400	6	ULS5	−190	−190	−158	307	248	0.76	0.23
PB531	IPE450	6	ULS13	−224	−227	−180	400	323	0.70	0.26
PB532	IPE400	6	ULS5	−129	−129	−108	307	248	0.52	0.16
PB533	IPE400	7	ULS5	−110	−110	−98	307	216	0.51	0.14
PB534	IPE400	6	ULS13	−60	−95	−75	307	238	0.40	0.11
PB535	IPE400	5	ULS13	−40	−71	−37	307	255	0.28	0.05
PB536	IPE400	6	ULS13	−67	−89	−78	307	235	0.38	0.11
PB537	IPE400	7	ULS13	−80	−120	−89	307	220	0.55	0.13
PB538	IPE400	6	ULS13	−130	−130	−112	307	246	0.53	0.16
PB539	IPE450	6	ULS13	−221	−221	−194	400	323	0.68	0.28
PB540	IPE400	6	ULS13	−191	−191	−164	307	246	0.78	0.24
PB541	IPE400	6	ULS13	−192	−192	−164	307	246	0.78	0.24
PB542	IPE450	6	ULS13	−221	−221	−194	400	323	0.68	0.28
PB543	IPE400	6	ULS13	−130	−130	−112	307	246	0.53	0.16
PB544	IPE400	7	ULS13	−47	−73	−51	307	225	0.32	0.07
PB545	IPE400	6	ULS13	−18	−74	−37	307	248	0.30	0.05
PB546	IPE400	5	ULS36	−66	−66	−44	307	260	0.25	0.06
PB547	IPE400	6	ULS48	−71	−71	−44	307	246	0.29	0.06
PB548	IPE400	7	ULS13	−32	−88	−46	307	231	0.38	0.07
PB600	IPE400	7	ULS48	−62	−62	−38	307	229	0.27	0.06
PB601	IPE400	6	ULS48	−55	−55	−36	307	244	0.22	0.05
PB602	IPE400	5	ULS36	50	50	−22	307	249	0.20	0.03
PB603	IPE400	6	ULS46	−55	−55	34	307	244	0.22	0.05
PB604	IPE400	7	ULS46	0	−62	−19	307	229	0.27	0.03
PB605	IPE400	6	ULS5	−81	−137	−89	307	230	0.59	0.13
PB606	IPE450	6	ULS5	−135	−251	−161	400	299	0.84	0.23
PB607	IPE400	6	ULS5	−123	−213	−137	307	230	0.93	0.20
PB608	IPE400	6	ULS5	−123	−213	−137	307	230	0.93	0.20
PB609	IPE450	6	ULS5	−135	−251	−161	400	299	0.84	0.23
PB610	IPE400	6	ULS5	−81	−137	−89	307	230	0.59	0.13
PB611	IPE400	7	ULS5	−81	−105	−92	307	213	0.49	0.13
PB612	IPE400	6	ULS5	−91	−91	−85	307	232	0.39	0.12
PB613	IPE400	5	ULS35	−95	−95	65	307	223	0.42	0.09
PB614	IPE400	6	ULS5	−78	−91	−80	307	232	0.39	0.12
PB615	IPE400	7	ULS5	−105	−105	−99	307	213	0.49	0.14
PB616	IPE400	6	ULS5	−124	−124	−102	307	245	0.51	0.15
PB617	IPE450	6	ULS5	−238	−238	−193	400	320	0.74	0.28

Frame	Section	Length	Comb	$M_{Ed,i}$(kNm)	$M_{Ed,j}$(kNm)	V_{Ed}(kN)	$M_{pl,Rd}$(kNm)	$M_{b,Rd}$(kNm)	$Eq.3.25$	$Eq.3.23$
PB618	IPE400	6	ULS5	−193	−193	−159	307	245	0.79	0.23
PB619	IPE400	6	ULS5	−193	−193	−159	307	245	0.79	0.23
PB620	IPE450	6	ULS5	−238	−238	−193	400	320	0.74	0.28
PB621	IPE400	6	ULS5	−124	−124	−102	307	245	0.51	0.15
PB622	IPE400	7	ULS5	−75	−108	−89	307	218	0.50	0.13
PB623	IPE400	6	ULS5	−80	−80	−82	307	231	0.34	0.12
PB624	IPE400	5	ULS5	−66	−66	−70	307	248	0.27	0.10
PB625	IPE400	6	ULS5	−78	−80	−81	307	231	0.34	0.12
PB626	IPE400	7	ULS5	−108	−108	−99	307	218	0.50	0.14
PB627	IPE400	6	ULS5	−123	−124	−102	307	245	0.51	0.15
PB628	IPE450	6	ULS5	−232	−238	−183	400	320	0.74	0.26
PB629	IPE400	6	ULS5	−191	−193	−158	307	245	0.79	0.23
PB630	IPE400	6	ULS5	−191	−193	−158	307	245	0.79	0.23
PB631	IPE450	6	ULS5	−232	−238	−183	400	320	0.74	0.26
PB632	IPE400	6	ULS5	−123	−124	−102	307	245	0.51	0.15
PB633	IPE400	7	ULS5	−81	−105	−92	307	213	0.49	0.13
PB634	IPE400	6	ULS5	−91	−91	−85	307	232	0.39	0.12
PB635	IPE400	5	ULS37	−95	−95	65	307	223	0.42	0.09
PB636	IPE400	6	ULS5	−78	−91	−80	307	232	0.39	0.12
PB637	IPE400	7	ULS5	−105	−105	−99	307	213	0.49	0.14
PB638	IPE400	6	ULS5	−137	−137	−114	307	230	0.59	0.16
PB639	IPE450	6	ULS5	−251	−251	−211	400	299	0.84	0.31
PB640	IPE400	6	ULS5	−213	−213	−177	307	230	0.93	0.26
PB641	IPE400	6	ULS5	−213	−213	−177	307	230	0.93	0.26
PB642	IPE450	6	ULS5	−251	−251	−211	400	299	0.84	0.31
PB643	IPE400	6	ULS5	−137	−137	−114	307	230	0.59	0.16
PB644	IPE400	7	ULS48	−62	−62	−38	307	229	0.27	0.06
PB645	IPE400	6	ULS48	−55	−55	−36	307	244	0.22	0.05
PB646	IPE400	5	ULS36	50	50	−22	307	249	0.20	0.03
PB647	IPE400	6	ULS46	−55	−55	34	307	244	0.22	0.05
PB648	IPE400	7	ULS46	0	−62	−19	307	229	0.27	0.03

Table A1.2 Verifications under SLS of the principal beams

Beam	Comb	$\gamma_{Total,deflection}$	$\gamma_{Q,deflection}$	Beam	Comb	$\gamma_{Total,deflection}$	$\gamma_{Q,deflection}$
PB105	SLS5	$L/2371$	$L/6772$	PB608	SLS5	L/806	L/1351
PB116	SLS5	$L/2883$	$L/7792$	PB619	SLS5	L/914	L/7109
PB127	SLS5	$L/2894$	$L/7812$	PB630	SLS5	L/917	L/7117
PB138	SLS5	$L/2577$	$L/7100$	PB641	SLS5	L/826	L/8733
PB106	SLS5	$L/1701$	$L/4643$	PB609	SLS5	L/810	L/1077
PB117	SLS5	$L/2012$	$L/4987$	PB620	SLS5	L/857	L/5952
PB118	SLS5	$L/1969$	$L/4827$	PB631	SLS5	L/850	L/5976
PB139	SLS5	$L/1803$	$L/4858$	PB642	SLS5	L/804	L/7237
PB107	SLS5	$L/1627$	$L/4316$	PB610	SLS5	L/1232	L/2097
PB118	SLS5	$L/1963$	$L/4987$	PB621	SLS5	L/1384	L/1109
PB119	SLS5	$L/1967$	$L/4983$	PB632	SLS5	L/1391	L/1111
PB140	SLS5	$L/1757$	$L/4545$	PB643	SLS5	L/1258	L/1357
PB108	SLS5	$L/1627$	$L/4316$	PB100	SLS5	L/4283	L/1343
PB119	SLS5	$L/1963$	$L/4987$	PB122	SLS5	L/2150	L/5577
PB130	SLS5	$L/1967$	$L/4983$	PB144	SLS5	L/4283	L/1343
PB141	SLS5	$L/1757$	$L/4545$	PB115	SLS5	L/1988	L/4964
PB109	SLS5	$L/1701$	$L/4643$	PB137	SLS5	L/1988	L/4964
PB120	SLS5	$L/2012$	$L/4987$	PB200	SLS5	L/3451	L/1109
PB131	SLS5	$L/1969$	$L/4827$	PB222	SLS5	L/1784	L/4871
PB142	SLS5	$L/1803$	$L/4858$	PB244	SLS5	L/3451	L/1109
PB110	SLS5	$L/2371$	$L/6772$	PB215	SLS5	L/1674	L/4530
PB121	SLS5	$L/2883$	$L/7792$	PB237	SLS5	L/1674	L/4530
PB132	SLS5	$L/2894$	$L/7812$	PB300	SLS5	L/2959	L/9722
PB143	SLS5	$L/2577$	$L/7100$	PB322	SLS5	L/1522	L/4281
PB205	SLS5	$L/2166$	$L/6557$	PB344	SLS5	L/2959	L/9722
PB216	SLS5	$L/2239$	$L/6637$	PB315	SLS5	L/1434	L/3993
PB227	SLS5	$L/2261$	$L/6622$	PB337	SLS5	L/1434	L/3993
PB238	SLS5	$L/2162$	$L/6410$	PB400	SLS5	L/2667	L/8997
PB206	SLS5	$L/1502$	$L/4411$	PB422	SLS5	L/1359	L/4020
PB217	SLS5	$L/1468$	$L/4282$	PB444	SLS5	L/2667	L/8997
PB218	SLS5	$L/1436$	$L/4316$	PB415	SLS5	L/1282	L/3771
PB239	SLS5	$L/1451$	$L/4264$	PB437	SLS5	L/1282	L/3771
PB207	SLS5	$L/1485$	$L/4189$	PB500	SLS57	L/2524	L/8599
PB218	SLS5	$L/1523$	$L/4246$	PB522	SLS5	L/1324	L/3769
PB219	SLS13	$L/1534$	$L/4237$	PB544	SLS57	L/2524	L/8599
PB240	SLS5	$L/1473$	$L/4109$	PB515	SLS5	L/1266	L/3521
PB208	SLS5	$L/1485$	$L/4189$	PB537	SLS5	L/1266	L/3521
PB219	SLS5	$L/1523$	$L/4246$	PB600	SLS5	L/2227	L/1548
PB230	SLS13	$L/1534$	$L/4237$	PB622	SLS5	L/976	L/7683
PB241	SLS5	$L/1473$	$L/4109$	PB644	SLS5	L/2227	L/1548

Beam	Comb	$\gamma_{Total,deflection}$	$\gamma_{Q,deflection}$	Beam	Comb	$\gamma_{Total,deflection}$	$\gamma_{Q,deflection}$
PB209	SLS5	$L/1502$	$L/4411$	PB615	SLS5	L/901	L/7600
PB220	SLS5	$L/1468$	$L/4282$	PB637	SLS5	L/901	L/7600
PB231	SLS5	$L/1436$	$L/4316$	PB101	SLS5	L/4995	L/1587
PB242	SLS5	$L/1451$	$L/4264$	PB112	SLS5	L/2682	L/6920
PB210	SLS5	$L/2166$	$L/6557$	PB123	SLS13	L/2631	L/7371
PB221	SLS5	$L/2239$	$L/6637$	PB134	SLS5	L/2682	L/6920
PB232	SLS5	$L/2261$	$L/6622$	PB145	SLS5	L/4995	L/1587
PB243	SLS5	$L/2162$	$L/6410$	PB103	SLS5	L/4995	L/1587
PB305	SLS5	$L/1924$	$L/6030$	PB114	SLS5	L/2682	L/6920
PB316	SLS5	$L/1899$	$L/5982$	PB125	SLS5	L/2683	L/7371
PB327	SLS5	$L/1920$	$L/5970$	PB136	SLS5	L/2682	L/6920
PB338	SLS5	$L/1866$	$L/5797$	PB147	SLS5	L/4995	L/1587
PB306	SLS5	$L/1308$	$L/4000$	PB201	SLS5	L/3562	L/1158
PB317	SLS5	$L/1214$	$L/3821$	PB212	SLS5	L/1837	L/5253
PB318	SLS5	$L/1200$	$L/3819$	PB223	SLS5	L/1898	L/5434
PB339	SLS5	$L/1223$	$L/3785$	PB234	SLS5	L/1837	L/5253
PB307	SLS5	$L/1319$	$L/3856$	PB245	SLS5	L/3562	L/1158
PB318	SLS5	$L/1290$	$L/3828$	PB203	SLS5	L/3562	L/1158
PB319	SLS5	$L/1301$	$L/3819$	PB214	SLS5	L/1837	L/5253
PB340	SLS5	$L/1270$	$L/3717$	PB225	SLS5	L/1898	L/5434
PB308	SLS5	$L/1319$	$L/3856$	PB236	SLS5	L/1837	L/5253
PB319	SLS5	$L/1290$	$L/3828$	PB247	SLS5	L/3562	L/1158
PB330	SLS5	$L/1301$	$L/3819$	PB301	SLS5	L/2891	L/9630
PB341	SLS5	$L/1270$	$L/3717$	PB312	SLS5	L/1482	L/4418
PB309	SLS5	$L/1308$	$L/4000$	PB323	SLS5	L/1529	L/4548
PB320	SLS5	$L/1214$	$L/3821$	PB334	SLS5	L/1482	L/4418
PB331	SLS5	$L/1200$	$L/3819$	PB345	SLS5	L/2891	L/9630
PB342	SLS5	$L/1223$	$L/3785$	PB303	SLS5	L/2891	L/9630
PB310	SLS5	$L/1924$	$L/6030$	PB314	SLS5	L/1482	L/4418
PB321	SLS5	$L/1899$	$L/5982$	PB325	SLS5	L/1529	L/4548
PB332	SLS5	$L/1920$	$L/5970$	PB336	SLS5	L/1482	L/4418
PB343	SLS5	$L/1866$	$L/5797$	PB347	SLS5	L/2891	L/9630
PB405	SLS5	$L/1765$	$L/5870$	PB401	SLS5	L/2528	L/8645
PB416	SLS5	$L/1703$	$L/5597$	PB412	SLS5	L/1293	L/3963
PB427	SLS5	$L/1721$	$L/5586$	PB423	SLS5	L/1331	L/4092
PB438	SLS5	$L/1683$	$L/5529$	PB434	SLS5	L/1293	L/3963
PB406	SLS5	$L/1186$	$L/3851$	PB445	SLS5	L/2528	L/8645
PB417	SLS5	$L/1070$	$L/3550$	PB403	SLS5	L/2528	L/8645
PB418	SLS5	$L/1065$	$L/3529$	PB414	SLS5	L/1293	L/3963
PB439	SLS5	$L/1088$	$L/3573$	PB425	SLS5	L/1331	L/4092
PB407	SLS5	$L/1207$	$L/3754$	PB436	SLS5	L/1293	L/3963

Beam	Comb	$\gamma_{Total,deflection}$	$\gamma_{Q,deflection}$	Beam	Comb	$\gamma_{Total,deflection}$	$\gamma_{Q,deflection}$
PB418	SLS5	$L/1155$	$L/3584$	PB447	SLS5	L/2528	L/8645
PB419	SLS5	$L/1165$	$L/3573$	PB501	SLS5	L/2326	L/8230
PB440	SLS5	$L/1143$	$L/3548$	PB512	SLS5	L/1168	L/3843
PB408	SLS5	$L/1207$	$L/3754$	PB523	SLS5	L/1215	L/3926
PB419	SLS5	$L/1155$	$L/3584$	PB534	SLS5	L/1168	L/3843
PB430	SLS5	$L/1165$	$L/3573$	PB545	SLS5	L/2326	L/8230
PB441	SLS5	$L/1143$	$L/3548$	PB503	SLS5	L/2326	L/8230
PB409	SLS5	$L/1186$	$L/3851$	PB514	SLS5	L/1168	L/3843
PB420	SLS5	$L/1070$	$L/3550$	PB525	SLS5	L/1215	L/3926
PB431	SLS5	$L/1065$	$L/3529$	PB536	SLS5	L/1168	L/3843
PB442	SLS5	$L/1088$	$L/3573$	PB547	SLS5	L/2326	L/8230
PB410	SLS5	$L/1765$	$L/5870$	PB601	SLS5	L/2160	L/1086
PB421	SLS5	$L/1703$	$L/5597$	PB612	SLS5	L/1067	L/4905
PB432	SLS5	$L/1721$	$L/5586$	PB623	SLS5	L/1079	L/5167
PB443	SLS5	$L/1683$	$L/5529$	PB634	SLS5	L/1067	L/4905
PB505	SLS29	$L/1779$	$L/5479$	PB645	SLS5	L/2160	L/1086
PB516	SLS5	$L/1577$	$L/5464$	PB603	SLS5	L/2160	L/1086
PB527	SLS5	$L/1597$	$L/5459$	PB614	SLS5	L/1067	L/4905
PB538	SLS5	$L/1622$	$L/5253$	PB625	SLS5	L/1079	L/5167
PB506	SLS5	$L/1180$	$L/3590$	PB636	SLS5	L/1067	L/4905
PB517	SLS5	$L/984$	$L/3438$	PB647	SLS5	L/2160	L/1086
PB518	SLS5	$L/982$	$L/3434$	PB102	SLS5	L/6976	L/2255
PB539	SLS5	$L/1038$	$L/3374$	PB112	SLS5	L/3783	L/1090
PB507	SLS5	$L/1224$	$L/3502$	PB123	SLS5	L/3861	L/1098
PB518	SLS5	$L/1068$	$L/3498$	PB134	SLS5	L/3783	L/1090
PB519	SLS5	$L/1080$	$L/3486$	PB146	SLS5	L/6976	L/2255
PB540	SLS5	$L/1104$	$L/3367$	PB202	SLS5	L/4583	L/1515
PB508	SLS5	$L/1224$	$L/3502$	PB212	SLS5	L/2442	L/7263
PB519	SLS5	$L/1068$	$L/3498$	PB223	SLS5	L/2487	L/7308
PB530	SLS5	$L/1080$	$L/3486$	PB234	SLS5	L/2442	L/7263
PB541	SLS5	$L/1104$	$L/3367$	PB246	SLS5	L/4583	L/1515
PB509	SLS5	$L/1180$	$L/3590$	PB302	SLS5	L/3592	L/1219
PB520	SLS5	$L/984$	$L/3438$	PB312	SLS5	L/1899	L/5876
PB531	SLS5	$L/982$	$L/3434$	PB323	SLS5	L/1938	L/5905
PB542	SLS5	$L/1038$	$L/3374$	PB334	SLS5	L/1899	L/5876
PB510	SLS29	$L/1779$	$L/5479$	PB346	SLS5	L/3592	L/1219
PB521	SLS5	$L/1577$	$L/5464$	PB402	SLS5	L/3084	L/1077
PB532	SLS5	$L/1597$	$L/5459$	PB412	SLS5	L/1625	L/5163
PB543	SLS5	$L/1622$	$L/5253$	PB423	SLS5	L/1658	L/5217
PB605	SLS5	$L/1232$	$L/2097$	PB434	SLS5	L/1625	L/5163
PB616	SLS5	$L/1384$	$L/1109$	PB446	SLS5	L/3084	L/1077

Beam	Comb	$\gamma_{Total,deflection}$	$\gamma_{Q,deflection}$	Beam	Comb	$\gamma_{Total,deflection}$	$\gamma_{Q,deflection}$
PB627	SLS5	$L/1391$	$L/1111$	PB502	SLS5	L/2802	L/1016
PB638	SLS5	$L/1258$	$L/1357$	PB512	SLS5	L/1463	L/4966
PB606	SLS5	$L/810$	$L/1077$	PB523	SLS5	L/1490	L/5000
PB617	SLS5	$L/857$	$L/5952$	PB534	SLS5	L/1463	L/4966
PB618	SLS5	$L/850$	$L/5976$	PB546	SLS5	L/2802	L/1016
PB639	SLS5	$L/804$	$L/7237$	PB602	SLS5	L/2659	L/1183
PB607	SLS5	$L/806$	$L/1351$	PB612	SLS5	L/1379	L/5479
PB618	SLS5	$L/914$	$L/7109$	PB623	SLS5	L/1408	L/5633
PB619	SLS5	$L/917$	$L/7117$	PB634	SLS5	L/1379	L/5479
PB640	SLS5	$L/826$	$L/8733$	PB646	SLS5	L/2659	L/1183

Table A1.3 Verification of the columns under ULS in the static condtions

Column	Comb	$N_{Ed}(kN)$	$M_{Ed,2}(kNm)$	$M_{Ed,3}(kNm)$	$V_{Ed,2}(kN)$	$V_{Ed,3}(kN)$	Ratio
AA1	ULS5	-1026	10	8	-7	-11	0.19
AA2	ULS5	-860	-69	-40	-24	-42	0.19
AB1	ULS13	-1654	15	20	21	-17	0.32
AB2	ULS13	-1370	-112	42	12	-46	0.29
AC1	ULS13	-1402	14	19	21	-16	0.28
AC2	ULS13	-1161	-101	44	15	-41	0.26
AD1	ULS13	-1439	14	21	18	-16	0.29
AD2	ULS13	-1191	-101	29	6	-41	0.25
AE1	ULS13	-1676	15	23	17	-17	0.32
AE2	ULS5	-1462	-113	-18	-11	-70	0.29
AF1	ULS13	-1011	10	17	23	-11	0.21
AF2	ULS13	-839	-69	52	23	-28	0.20
BA1	ULS5	-1947	-9	-7	-5	10	0.31
BA2	ULS5	-1623	61	30	18	37	0.28
BB1	ULS5	-3441	1	-11	14	-7	0.51
BB2	ULS5	-2853	-27	53	-24	2	0.44
BC1	ULS5	-2900	1	-11	12	-5	0.42
BC2	ULS5	-2412	-21	46	-20	1	0.37
BD1	ULS5	-2900	-1	-11	-8	-1	0.42
BD2	ULS5	-2412	21	46	27	13	0.37
BE1	ULS5	-3441	-1	-11	-9	-1	0.51
BE2	ULS5	-2853	27	53	31	17	0.44
BF1	ULS5	-1947	9	-7	8	-14	0.31
BF2	ULS5	-1623	-61	30	-13	-25	0.28
CA1	ULS5	-1915	-8	-5	-7	9	0.30
CA2	ULS5	-1600	59	-26	15	24	0.27
CB1	ULS13	-3182	-10	60	15	8	0.50

Column	Comb	$N_{Ed}(kN)$	$M_{Ed,2}(kNm)$	$M_{Ed,3}(kNm)$	$V_{Ed,2}(kN)$	$V_{Ed,3}(kN)$	Ratio
CB2	ULS5	-2799	-32	34	-3	20	0.44
CC1	ULS5	-2863	0	-15	10	-5	0.41
CC2	ULS5	-2385	-20	39	-23	1	0.36
CD1	ULS5	-2863	0	-15	-10	0	0.41
CD2	ULS5	-2385	20	-39	23	-1	0.36
CE1	ULS5	-3363	-10	1	-9	8	0.50
CE2	ULS5	-2799	-32	-34	-21	-20	0.44
CF1	ULS5	-1915	8	-5	7	-14	0.30
CF2	ULS5	-1600	-59	26	-15	-24	0.27
DA1	ULS5	-1947	-9	7	-8	14	0.31
DA2	ULS5	-1623	61	-30	13	25	0.28
DB1	ULS5	-3441	1	11	9	1	0.51
DB2	ULS5	-2853	-27	-53	-31	-17	0.44
DC1	ULS5	-2900	1	11	8	1	0.42
DC2	ULS5	-2412	-21	-46	-27	-13	0.37
DD1	ULS5	-2900	-1	11	-12	5	0.42
DD2	ULS5	-2412	21	-46	20	-1	0.37
DE1	ULS5	-3441	-1	11	-14	7	0.51
DE2	ULS5	-2853	27	-53	24	-2	0.44
DF1	ULS5	-1947	9	7	5	-10	0.31
DF2	ULS5	-1623	-61	-30	-18	-37	0.28
EA1	ULS5	-1026	-10	8	-10	16	0.19
EA2	ULS5	-860	69	-40	-17	28	0.19
EB1	ULS13	-1654	-15	20	15	26	0.32
EB2	ULS13	-1370	112	42	25	70	0.29
EC1	ULS13	-1402	-14	19	17	24	0.28
EC2	ULS13	-1161	101	44	26	62	0.26
ED1	ULS13	-1439	-14	21	13	24	0.29
ED2	ULS13	-1191	101	29	17	62	0.25
EE1	ULS13	-1676	-15	23	11	26	0.32
EE2	ULS5	-1462	113	-18	2	47	0.29
EF1	ULS13	-1011	-10	17	20	16	0.21
EF2	ULS13	-839	69	52	30	42	0.20
AA3	ULS5	-680	1	1	-15	-24	0.15
AB3	ULS13	-1071	2	1	23	-41	0.24
AC3	ULS13	-905	1	1	25	-35	0.21
AD3	ULS5	-1000	1	1	1	-36	0.20
AE3	ULS5	-1161	1	1	2	-41	0.23
AF3	ULS13	-653	1	1	28	-24	0.16
BA3	ULS5	-1291	-1	-1	-13	21	0.22
BB3	ULS5	-2280	5	36	24	3	0.35
BC3	ULS5	-1930	2	-31	22	-13	0.30
BD3	ULS5	-1930	-2	-31	-20	-1	0.30

Column	Comb	$N_{Ed}(kN)$	$M_{Ed,2}(kNm)$	$M_{Ed,3}(kNm)$	$V_{Ed,2}(kN)$	$V_{Ed,3}(kN)$	Ratio
BE3	ULS5	-2280	-5	36	-25	14	0.35
BF3	ULS5	-1291	1	-1	14	-32	0.22
CA3	ULS5	-1273	-1	1	-14	31	0.22
CB3	ULS5	-2238	-28	-6	-4	-18	0.36
CC3	ULS5	-1909	2	-31	21	-12	0.29
CD3	ULS5	-1909	-2	-31	-21	-1	0.29
CE3	ULS5	-2238	28	6	4	18	0.36
CF3	ULS5	-1273	1	-1	14	-31	0.22
DA3	ULS5	-1291	-1	1	-14	32	0.22
DB3	ULS5	-2280	5	-36	25	-14	0.35
DC3	ULS5	-1930	2	31	20	1	0.30
DD3	ULS5	-1930	-2	31	-22	13	0.30
DE3	ULS5	-2280	-5	-36	-24	-3	0.35
DF3	ULS5	-1291	1	1	13	-21	0.22
EA3	ULS5	-680	-1	1	-21	37	0.15
EB3	ULS13	-1071	-2	1	12	62	0.24
EC3	ULS13	-905	-1	1	15	54	0.21
ED3	ULS5	-1000	-1	1	-9	54	0.20
EE3	ULS5	-1161	-1	1	-9	63	0.23
EF3	ULS13	-653	-1	1	22	36	0.16
AA4	ULS5	-505	1	1	-16	-27	0.14
AB4	ULS13	-782	-101	36	12	-45	0.20
AC4	ULS13	-654	1	-1	26	-57	0.18
AD4	ULS5	-745	2	0	1	-40	0.18
AE4	ULS5	-864	2	0	2	-68	0.20
AF4	ULS13	-477	-60	45	23	-26	0.14
BA4	ULS5	-964	-1	0	-13	35	0.18
BB4	ULS5	-1711	5	-39	25	-15	0.28
BC4	ULS5	-1449	2	36	23	1	0.24
BD4	ULS5	-1449	-2	36	-20	14	0.24
BE4	ULS5	-1711	-5	-39	-25	-3	0.28
BF4	ULS5	-964	1	0	15	-25	0.18
CA4	ULS5	-950	-1	-1	-14	24	0.18
CB4	ULS5	-1679	29	-6	19	-19	0.29
CC4	ULS5	-1431	2	33	21	1	0.23
CD4	ULS5	-1431	-2	33	-21	13	0.23
CE4	ULS5	-1679	-29	6	-19	19	0.29
CF4	ULS5	-950	1	1	14	-24	0.18
DA4	ULS5	-964	-1	0	-15	25	0.18
DB4	ULS5	-1711	5	39	25	3	0.28
DC4	ULS5	-1449	2	-36	20	-14	0.24
DD4	ULS5	-1449	-2	-36	-23	-1	0.24
DE4	ULS5	-1711	-5	39	-25	15	0.28

Column	Comb	$N_{Ed}(kN)$	$M_{Ed,2}(kNm)$	$M_{Ed,3}(kNm)$	$V_{Ed,2}(kN)$	$V_{Ed,3}(kN)$	Ratio
DF4	ULS5	-964	1	0	13	-35	0.18
EA4	ULS5	-505	-1	1	-23	40	0.14
EB4	ULS13	-782	101	36	24	66	0.20
EC4	ULS13	-654	-1	-1	15	39	0.18
ED4	ULS5	-745	-2	0	-10	59	0.18
EE4	ULS5	-864	-2	0	-10	46	0.20
EF4	ULS13	-477	60	45	29	39	0.14
AA5	ULS13	-259	-59	-25	-14	-38	0.11
AB5	ULS13	-487	-100	35	11	-40	0.19
AC5	ULS13	-406	-87	38	13	-34	0.16
AD5	ULS13	-416	-87	26	7	-34	0.16
AE5	ULS13	-494	-100	24	4	-40	0.19
AF5	ULS13	-290	-2	-2	22	-38	0.12
BA5	ULS5	-642	50	23	15	30	0.14
BB5	ULS5	-1143	-23	38	-33	6	0.22
BC5	ULS5	-967	-22	35	-27	2	0.19
BD5	ULS5	-967	22	35	22	14	0.19
BE5	ULS5	-1143	23	38	24	14	0.22
BF5	ULS5	-642	-50	23	-17	-18	0.14
CA5	ULS5	-631	49	23	16	30	0.14
CB5	ULS5	-1119	31	27	17	21	0.22
CC5	ULS5	-954	-21	-35	-24	-14	0.18
CD5	ULS5	-954	21	-35	24	-2	0.18
CE5	ULS5	-1119	31	-27	8	-21	0.22
CF5	ULS5	-631	-49	23	-16	-18	0.14
DA5	ULS5	-642	50	-23	17	18	0.14
DB5	ULS5	-1143	-23	-38	-24	-14	0.22
DC5	ULS5	-967	-22	-35	-22	-14	0.19
DD5	ULS5	-967	22	-35	27	-2	0.19
DE5	ULS5	-1143	23	-38	33	-6	0.22
DF5	ULS5	-642	-50	-23	-15	-30	0.14
EA5	ULS13	-259	59	-25	-7	23	0.11
EB5	ULS13	-487	100	35	25	65	0.19
EC5	ULS13	-406	87	38	25	55	0.16
ED5	ULS13	-416	87	26	19	55	0.16
EE5	ULS13	-494	100	24	17	65	0.19
EF5	ULS13	-290	2	-2	29	23	0.12
AA6	ULS5	-145	95	59	-28	-47	0.18
AB6	ULS5	-262	161	-15	10	-93	0.30
AC6	ULS5	-225	147	-19	11	-82	0.27
AD6	ULS5	-225	147	19	-2	-72	0.27
AE6	ULS5	-262	161	15	-1	-81	0.30
AF6	ULS5	-145	95	-59	32	-54	0.18

Column	Comb	$N_{Ed}(kN)$	$M_{Ed,2}(kNm)$	$M_{Ed,3}(kNm)$	$V_{Ed,2}(kN)$	$V_{Ed,3}(kN)$	Ratio
BA6	ULS5	-308	-92	-16	-4	45	0.17
BB6	ULS5	-595	1	-34	19	-16	0.13
BC6	ULS47	-214	16	-28	42	-28	0.14
BD6	ULS47	-214	-16	-28	26	20	0.14
BE6	ULS5	-595	-1	-34	-10	4	0.13
BF6	ULS5	-308	92	-16	11	-51	0.17
CA6	ULS5	-297	-89	-7	-8	44	0.17
CB6	ULS5	-571	-23	-3	6	-12	0.13
CC6	ULS46	-229	75	-8	9	-41	0.14
CD6	ULS48	-229	-75	-8	-9	32	0.14
CE6	ULS5	-571	-23	3	-21	12	0.13
CF6	ULS5	-297	89	-7	8	-50	0.17
DA6	ULS5	-308	-92	16	-11	51	0.17
DB6	ULS5	-595	1	34	10	-4	0.13
DC6	ULS49	-214	16	28	-26	-20	0.14
DD6	ULS49	-214	-16	28	-42	28	0.14
DE6	ULS5	-595	-1	34	-19	16	0.13
DF6	ULS5	-308	92	16	4	-45	0.17
EA6	ULS5	-145	-95	59	-32	54	0.18
EB6	ULS5	-262	-161	-15	1	81	0.30
EC6	ULS5	-225	-147	-19	2	72	0.27
ED6	ULS5	-225	-147	19	-11	82	0.27
EE6	ULS5	-262	-161	15	-10	93	0.30
EF6	ULS5	-145	-95	-59	28	47	0.18

ANNEX 2

The annex 2 presents the capacity design verifications for the primary elements. Tables A2.1 and A.2 show the bending and shear designing forces according to the section 3.6.2, obtained from the linear modal response spectrum analysis, as well as the overstrengh factors to be accounted for the non-dissipative elements.

In the Tables A2.3 and A2.4 has been specified the designing forces applied to the non-dissipative elements and the verifications of the cross-sections according to the section 3.6.3, considering the top and bottom ends.

Table A2.1 Verifications of the dissipative elements under bending forces

Direction	Item	Profile	M_{Ed_G}(kNm)	M_{Ed_E}(kNm)	α	M_{Ed_Total}(kNm)	$M_{pl,Rd}$(kNm)	Ω	Eq.2.2
X	PB100	IPE400	20	72	1.21	87	108	2.85	0.35
X	PB101	IPE400	15	78	1.21	95	110	2.79	0.36
X	PB102	IPE400	10	91	1.21	110	120	2.56	0.39
X	PB103	IPE400	15	77	1.21	94	109	2.83	0.35
X	PB104	IPE400	20	70	1.21	85	105	2.93	0.34
X	PB111	IPE400	30	54	1.21	65	95	3.24	0.31
X	PB112	IPE400	27	51	1.21	61	88	3.49	0.29
X	PB113	IPE400	18	57	1.21	69	86	3.55	0.28
X	PB114	IPE400	23	49	1.21	60	83	3.70	0.27
X	PB115	IPE400	35	49	1.21	59	94	3.27	0.31
X	PB122	IPE400	29	55	1.21	67	96	3.20	0.31
X	PB123	IPE400	25	61	1.21	74	99	3.09	0.32
X	PB124	IPE400	18	51	1.21	62	80	3.86	0.26
X	PB125	IPE400	24	52	1.21	63	87	3.53	0.28
X	PB126	IPE400	35	58	1.21	70	105	2.93	0.34
X	PB133	IPE400	30	54	1.21	65	95	3.24	0.31
X	PB134	IPE400	27	51	1.21	61	88	3.49	0.29
X	PB135	IPE400	18	57	1.21	69	86	3.55	0.28
X	PB136	IPE400	23	49	1.21	60	83	3.70	0.27
X	PB137	IPE400	35	49	1.21	59	94	3.27	0.31
X	PB144	IPE400	20	72	1.21	87	108	2.85	0.35
X	PB145	IPE400	15	78	1.21	95	110	2.79	0.36
X	PB146	IPE400	10	91	1.21	110	120	2.56	0.39
X	PB147	IPE400	15	77	1.21	94	109	2.83	0.35
X	PB148	IPE400	20	70	1.21	85	105	2.93	0.34
X	PB200	IPE400	22	71	1.27	90	112	2.75	0.36
X	PB201	IPE400	15	79	1.27	101	115	2.66	0.38
X	PB202	IPE400	10	91	1.27	116	127	2.43	0.41
X	PB203	IPE400	15	78	1.27	100	115	2.67	0.37
X	PB204	IPE400	20	69	1.27	88	108	2.85	0.35
X	PB211	IPE400	33	55	1.27	70	103	2.97	0.34
X	PB212	IPE400	25	55	1.27	70	96	3.21	0.31
X	PB213	IPE400	18	62	1.27	79	96	3.19	0.31
X	PB214	IPE400	25	54	1.27	69	93	3.29	0.30

Direction	Item	Profile	M_{Ed_G}(kNm)	M_{Ed_E}(kNm)	α	M_{Ed_Total}(kNm)	$M_{pl,Rd}$(kNm)	Ω	Eq.2.2
X	PB215	IPE400	33	52	1.27	66	99	3.11	0.32
X	PB222	IPE400	32	56	1.27	72	104	2.95	0.34
X	PB223	IPE400	24	63	1.27	80	104	2.95	0.34
X	PB224	IPE400	18	57	1.27	72	90	3.41	0.29
X	PB225	IPE400	25	56	1.27	71	95	3.22	0.31
X	PB226	IPE400	33	58	1.27	74	107	2.88	0.35
X	PB233	IPE400	33	55	1.27	70	103	2.97	0.34
X	PB234	IPE400	25	55	1.27	70	96	3.21	0.31
X	PB235	IPE400	18	62	1.27	79	96	3.19	0.31
X	PB236	IPE400	25	54	1.27	69	93	3.29	0.30
X	PB237	IPE400	33	52	1.27	66	99	3.11	0.32
X	PB244	IPE400	22	71	1.27	90	112	2.75	0.36
X	PB245	IPE400	15	79	1.27	101	115	2.66	0.38
X	PB246	IPE400	10	91	1.27	116	127	2.43	0.41
X	PB247	IPE400	15	78	1.27	100	115	2.67	0.37
X	PB248	IPE400	20	69	1.27	88	108	2.85	0.35
X	PB300	IPE400	22	62	1.21	76	98	3.15	0.32
X	PB301	IPE400	15	70	1.21	84	99	3.11	0.32
X	PB302	IPE400	10	80	1.21	97	107	2.87	0.35
X	PB303	IPE400	16	69	1.21	83	99	3.11	0.32
X	PB304	IPE400	19	61	1.21	74	93	3.31	0.30
X	PB311	IPE400	33	48	1.21	59	92	3.33	0.30
X	PB312	IPE400	25	48	1.21	58	83	3.68	0.27
X	PB313	IPE400	18	54	1.21	65	83	3.71	0.27
X	PB314	IPE400	25	47	1.21	57	82	3.75	0.27
X	PB315	IPE400	32	45	1.21	55	87	3.54	0.28
X	PB322	IPE400	33	50	1.21	60	93	3.31	0.30
X	PB323	IPE400	24	55	1.21	67	91	3.38	0.30
X	PB324	IPE400	18	50	1.21	60	78	3.95	0.25
X	PB325	IPE400	25	49	1.21	59	84	3.65	0.27
X	PB326	IPE400	32	51	1.21	62	94	3.26	0.31
X	PB333	IPE400	33	48	1.21	59	92	3.33	0.30
X	PB334	IPE400	25	48	1.21	58	83	3.68	0.27
X	PB335	IPE400	18	54	1.21	65	83	3.71	0.27
X	PB336	IPE400	25	47	1.21	57	82	3.75	0.27
X	PB337	IPE400	32	45	1.21	55	87	3.54	0.28
X	PB344	IPE400	22	62	1.21	76	98	3.15	0.32
X	PB345	IPE400	15	70	1.21	84	99	3.11	0.32
X	PB346	IPE400	10	80	1.21	97	107	2.87	0.35
X	PB347	IPE400	16	69	1.21	83	99	3.11	0.32
X	PB348	IPE400	19	61	1.21	74	93	3.31	0.30
X	PB400	IPE400	22	50	1.15	57	80	3.86	0.26
X	PB401	IPE400	14	56	1.15	64	79	3.91	0.26
X	PB402	IPE400	10	63	1.15	73	83	3.69	0.27
X	PB403	IPE400	16	55	1.15	64	79	3.88	0.26
X	PB404	IPE400	19	49	1.15	56	75	4.11	0.24
X	PB411	IPE400	34	39	1.15	45	78	3.92	0.26
X	PB412	IPE400	25	39	1.15	45	69	4.43	0.23
X	PB413	IPE400	18	43	1.15	49	67	4.57	0.22

Direction	Item	Profile	M_{Ed_G}(kNm)	M_{Ed_E}(kNm)	α	M_{Ed_Total}(kNm)	$M_{pl,Rd}$(kNm)	Ω	Eq.2.2
X	PB414	IPE400	25	38	1.15	44	69	4.46	0.22
X	PB415	IPE400	32	36	1.15	42	73	4.20	0.24
X	PB422	IPE400	33	40	1.15	46	79	3.90	0.26
X	PB423	IPE400	24	45	1.15	51	75	4.10	0.24
X	PB424	IPE400	18	40	1.15	46	64	4.82	0.21
X	PB425	IPE400	25	39	1.15	45	71	4.35	0.23
X	PB426	IPE400	32	41	1.15	47	79	3.89	0.26
X	PB433	IPE400	34	39	1.15	45	78	3.92	0.26
X	PB434	IPE400	25	39	1.15	45	69	4.43	0.23
X	PB435	IPE400	18	43	1.15	49	67	4.57	0.22
X	PB436	IPE400	25	38	1.15	44	69	4.46	0.22
X	PB437	IPE400	32	36	1.15	42	73	4.20	0.24
X	PB444	IPE400	22	50	1.15	57	80	3.86	0.26
X	PB445	IPE400	14	56	1.15	64	79	3.91	0.26
X	PB446	IPE400	10	63	1.15	73	83	3.69	0.27
X	PB447	IPE400	16	55	1.15	64	79	3.88	0.26
X	PB448	IPE400	19	49	1.15	56	75	4.11	0.24
X	PB500	IPE400	23	34	-	34	57	5.37	0.19
X	PB501	IPE400	14	39	-	39	53	5.77	0.17
X	PB502	IPE400	10	44	-	44	54	5.67	0.18
X	PB503	IPE400	16	39	-	39	55	5.61	0.18
X	PB504	IPE400	18	34	-	34	52	5.89	0.17
X	PB511	IPE400	36	27	-	27	63	4.84	0.21
X	PB512	IPE400	24	28	-	28	52	5.96	0.17
X	PB513	IPE400	18	30	-	30	48	6.38	0.16
X	PB514	IPE400	26	27	-	27	53	5.77	0.17
X	PB515	IPE400	31	26	-	26	56	5.46	0.18
X	PB522	IPE400	35	28	-	28	63	4.84	0.21
X	PB523	IPE400	23	31	-	31	54	5.66	0.18
X	PB524	IPE400	18	29	-	29	46	6.62	0.15
X	PB525	IPE400	26	28	-	28	54	5.70	0.18
X	PB526	IPE400	31	29	-	29	59	5.18	0.19
X	PB533	IPE400	36	27	-	27	63	4.84	0.21
X	PB534	IPE400	24	28	-	28	52	5.96	0.17
X	PB535	IPE400	18	30	-	30	48	6.38	0.16
X	PB536	IPE400	26	27	-	27	53	5.77	0.17
X	PB537	IPE400	31	26	-	26	56	5.46	0.18
X	PB544	IPE400	23	34	-	34	57	5.37	0.19
X	PB545	IPE400	14	39	-	39	53	5.77	0.17
X	PB546	IPE400	10	44	-	44	54	5.67	0.18
X	PB547	IPE400	16	39	-	39	55	5.61	0.18
X	PB548	IPE400	18	34	-	34	52	5.89	0.17
X	PB600	IPE400	19	21	-	21	40	7.68	0.13
X	PB601	IPE400	12	23	-	23	36	8.65	0.12
X	PB602	IPE400	9	25	-	25	34	9.08	0.11
X	PB603	IPE400	13	23	-	23	36	8.50	0.12
X	PB604	IPE400	16	20	-	20	36	8.47	0.12
X	PB611	IPE400	28	14	-	14	43	7.17	0.14
X	PB612	IPE400	27	13	-	13	40	7.68	0.13

Direction	Item	Profile	M_{Ed_G}(kNm)	M_{Ed_E}(kNm)	α	M_{Ed_Total}(kNm)	$M_{pl,Rd}$(kNm)	Ω	Eq.2.2
X	PB613	IPE400	18	14	-	14	33	9.44	0.11
X	PB614	IPE400	24	13	-	13	37	8.33	0.12
X	PB615	IPE400	33	13	-	13	46	6.75	0.15
X	PB622	IPE400	27	15	-	15	43	7.16	0.14
X	PB623	IPE400	25	18	-	18	43	7.22	0.14
X	PB624	IPE400	19	13	-	13	31	9.84	0.10
X	PB625	IPE400	24	15	-	15	38	7.99	0.13
X	PB626	IPE400	34	17	-	17	50	6.12	0.16
X	PB633	IPE400	28	14	-	14	43	7.17	0.14
X	PB634	IPE400	27	13	-	13	40	7.68	0.13
X	PB635	IPE400	18	14	-	14	33	9.44	0.11
X	PB636	IPE400	24	13	-	13	37	8.33	0.12
X	PB637	IPE400	33	13	-	13	46	6.75	0.15
X	PB644	IPE400	19	21	-	21	40	7.68	0.13
X	PB645	IPE400	12	23	-	23	36	8.65	0.12
X	PB646	IPE400	9	25	-	25	34	9.08	0.11
X	PB647	IPE400	13	23	-	23	36	8.50	0.12
X	PB648	IPE400	16	20	-	20	36	8.47	0.12
Y	PB105	IPE400	34	71	1.2	85	120	2.57	0.39
Y	PB106	IPE450	55	86	1.2	103	158	2.53	0.40
Y	PB107	IPE400	50	60	1.2	72	122	2.51	0.40
Y	PB108	IPE400	50	60	1.2	72	122	2.51	0.40
Y	PB109	IPE450	55	86	1.2	103	158	2.53	0.40
Y	PB110	IPE400	34	71	1.2	85	120	2.57	0.39
Y	PB116	IPE400	42	79	1.2	95	137	2.25	0.44
Y	PB117	IPE450	74	84	1.2	100	175	2.29	0.44
Y	PB118	IPE400	62	67	1.2	80	142	2.17	0.46
Y	PB119	IPE400	62	67	1.2	80	142	2.17	0.46
Y	PB120	IPE450	74	84	1.2	100	175	2.29	0.44
Y	PB121	IPE400	42	79	1.2	95	137	2.25	0.44
Y	PB127	IPE400	42	79	1.2	94	136	2.26	0.44
Y	PB128	IPE450	73	69	1.2	82	155	2.58	0.39
Y	PB129	IPE400	61	67	1.2	80	141	2.18	0.46
Y	PB130	IPE400	61	67	1.2	80	141	2.18	0.46
Y	PB131	IPE450	73	69	1.2	82	155	2.58	0.39
Y	PB132	IPE400	42	79	1.2	94	136	2.26	0.44
Y	PB138	IPE400	45	74	1.2	89	135	2.28	0.44
Y	PB139	IPE450	80	92	1.2	110	190	2.11	0.47
Y	PB140	IPE400	66	63	1.2	75	142	2.16	0.46
Y	PB141	IPE400	66	63	1.2	75	142	2.16	0.46
Y	PB142	IPE450	80	92	1.2	110	190	2.11	0.47
Y	PB143	IPE400	45	74	1.2	89	135	2.28	0.44
Y	PB205	IPE400	38	72	1.25	90	128	2.39	0.42
Y	PB206	IPE450	64	89	1.25	111	175	2.28	0.44
Y	PB207	IPE400	56	61	1.25	77	132	2.32	0.43
Y	PB208	IPE400	56	61	1.25	77	132	2.32	0.43
Y	PB209	IPE450	64	89	1.25	111	175	2.28	0.44
Y	PB210	IPE400	38	72	1.25	90	128	2.39	0.42
Y	PB216	IPE400	42	78	1.25	98	140	2.20	0.46

Direction	Item	Profile	M_{Ed_G}(kNm)	M_{Ed_E}(kNm)	α	M_{Ed_Total}(kNm)	$M_{pl,Rd}$(kNm)	Ω	Eq.2.2
Y	PB217	IPE450	73	87	1.25	109	182	2.19	0.46
Y	PB218	IPE400	61	67	1.25	83	144	2.13	0.47
Y	PB219	IPE400	61	67	1.25	83	144	2.13	0.47
Y	PB220	IPE450	73	87	1.25	109	182	2.19	0.46
Y	PB221	IPE400	42	78	1.25	98	140	2.20	0.46
Y	PB227	IPE400	42	78	1.25	98	140	2.20	0.46
Y	PB228	IPE450	73	75	1.25	94	167	2.39	0.42
Y	PB229	IPE400	61	66	1.25	83	144	2.13	0.47
Y	PB230	IPE400	61	66	1.25	83	144	2.13	0.47
Y	PB231	IPE450	73	75	1.25	94	167	2.39	0.42
Y	PB232	IPE400	42	78	1.25	98	140	2.20	0.46
Y	PB238	IPE400	43	75	1.25	93	136	2.25	0.44
Y	PB239	IPE450	75	93	1.25	116	191	2.09	0.48
Y	PB240	IPE400	63	63	1.25	79	142	2.16	0.46
Y	PB241	IPE400	63	63	1.25	79	142	2.16	0.46
Y	PB242	IPE450	75	93	1.25	116	191	2.09	0.48
Y	PB243	IPE400	43	75	1.25	93	136	2.25	0.44
Y	PB305	IPE400	38	63	1.2	75	113	2.71	0.37
Y	PB306	IPE450	64	77	1.2	92	157	2.55	0.39
Y	PB307	IPE400	56	54	1.2	64	120	2.56	0.39
Y	PB308	IPE400	56	54	1.2	64	120	2.56	0.39
Y	PB309	IPE450	64	77	1.2	92	157	2.55	0.39
Y	PB310	IPE400	38	63	1.2	75	113	2.71	0.37
Y	PB316	IPE400	42	69	1.2	82	124	2.48	0.40
Y	PB317	IPE450	73	76	1.2	91	165	2.43	0.41
Y	PB318	IPE400	61	59	1.2	70	131	2.34	0.43
Y	PB319	IPE400	61	59	1.2	70	131	2.34	0.43
Y	PB320	IPE450	73	76	1.2	91	165	2.43	0.41
Y	PB321	IPE400	42	69	1.2	82	124	2.48	0.40
Y	PB327	IPE400	42	68	1.2	82	124	2.48	0.40
Y	PB328	IPE450	73	65	1.2	78	152	2.64	0.38
Y	PB329	IPE400	61	59	1.2	70	132	2.34	0.43
Y	PB330	IPE400	61	59	1.2	70	132	2.34	0.43
Y	PB331	IPE450	73	65	1.2	78	152	2.64	0.38
Y	PB332	IPE400	42	68	1.2	82	124	2.48	0.40
Y	PB338	IPE400	43	65	1.2	78	120	2.55	0.39
Y	PB339	IPE450	73	81	1.2	97	170	2.35	0.42
Y	PB340	IPE400	62	55	1.2	66	129	2.39	0.42
Y	PB341	IPE400	62	55	1.2	66	129	2.39	0.42
Y	PB342	IPE450	73	81	1.2	97	170	2.35	0.42
Y	PB343	IPE400	43	65	1.2	78	120	2.55	0.39
Y	PB405	IPE400	38	49	1.14	56	95	3.25	0.31
Y	PB406	IPE450	65	61	1.14	69	134	2.98	0.34
Y	PB407	IPE400	56	43	1.14	49	105	2.94	0.34
Y	PB408	IPE400	56	43	1.14	49	105	2.94	0.34
Y	PB409	IPE450	65	61	1.14	69	134	2.98	0.34
Y	PB410	IPE400	38	49	1.14	56	95	3.25	0.31
Y	PB416	IPE400	42	54	1.14	62	104	2.96	0.34
Y	PB417	IPE450	73	61	1.14	69	142	2.81	0.36

Direction	Item	Profile	M_{Ed_G}(kNm)	M_{Ed_E}(kNm)	α	M_{Ed_Total}(kNm)	$M_{pl,Rd}$(kNm)	Ω	Eq.2.2
Y	PB418	IPE400	61	47	1.14	53	115	2.68	0.37
Y	PB419	IPE400	61	47	1.14	53	115	2.68	0.37
Y	PB420	IPE450	73	61	1.14	69	142	2.81	0.36
Y	PB421	IPE400	42	54	1.14	62	104	2.96	0.34
Y	PB427	IPE400	42	54	1.14	62	104	2.96	0.34
Y	PB428	IPE450	73	52	1.14	60	133	3.01	0.33
Y	PB429	IPE400	61	47	1.14	53	115	2.68	0.37
Y	PB430	IPE400	61	47	1.14	53	115	2.68	0.37
Y	PB431	IPE450	73	52	1.14	60	133	3.01	0.33
Y	PB432	IPE400	42	54	1.14	62	104	2.96	0.34
Y	PB438	IPE400	42	51	1.14	58	100	3.06	0.33
Y	PB439	IPE450	72	64	1.14	73	144	2.77	0.36
Y	PB440	IPE400	62	44	1.14	50	112	2.75	0.36
Y	PB441	IPE400	62	44	1.14	50	112	2.75	0.36
Y	PB442	IPE450	72	64	1.14	73	144	2.77	0.36
Y	PB443	IPE400	42	51	1.14	58	100	3.06	0.33
Y	PB505	IPE400	41	34	-	34	75	4.10	0.24
Y	PB506	IPE450	70	42	-	42	112	3.56	0.28
Y	PB507	IPE400	60	30	-	30	90	3.43	0.29
Y	PB508	IPE400	60	30	-	30	90	3.43	0.29
Y	PB509	IPE450	70	42	-	42	112	3.56	0.28
Y	PB510	IPE400	41	34	-	34	75	4.10	0.24
Y	PB516	IPE400	42	37	-	37	79	3.89	0.26
Y	PB517	IPE450	72	42	-	42	115	3.48	0.29
Y	PB518	IPE400	61	32	-	32	93	3.30	0.30
Y	PB519	IPE400	61	32	-	32	93	3.30	0.30
Y	PB520	IPE450	72	42	-	42	115	3.48	0.29
Y	PB521	IPE400	42	37	-	37	79	3.89	0.26
Y	PB527	IPE400	42	37	-	37	79	3.87	0.26
Y	PB528	IPE450	74	37	-	37	111	3.61	0.28
Y	PB529	IPE400	62	32	-	32	94	3.27	0.31
Y	PB530	IPE400	62	32	-	32	94	3.27	0.31
Y	PB531	IPE450	74	37	-	37	111	3.61	0.28
Y	PB532	IPE400	42	37	-	37	79	3.87	0.26
Y	PB538	IPE400	41	35	-	35	76	4.05	0.25
Y	PB539	IPE450	69	43	-	43	113	3.55	0.28
Y	PB540	IPE400	60	30	-	30	90	3.42	0.29
Y	PB541	IPE400	60	30	-	30	90	3.42	0.29
Y	PB542	IPE450	69	43	-	43	113	3.55	0.28
Y	PB543	IPE400	41	35	-	35	76	4.05	0.25
Y	PB605	IPE400	30	18	-	18	47	6.47	0.15
Y	PB606	IPE450	50	21	-	21	71	5.64	0.18
Y	PB607	IPE400	45	15	-	15	61	5.05	0.20
Y	PB608	IPE400	45	15	-	15	61	5.05	0.20
Y	PB609	IPE450	50	21	-	21	71	5.64	0.18
Y	PB610	IPE400	30	18	-	18	47	6.47	0.15
Y	PB616	IPE400	40	22	-	22	62	4.97	0.20
Y	PB617	IPE450	74	22	-	22	97	4.14	0.24
Y	PB618	IPE400	62	19	-	19	81	3.80	0.26

Direction	Item	Profile	M_{Ed_G}(kNm)	M_{Ed_E}(kNm)	α	M_{Ed_Total}(kNm)	$M_{pl,Rd}$(kNm)	Ω	Eq.2.2
Y	PB619	IPE400	62	19	-	19	81	3.80	0.26
Y	PB620	IPE450	74	22	-	22	97	4.14	0.24
Y	PB621	IPE400	40	22	-	22	62	4.97	0.20
Y	PB627	IPE400	40	21	-	21	61	5.02	0.20
Y	PB628	IPE450	73	17	-	17	90	4.44	0.23
Y	PB629	IPE400	61	19	-	19	80	3.86	0.26
Y	PB630	IPE400	61	19	-	19	80	3.86	0.26
Y	PB631	IPE450	73	17	-	17	90	4.44	0.23
Y	PB632	IPE400	40	21	-	21	61	5.02	0.20
Y	PB638	IPE400	43	19	-	19	62	4.99	0.20
Y	PB639	IPE450	77	23	-	23	100	3.99	0.25
Y	PB640	IPE400	66	16	-	16	82	3.73	0.27
Y	PB641	IPE400	66	16	-	16	82	3.73	0.27
Y	PB642	IPE450	77	23	-	23	100	3.99	0.25
Y	PB643	IPE400	43	19	-	19	62	4.99	0.20

Table A2 3. Shear designing forces applied to the dissipative elements under rare seismic actions

Direction	Item	Profile	L(m)	L_h(m)	$V_{Ed,G}$(kN)	$V_{Ed,M}$ (kN)	α	V_{Ed_total}(kN)	Eq. 2.4
X	PB100	IPE400	7	6.45	19	95	1.21	134	0.23
X	PB101	IPE400	6	5.45	16	113	1.21	153	0.26
X	PB102	IPE400	5	4.45	13	138	1.21	180	0.31
X	PB103	IPE400	6	5.45	16	113	1.21	152	0.26
X	PB104	IPE400	7	6.45	19	95	1.21	134	0.23
X	PB111	IPE400	7	7.00	30	88	1.21	136	0.24
X	PB112	IPE400	6	6.00	27	102	1.21	151	0.26
X	PB113	IPE400	5	5.00	22	123	1.21	170	0.29
X	PB114	IPE400	6	6.00	26	102	1.21	150	0.26
X	PB115	IPE400	7	7.00	32	88	1.21	138	0.24
X	PB122	IPE400	7	6.73	30	91	1.21	140	0.24
X	PB123	IPE400	6	5.73	26	107	1.21	156	0.27
X	PB124	IPE400	5	5.00	22	123	1.21	170	0.29
X	PB125	IPE400	6	5.73	26	107	1.21	156	0.27
X	PB126	IPE400	7	6.73	32	91	1.21	142	0.25
X	PB133	IPE400	7	7.00	30	88	1.21	136	0.24
X	PB134	IPE400	6	6.00	27	102	1.21	151	0.26
X	PB135	IPE400	5	5.00	22	123	1.21	170	0.29
X	PB136	IPE400	6	6.00	26	102	1.21	150	0.26
X	PB137	IPE400	7	7.00	32	88	1.21	138	0.24
X	PB144	IPE400	7	6.45	19	95	1.21	134	0.23
X	PB145	IPE400	6	5.45	16	113	1.21	153	0.26
X	PB146	IPE400	5	4.45	13	138	1.21	180	0.31
X	PB147	IPE400	6	5.45	16	113	1.21	152	0.26
X	PB148	IPE400	7	6.45	19	95	1.21	134	0.23
X	PB200	IPE400	7	6.45	19	95	1.27	140	0.24
X	PB201	IPE400	6	5.45	16	113	1.27	159	0.27
X	PB202	IPE400	5	4.45	13	138	1.27	189	0.33

Direction	Item	Profile	L(m)	L_h(m)	$V_{Ed,G}$(kN)	$V_{Ed,M}$ (kN)	α	V_{Ed_total}(kN)	Eq. 2.4
X	PB203	IPE400	6	5.45	16	113	1.27	159	0.28
X	PB204	IPE400	7	6.45	19	95	1.27	140	0.24
X	PB211	IPE400	7	7.00	31	88	1.27	142	0.25
X	PB212	IPE400	6	6.00	26	102	1.27	156	0.27
X	PB213	IPE400	5	5.00	22	123	1.27	178	0.31
X	PB214	IPE400	6	6.00	26	102	1.27	156	0.27
X	PB215	IPE400	7	7.00	31	88	1.27	142	0.25
X	PB222	IPE400	7	6.73	31	91	1.27	147	0.25
X	PB223	IPE400	6	5.73	26	107	1.27	162	0.28
X	PB224	IPE400	5	5.00	22	123	1.27	178	0.31
X	PB225	IPE400	6	5.73	26	107	1.27	162	0.28
X	PB226	IPE400	7	6.73	31	91	1.27	147	0.25
X	PB233	IPE400	7	7.00	31	88	1.27	142	0.25
X	PB234	IPE400	6	6.00	26	102	1.27	156	0.27
X	PB235	IPE400	5	5.00	22	123	1.27	178	0.31
X	PB236	IPE400	6	6.00	26	102	1.27	156	0.27
X	PB237	IPE400	7	7.00	31	88	1.27	142	0.25
X	PB244	IPE400	7	6.45	19	95	1.27	140	0.24
X	PB245	IPE400	6	5.45	16	113	1.27	159	0.27
X	PB246	IPE400	5	4.45	13	138	1.27	189	0.33
X	PB247	IPE400	6	5.45	16	113	1.27	159	0.28
X	PB248	IPE400	7	6.45	19	95	1.27	140	0.24
X	PB300	IPE400	7	6.45	19	95	1.21	135	0.23
X	PB301	IPE400	6	5.45	16	113	1.21	152	0.26
X	PB302	IPE400	5	4.45	13	138	1.21	180	0.31
X	PB303	IPE400	6	5.45	16	113	1.21	153	0.26
X	PB304	IPE400	7	6.45	19	95	1.21	134	0.23
X	PB311	IPE400	7	7.00	31	88	1.21	137	0.24
X	PB312	IPE400	6	6.00	26	102	1.21	150	0.26
X	PB313	IPE400	5	5.00	22	123	1.21	170	0.29
X	PB314	IPE400	6	6.00	26	102	1.21	150	0.26
X	PB315	IPE400	7	7.00	31	88	1.21	137	0.24
X	PB322	IPE400	7	6.73	31	91	1.21	141	0.24
X	PB323	IPE400	6	5.73	26	107	1.21	156	0.27
X	PB324	IPE400	5	5.00	22	123	1.21	170	0.29
X	PB325	IPE400	6	5.73	26	107	1.21	156	0.27
X	PB326	IPE400	7	6.73	31	91	1.21	141	0.24
X	PB333	IPE400	7	7.00	31	88	1.21	137	0.24
X	PB334	IPE400	6	6.00	26	102	1.21	150	0.26
X	PB335	IPE400	5	5.00	22	123	1.21	170	0.29
X	PB336	IPE400	6	6.00	26	102	1.21	150	0.26
X	PB337	IPE400	7	7.00	31	88	1.21	137	0.24
X	PB344	IPE400	7	6.45	19	95	1.21	135	0.23
X	PB345	IPE400	6	5.45	16	113	1.21	152	0.26
X	PB346	IPE400	5	4.45	13	138	1.21	180	0.31
X	PB347	IPE400	6	5.45	16	113	1.21	153	0.26
X	PB348	IPE400	7	6.45	19	95	1.21	134	0.23
X	PB400	IPE400	7	6.45	20	95	1.15	129	0.22

Direction	Item	Profile	L(m)	L_h(m)	$V_{Ed,G}$(kN)	$V_{Ed,M}$ (kN)	α	V_{Ed_total}(kN)	Eq. 2.4
X	PB401	IPE400	6	5.45	16	113	1.15	146	0.25
X	PB402	IPE400	5	4.45	13	138	1.15	172	0.30
X	PB403	IPE400	6	5.45	16	113	1.15	146	0.25
X	PB404	IPE400	7	6.45	18	95	1.15	128	0.22
X	PB411	IPE400	7	7.00	31	88	1.15	132	0.23
X	PB412	IPE400	6	6.00	26	102	1.15	144	0.25
X	PB413	IPE400	5	5.00	22	123	1.15	163	0.28
X	PB414	IPE400	6	6.00	26	102	1.15	144	0.25
X	PB415	IPE400	7	7.00	31	88	1.15	132	0.23
X	PB422	IPE400	7	6.73	31	91	1.15	136	0.23
X	PB423	IPE400	6	5.73	26	107	1.15	149	0.26
X	PB424	IPE400	5	5.00	22	123	1.15	163	0.28
X	PB425	IPE400	6	5.73	26	107	1.15	150	0.26
X	PB426	IPE400	7	6.73	31	91	1.15	136	0.23
X	PB433	IPE400	7	7.00	31	88	1.15	132	0.23
X	PB434	IPE400	6	6.00	26	102	1.15	144	0.25
X	PB435	IPE400	5	5.00	22	123	1.15	163	0.28
X	PB436	IPE400	6	6.00	26	102	1.15	144	0.25
X	PB437	IPE400	7	7.00	31	88	1.15	132	0.23
X	PB444	IPE400	7	6.45	20	95	1.15	129	0.22
X	PB445	IPE400	6	5.45	16	113	1.15	146	0.25
X	PB446	IPE400	5	4.45	13	138	1.15	172	0.30
X	PB447	IPE400	6	5.45	16	113	1.15	146	0.25
X	PB448	IPE400	7	6.45	18	95	1.15	128	0.22
X	PB500	IPE400	7	6.45	20	95	-	115	0.20
X	PB501	IPE400	6	5.45	16	113	-	129	0.22
X	PB502	IPE400	5	4.45	13	138	-	151	0.26
X	PB503	IPE400	6	5.45	16	113	-	129	0.22
X	PB504	IPE400	7	6.45	18	95	-	114	0.20
X	PB511	IPE400	7	7.00	32	88	-	120	0.21
X	PB512	IPE400	6	6.00	26	102	-	128	0.22
X	PB513	IPE400	5	5.00	22	123	-	145	0.25
X	PB514	IPE400	6	6.00	27	102	-	129	0.22
X	PB515	IPE400	7	7.00	30	88	-	118	0.20
X	PB522	IPE400	7	6.73	31	91	-	123	0.21
X	PB523	IPE400	6	5.73	26	107	-	133	0.23
X	PB524	IPE400	5	5.00	22	123	-	145	0.25
X	PB525	IPE400	6	5.73	27	107	-	134	0.23
X	PB526	IPE400	7	6.73	30	91	-	121	0.21
X	PB533	IPE400	7	7.00	32	88	-	120	0.21
X	PB534	IPE400	6	6.00	26	102	-	128	0.22
X	PB535	IPE400	5	5.00	22	123	-	145	0.25
X	PB536	IPE400	6	6.00	27	102	-	129	0.22
X	PB537	IPE400	7	7.00	30	88	-	118	0.20
X	PB544	IPE400	7	6.45	20	95	-	115	0.20
X	PB545	IPE400	6	5.45	16	113	-	129	0.22
X	PB546	IPE400	5	4.45	13	138	-	151	0.26
X	PB547	IPE400	6	5.45	16	113	-	129	0.22

Direction	Item	Profile	L(m)	L_h(m)	$V_{Ed,G}$(kN)	$V_{Ed,M}$ (kN)	α	V_{Ed_total}(kN)	Eq. 2.4
X	PB548	IPE400	7	6.45	18	95	-	114	0.20
X	PB600	IPE400	7	6.45	17	95	-	112	0.19
X	PB601	IPE400	6	5.45	14	113	-	126	0.22
X	PB602	IPE400	5	4.45	11	138	-	149	0.26
X	PB603	IPE400	6	5.45	14	113	-	127	0.22
X	PB604	IPE400	7	6.45	16	95	-	111	0.19
X	PB611	IPE400	7	7.00	30	88	-	118	0.20
X	PB612	IPE400	6	6.00	27	102	-	129	0.22
X	PB613	IPE400	5	5.00	22	123	-	145	0.25
X	PB614	IPE400	6	6.00	26	102	-	128	0.22
X	PB615	IPE400	7	7.00	32	88	-	119	0.21
X	PB622	IPE400	7	6.73	30	91	-	121	0.21
X	PB623	IPE400	6	5.73	26	107	-	134	0.23
X	PB624	IPE400	5	5.00	22	123	-	145	0.25
X	PB625	IPE400	6	5.73	26	107	-	133	0.23
X	PB626	IPE400	7	6.73	32	91	-	123	0.21
X	PB633	IPE400	7	7.00	30	88	-	118	0.20
X	PB634	IPE400	6	6.00	27	102	-	129	0.22
X	PB635	IPE400	5	5.00	22	123	-	145	0.25
X	PB636	IPE400	6	6.00	26	102	-	128	0.22
X	PB637	IPE400	7	7.00	32	88	-	119	0.21
X	PB644	IPE400	7	6.45	17	95	-	112	0.19
X	PB645	IPE400	6	5.45	14	113	-	126	0.22
X	PB646	IPE400	5	4.45	11	138	-	149	0.26
X	PB647	IPE400	6	5.45	14	113	-	127	0.22
X	PB648	IPE400	7	6.45	16	95	-	111	0.19
Y	PB105	IPE400	6	5.73	33	107	1.2	162	0.28
Y	PB106	IPE450	6	5.73	55	140	1.2	223	0.32
Y	PB107	IPE400	6	5.73	47	107	1.2	176	0.30
Y	PB108	IPE400	6	5.73	47	107	1.2	176	0.30
Y	PB109	IPE450	6	5.73	55	140	1.2	223	0.32
Y	PB110	IPE400	6	5.73	33	107	1.2	162	0.28
Y	PB116	IPE400	6	5.45	35	113	1.2	171	0.29
Y	PB117	IPE450	6	5.73	61	140	1.2	228	0.33
Y	PB118	IPE400	6	5.45	51	113	1.2	186	0.32
Y	PB119	IPE400	6	5.45	51	113	1.2	186	0.32
Y	PB120	IPE450	6	5.73	61	140	1.2	228	0.33
Y	PB121	IPE400	6	5.45	35	113	1.2	171	0.29
Y	PB127	IPE400	6	5.45	35	113	1.2	170	0.29
Y	PB128	IPE450	6	5.73	59	140	1.2	227	0.33
Y	PB129	IPE400	6	5.45	50	113	1.2	186	0.32
Y	PB130	IPE400	6	5.45	50	113	1.2	186	0.32
Y	PB131	IPE450	6	5.73	59	140	1.2	227	0.33
Y	PB132	IPE400	6	5.45	35	113	1.2	170	0.29
Y	PB138	IPE400	6	5.73	37	107	1.2	166	0.29
Y	PB139	IPE450	6	5.73	65	140	1.2	232	0.34
Y	PB140	IPE400	6	5.73	54	107	1.2	183	0.32
Y	PB141	IPE400	6	5.73	54	107	1.2	183	0.32

Direction	Item	Profile	L(m)	L_h(m)	$V_{Ed,G}$(kN)	$V_{Ed,M}$ (kN)	α	V_{Ed_total}(kN)	Eq. 2.4
Y	PB142	IPE450	6	5.73	65	140	1.2	232	0.34
Y	PB143	IPE400	6	5.73	37	107	1.2	166	0.29
Y	PB205	IPE400	6	5.73	34	107	1.25	168	0.29
Y	PB206	IPE450	6	5.73	57	140	1.25	232	0.34
Y	PB207	IPE400	6	5.73	49	107	1.25	183	0.32
Y	PB208	IPE400	6	5.73	49	107	1.25	183	0.32
Y	PB209	IPE450	6	5.73	57	140	1.25	232	0.34
Y	PB210	IPE400	6	5.73	34	107	1.25	168	0.29
Y	PB216	IPE400	6	5.45	35	113	1.25	176	0.30
Y	PB217	IPE450	6	5.73	60	140	1.25	235	0.34
Y	PB218	IPE400	6	5.45	50	113	1.25	191	0.33
Y	PB219	IPE400	6	5.45	50	113	1.25	191	0.33
Y	PB220	IPE450	6	5.73	60	140	1.25	235	0.34
Y	PB221	IPE400	6	5.45	35	113	1.25	176	0.30
Y	PB227	IPE400	6	5.45	35	113	1.25	176	0.30
Y	PB228	IPE450	6	5.73	59	140	1.25	234	0.34
Y	PB229	IPE400	6	5.45	51	113	1.25	191	0.33
Y	PB230	IPE400	6	5.45	51	113	1.25	191	0.33
Y	PB231	IPE450	6	5.73	59	140	1.25	234	0.34
Y	PB232	IPE400	6	5.45	35	113	1.25	176	0.30
Y	PB238	IPE400	6	5.73	36	107	1.25	171	0.29
Y	PB239	IPE450	6	5.73	62	140	1.25	237	0.34
Y	PB240	IPE400	6	5.73	52	107	1.25	186	0.32
Y	PB241	IPE400	6	5.73	52	107	1.25	186	0.32
Y	PB242	IPE450	6	5.73	62	140	1.25	237	0.34
Y	PB243	IPE400	6	5.73	36	107	1.25	171	0.29
Y	PB305	IPE400	6	5.73	34	107	1.2	163	0.28
Y	PB306	IPE450	6	5.73	58	140	1.2	226	0.33
Y	PB307	IPE400	6	5.73	49	107	1.2	178	0.31
Y	PB308	IPE400	6	5.73	49	107	1.2	178	0.31
Y	PB309	IPE450	6	5.73	58	140	1.2	226	0.33
Y	PB310	IPE400	6	5.73	34	107	1.2	163	0.28
Y	PB316	IPE400	6	5.45	35	113	1.2	170	0.29
Y	PB317	IPE450	6	5.73	60	140	1.2	228	0.33
Y	PB318	IPE400	6	5.45	50	113	1.2	186	0.32
Y	PB319	IPE400	6	5.45	50	113	1.2	186	0.32
Y	PB320	IPE450	6	5.73	60	140	1.2	228	0.33
Y	PB321	IPE400	6	5.45	35	113	1.2	170	0.29
Y	PB327	IPE400	6	5.45	35	113	1.2	171	0.29
Y	PB328	IPE450	6	5.73	59	140	1.2	227	0.33
Y	PB329	IPE400	6	5.45	51	113	1.2	186	0.32
Y	PB330	IPE400	6	5.45	51	113	1.2	186	0.32
Y	PB331	IPE450	6	5.73	59	140	1.2	227	0.33
Y	PB332	IPE400	6	5.45	35	113	1.2	171	0.29
Y	PB338	IPE400	6	5.73	36	107	1.2	165	0.28
Y	PB339	IPE450	6	5.73	62	140	1.2	229	0.33
Y	PB340	IPE400	6	5.73	52	107	1.2	181	0.31
Y	PB341	IPE400	6	5.73	52	107	1.2	181	0.31

Direction	Item	Profile	L(m)	L_h(m)	$V_{Ed,G}$(kN)	$V_{Ed,M}$ (kN)	α	V_{Ed_total}(kN)	Eq. 2.4
Y	PB342	IPE450	6	5.73	62	140	1.2	229	0.33
Y	PB343	IPE400	6	5.73	36	107	1.2	165	0.28
Y	PB405	IPE400	6	5.73	34	107	1.14	157	0.27
Y	PB406	IPE450	6	5.73	58	140	1.14	217	0.32
Y	PB407	IPE400	6	5.73	49	107	1.14	171	0.30
Y	PB408	IPE400	6	5.73	49	107	1.14	171	0.30
Y	PB409	IPE450	6	5.73	58	140	1.14	217	0.32
Y	PB410	IPE400	6	5.73	34	107	1.14	157	0.27
Y	PB416	IPE400	6	5.45	35	113	1.14	164	0.28
Y	PB417	IPE450	6	5.73	60	140	1.14	220	0.32
Y	PB418	IPE400	6	5.45	50	113	1.14	179	0.31
Y	PB419	IPE400	6	5.45	50	113	1.14	179	0.31
Y	PB420	IPE450	6	5.73	60	140	1.14	220	0.32
Y	PB421	IPE400	6	5.45	35	113	1.14	164	0.28
Y	PB427	IPE400	6	5.45	35	113	1.14	164	0.28
Y	PB428	IPE450	6	5.73	59	140	1.14	219	0.32
Y	PB429	IPE400	6	5.45	51	113	1.14	179	0.31
Y	PB430	IPE400	6	5.45	51	113	1.14	179	0.31
Y	PB431	IPE450	6	5.73	59	140	1.14	219	0.32
Y	PB432	IPE400	6	5.45	35	113	1.14	164	0.28
Y	PB438	IPE400	6	5.73	36	107	1.14	159	0.27
Y	PB439	IPE450	6	5.73	61	140	1.14	221	0.32
Y	PB440	IPE400	6	5.73	52	107	1.14	174	0.30
Y	PB441	IPE400	6	5.73	52	107	1.14	174	0.30
Y	PB442	IPE450	6	5.73	61	140	1.14	221	0.32
Y	PB443	IPE400	6	5.73	36	107	1.14	159	0.27
Y	PB505	IPE400	6	5.73	35	107	-	142	0.25
Y	PB506	IPE450	6	5.73	60	140	-	199	0.29
Y	PB507	IPE400	6	5.73	50	107	-	158	0.27
Y	PB508	IPE400	6	5.73	50	107	-	158	0.27
Y	PB509	IPE450	6	5.73	60	140	-	199	0.29
Y	PB510	IPE400	6	5.73	35	107	-	142	0.25
Y	PB516	IPE400	6	5.45	35	113	-	148	0.26
Y	PB517	IPE450	6	5.73	60	140	-	200	0.29
Y	PB518	IPE400	6	5.45	50	113	-	163	0.28
Y	PB519	IPE400	6	5.45	50	113	-	163	0.28
Y	PB520	IPE450	6	5.73	60	140	-	200	0.29
Y	PB521	IPE400	6	5.45	35	113	-	148	0.26
Y	PB527	IPE400	6	5.45	35	113	-	148	0.26
Y	PB528	IPE450	6	5.73	60	140	-	199	0.29
Y	PB529	IPE400	6	5.45	51	113	-	163	0.28
Y	PB530	IPE400	6	5.45	51	113	-	163	0.28
Y	PB531	IPE450	6	5.73	60	140	-	199	0.29
Y	PB532	IPE400	6	5.45	35	113	-	148	0.26
Y	PB538	IPE400	6	5.73	35	107	-	143	0.25
Y	PB539	IPE450	6	5.73	60	140	-	200	0.29
Y	PB540	IPE400	6	5.73	51	107	-	158	0.27
Y	PB541	IPE400	6	5.73	51	107	-	158	0.27

Direction	Item	Profile	L(m)	L_h(m)	$V_{Ed,G}$(kN)	$V_{Ed,M}$ (kN)	α	V_{Ed_total}(kN)	Eq. 2.4
Y	PB542	IPE450	6	5.73	60	140	-	200	0.29
Y	PB543	IPE400	6	5.73	35	107	-	143	0.25
Y	PB605	IPE400	6	5.73	30	107	-	138	0.24
Y	PB606	IPE450	6	5.73	55	140	-	194	0.28
Y	PB607	IPE400	6	5.73	47	107	-	154	0.27
Y	PB608	IPE400	6	5.73	47	107	-	154	0.27
Y	PB609	IPE450	6	5.73	55	140	-	194	0.28
Y	PB610	IPE400	6	5.73	30	107	-	138	0.24
Y	PB616	IPE400	6	5.45	33	113	-	146	0.25
Y	PB617	IPE450	6	5.73	61	140	-	200	0.29
Y	PB618	IPE400	6	5.45	51	113	-	163	0.28
Y	PB619	IPE400	6	5.45	51	113	-	163	0.28
Y	PB620	IPE450	6	5.73	61	140	-	200	0.29
Y	PB621	IPE400	6	5.45	33	113	-	146	0.25
Y	PB627	IPE400	6	5.45	33	113	-	146	0.25
Y	PB628	IPE450	6	5.73	59	140	-	199	0.29
Y	PB629	IPE400	6	5.45	50	113	-	163	0.28
Y	PB630	IPE400	6	5.45	50	113	-	163	0.28
Y	PB631	IPE450	6	5.73	59	140	-	199	0.29
Y	PB632	IPE400	6	5.45	33	113	-	146	0.25
Y	PB638	IPE400	6	5.73	35	107	-	143	0.25
Y	PB639	IPE450	6	5.73	65	140	-	205	0.30
Y	PB640	IPE400	6	5.73	55	107	-	162	0.28
Y	PB641	IPE400	6	5.73	55	107	-	162	0.28
Y	PB642	IPE450	6	5.73	65	140	-	205	0.30
Y	PB643	IPE400	6	5.73	35	107	-	143	0.25

Table A2. 3. Axial and bending designing forces applied to the non-dissipative elements

Item	End	ϴ	Ω_x	Ω_y	N_{Ed}(kN)	$M_{2,Ed}$(kNm)	$M_{3,Ed}$(kNm)	Eq. 3.33	Eq. 3.40	Eq. 3.41
AA1	Top	90º	2.43	2.09	869	113	126	0.22	0.36	0.48
AA2	Top	90º	2.43	2.09	694	163	209	0.33	0.43	0.48
AA3	Top	90º	2.43	2.09	515	147	227	0.30	0.37	0.51
AA4	Top	90º	2.43	2.09	349	125	201	0.26	0.29	0.42
AA5	Top	90º	2.43	2.09	203	88	167	0.18	0.21	0.30
AA6	Top	90º	2.43	2.09	81	82	96	0.16	0.15	0.21
AB1	Top	90º	2.43	2.09	1171	135	227	0.28	0.46	0.57
AB2	Top	90º	2.43	2.09	941	205	361	0.45	0.65	0.83
AB3	Top	90º	2.43	2.09	705	181	351	0.40	0.53	0.70
AB4	Top	90º	2.43	2.09	486	156	300	0.34	0.42	0.57
AB5	Top	90º	2.43	2.09	289	110	222	0.23	0.29	0.40
AB6	Top	90º	2.43	2.09	120	111	151	0.22	0.21	0.31
AC1	Top	90º	2.43	2.09	963	104	268	0.23	0.42	0.51
AC2	Top	90º	2.43	2.09	775	150	416	0.37	0.59	0.73
AC3	Top	90º	2.43	2.09	584	136	395	0.34	0.49	0.63
AC4	Top	90º	2.43	2.09	405	120	335	0.28	0.40	0.52
AC5	Top	90º	2.43	2.09	243	86	243	0.19	0.27	0.37

Item	End	Θ	Ω_x	Ω_y	N_{Ed}(kN)	$M_{2,Ed}$(kNm)	$M_{3,Ed}$(kNm)	Eq. 3.33	Eq. 3.40	Eq. 3.41
AC6	Top	90º	2.43	2.09	102	92	169	0.19	0.20	0.29
AD1	Top	90º	2.43	2.09	963	104	268	0.23	0.38	0.46
AD2	Top	90º	2.43	2.09	775	150	416	0.37	0.60	0.73
AD3	Top	90º	2.43	2.09	584	136	395	0.34	0.50	0.63
AD4	Top	90º	2.43	2.09	405	120	335	0.28	0.50	0.52
AD5	Top	90º	2.43	2.09	243	86	243	0.19	0.30	0.37
AD6	Top	90º	2.43	2.09	102	92	169	0.19	0.23	0.29
AE1	Top	90º	2.43	2.09	1171	135	227	0.28	0.45	0.57
AE2	Top	90º	2.43	2.09	941	205	361	0.45	0.64	0.81
AE3	Top	90º	2.43	2.09	705	181	351	0.40	0.53	0.70
AE4	Top	90º	2.43	2.09	486	156	300	0.34	0.42	0.57
AE5	Top	90º	2.43	2.09	289	110	222	0.23	0.28	0.40
AE6	Top	90º	2.43	2.09	120	111	151	0.22	0.21	0.31
AF1	Top	90º	2.43	2.09	869	113	126	0.22	0.36	0.48
AF2	Top	90º	2.43	2.09	694	163	209	0.33	0.44	0.59
AF3	Top	90º	2.43	2.09	515	147	227	0.30	0.37	0.51
AF4	Top	90º	2.43	2.09	349	125	201	0.26	0.29	0.43
AF5	Top	90º	2.43	2.09	203	88	167	0.18	0.20	0.28
AF6	Top	90º	2.43	2.09	81	82	96	0.16	0.15	0.20
BA1	Top	0º	2.43	2.09	953	97	215	0.21	0.39	0.48
BA2	Top	0º	2.43	2.09	777	144	322	0.32	0.51	0.63
BA3	Top	0º	2.43	2.09	599	133	310	0.30	0.43	0.54
BA4	Top	0º	2.43	2.09	427	115	261	0.25	0.35	0.47
BA5	Top	0º	2.43	2.09	267	83	193	0.18	0.23	0.32
BA6	Top	0º	2.43	2.09	119	78	123	0.15	0.14	0.22
BB1	Top	0º	2.43	2.09	1219	152	237	0.31	0.56	0.67
BB2	Top	0º	2.43	2.09	1008	241	363	0.52	0.70	0.92
BB3	Top	0º	2.43	2.09	799	210	341	0.46	0.62	0.85
BB4	Top	0º	2.43	2.09	592	173	285	0.37	0.45	0.61
BB5	Top	0º	2.43	2.09	389	116	209	0.24	0.30	0.42
BB6	Top	0º	2.43	2.09	193	91	135	0.18	0.19	0.28
BC1	Top	0º	2.43	2.09	1097	164	185	0.33	0.43	0.55
BC2	Top	0º	2.43	2.09	905	264	272	0.53	0.63	0.85
BC3	Top	0º	2.43	2.09	712	231	263	0.47	0.53	0.73
BC4	Top	0º	2.43	2.09	523	189	224	0.38	0.42	0.59
BC5	Top	0º	2.43	2.09	340	128	168	0.25	0.28	0.40
BC6	Top	0º	2.43	2.09	164	95	109	0.19	0.18	0.27
BD1	Top	0º	2.43	2.09	1097	164	185	0.33	0.45	0.60
BD2	Top	0º	2.43	2.09	905	264	272	0.53	0.63	0.85
BD3	Top	0º	2.43	2.09	712	231	263	0.47	0.53	0.53
BD4	Top	0º	2.43	2.09	523	189	224	0.38	0.42	0.52
BD5	Top	0º	2.43	2.09	340	128	168	0.25	0.28	0.40
BD6	Top	0º	2.43	2.09	164	95	109	0.19	0.18	0.26
BE1	Top	0º	2.43	2.09	1219	152	237	0.31	0.47	0.59
BE2	Top	0º	2.43	2.09	1008	241	363	0.52	0.70	0.92
BE3	Top	0º	2.43	2.09	799	210	341	0.46	0.57	0.76
BE4	Top	0º	2.43	2.09	592	173	285	0.37	0.45	0.61
BE5	Top	0º	2.43	2.09	389	116	209	0.24	0.30	0.41
BE6	Top	0º	2.43	2.09	193	91	135	0.18	0.19	0.28

Item	End	Θ	Ω_x	Ω_y	N_{Ed}(kN)	$M_{2,Ed}$(kNm)	$M_{3,Ed}$(kNm)	Eq. 3.33	Eq. 3.40	Eq. 3.41
BF1	Top	0º	2.43	2.09	953	97	215	0.21	0.39	0.48
BF2	Top	0º	2.43	2.09	777	144	322	0.32	0.51	0.63
BF3	Top	0º	2.43	2.09	599	133	310	0.30	0.43	0.56
BF4	Top	0º	2.43	2.09	427	115	261	0.25	0.34	0.45
BF5	Top	0º	2.43	2.09	267	83	193	0.18	0.23	0.32
BF6	Top	0º	2.43	2.09	119	78	123	0.15	0.16	0.23
CA1	Top	0º	2.43	2.09	959	100	220	0.21	0.29	0.36
CA2	Top	0º	2.43	2.09	781	146	328	0.33	0.52	0.64
CA3	Top	0º	2.43	2.09	601	134	316	0.30	0.43	0.56
CA4	Top	0º	2.43	2.09	428	116	267	0.26	0.33	0.46
CA5	Top	0º	2.43	2.09	266	82	195	0.17	0.26	0.36
CA6	Top	0º	2.43	2.09	118	80	128	0.16	0.16	0.24
CB1	Top	90º	2.43	2.09	1185	177	183	0.35	0.46	0.60
CB2	Top	90º	2.43	2.09	984	285	297	0.58	0.65	0.88
CB3	Top	90º	2.43	2.09	781	245	293	0.51	0.57	0.59
CB4	Top	90º	2.43	2.09	579	198	254	0.41	0.51	0.73
CB5	Top	90º	2.43	2.09	380	130	193	0.26	0.30	0.43
CB6	Top	90º	2.43	2.09	184	97	127	0.19	0.23	0.36
CC1	Top	0º	2.43	2.09	1004	161	188	0.32	0.42	0.54
CC2	Top	0º	2.43	2.09	837	257	277	0.52	0.62	0.84
CC3	Top	0º	2.43	2.09	663	225	268	0.46	0.52	0.72
CC4	Top	0º	2.43	2.09	490	185	229	0.37	0.45	0.60
CC5	Top	0º	2.43	2.09	320	124	169	0.25	0.27	0.39
CC6	Top	0º	2.43	2.09	153	96	111	0.19	0.18	0.27
CD1	Top	0º	2.43	2.09	1004	161	188	0.32	0.42	0.54
CD2	Top	0º	2.43	2.09	837	257	277	0.52	0.62	0.84
CD3	Top	0º	2.43	2.09	663	225	268	0.46	0.52	0.71
CD4	Top	0º	2.43	2.09	490	185	229	0.37	0.51	0.58
CD5	Top	0º	2.43	2.09	320	124	169	0.25	0.27	0.39
CD6	Top	0º	2.43	2.09	153	96	111	0.19	0.18	0.25
CE1	Top	90º	2.43	2.09	1185	177	183	0.35	0.46	0.60
CE2	Top	90º	2.43	2.09	984	285	297	0.58	0.65	0.88
CE3	Top	90º	2.43	2.09	781	245	293	0.51	0.57	0.79
CE4	Top	90º	2.43	2.09	579	198	254	0.41	0.45	0.64
CE5	Top	90º	2.43	2.09	380	130	193	0.26	0.30	0.43
CE6	Top	90º	2.43	2.09	184	97	127	0.19	0.18	0.26
CF1	Top	0º	2.43	2.09	959	100	220	0.21	0.40	0.49
CF2	Top	0º	2.43	2.09	781	146	328	0.33	0.52	0.65
CF3	Top	0º	2.43	2.09	601	134	316	0.30	0.43	0.56
CF4	Top	0º	2.43	2.09	428	116	267	0.26	0.35	0.46
CF5	Top	0º	2.43	2.09	266	82	195	0.17	0.27	0.39
CF6	Top	0º	2.43	2.09	118	80	128	0.16	0.16	0.24
DA1	Top	0º	2.43	2.09	953	97	215	0.21	0.39	0.48
DA2	Top	0º	2.43	2.09	777	144	322	0.32	0.51	0.63
DA3	Top	0º	2.43	2.09	599	133	310	0.30	0.43	0.54
DA4	Top	0º	2.43	2.09	427	115	261	0.25	0.35	0.47
DA5	Top	0º	2.43	2.09	267	83	193	0.18	0.23	0.32
DA6	Top	0º	2.43	2.09	119	78	123	0.15	0.14	0.22
DB1	Top	0º	2.43	2.09	1219	152	237	0.31	0.56	0.67

Item	End	Θ	Ω_x	Ω_y	N_{Ed}(kN)	$M_{2,Ed}$(kNm)	$M_{3,Ed}$(kNm)	Eq. 3.33	Eq. 3.40	Eq. 3.41
DB2	Top	0º	2.43	2.09	1008	241	363	0.52	0.70	0.92
DB3	Top	0º	2.43	2.09	799	210	341	0.46	0.62	0.85
DB4	Top	0º	2.43	2.09	592	173	285	0.37	0.45	0.61
DB5	Top	0º	2.43	2.09	389	116	209	0.24	0.30	0.42
DB6	Top	0º	2.43	2.09	193	91	135	0.18	0.19	0.28
DC1	Top	0º	2.43	2.09	1097	164	185	0.33	0.43	0.55
DC2	Top	0º	2.43	2.09	905	264	272	0.53	0.63	0.85
DC3	Top	0º	2.43	2.09	712	231	263	0.47	0.53	0.73
DC4	Top	0º	2.43	2.09	523	189	224	0.38	0.42	0.59
DC5	Top	0º	2.43	2.09	340	128	168	0.25	0.28	0.40
DC6	Top	0º	2.43	2.09	164	95	109	0.19	0.18	0.27
DD1	Top	0º	2.43	2.09	1097	164	185	0.33	0.45	0.60
DD2	Top	0º	2.43	2.09	905	264	272	0.53	0.63	0.85
DD3	Top	0º	2.43	2.09	712	231	263	0.47	0.53	0.53
DD4	Top	0º	2.43	2.09	523	189	224	0.38	0.42	0.52
DD5	Top	0º	2.43	2.09	340	128	168	0.25	0.28	0.40
DD6	Top	0º	2.43	2.09	164	95	109	0.19	0.18	0.26
DE1	Top	0º	2.43	2.09	1219	152	237	0.31	0.47	0.59
DE2	Top	0º	2.43	2.09	1008	241	363	0.52	0.70	0.92
DE3	Top	0º	2.43	2.09	799	210	341	0.46	0.57	0.76
DE4	Top	0º	2.43	2.09	592	173	285	0.37	0.45	0.61
DE5	Top	0º	2.43	2.09	389	116	209	0.24	0.30	0.41
DE6	Top	0º	2.43	2.09	193	91	135	0.18	0.19	0.28
DF1	Top	0º	2.43	2.09	953	97	215	0.21	0.39	0.48
DF2	Top	0º	2.43	2.09	777	144	322	0.32	0.51	0.63
DF3	Top	0º	2.43	2.09	599	133	310	0.30	0.43	0.56
DF4	Top	0º	2.43	2.09	427	115	261	0.25	0.34	0.45
DF5	Top	0º	2.43	2.09	267	83	193	0.18	0.23	0.32
DF6	Top	0º	2.43	2.09	119	78	123	0.15	0.16	0.23
EA1	Top	90º	2.43	2.09	869	113	126	0.22	0.36	0.48
EA2	Top	90º	2.43	2.09	694	163	209	0.33	0.43	0.48
EA3	Top	90º	2.43	2.09	515	147	227	0.30	0.37	0.51
EA4	Top	90º	2.43	2.09	349	125	201	0.26	0.29	0.42
EA5	Top	90º	2.43	2.09	203	88	167	0.18	0.21	0.30
EA6	Top	90º	2.43	2.09	81	82	96	0.16	0.15	0.21
EB1	Top	90º	2.43	2.09	1171	135	227	0.28	0.46	0.57
EB2	Top	90º	2.43	2.09	941	205	361	0.45	0.65	0.83
EB3	Top	90º	2.43	2.09	705	181	351	0.40	0.53	0.70
EB4	Top	90º	2.43	2.09	486	156	300	0.34	0.42	0.57
EB5	Top	90º	2.43	2.09	289	110	222	0.23	0.29	0.40
EB6	Top	90º	2.43	2.09	120	111	151	0.22	0.21	0.31
EC1	Top	90º	2.43	2.09	963	104	268	0.23	0.42	0.51
EC2	Top	90º	2.43	2.09	775	150	416	0.37	0.59	0.73
EC3	Top	90º	2.43	2.09	584	136	395	0.34	0.49	0.63
EC4	Top	90º	2.43	2.09	405	120	335	0.28	0.40	0.52
EC5	Top	90º	2.43	2.09	243	86	243	0.19	0.27	0.37
EC6	Top	90º	2.43	2.09	102	92	169	0.19	0.20	0.29
ED1	Top	90º	2.43	2.09	963	104	268	0.23	0.38	0.46
ED2	Top	90º	2.43	2.09	775	150	416	0.37	0.60	0.73

Item	End	Θ	Ω_x	Ω_y	N_{Ed}(kN)	$M_{2,Ed}$(kNm)	$M_{3,Ed}$(kNm)	Eq. 3.33	Eq. 3.40	Eq. 3.41
ED3	Top	90º	2.43	2.09	584	136	395	0.34	0.50	0.63
ED4	Top	90º	2.43	2.09	405	120	335	0.28	0.50	0.52
ED5	Top	90º	2.43	2.09	243	86	243	0.19	0.30	0.37
ED6	Top	90º	2.43	2.09	102	92	169	0.19	0.23	0.29
EE1	Top	90º	2.43	2.09	1171	135	227	0.28	0.45	0.57
EE2	Top	90º	2.43	2.09	941	205	361	0.45	0.64	0.81
EE3	Top	90º	2.43	2.09	705	181	351	0.40	0.53	0.70
EE4	Top	90º	2.43	2.09	486	156	300	0.34	0.42	0.57
EE5	Top	90º	2.43	2.09	289	110	222	0.23	0.28	0.40
EE6	Top	90º	2.43	2.09	120	111	151	0.22	0.21	0.31
EF1	Top	90º	2.43	2.09	869	113	126	0.22	0.36	0.48
EF2	Top	90º	2.43	2.09	694	163	209	0.33	0.44	0.59
EF3	Top	90º	2.43	2.09	515	147	227	0.30	0.37	0.51
EF4	Top	90º	2.43	2.09	349	125	201	0.26	0.29	0.43
EF5	Top	90º	2.43	2.09	203	88	167	0.18	0.20	0.28
EF6	Top	90º	2.43	2.09	81	82	96	0.16	0.15	0.20
AA1	Bottom	90º	2.43	2.09	520	75	224	0.17	0.36	0.48
AA2	Bottom	90º	2.43	2.09	721	169	187	0.34	0.43	0.48
AA3	Bottom	90º	2.43	2.09	524	129	141	0.25	0.37	0.51
AA4	Bottom	90º	2.43	2.09	348	103	101	0.20	0.29	0.42
AA5	Bottom	90º	2.43	2.09	195	68	65	0.13	0.21	0.30
AA6	Bottom	90º	2.43	2.09	83	50	68	0.10	0.15	0.21
AB1	Bottom	90º	2.43	2.09	775	78	237	0.18	0.46	0.57
AB2	Bottom	90º	2.43	2.09	971	216	363	0.47	0.65	0.83
AB3	Bottom	90º	2.43	2.09	714	165	261	0.35	0.53	0.70
AB4	Bottom	90º	2.43	2.09	484	137	187	0.28	0.42	0.57
AB5	Bottom	90º	2.43	2.09	280	94	104	0.18	0.29	0.40
AB6	Bottom	90º	2.43	2.09	122	76	48	0.14	0.21	0.31
AC1	Bottom	90º	2.43	2.09	658	68	242	0.16	0.42	0.51
AC2	Bottom	90º	2.43	2.09	800	157	423	0.39	0.59	0.73
AC3	Bottom	90º	2.43	2.09	593	121	309	0.28	0.49	0.63
AC4	Bottom	90º	2.43	2.09	405	101	225	0.22	0.40	0.52
AC5	Bottom	90º	2.43	2.09	237	70	129	0.14	0.27	0.37
AC6	Bottom	90º	2.43	2.09	105	59	61	0.11	0.20	0.29
AD1	Bottom	90º	2.43	2.09	658	68	242	0.16	0.38	0.46
AD2	Bottom	90º	2.43	2.09	800	157	423	0.39	0.60	0.73
AD3	Bottom	90º	2.43	2.09	593	121	309	0.28	0.50	0.63
AD4	Bottom	90º	2.43	2.09	405	101	225	0.22	0.50	0.52
AD5	Bottom	90º	2.43	2.09	237	70	129	0.14	0.30	0.37
AD6	Bottom	90º	2.43	2.09	105	59	61	0.11	0.23	0.29
AE1	Bottom	90º	2.43	2.09	775	78	237	0.18	0.45	0.57
AE2	Bottom	90º	2.43	2.09	971	216	363	0.47	0.64	0.81
AE3	Bottom	90º	2.43	2.09	714	165	261	0.35	0.53	0.70
AE4	Bottom	90º	2.43	2.09	484	137	187	0.28	0.42	0.57
AE5	Bottom	90º	2.43	2.09	280	94	104	0.18	0.28	0.40
AE6	Bottom	90º	2.43	2.09	122	76	48	0.14	0.21	0.31
AF1	Bottom	90º	2.43	2.09	520	75	224	0.17	0.36	0.48
AF2	Bottom	90º	2.43	2.09	721	169	187	0.34	0.44	0.59
AF3	Bottom	90º	2.43	2.09	524	129	141	0.25	0.37	0.51

Item	End	Θ	Ω_x	Ω_y	N_{Ed}(kN)	$M_{2,Ed}$(kNm)	$M_{3,Ed}$(kNm)	Eq. 3.33	Eq. 3.40	Eq. 3.41
AF4	Bottom	90º	2.43	2.09	348	103	101	0.20	0.29	0.43
AF5	Bottom	90º	2.43	2.09	195	68	65	0.13	0.20	0.28
AF6	Bottom	90º	2.43	2.09	83	50	68	0.10	0.15	0.20
BA1	Bottom	0º	2.43	2.09	759	66	242	0.15	0.39	0.48
BA2	Bottom	0º	2.43	2.09	796	147	317	0.33	0.51	0.63
BA3	Bottom	0º	2.43	2.09	607	115	232	0.24	0.43	0.54
BA4	Bottom	0º	2.43	2.09	430	91	162	0.19	0.35	0.47
BA5	Bottom	0º	2.43	2.09	265	60	88	0.12	0.23	0.32
BA6	Bottom	0º	2.43	2.09	124	45	36	0.08	0.14	0.22
BB1	Bottom	0º	2.43	2.09	1175	71	230	0.16	0.56	0.67
BB2	Bottom	0º	2.43	2.09	1019	252	365	0.54	0.69	0.90
BB3	Bottom	0º	2.43	2.09	806	194	273	0.40	0.62	0.85
BB4	Bottom	0º	2.43	2.09	598	153	196	0.31	0.45	0.61
BB5	Bottom	0º	2.43	2.09	395	97	112	0.19	0.30	0.42
BB6	Bottom	0º	2.43	2.09	200	63	48	0.12	0.19	0.28
BC1	Bottom	0º	2.43	2.09	1014	72	206	0.16	0.43	0.55
BC2	Bottom	0º	2.43	2.09	918	274	270	0.55	0.63	0.85
BC3	Bottom	0º	2.43	2.09	720	216	201	0.43	0.53	0.73
BC4	Bottom	0º	2.43	2.09	529	171	143	0.33	0.42	0.59
BC5	Bottom	0º	2.43	2.09	344	109	79	0.21	0.28	0.40
BC6	Bottom	0º	2.43	2.09	170	71	34	0.13	0.18	0.27
BD1	Bottom	0º	2.43	2.09	1014	72	206	0.16	0.45	0.60
BD2	Bottom	0º	2.43	2.09	918	274	270	0.55	0.63	0.85
BD3	Bottom	0º	2.43	2.09	720	216	201	0.43	0.53	0.53
BD4	Bottom	0º	2.43	2.09	529	171	143	0.33	0.42	0.52
BD5	Bottom	0º	2.43	2.09	344	109	79	0.21	0.28	0.40
BD6	Bottom	0º	2.43	2.09	170	71	34	0.13	0.18	0.26
BE1	Bottom	0º	2.43	2.09	1175	71	230	0.16	0.47	0.59
BE2	Bottom	0º	2.43	2.09	1019	252	365	0.54	0.70	0.92
BE3	Bottom	0º	2.43	2.09	806	194	273	0.40	0.57	0.76
BE4	Bottom	0º	2.43	2.09	598	153	196	0.31	0.45	0.61
BE5	Bottom	0º	2.43	2.09	395	97	112	0.19	0.30	0.41
BE6	Bottom	0º	2.43	2.09	200	63	48	0.12	0.19	0.28
BF1	Bottom	0º	2.43	2.09	759	66	242	0.15	0.39	0.48
BF2	Bottom	0º	2.43	2.09	796	147	317	0.33	0.51	0.63
BF3	Bottom	0º	2.43	2.09	607	115	232	0.24	0.43	0.56
BF4	Bottom	0º	2.43	2.09	430	91	162	0.19	0.34	0.45
BF5	Bottom	0º	2.43	2.09	265	60	88	0.12	0.23	0.32
BF6	Bottom	0º	2.43	2.09	124	45	36	0.08	0.16	0.23
CA1	Bottom	0º	2.43	2.09	753	63	243	0.15	0.29	0.36
CA2	Bottom	0º	2.43	2.09	801	152	325	0.34	0.52	0.64
CA3	Bottom	0º	2.43	2.09	610	116	238	0.25	0.43	0.56
CA4	Bottom	0º	2.43	2.09	430	95	167	0.19	0.33	0.46
CA5	Bottom	0º	2.43	2.09	264	62	92	0.12	0.26	0.36
CA6	Bottom	0º	2.43	2.09	122	47	38	0.09	0.16	0.24
CB1	Bottom	90º	2.43	2.09	1148	78	206	0.17	0.46	0.60
CB2	Bottom	90º	2.43	2.09	994	299	295	0.61	0.65	0.88
CB3	Bottom	90º	2.43	2.09	788	234	219	0.46	0.57	0.59
CB4	Bottom	90º	2.43	2.09	585	185	158	0.36	0.51	0.73

Item	End	Θ	Ω_x	Ω_y	N_{Ed}(kN)	$M_{2,Ed}$(kNm)	$M_{3,Ed}$(kNm)	Eq. 3.33	Eq. 3.40	Eq. 3.41
CB5	Bottom	90º	2.43	2.09	386	117	90	0.22	0.30	0.43
CB6	Bottom	90º	2.43	2.09	191	75	45	0.14	0.23	0.36
CC1	Bottom	0º	2.43	2.09	979	69	206	0.15	0.42	0.54
CC2	Bottom	0º	2.43	2.09	847	268	275	0.54	0.62	0.84
CC3	Bottom	0º	2.43	2.09	670	211	206	0.42	0.52	0.72
CC4	Bottom	0º	2.43	2.09	497	168	148	0.33	0.45	0.60
CC5	Bottom	0º	2.43	2.09	327	108	82	0.21	0.27	0.39
CC6	Bottom	0º	2.43	2.09	160	71	35	0.13	0.18	0.27
CD1	Bottom	0º	2.43	2.09	979	69	206	0.15	0.42	0.54
CD2	Bottom	0º	2.43	2.09	847	268	275	0.54	0.62	0.84
CD3	Bottom	0º	2.43	2.09	670	211	206	0.42	0.52	0.71
CD4	Bottom	0º	2.43	2.09	497	168	148	0.33	0.51	0.58
CD5	Bottom	0º	2.43	2.09	327	108	82	0.21	0.27	0.39
CD6	Bottom	0º	2.43	2.09	160	71	35	0.13	0.18	0.25
CE1	Bottom	90º	2.43	2.09	1148	78	206	0.17	0.46	0.60
CE2	Bottom	90º	2.43	2.09	994	299	295	0.61	0.65	0.88
CE3	Bottom	90º	2.43	2.09	788	234	219	0.46	0.57	0.79
CE4	Bottom	90º	2.43	2.09	585	185	158	0.36	0.45	0.64
CE5	Bottom	90º	2.43	2.09	386	117	90	0.22	0.30	0.43
CE6	Bottom	90º	2.43	2.09	191	75	45	0.14	0.18	0.26
CF1	Bottom	0º	2.43	2.09	753	63	243	0.15	0.40	0.49
CF2	Bottom	0º	2.43	2.09	801	152	325	0.34	0.52	0.65
CF3	Bottom	0º	2.43	2.09	610	116	238	0.25	0.43	0.56
CF4	Bottom	0º	2.43	2.09	430	95	167	0.19	0.35	0.46
CF5	Bottom	0º	2.43	2.09	264	62	92	0.12	0.27	0.39
CF6	Bottom	0º	2.43	2.09	122	47	38	0.09	0.16	0.24
DA1	Bottom	0º	2.43	2.09	759	66	242	0.15	0.39	0.48
DA2	Bottom	0º	2.43	2.09	796	147	317	0.33	0.51	0.63
DA3	Bottom	0º	2.43	2.09	607	115	232	0.24	0.43	0.54
DA4	Bottom	0º	2.43	2.09	430	91	162	0.19	0.35	0.47
DA5	Bottom	0º	2.43	2.09	265	60	88	0.12	0.23	0.32
DA6	Bottom	0º	2.43	2.09	124	45	36	0.08	0.14	0.22
DB1	Bottom	0º	2.43	2.09	1175	71	230	0.16	0.56	0.67
DB2	Bottom	0º	2.43	2.09	1019	252	365	0.54	0.69	0.90
DB3	Bottom	0º	2.43	2.09	806	194	273	0.40	0.62	0.85
DB4	Bottom	0º	2.43	2.09	598	153	196	0.31	0.45	0.61
DB5	Bottom	0º	2.43	2.09	395	97	112	0.19	0.30	0.42
DB6	Bottom	0º	2.43	2.09	200	63	48	0.12	0.19	0.28
DC1	Bottom	0º	2.43	2.09	1014	72	206	0.16	0.43	0.55
DC2	Bottom	0º	2.43	2.09	918	274	270	0.55	0.63	0.85
DC3	Bottom	0º	2.43	2.09	720	216	201	0.43	0.53	0.73
DC4	Bottom	0º	2.43	2.09	529	171	143	0.33	0.42	0.59
DC5	Bottom	0º	2.43	2.09	344	109	79	0.21	0.28	0.40
DC6	Bottom	0º	2.43	2.09	170	71	34	0.13	0.18	0.27
DD1	Bottom	0º	2.43	2.09	1014	72	206	0.16	0.45	0.60
DD2	Bottom	0º	2.43	2.09	918	274	270	0.55	0.63	0.85
DD3	Bottom	0º	2.43	2.09	720	216	201	0.43	0.53	0.53
DD4	Bottom	0º	2.43	2.09	529	171	143	0.33	0.42	0.52
DD5	Bottom	0º	2.43	2.09	344	109	79	0.21	0.28	0.40

Item	End	Θ	Ω_x	Ω_y	N_{Ed}(kN)	$M_{2,Ed}$(kNm)	$M_{3,Ed}$(kNm)	Eq. 3.33	Eq. 3.40	Eq. 3.41
DD6	Bottom	0º	2.43	2.09	170	71	34	0.13	0.18	0.26
DE1	Bottom	0º	2.43	2.09	1175	71	230	0.16	0.47	0.59
DE2	Bottom	0º	2.43	2.09	1019	252	365	0.54	0.70	0.92
DE3	Bottom	0º	2.43	2.09	806	194	273	0.40	0.57	0.76
DE4	Bottom	0º	2.43	2.09	598	153	196	0.31	0.45	0.61
DE5	Bottom	0º	2.43	2.09	395	97	112	0.19	0.30	0.41
DE6	Bottom	0º	2.43	2.09	200	63	48	0.12	0.19	0.28
DF1	Bottom	0º	2.43	2.09	759	66	242	0.15	0.39	0.48
DF2	Bottom	0º	2.43	2.09	796	147	317	0.33	0.51	0.63
DF3	Bottom	0º	2.43	2.09	607	115	232	0.24	0.43	0.56
DF4	Bottom	0º	2.43	2.09	430	91	162	0.19	0.34	0.45
DF5	Bottom	0º	2.43	2.09	265	60	88	0.12	0.23	0.32
DF6	Bottom	0º	2.43	2.09	124	45	36	0.08	0.16	0.23
EA1	Bottom	90º	2.43	2.09	520	75	224	0.17	0.36	0.48
EA2	Bottom	90º	2.43	2.09	721	169	187	0.34	0.43	0.48
EA3	Bottom	90º	2.43	2.09	524	129	141	0.25	0.37	0.51
EA4	Bottom	90º	2.43	2.09	348	103	101	0.20	0.29	0.42
EA5	Bottom	90º	2.43	2.09	195	68	65	0.13	0.21	0.30
EA6	Bottom	90º	2.43	2.09	83	50	68	0.10	0.15	0.21
EB1	Bottom	90º	2.43	2.09	775	78	237	0.18	0.46	0.57
EB2	Bottom	90º	2.43	2.09	971	216	363	0.47	0.65	0.83
EB3	Bottom	90º	2.43	2.09	714	165	261	0.35	0.53	0.70
EB4	Bottom	90º	2.43	2.09	484	137	187	0.28	0.42	0.57
EB5	Bottom	90º	2.43	2.09	280	94	104	0.18	0.29	0.40
EB6	Bottom	90º	2.43	2.09	122	76	48	0.14	0.21	0.31
EC1	Bottom	90º	2.43	2.09	658	68	242	0.16	0.42	0.51
EC2	Bottom	90º	2.43	2.09	800	157	423	0.39	0.59	0.73
EC3	Bottom	90º	2.43	2.09	593	121	309	0.28	0.49	0.63
EC4	Bottom	90º	2.43	2.09	405	101	225	0.22	0.40	0.52
EC5	Bottom	90º	2.43	2.09	237	70	129	0.14	0.27	0.37
EC6	Bottom	90º	2.43	2.09	105	59	61	0.11	0.20	0.29
ED1	Bottom	90º	2.43	2.09	658	68	242	0.16	0.38	0.46
ED2	Bottom	90º	2.43	2.09	800	157	423	0.39	0.60	0.73
ED3	Bottom	90º	2.43	2.09	593	121	309	0.28	0.50	0.63
ED4	Bottom	90º	2.43	2.09	405	101	225	0.22	0.50	0.52
ED5	Bottom	90º	2.43	2.09	237	70	129	0.14	0.30	0.37
ED6	Bottom	90º	2.43	2.09	105	59	61	0.11	0.23	0.29
EE1	Bottom	90º	2.43	2.09	775	78	237	0.18	0.45	0.57
EE2	Bottom	90º	2.43	2.09	971	216	363	0.47	0.64	0.81
EE3	Bottom	90º	2.43	2.09	714	165	261	0.35	0.53	0.70
EE4	Bottom	90º	2.43	2.09	484	137	187	0.28	0.42	0.57
EE5	Bottom	90º	2.43	2.09	280	94	104	0.18	0.28	0.40
EE6	Bottom	90º	2.43	2.09	122	76	48	0.14	0.21	0.31
EF1	Bottom	90º	2.43	2.09	520	75	224	0.17	0.36	0.48
EF2	Bottom	90º	2.43	2.09	721	169	187	0.34	0.44	0.59
EF3	Bottom	90º	2.43	2.09	524	129	141	0.25	0.37	0.51
EF4	Bottom	90º	2.43	2.09	348	103	101	0.20	0.29	0.43
EF5	Bottom	90º	2.43	2.09	195	68	65	0.13	0.20	0.28
EF6	Bottom	90º	2.43	2.09	83	50	68	0.10	0.15	0.20

Table A2.3 Shear forces applied to the non-dissipative elements

Item	End	ϴ	Ω_x	Ω_y	$V_{Ed,2}$(kN)	$V_{Ed,3}$ (kN)	Eq. 2.4 (2)	Eq. 2.4 (3)
AA1	End	90º	2.43	2.09	233	85	0.14	0.05
AA2	Top	90º	2.43	2.09	122	107	0.07	0.07
AA3	Top	90º	2.43	2.09	110	88	0.07	0.05
AA4	Top	90º	2.43	2.09	85	73	0.05	0.05
AA5	Top	90º	2.43	2.09	62	50	0.04	0.03
AA6	Top	90º	2.43	2.09	30	42	0.02	0.03
AB1	Top	90º	2.43	2.09	277	92	0.17	0.06
AB2	Top	90º	2.43	2.09	235	138	0.14	0.08
AB3	Top	90º	2.43	2.09	196	113	0.12	0.07
AB4	Top	90º	2.43	2.09	155	96	0.10	0.06
AB5	Top	90º	2.43	2.09	103	67	0.06	0.04
AB6	Top	90º	2.43	2.09	60	61	0.04	0.04
AC1	Top	90º	2.43	2.09	290	75	0.18	0.05
AC2	Top	90º	2.43	2.09	269	99	0.17	0.06
AC3	Top	90º	2.43	2.09	224	83	0.14	0.05
AC4	Top	90º	2.43	2.09	177	71	0.11	0.04
AC5	Top	90º	2.43	2.09	117	50	0.07	0.03
AC6	Top	90º	2.43	2.09	71	48	0.04	0.03
AD1	Top	90º	2.43	2.09	290	75	0.18	0.05
AD2	Top	90º	2.43	2.09	269	99	0.17	0.06
AD3	Top	90º	2.43	2.09	224	83	0.14	0.05
AD4	Top	90º	2.43	2.09	177	71	0.11	0.04
AD5	Top	90º	2.43	2.09	117	50	0.07	0.03
AD6	Top	90º	2.43	2.09	71	48	0.04	0.03
AE1	Top	90º	2.43	2.09	277	92	0.17	0.06
AE2	Top	90º	2.43	2.09	235	138	0.14	0.08
AE3	Top	90º	2.43	2.09	196	113	0.12	0.07
AE4	Top	90º	2.43	2.09	155	96	0.10	0.06
AE5	Top	90º	2.43	2.09	103	67	0.06	0.04
AE6	Top	90º	2.43	2.09	60	61	0.04	0.04
AF1	Top	90º	2.43	2.09	233	85	0.14	0.05
AF2	Top	90º	2.43	2.09	122	107	0.07	0.07
AF3	Top	90º	2.43	2.09	110	88	0.07	0.05
AF4	Top	90º	2.43	2.09	85	73	0.05	0.05
AF5	Top	90º	2.43	2.09	62	50	0.04	0.03
AF6	Top	90º	2.43	2.09	30	42	0.02	0.03
BA1	Top	0º	2.43	2.09	246	82	0.15	0.05
BA2	Top	0º	2.43	2.09	204	94	0.13	0.06
BA3	Top	0º	2.43	2.09	172	79	0.11	0.05

Item	End	ϴ	Ω_x	Ω_y	$V_{Ed,2}$(kN)	$V_{Ed,3}$ (kN)	Eq. 2.4 (2)	Eq. 2.4 (3)
BA4	Top	0º	2.43	2.09	133	66	0.08	0.04
BA5	Top	0º	2.43	2.09	88	46	0.05	0.03
BA6	Top	0º	2.43	2.09	47	39	0.03	0.02
BB1	Top	0º	2.43	2.09	244	105	0.15	0.06
BB2	Top	0º	2.43	2.09	237	161	0.15	0.10
BB3	Top	0º	2.43	2.09	199	132	0.12	0.08
BB4	Top	0º	2.43	2.09	155	107	0.10	0.07
BB5	Top	0º	2.43	2.09	103	70	0.06	0.04
BB6	Top	0º	2.43	2.09	57	50	0.04	0.03
BC1	Top	0º	2.43	2.09	210	109	0.13	0.07
BC2	Top	0º	2.43	2.09	173	173	0.11	0.11
BC3	Top	0º	2.43	2.09	147	144	0.09	0.09
BC4	Top	0º	2.43	2.09	115	116	0.07	0.07
BC5	Top	0º	2.43	2.09	77	76	0.05	0.05
BC6	Top	0º	2.43	2.09	42	53	0.03	0.03
BD1	Top	0º	2.43	2.09	210	109	0.13	0.07
BD2	Top	0º	2.43	2.09	173	173	0.11	0.11
BD3	Top	0º	2.43	2.09	147	144	0.09	0.09
BD4	Top	0º	2.43	2.09	115	116	0.07	0.07
BD5	Top	0º	2.43	2.09	77	76	0.05	0.05
BD6	Top	0º	2.43	2.09	42	53	0.03	0.03
BE1	Top	0º	2.43	2.09	244	105	0.15	0.06
BE2	Top	0º	2.43	2.09	237	161	0.15	0.10
BE3	Top	0º	2.43	2.09	199	132	0.12	0.08
BE4	Top	0º	2.43	2.09	155	107	0.10	0.07
BE5	Top	0º	2.43	2.09	103	70	0.06	0.04
BE6	Top	0º	2.43	2.09	57	50	0.04	0.03
BF1	Top	0º	2.43	2.09	246	82	0.15	0.05
BF2	Top	0º	2.43	2.09	204	94	0.13	0.06
BF3	Top	0º	2.43	2.09	172	79	0.11	0.05
BF4	Top	0º	2.43	2.09	133	66	0.08	0.04
BF5	Top	0º	2.43	2.09	88	46	0.05	0.03
BF6	Top	0º	2.43	2.09	47	39	0.03	0.02
CA1	Top	0º	2.43	2.09	248	80	0.15	0.05
CA2	Top	0º	2.43	2.09	209	96	0.13	0.06
CA3	Top	0º	2.43	2.09	176	80	0.11	0.05
CA4	Top	0º	2.43	2.09	137	68	0.08	0.04
CA5	Top	0º	2.43	2.09	90	46	0.06	0.03
CA6	Top	0º	2.43	2.09	50	41	0.03	0.02
CB1	Top	90º	2.43	2.09	236	109	0.15	0.07
CB2	Top	90º	2.43	2.09	191	192	0.12	0.12
CB3	Top	90º	2.43	2.09	163	157	0.10	0.10
CB4	Top	90º	2.43	2.09	129	126	0.08	0.08

Item	End	ϴ	Ω_x	Ω_y	$V_{Ed,2}$(kN)	$V_{Ed,3}$ (kN)	Eq. 2.4 (2)	Eq. 2.4 (3)
CB5	Top	90º	2.43	2.09	88	81	0.05	0.05
CB6	Top	90º	2.43	2.09	49	56	0.03	0.03
CC1	Top	0º	2.43	2.09	211	104	0.13	0.06
CC2	Top	0º	2.43	2.09	176	169	0.11	0.10
CC3	Top	0º	2.43	2.09	150	140	0.09	0.09
CC4	Top	0º	2.43	2.09	118	114	0.07	0.07
CC5	Top	0º	2.43	2.09	78	75	0.05	0.05
CC6	Top	0º	2.43	2.09	43	54	0.03	0.03
CD1	Top	0º	2.43	2.09	211	104	0.13	0.06
CD2	Top	0º	2.43	2.09	176	169	0.11	0.10
CD3	Top	0º	2.43	2.09	150	140	0.09	0.09
CD4	Top	0º	2.43	2.09	118	114	0.07	0.07
CD5	Top	0º	2.43	2.09	78	75	0.05	0.05
CD6	Top	0º	2.43	2.09	43	54	0.03	0.03
CE1	Top	90º	2.43	2.09	236	109	0.15	0.07
CE2	Top	90º	2.43	2.09	191	192	0.12	0.12
CE3	Top	90º	2.43	2.09	163	157	0.10	0.10
CE4	Top	90º	2.43	2.09	129	126	0.08	0.08
CE5	Top	90º	2.43	2.09	88	81	0.05	0.05
CE6	Top	90º	2.43	2.09	49	56	0.03	0.03
CF1	Top	0º	2.43	2.09	248	80	0.15	0.05
CF2	Top	0º	2.43	2.09	209	96	0.13	0.06
CF3	Top	0º	2.43	2.09	176	80	0.11	0.05
CF4	Top	0º	2.43	2.09	137	68	0.08	0.04
CF5	Top	0º	2.43	2.09	90	46	0.06	0.03
CF6	Top	0º	2.43	2.09	50	41	0.03	0.02
DA1	Top	0º	2.43	2.09	246	82	0.15	0.05
DA2	Top	0º	2.43	2.09	204	94	0.13	0.06
DA3	Top	0º	2.43	2.09	172	79	0.11	0.05
DA4	Top	0º	2.43	2.09	133	66	0.08	0.04
DA5	Top	0º	2.43	2.09	88	46	0.05	0.03
DA6	Top	0º	2.43	2.09	47	39	0.03	0.02
DB1	Top	0º	2.43	2.09	244	105	0.15	0.06
DB2	Top	0º	2.43	2.09	237	161	0.15	0.10
DB3	Top	0º	2.43	2.09	199	132	0.12	0.08
DB4	Top	0º	2.43	2.09	155	107	0.10	0.07
DB5	Top	0º	2.43	2.09	103	70	0.06	0.04
DB6	Top	0º	2.43	2.09	57	50	0.04	0.03
DC1	Top	0º	2.43	2.09	210	109	0.13	0.07
DC2	Top	0º	2.43	2.09	173	173	0.11	0.11
DC3	Top	0º	2.43	2.09	147	144	0.09	0.09
DC4	Top	0º	2.43	2.09	115	116	0.07	0.07
DC5	Top	0º	2.43	2.09	77	76	0.05	0.05

Item	End	Θ	Ω_x	Ω_y	$V_{Ed,2}$(kN)	$V_{Ed,3}$ (kN)	Eq. 2.4 (2)	Eq. 2.4 (3)
DC6	Top	0º	2.43	2.09	42	53	0.03	0.03
DD1	Top	0º	2.43	2.09	210	109	0.13	0.07
DD2	Top	0º	2.43	2.09	173	173	0.11	0.11
DD3	Top	0º	2.43	2.09	147	144	0.09	0.09
DD4	Top	0º	2.43	2.09	115	116	0.07	0.07
DD5	Top	0º	2.43	2.09	77	76	0.05	0.05
DD6	Top	0º	2.43	2.09	42	53	0.03	0.03
DE1	Top	0º	2.43	2.09	244	105	0.15	0.06
DE2	Top	0º	2.43	2.09	237	161	0.15	0.10
DE3	Top	0º	2.43	2.09	199	132	0.12	0.08
DE4	Top	0º	2.43	2.09	155	107	0.10	0.07
DE5	Top	0º	2.43	2.09	103	70	0.06	0.04
DE6	Top	0º	2.43	2.09	57	50	0.04	0.03
DF1	Top	0º	2.43	2.09	246	82	0.15	0.05
DF2	Top	0º	2.43	2.09	204	94	0.13	0.06
DF3	Top	0º	2.43	2.09	172	79	0.11	0.05
DF4	Top	0º	2.43	2.09	133	66	0.08	0.04
DF5	Top	0º	2.43	2.09	88	46	0.05	0.03
DF6	Top	0º	2.43	2.09	47	39	0.03	0.02
EA1	Top	90º	2.43	2.09	233	85	0.14	0.05
EA2	Top	90º	2.43	2.09	122	107	0.07	0.07
EA3	Top	90º	2.43	2.09	110	88	0.07	0.05
EA4	Top	90º	2.43	2.09	85	73	0.05	0.05
EA5	Top	90º	2.43	2.09	62	50	0.04	0.03
EA6	Top	90º	2.43	2.09	30	42	0.02	0.03
EB1	Top	90º	2.43	2.09	277	92	0.17	0.06
EB2	Top	90º	2.43	2.09	235	138	0.14	0.08
EB3	Top	90º	2.43	2.09	196	113	0.12	0.07
EB4	Top	90º	2.43	2.09	155	96	0.10	0.06
EB5	Top	90º	2.43	2.09	103	67	0.06	0.04
EB6	Top	90º	2.43	2.09	60	61	0.04	0.04
EC1	Top	90º	2.43	2.09	290	75	0.18	0.05
EC2	Top	90º	2.43	2.09	269	99	0.17	0.06
EC3	Top	90º	2.43	2.09	224	83	0.14	0.05
EC4	Top	90º	2.43	2.09	177	71	0.11	0.04
EC5	Top	90º	2.43	2.09	117	50	0.07	0.03
EC6	Top	90º	2.43	2.09	71	48	0.04	0.03
ED1	Top	90º	2.43	2.09	290	75	0.18	0.05
ED2	Top	90º	2.43	2.09	269	99	0.17	0.06
ED3	Top	90º	2.43	2.09	224	83	0.14	0.05
ED4	Top	90º	2.43	2.09	177	71	0.11	0.04
ED5	Top	90º	2.43	2.09	117	50	0.07	0.03
ED6	Top	90º	2.43	2.09	71	48	0.04	0.03

Item	End	Θ	Ω_x	Ω_y	$V_{Ed,2}$(kN)	$V_{Ed,3}$ (kN)	Eq. 2.4 (2)	Eq. 2.4 (3)
EE1	Top	90º	2.43	2.09	277	92	0.17	0.06
EE2	Top	90º	2.43	2.09	235	138	0.14	0.08
EE3	Top	90º	2.43	2.09	196	113	0.12	0.07
EE4	Top	90º	2.43	2.09	155	96	0.10	0.06
EE5	Top	90º	2.43	2.09	103	67	0.06	0.04
EE6	Top	90º	2.43	2.09	60	61	0.04	0.04
EF1	Top	90º	2.43	2.09	233	85	0.14	0.05
EF2	Top	90º	2.43	2.09	122	107	0.07	0.07
EF3	Top	90º	2.43	2.09	110	88	0.07	0.05
EF4	Top	90º	2.43	2.09	85	73	0.05	0.05
EF5	Top	90º	2.43	2.09	62	50	0.04	0.03
EF6	Top	90º	2.43	2.09	233	85	0.14	0.05
AA1	Bottom	90º	2.43	2.09	122	107	0.07	0.07
AA2	Bottom	90º	2.43	2.09	110	88	0.07	0.05
AA3	Bottom	90º	2.43	2.09	85	73	0.05	0.05
AA4	Bottom	90º	2.43	2.09	62	50	0.04	0.03
AA5	Bottom	90º	2.43	2.09	30	42	0.02	0.03
AA6	Bottom	90º	2.43	2.09	277	92	0.17	0.06
AB1	Bottom	90º	2.43	2.09	235	138	0.14	0.08
AB2	Bottom	90º	2.43	2.09	196	113	0.12	0.07
AB3	Bottom	90º	2.43	2.09	155	96	0.10	0.06
AB4	Bottom	90º	2.43	2.09	103	67	0.06	0.04
AB5	Bottom	90º	2.43	2.09	60	61	0.04	0.04
AB6	Bottom	90º	2.43	2.09	290	75	0.18	0.05
AC1	Bottom	90º	2.43	2.09	269	99	0.17	0.06
AC2	Bottom	90º	2.43	2.09	224	83	0.14	0.05
AC3	Bottom	90º	2.43	2.09	177	71	0.11	0.04
AC4	Bottom	90º	2.43	2.09	117	50	0.07	0.03
AC5	Bottom	90º	2.43	2.09	71	48	0.04	0.03
AC6	Bottom	90º	2.43	2.09	290	75	0.18	0.05
AD1	Bottom	90º	2.43	2.09	269	99	0.17	0.06
AD2	Bottom	90º	2.43	2.09	224	83	0.14	0.05
AD3	Bottom	90º	2.43	2.09	177	71	0.11	0.04
AD4	Bottom	90º	2.43	2.09	117	50	0.07	0.03
AD5	Bottom	90º	2.43	2.09	71	48	0.04	0.03
AD6	Bottom	90º	2.43	2.09	277	92	0.17	0.06
AE1	Bottom	90º	2.43	2.09	235	138	0.14	0.08
AE2	Bottom	90º	2.43	2.09	196	113	0.12	0.07
AE3	Bottom	90º	2.43	2.09	155	96	0.10	0.06
AE4	Bottom	90º	2.43	2.09	103	67	0.06	0.04
AE5	Bottom	90º	2.43	2.09	60	61	0.04	0.04
AE6	Bottom	90º	2.43	2.09	233	85	0.14	0.05
AF1	Bottom	90º	2.43	2.09	122	107	0.07	0.07

Item	End	Θ	Ω_x	Ω_y	$V_{Ed,2}$(kN)	$V_{Ed,3}$ (kN)	Eq. 2.4 (2)	Eq. 2.4 (3)
AF2	Bottom	90º	2.43	2.09	110	88	0.07	0.05
AF3	Bottom	90º	2.43	2.09	85	73	0.05	0.05
AF4	Bottom	90º	2.43	2.09	62	50	0.04	0.03
AF5	Bottom	90º	2.43	2.09	30	42	0.02	0.03
AF6	Bottom	90º	2.43	2.09	246	82	0.15	0.05
BA1	Bottom	0º	2.43	2.09	204	94	0.13	0.06
BA2	Bottom	0º	2.43	2.09	172	79	0.11	0.05
BA3	Bottom	0º	2.43	2.09	133	66	0.08	0.04
BA4	Bottom	0º	2.43	2.09	88	46	0.05	0.03
BA5	Bottom	0º	2.43	2.09	47	39	0.03	0.02
BA6	Bottom	0º	2.43	2.09	244	105	0.15	0.06
BB1	Bottom	0º	2.43	2.09	237	161	0.15	0.10
BB2	Bottom	0º	2.43	2.09	199	132	0.12	0.08
BB3	Bottom	0º	2.43	2.09	155	107	0.10	0.07
BB4	Bottom	0º	2.43	2.09	103	70	0.06	0.04
BB5	Bottom	0º	2.43	2.09	57	50	0.04	0.03
BB6	Bottom	0º	2.43	2.09	210	109	0.13	0.07
BC1	Bottom	0º	2.43	2.09	173	173	0.11	0.11
BC2	Bottom	0º	2.43	2.09	147	144	0.09	0.09
BC3	Bottom	0º	2.43	2.09	115	116	0.07	0.07
BC4	Bottom	0º	2.43	2.09	77	76	0.05	0.05
BC5	Bottom	0º	2.43	2.09	42	53	0.03	0.03
BC6	Bottom	0º	2.43	2.09	210	109	0.13	0.07
BD1	Bottom	0º	2.43	2.09	173	173	0.11	0.11
BD2	Bottom	0º	2.43	2.09	147	144	0.09	0.09
BD3	Bottom	0º	2.43	2.09	115	116	0.07	0.07
BD4	Bottom	0º	2.43	2.09	77	76	0.05	0.05
BD5	Bottom	0º	2.43	2.09	42	53	0.03	0.03
BD6	Bottom	0º	2.43	2.09	244	105	0.15	0.06
BE1	Bottom	0º	2.43	2.09	237	161	0.15	0.10
BE2	Bottom	0º	2.43	2.09	199	132	0.12	0.08
BE3	Bottom	0º	2.43	2.09	155	107	0.10	0.07
BE4	Bottom	0º	2.43	2.09	103	70	0.06	0.04
BE5	Bottom	0º	2.43	2.09	57	50	0.04	0.03
BE6	Bottom	0º	2.43	2.09	246	82	0.15	0.05
BF1	Bottom	0º	2.43	2.09	204	94	0.13	0.06
BF2	Bottom	0º	2.43	2.09	172	79	0.11	0.05
BF3	Bottom	0º	2.43	2.09	133	66	0.08	0.04
BF4	Bottom	0º	2.43	2.09	88	46	0.05	0.03
BF5	Bottom	0º	2.43	2.09	47	39	0.03	0.02
BF6	Bottom	0º	2.43	2.09	248	80	0.15	0.05
CA1	Bottom	0º	2.43	2.09	209	96	0.13	0.06
CA2	Bottom	0º	2.43	2.09	176	80	0.11	0.05

Item	End	Θ	Ω_x	Ω_y	$V_{Ed,2}$(kN)	$V_{Ed,3}$ (kN)	Eq. 2.4 (2)	Eq. 2.4 (3)
CA3	Bottom	0º	2.43	2.09	137	68	0.08	0.04
CA4	Bottom	0º	2.43	2.09	90	46	0.06	0.03
CA5	Bottom	0º	2.43	2.09	50	41	0.03	0.02
CA6	Bottom	0º	2.43	2.09	236	109	0.15	0.07
CB1	Bottom	90º	2.43	2.09	191	192	0.12	0.12
CB2	Bottom	90º	2.43	2.09	163	157	0.10	0.10
CB3	Bottom	90º	2.43	2.09	129	126	0.08	0.08
CB4	Bottom	90º	2.43	2.09	88	81	0.05	0.05
CB5	Bottom	90º	2.43	2.09	49	56	0.03	0.03
CB6	Bottom	90º	2.43	2.09	211	104	0.13	0.06
CC1	Bottom	0º	2.43	2.09	176	169	0.11	0.10
CC2	Bottom	0º	2.43	2.09	150	140	0.09	0.09
CC3	Bottom	0º	2.43	2.09	118	114	0.07	0.07
CC4	Bottom	0º	2.43	2.09	78	75	0.05	0.05
CC5	Bottom	0º	2.43	2.09	43	54	0.03	0.03
CC6	Bottom	0º	2.43	2.09	211	104	0.13	0.06
CD1	Bottom	0º	2.43	2.09	176	169	0.11	0.10
CD2	Bottom	0º	2.43	2.09	150	140	0.09	0.09
CD3	Bottom	0º	2.43	2.09	118	114	0.07	0.07
CD4	Bottom	0º	2.43	2.09	78	75	0.05	0.05
CD5	Bottom	0º	2.43	2.09	43	54	0.03	0.03
CD6	Bottom	0º	2.43	2.09	236	109	0.15	0.07
CE1	Bottom	90º	2.43	2.09	191	192	0.12	0.12
CE2	Bottom	90º	2.43	2.09	163	157	0.10	0.10
CE3	Bottom	90º	2.43	2.09	129	126	0.08	0.08
CE4	Bottom	90º	2.43	2.09	88	81	0.05	0.05
CE5	Bottom	90º	2.43	2.09	49	56	0.03	0.03
CE6	Bottom	90º	2.43	2.09	248	80	0.15	0.05
CF1	Bottom	0º	2.43	2.09	209	96	0.13	0.06
CF2	Bottom	0º	2.43	2.09	176	80	0.11	0.05
CF3	Bottom	0º	2.43	2.09	137	68	0.08	0.04
CF4	Bottom	0º	2.43	2.09	90	46	0.06	0.03
CF5	Bottom	0º	2.43	2.09	50	41	0.03	0.02
CF6	Bottom	0º	2.43	2.09	246	82	0.15	0.05
DA1	Bottom	0º	2.43	2.09	204	94	0.13	0.06
DA2	Bottom	0º	2.43	2.09	172	79	0.11	0.05
DA3	Bottom	0º	2.43	2.09	133	66	0.08	0.04
DA4	Bottom	0º	2.43	2.09	88	46	0.05	0.03
DA5	Bottom	0º	2.43	2.09	47	39	0.03	0.02
DA6	Bottom	0º	2.43	2.09	244	105	0.15	0.06
DB1	Bottom	0º	2.43	2.09	237	161	0.15	0.10
DB2	Bottom	0º	2.43	2.09	199	132	0.12	0.08
DB3	Bottom	0º	2.43	2.09	155	107	0.10	0.07

Item	End	Θ	Ω_x	Ω_y	$V_{Ed,2}$(kN)	$V_{Ed,3}$ (kN)	Eq. 2.4 (2)	Eq. 2.4 (3)
DB4	Bottom	0º	2.43	2.09	103	70	0.06	0.04
DB5	Bottom	0º	2.43	2.09	57	50	0.04	0.03
DB6	Bottom	0º	2.43	2.09	210	109	0.13	0.07
DC1	Bottom	0º	2.43	2.09	173	173	0.11	0.11
DC2	Bottom	0º	2.43	2.09	147	144	0.09	0.09
DC3	Bottom	0º	2.43	2.09	115	116	0.07	0.07
DC4	Bottom	0º	2.43	2.09	77	76	0.05	0.05
DC5	Bottom	0º	2.43	2.09	42	53	0.03	0.03
DC6	Bottom	0º	2.43	2.09	210	109	0.13	0.07
DD1	Bottom	0º	2.43	2.09	173	173	0.11	0.11
DD2	Bottom	0º	2.43	2.09	147	144	0.09	0.09
DD3	Bottom	0º	2.43	2.09	115	116	0.07	0.07
DD4	Bottom	0º	2.43	2.09	77	76	0.05	0.05
DD5	Bottom	0º	2.43	2.09	42	53	0.03	0.03
DD6	Bottom	0º	2.43	2.09	244	105	0.15	0.06
DE1	Bottom	0º	2.43	2.09	237	161	0.15	0.10
DE2	Bottom	0º	2.43	2.09	199	132	0.12	0.08
DE3	Bottom	0º	2.43	2.09	155	107	0.10	0.07
DE4	Bottom	0º	2.43	2.09	103	70	0.06	0.04
DE5	Bottom	0º	2.43	2.09	57	50	0.04	0.03
DE6	Bottom	0º	2.43	2.09	246	82	0.15	0.05
DF1	Bottom	0º	2.43	2.09	204	94	0.13	0.06
DF2	Bottom	0º	2.43	2.09	172	79	0.11	0.05
DF3	Bottom	0º	2.43	2.09	133	66	0.08	0.04
DF4	Bottom	0º	2.43	2.09	88	46	0.05	0.03
DF5	Bottom	0º	2.43	2.09	47	39	0.03	0.02
DF6	Bottom	0º	2.43	2.09	233	85	0.14	0.05
EA1	Bottom	90º	2.43	2.09	122	107	0.07	0.07
EA2	Bottom	90º	2.43	2.09	110	88	0.07	0.05
EA3	Bottom	90º	2.43	2.09	85	73	0.05	0.05
EA4	Bottom	90º	2.43	2.09	62	50	0.04	0.03
EA5	Bottom	90º	2.43	2.09	30	42	0.02	0.03
EA6	Bottom	90º	2.43	2.09	277	92	0.17	0.06
EB1	Bottom	90º	2.43	2.09	235	138	0.14	0.08
EB2	Bottom	90º	2.43	2.09	196	113	0.12	0.07
EB3	Bottom	90º	2.43	2.09	155	96	0.10	0.06
EB4	Bottom	90º	2.43	2.09	103	67	0.06	0.04
EB5	Bottom	90º	2.43	2.09	60	61	0.04	0.04
EB6	Bottom	90º	2.43	2.09	290	75	0.18	0.05
EC1	Bottom	90º	2.43	2.09	269	99	0.17	0.06
EC2	Bottom	90º	2.43	2.09	224	83	0.14	0.05
EC3	Bottom	90º	2.43	2.09	177	71	0.11	0.04
EC4	Bottom	90º	2.43	2.09	117	50	0.07	0.03

Item	End	ϴ	Ω_x	Ω_y	$V_{Ed,2}$(kN)	$V_{Ed,3}$ (kN)	Eq. 2.4 (2)	Eq. 2.4 (3)
EC5	Bottom	90º	2.43	2.09	71	48	0.04	0.03
EC6	Bottom	90º	2.43	2.09	290	75	0.18	0.05
ED1	Bottom	90º	2.43	2.09	269	99	0.17	0.06
ED2	Bottom	90º	2.43	2.09	224	83	0.14	0.05
ED3	Bottom	90º	2.43	2.09	177	71	0.11	0.04
ED4	Bottom	90º	2.43	2.09	117	50	0.07	0.03
ED5	Bottom	90º	2.43	2.09	71	48	0.04	0.03
ED6	Bottom	90º	2.43	2.09	277	92	0.17	0.06
EE1	Bottom	90º	2.43	2.09	235	138	0.14	0.08
EE2	Bottom	90º	2.43	2.09	196	113	0.12	0.07
EE3	Bottom	90º	2.43	2.09	155	96	0.10	0.06
EE4	Bottom	90º	2.43	2.09	103	67	0.06	0.04
EE5	Bottom	90º	2.43	2.09	60	61	0.04	0.04
EE6	Bottom	90º	2.43	2.09	233	85	0.14	0.05
EF1	Bottom	90º	2.43º	2.09	122	107	0.07	0.07
EF2	Bottom	90º	2.43	2.09	110	88	0.07	0.05
EF3	Bottom	90º	2.43	2.09	85	73	0.05	0.05
EF4	Bottom	90º	2.43	2.09	62	50	0.04	0.03
EF5	Bottom	90º	2.43	2.09	62	50	0.04	0.03
EF6	Bottom	90º	2.43	2.09	30	42	0.02	0.03

BIBLIOGRAPHY

ASCE (2000),'American Society of Civil Engineers, FEMA 356, Prestandard and Commentary for the Seismic Rehabilitation of Building', *Rehabilitation (2000).*

CEN (2002) 'EN 1991-1, *Eurocode 1, Actions on structures - Part 1-1: General actions - Densities, self-weight, imposed loads for buildings*'.

CEN (2004a) 'EN 1991-4, *Eurocode 1, Actions on structures - Part 1-4: General actions - Wind actions*'.

CEN (2004b) 'EN 1994-1, *Eurocode 4, Design of composite steel and concrete structures - Part 1-1: General rules and rules for buildings*'.

CEN (2004c) 'EN 1998-1, *Eurocode 8, Design of structures for earthquake resistance - Part 1: General rules, seismic actions and rules for buildings*'.

CEN (2005a) 'EN 1990, *Eurocode, Basis of structural design*'.

CEN (2005b) 'EN 1993-1, *Eurocode 3, Design of steel structures - Part 1-1: General rules and rules for buildings*'.

CEN (2005c) 'EN 1993-1-8, *Eurocode 3, Design of steel structures - Part 1-8: Design of joints*'.

Chopra, A.K. (2019) '*Dynamics of Structures Theory and Application to Earthquake Engineering*' . Pearson.

Chopra, A.K. (2005) 'Earthquake dynamics of structures A primer', *University of California, Berkeley*, pp. 809–834.

Fajfar, P. (2000) 'A Nonlinear Analysis Method for Performance-Based Seismic Design', *Earthquake Spectra*, 16(3), pp. 573–592. doi: 10.1193/1.1586128.

Jaspart, J. P. and Weynand, K. (2016) '*Design of joints in steel and composite structures*'. ECCS.

Landolfo, R., Mazzolani, F., Dubina, D. and Simoes da Silva, L. (2017) '*Design of Steel Structures for Buildings in Seismic Areas*'. ECCS.

Landolfo, R. D'Aniello, M., Costanzo, S., Tartaglia, R., Demonceau, J.F., Jaspart, J.P., Stratan, A., Jaka, D., Dubina, D., Elghazouli, A. and Bompa, D. (2018) '*Equaljoints PLUS: Volume with information brochures for 4 seismically qualified joints*'. Available at: https://www.steelconstruct.com/wp-content/uploads/DWP2-3_EJplus_FINAL_v2-compressed.pdf.

MeTecno (2020) 'HI-BOND - Trapezoidal sheets for concrete slabs'.

Ministerio delle Infraestructure e dei Transporti (2018) *'Aggiornamento delle NTC 2018 Norme Tecniche per le Costruzioni'*, pp. 1-198.

Ministerio delle Infraestructure e dei Transporti (2018) *'Circolare NTC 18 - AZIONI SULLE COSTRUZIONI'.*

Mirambell, E. (2020) 'Estructuras Mixtas Acero – Hormigón'.

Petrini, L., Pinho, R. and Michele Calvi, G. (2004) '*Criteri di Progettazione Antisimica degli Edifici*'. Iuss Press, Pavia.

Simoes da Silva, L., Simoes, R. and Gervasio, H. (2013) '*Design of Steel Structures*'. ECCS.

Studio viscogliosi tomassi (2010) '*RELAZIONE GEOLOGICA E SISMICA AI SENSI DEL D.M. DEL 14/01/2008 - "NUOVE NORME TECNICHE PER LE COSTRUZIONI" E CIRCOLARE 2 FEBBRAIO 2009, N. 617, C.S.LL.PP*'.

Di Trapani, F. and Cavalieri, L. (2018) 'Nonlinear Static Analysis', pp. 169–240. doi: 10.1007/978-1-4757-3546-8_4.

Tullini, N. (2019) 'Solai in lamiera grecata e soletta in calcestruzzo: Tipologie, progetto e verifiche'.